CHEMICAL REVIEWS

Interactions between Metal Oxides and Biomolecules: from Fundamental Understanding to Applications
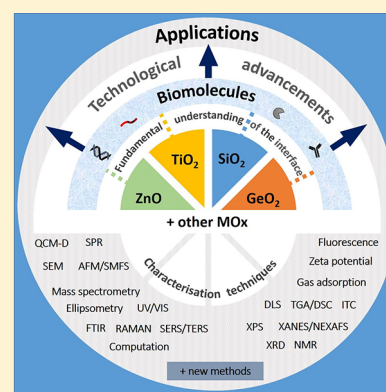
Marion J. Limo,[∥,†,‡] Anna Sola-Rabada,[∥,†] Estefania Boix,[∥,†,§] Veeranjaneyulu Thota,[†] Zayd C. Westcott,[†] Valeria Puddu,[†] and Carole C. Perry*[,†]

[†]Interdisciplinary Biomedical Research Centre, School of Science and Technology, Nottingham Trent University, Clifton Lane, Nottingham NG11 8NS, United Kingdom

[‡]Interface and Surface Analysis Centre, School of Pharmacy, University of Nottingham, University Park, Nottingham NG7 2RD, United Kingdom

[§]Department of Bioproducts and Biosystems, Aalto University, P.O. Box 16100, FI-00076 Aalto, Finland

ABSTRACT: Metallo-oxide (MO)-based bioinorganic nanocomposites promise unique structures, physicochemical properties, and novel biochemical functionalities, and within the past decade, investment in research on materials such as ZnO, TiO$_2$, SiO$_2$, and GeO$_2$ has significantly increased. Besides traditional approaches, the synthesis, shaping, structural patterning, and postprocessing chemical functionalization of the materials surface is inspired by strategies which mimic processes in nature. Would such materials deliver new technologies? Answering this question requires the merging of historical knowledge and current research from different fields of science. Practically, we need an effective defragmentation of the research area. From our perspective, the superficial accounting of material properties, chemistry of the surfaces, and the behavior of biomolecules next to such surfaces is a problem. This is particularly of concern when we wish to bridge between technologies in vitro and biotechnologies in vivo. Further, besides the potential practical technological efficiency and advantages such materials might exhibit, we have to consider the wider long-term implications of material stability and toxicity. In this contribution, we present a critical review of recent advances in the chemistry and engineering of MO-based biocomposites, highlighting the role of interactions at the interface and the techniques by which these can be studied. At the end of the article, we outline the challenges which hamper progress in research and extrapolate to developing and promising directions including additive manufacturing and synthetic biology that could benefit from molecular level understanding of interactions occurring between inanimate (abiotic) and living (biotic) materials.

CONTENTS

1. INTRODUCTION

Metal/metalloid oxides hereafter referred to as MOs are important materials that have the potential for programmable structures to be engineered with integrated properties. They display a wide range of structures and have exceptional optical, electrical, and magnetic properties, making them useful for a large variety of applications.[1] They can act as semiconductors through to insulators, and much research effort is focused toward advancements for technological use in catalysis, optoelectronics, ceramics, sensing, transparent conductive films, biomedical devices, and environmental remediation, as examples. Their unique properties are associated with variations in bonding, electronic structure, and the presence of ordered or extended defects.[2] For instance, many MOs have good chemical and thermal stability attributed to their completely filled s-shells.[3,4] However, a number of commercially important MOs also have incomplete d shells, giving them properties such as wide band gaps, reactive electronic transitions, and high dielectric constants, coupled with good optical, electrical, and electrochromic characteristics.[3,5] The properties of bulk materials differ from nanoparticle (NP) counterparts of the same chemical composition. For example, the chemical and thermal stability of NPs may be reduced in comparison to bulk materials, but NPs exhibit unique features such as size, shape, composition, interparticle distance-dependent quantum effects, and a large surface area to volume ratio. The high levels of surface active atoms can additionally be functionalized with ligands exhibiting a wide range of chemical functionality for a wide range of applications.[6−9]

The application of MOs depends on control over their physicochemical properties, including composition, chemical structure (including the surface), and morphology, all of which are directly influenced by the synthesis process. Material synthesis strategies can largely be classified into two approaches, the top-down and the bottom-up approach.[9−12] The top-down rationale involves miniaturization processes using physical or chemical means for printing and patterning predesigned forms at a micro and nanoscale (microlithography and nanolithography).[13] Top-down methods are costly and limited to molecular level precision, currently unable to mass produce identical nanostructures especially below 100 nm.[12−15]

These limitations are overcome in the bottom-up approach whereby functional materials are assembled from chemically synthesized nanoscale building blocks. Bottom-up strategies

employ solution phase methods in aqueous or nonhydrolytic media. Hydrothermal methods are particularly attractive for their simplicity and low cost sustainable green chemistry approach.[16,17] Additionally, solution synthesis methods allow for control over nano/microparticle nucleation, growth, and aging mechanisms, thereby controlling the material's properties. This is achieved by controlling the growth conditions (i.e., solution composition such as precursors and solvents used, reaction temperature, pressure, and pH), thereby tuning the relative surface energy of the different growth facets, manipulating the rate and direction of crystal growth.[18,19]

Using hydrothermal synthesis routes, a wide range of MO materials having amorphous/crystalline structure and different morphologies have been generated.[20−22] Further structural modification has been achieved using structure directing agents (SDAs) such as citrate ions,[23] amines,[24−26] polymers,[27−31] biomolecules,[21,32−40] and the use of mixed solvent systems, including microemulsions and different acids.[41,42] Though more complex and costly to work with, biomolecules, particularly proteins, have great potential to assist in controlling the synthesis, structure, and/or function of materials, including MOs.[43−45]

The association between biomolecules and MOs is observed in nature. Through the process of biomineralization, complex hierarchical and functional inorganic structures, including MOs, are produced in certain species. For example, magnetosome crystals consisting of the magnetic iron oxide, magnetite, are found in magnetotactic bacteria,[46] and detailed silica structures are manufactured by diatoms, marine sponges, and higher plants.[47−49] The reproducible formation of intricate biominerals by nature is unequaled and remains unattainable using artificial synthesis processes. To emulate nature's biomaterials synthesis tools, the conventional approach taken in biomimetic studies has been to extract, isolate, fully characterize, and understand the role of biomolecules involved in biomineralization.[50−53] In fact, there is evidence of successful in vitro mineralization activity utilizing these proteins and their shorter sequences (peptides) not just in the synthesis of biominerals produced by the organism from which they were obtained but also in controlling the synthesis of other materials of interest.[54,55]

However, this approach has challenges that include difficulties in obtaining and culturing biomineralizing species. Those avaliable present a limited repertoire of identified biomineralizing molecules (including proteins) that can control the synthesis of a broader spectrum of commercially relevant inorganic materials, such as semiconductors and metals not routinely formed through biomineralization processes.[56,57] Improvements have been made in biomolecule extraction techniques, and quantities can be synthesized using recombinant DNA protocols for the expression and purification of proteins.[38,56,58] Even so, few biomineralizing proteins have been sequenced.[54,59,60] In addition, there are serious deficiencies with respect to the level of understanding as to how such biomolecules either interact with and/or influence mineral formation, due to the difficulties in understanding the behavior of the biomolecules in aqueous media or in the local environment in which they are found. For example, no crystal structure (and hence detailed molecular understanding) of any of the purported molecules involved in the silicification of diatoms or sponges (e.g., silicateins or silaffins) is known.

Different approaches are needed. One recognized strategy is the use of combinatorial techniques [i.e., cell-surface display (CSD), ribosome display (RD), and phage display (PD)] to identify peptide sequences that can bind specifically to a given target material.[38,61,62] The identified peptides have practical applications in inorganic synthesis, surface functionalization, and immobilization of other molecules or NPs onto an inorganic surface.[56,61−63] Further, the prospect of creating novel hybrid materials using biological linkers to combine more than one material in order to incorporate different electronic, magnetic, and mechanical properties, for example, to generate unique combinations of properties is becoming feasible.[61,64]

To date, the principles governing and driving MO−biomolecule interfacial interactions are poorly understood. This includes the influence of biomolecules on composite functionality as well as matters such as stability and toxicity. For a given set of biomolecules and MOs, interactions seem to occur in a unique manner currently necessitating analysis to be carried out on an individual basis.[65]

1.1. Approaches Used in the Study of MO-Biomolecule Interactions

Numerous experimental techniques and computational tools are being used to investigate and characterize MO-biomolecule interactions, probing binding selectivity, elucidation of biomolecule conformation when unbound/free and surface bound, surface coverage, kinetic and thermodynamic changes during interaction, and the stability of interactions. Experimental techniques include atomic force microscopy (AFM), single molecule force spectroscopy (SMFS), quartz crystal microbalance with dissipation monitoring (QCM-D), isothermal titration calorimetry (ITC), ellipsometry, optical waveguide lightmode spectroscopy (OWLS), surface plasmon resonance (SPR) spectroscopy, sum-frequency generation (SFG) spectroscopy, fluorescence spectroscopy, ultraviolet−visible (UV/vis) spectroscopy, circular dichroism (CD) spectroscopy, Fourier transform infrared spectroscopy (FTIR), Raman spectroscopy, nuclear magnetic resonance (NMR) spectroscopy, dynamic light scattering (DLS), zeta potential measurements, X-ray photoelectron spectroscopy (XPS), X-ray absorption near edge spectroscopy (XANES), and high-resolution powder X-ray diffraction (HR-XRD).

These techniques have different working principles/measurement modes, advantages and disadvantages, and thus there are differences in the information that can be obtained when each is used. At the end of this article, a summary of key information on experimental techniques that have significantly contributed toward enhancing our understanding of MO-biomolecule interactions is given. The table draws together the experience of researchers in this field and serves as a guide to enable other researchers to select appropriate tools for their studies. It should be noted that, in many cases, the application of multiple techniques will be necessary to fully characterize the materials and interface. The use of these techniques will be discussed in this article with examples.

Approaches used by the community include the use of bioinformatics and computational tools including molecular dynamics (MD) simulations.

For experimentalists, the principles behind computational modeling as applied to the material biomolecule interface might be less clear than many of the methods encountered in the laboratory, so a short introduction to the principles

underlying the approach is given here. This is so that terms such as computer model, force field, parameter set, and conformational sampling will be understood when they appear in the rest of the review.

Why should we want to make use of simulations in our study of the biomolecule−material interface? Such interactions when studied by experimental approaches are limited in their ability to provide detail at the atomistic level and are seldom able to provide information on biomolecule orientation and conformation at a particular surface. There are some exceptions as we will discuss later in this review article. Application of computer simulations to study the complex environment at the center of a biomolecule-material construct can yield information at a level currently unobtainable by experiment. Laboratory-based experiments, on the whole, yield data for ensembles of molecules interacting with materials. With computer simulation, it is possible to obtain information for a specific molecule interacting with a specific predefined surface. This is generally limited to a single molecule at this time, at least for oxides, although studies on multiple peptides, proteins, and polymers on surfaces have all been reported.[66,67]

The size of the computational problem, including the numbers of atoms required to represent a molecule (even a small peptide) interacting with a surface is considerable and on the order of tens of thousands of atoms. This means that at present a full quantum level description of the events occurring during adsorption or desorption of a biomolecule on a surface is not possible. For quantum chemistry approaches, the current limit is on the order of a few hundred atoms, though as computer power and access increases this will no doubt increase considerably.

A more feasible approach is to use empirical force field-based molecular modeling which is able to predict molecular interactions at the atomistic level for systems up to several 100000 atoms, though numbers ∼10 times higher than this can be explored at the expense of accuracy or time scale/sampling. For this approach, a physical model has to be described by equations (a force field), using a series of parameters to describe (as accurately as possible) ALL of the interactions between the atoms contained in the molecular system in question. Further, in order to obtain a statistically valid representation of the system's behavior, it is important to "sample" the configurational space (sampling of all conformations possible for a molecule/system being explored).

If we consider the interaction of a small biomolecule (e.g., peptide) with a surface in aqueous media, we further need to use a model and parameter set that is able to handle the mineral, biomolecule, and interface between the two. It is usual that a compromise has to be made which may be to limit the description of the charge of a surface, to simplify the model used to describe water at the interface or to limit the conformational space explored during the simulation. A recently published review by Walsh in 2017 clearly describes the current challenges in the field which include the development of structural models, issues to do with force field development and conformational sampling, albeit that the examples used to illustrate progress to date relate mainly to noble face centered cubic (fcc) metals such as gold and silver, graphitic substrates, and to a lesser extent the oxide, titania.[68]

1.2. Choice of Metal (Metalloid) Oxide Systems

The study of MO-biomolecule interactions is being pursued by researchers worldwide. Some of the MOs which have been studied using a biomimetic approach and/or for which applications are being developed that make use of MO−biomolecule interfacial interactions include silica (SiO_2),[69−75] zinc oxide (ZnO),[33,44,76−82] titania (TiO_2),[37,83−87] germania (GeO_2),[21,88−97] gallium oxide (Ga_2O_3),[98,99] iron oxide (Fe_3O_4),[41,76,100,101] cobalt oxide (Co_3O_4),[102,103] and manganese oxide (Mn_3O_4).[104] Newly developing technologies that exploit MO−biomolecule interfaces have applications that span from materials chemistry through to biotechnology and biomedical engineering.[11,105−108] However, to fully realize the potential of this field, further detailed, comprehensive, and innovative studies of the interface will be required. Figure 1 illustrates the link between a fundamental understanding of the interface and development of applications.
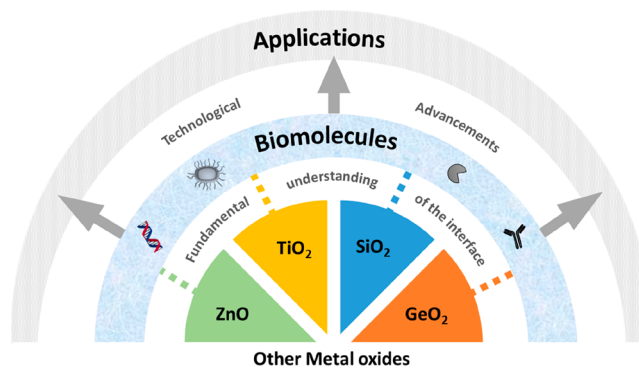
Figure 1. Schematic depicting the importance of a fundamental understanding of interactions at the metal oxide−biomolecule interface for the advancement of applications.

In exploring these interactions, it is important that a distinction is made between biomolecules that can recognize a metal oxide surface (i.e., surfaces that already exist-as in phage display) and biomolecules that can be used in the biomimetic growth of (nano)particles from solution. Note that depending on the strength of binding or specific interaction pattern, biomolecules can also be used to change morphology by limiting growth in particular directions as well as change the phase or even chemical composition of the material that forms. Examples of all these types of behavior are showcased in the studies of MO_x biomolecule interactions described in sections 2−7 below. We note that a recent review by Walsh and Knecht[109] provides similar information for other classes of materials, including semiconductors, catalysts, and quantum dot materials.

Studies within our research group have focused toward understanding the specificity, interaction mechanisms, and identifying/developing functionality of inorganic binding biomolecules including peptides. The MOs that we have studied extensively, gained a wealth of knowledge on, and report on here are ZnO, TiO_2, SiO_2, and GeO_2, selected for their exceptional properties which will be discussed in detail below. For these particular MOs, a précis of key contributions reported in the literature, highlighting developing applications and discussion of techniques and methods that have significantly contributed toward enhancing our understanding of MO-biomolecule interactions will be provided. Using these MOs as exemplars, the objective is to showcase important findings, point out problems, and put forward steps that can be taken toward advancing the wider field of research on MO-biomolecule interactions.
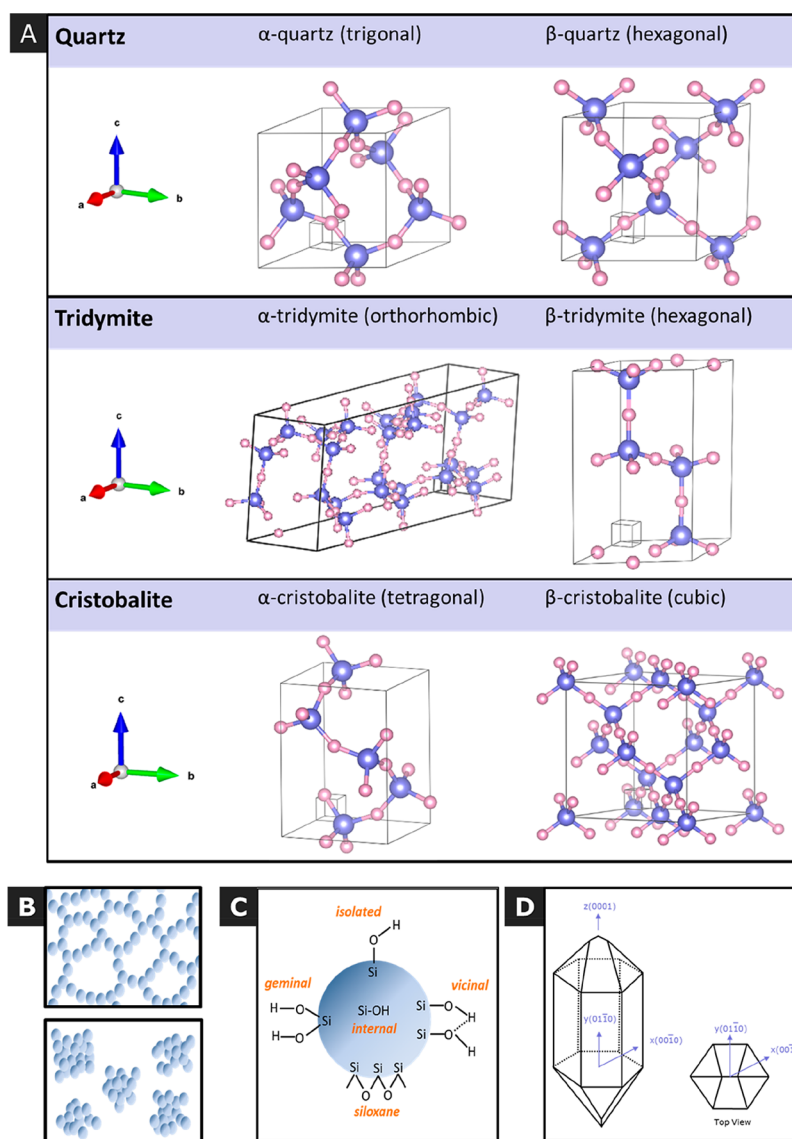
Figure 2. (A) Images were drawn using VESTA[138] and lattice parameters imported from Crystallography Open Database:[139] alpha-quartz (COD 1011097), beta-quartz (COD 1011200), alpha-tridymite (COD-9013393), beta-tridymite (COD 5910147), alpha-cristobalite (COD 1010938), and beta-cristobalite (COD 1010944). Note that alpha-tridymite is a cut section of the unit cell. (B) Two-dimensional representation of silica units distributed in a gel (top) and a precipitate (bottom). (C) The silanol chemistry of silica particles: isolated, geminal, vicinal, and internal. Illustration adapted with permission from ref 140. Copyright 2000 Elsevier. (D) Main quartz planes during crystal growth. Adapted with permission from ref 141. Copyright 2012 IOP Publishing.

In particular, we emphasize the need to understand the materials being worked with whether these be commercially sourced (i.e., particulates, surfaces, sensors, and biomolecules) or prepared in the laboratory. Interactions between molecules and materials occur at the interface between the two, and therefore, we need to understand the surfaces of the materials and the environment in which any interactions take place. Full reporting of these facts will enable the field to move forward in a more timely manner than present. For studies using computational simulations, we provide pointers as to what to look out for to determine whether the information obtained from such studies is reasonable as well as pointing out limitations and issues with the approach taken.

Although nanotechnology promises to have great benefits for society, there is increasing concern that human and environmental exposure to engineered nanomaterials may result in harm to those exposed to such materials,[110,111] and

thus, we also present brief summaries of what is known concerning the nanotoxicology of the chosen materials together with comments concerning the likely effect of surface-associated biomolecules on their toxicity. Again, as responsible scientists, it is imperative that we fully describe the nature of the materials we study/generate so that the hazards associated with such materials can be fully appreciated as they will no doubt impinge on potential applications of the same. At the end of the review, we highlight some newly developing areas in both the engineering and bioscience communities where increased understanding of biomolecule-mineral inter-actions may enhance progress in areas such as additive manufacturing and synthetic biology. We conclude with some "take home messages" for those both new to and already working in the field.

2. SiO$_2$

2.1. Introduction to SiO$_2$ as a Material

SiO$_2$ is a common material in nature and is the second most common biogenic mineral after carbonates.[112] Silica can be found in nature either in amorphous or crystalline forms (i.e., quartz, cristobalite, trydimite), Figure 2A. Crystalline silica, commonly α-quartz, is a basic compound of soil, sands, and rocks, whereas amorphous silica is commonly deposited in living organisms, including land plants (i.e., rice, cucumber, mares tail), single cellular organisms such as diatoms, and multicellular organisms like sponges.[60,113−115] Amorphous silica can also be found in its hydrated form (SiO$_2$·nH$_2$O), forming part of minerals such as limonite, sandstone, rhyolite, marl, and basalt and the semiprecious gem, opal. The biosilicification process to make biogenic or natural hydrated silica involves a range of inorganic polymerization reactions in the presence of organic species such as proteins and proteoglycans, which are considered possible control molecules during the biomineralization process.[116] The role of the organic matrix in silica formation and the overall biosilicification process has been widely studied as a way to design new materials inspired by nature.[69,116−118] Silica, in all its different forms, is currently one of the most studied compounds in the fields of chemistry, physics, engineering, and (bio)medicine, and its popularity is still on the rise.
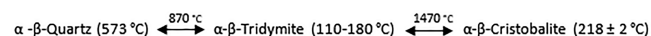
Synthetic silica nanoparticles (SiNPs), especially amorphous silica, have received much attention in recent years for a variety of technological and biomedical applications due to their tunable high surface area and permeability across membranes, resulting in high interaction with cellular systems;[119] unfortunately some forms of crystalline silica show toxic effects when interacting with biological systems.[120] The cytotoxicity of SiNPs on cells is dependent on the amount of material used, time of exposure to the cells, and size of the nanoparticles; where smaller particles (<20 nm) show higher toxicity.[119] Amorphous silicas in particular can be readily reabsorbed from aqueous media and together with their biocompatibility and easy chemical functionalization makes them ideal candidates for biomedical applications. Parameters such as size, shape, chemical composition, surface properties, and crystallinity determine the viability of using SiNPs, for example as drug delivery supports. Larger, micron-sized silica particles have been extensively used as inorganic supports (i.e., chromatography columns) for applications including isolation of polypeptides, proteins, nucleic acids, or DNA fragments.[121] In the last decades, the use of chromatography columns made with either nonporous or porous silica has also been investigated.[121,122] These materials can have pore diameters that vary from micropores (<2 nm) to mesopores (<50 nm) and macropores (>50 nm) that can be tuned by choice of method of synthesis. As examples, microporous (or nonporous) stationary phases have shown outstanding speed of separation of macromolecules due to excellent mass transfer characteristics.[121] Further, porous silica-based materials have attracted great interest for enzyme immobilization since biomolecules can be hosted within the pores of mesoporous supports, allowing expensive biological catalysts to be used repeatedly for as long as they remain active.[123,124] Mesoporous silica nanoparticles (MSNs) have also gained considerable interest as the surface area, pore size, and the shape of the MSNs can be tuned in such a way that a range of materials (e.g., dyes, drugs, and metal oxides) can selectively be encapsulated.[125−127] As MSNs possess high biological compatibility, from molecules through to cell, blood, and tissue,[127−131] they have emerged as ideal candidates for controlled drug delivery, biosensors, imaging, and cellular uptake processes.[127,132−136] Note that in this review, we mainly focus on amorphous (noncrystalline) silica and biomolecule interactions for their widespread application in biomaterials science; however, some examples of studies on quartz SiO$_2$-binding peptide interactions are also given as extensive research has been performed in this area.

2.2. Silica Structure and Synthesis Methods

To understand the nature of the material we use to investigate biomolecule-mineral interactions, we need to know something about the material itself. The method of synthesis, its crystallinity or amorphous state, its surface chemistry, and the behavior of the material in the reaction environment chosen for binding studies are all important. What follows is a brief introduction to these aspects together with illustrative examples, chosen, wherever possible, from within the field of biomolecule-mineral interaction studies.

We first consider the various polymorphic crystalline structures of silica: quartz, cristobalite, trydimite (Figure 2A), as well as alpha quartz, which is the only stable form under normal conditions. Among facets of alpha-quartz, the (0001) surface is the most stable (Figure 2D). Tridymite can occur in several crystalline forms, but the most common at standard pressure are α and β. The transformation from low to high temperature modifications between and within polymorphs[137] are as follows.

$$\alpha\text{-}\beta\text{-Quartz (573 °C)} \xrightleftharpoons{870\,°C} \alpha\text{-}\beta\text{-Tridymite (110-180 °C)} \xrightleftharpoons{1470\,°C} \alpha\text{-}\beta\text{-Cristobalite (218 ± 2 °C)}$$

Now we turn our attention to monodisperse silica particles (at the nano- and microscale) that have been widely synthesized using the sol−gel method, which consists of the hydrolysis of a silica precursor followed by condensation into oligomers and then formation of silica particles.[142,143] The addition of an acid (i.e., HCl) or a base (i.e., NH$_3$), due to the increase of either hydronium or hydroxide ions, can increase the rate of hydrolysis and condensation in the system. In 1968, Stöber and Fink reported an effective route for the synthesis of silica particles in basic conditions where the particle size, from 10 nm to 2 μm, was controlled by changing the concentrations of the reactants.[144] Early in the 1990s, Osseo-Asare and Arriagada developed a microemulsion method (also in basic conditions) for the synthesis of SiNPs by controlling the hydrolysis of the silica precursor in an inverse microemulsion system.[145] The growth of silica microparticles has also been investigated under acidic conditions using acetic acid,[146] tartaric acid,[147] or nitric acid.[148] Karmakar and co-workers developed a method to synthesize highly dense microspheres, with densities between 2.10 and 2.16 g cm^{-3},[146] being also named glasslike silica spheres.[149] In general, at low pH, structures with low porosity are obtained, and consequently, these are more dense particles, whereas for materials made under alkaline conditions, mesoporous spheres (from 2 to 50 nm) are typically achieved. More recently, SiNPs have been prepared through microwave-assisted acid catalysis using HCl.[150] SiNPs have also been commercially produced by chemical vapor condensation (CVC), a process which involves the decomposition of metal−organic precursors, or SiCl$_4$, under flame treatment at high temperature.[151] With dependence on the reaction conditions, the silica units can

interconnect to give chains eventually forming a gel or stay separated to form a sol or powder (Figure 2B). Generally, at acidic pH the particles are less negatively charged, there is a minimum repulsion, and they can aggregate into gel networks.[113] At basic pH, where silica carries a negative charge, there is repulsion among particles which results in the formation of discrete units (particles). Nonetheless, the presence of salts (and these do not exclusively have to be simple metal cation anion pairs such as NaCl or KCl) above 0.2−0.3 M can neutralize the negative charge of the silica particles allowing gelation to occur.[113]

Although we describe above routes to silica particles that appear straightforward, the difficulty in reproducing syntheses is often ignored by those working in the community. In part, this is due to a lack of knowledge about the fundamental chemical reactions occurring during synthesis and further ignorance concerning what nucleation and growth mean for an amorphous material. This understanding, although incomplete is much better advanced for crystalline materials such as gold[152] and is an area of investigation where there is certainly still room for improvement. In the context of this review, the precise synthesis/fabrication conditions materially affect the surface chemistry of the materials (particles or surfaces) which taken together affects their interaction with other materials including biomolecules.

2.3. Silica Surface Chemistry

The mineral, as for all other oxides discussed in this review, comprises both a bulk or internal structure and also, very importantly, a surface, the latter being exposed to the medium in which the material is found, and through which any interactions with biomolecules will occur. In order to understand interactions at the molecular scale, it is imperative that we understand the nature of the material we are working with, its surface chemistry, and the effect of the environment, including any time-dependent changes as this will affect the nature of any potential interactions.

2.3.1. Surface Speciation and Associated Properties.

We now consider the chemical nature of the material, both bulk and surface, under discussion. In bulk silica, silicon atoms are mostly bound to four bridging oxygen atoms forming $[SiO_4]$ tetrahedra. Synthesized silica particles are mainly composed of siloxanes (Si−O−Si), silanols (Si−OH), and ionic siloxide (Si−O$^-$) and/or the presence of water molecules adsorbed on the surface by hydrogen bonding, Figure 2C. The Si−O bond character and basicity of Si−O−Si bridging groups strongly depends on the local siloxane angle as shown by both experimental and computational studies.[153] At smaller Si−O−Si angles (near the tetrahedral angle), the Si−O bond units become more covalent and the siloxane linkages increase in basicity and can act as hydrogen bond acceptors.[153] Silanol groups can be found in different forms: isolated, geminal, vicinal, and internal (Figure 2C). In general, an increase of surface ionization with particle size is believed to be due to the presence of a higher population of isolated silanol groups (Si−OH), leading to a higher surface acidity.[154] The silanol density in fully hydroxylated silica (at 500 K) has been reported to be from 4.5 to 5.8 OH nm^{-2}.[140,155,156] Knowing the silanol density is important both to directly study biomolecule−surface interactions but also in the modification of surfaces by chemical functionalization. However, these values (given for the bulk material) include all of the different silanol groups (isolated, geminal, vicinal, and internal) that can be present on

a silica particle or fabricated surface (for instance in commercial sensors). The size of particles affects the proportion of internal versus external silanol groups; for larger particles, a higher fraction of internal silanol groups has been reported compared with smaller particles.[155] The level but not the chemical identity of silanol groups on amorphous silica particles can be determined by thermal methods.[140] With dependence on the extent of these species on the silica surface, a more hydrophilic (silanol) or hydrophobic (siloxane) character of the particles can be achieved, which on interaction with biomolecules may at the extreme scale of interaction cause protein folding/unfolding[157−159] or membrane rupture.[160]

In general, silica is usually hydrophilic; however, the hydrophobic sites (siloxanes) present on the silica surface may provide sites for possible hydrophobic interactions with certain biomolecules. For example, DNA is negatively charged (at pH values above its isoelectric point near pH 3), and it is suggested that this molecule interacts with silica via DNA phosphate and surface silanol groups, though hydrophobic bonding between DNA bases and silica hydrophobic regions has been recently documented as a principal mechanism for binding DNA to silica.[161] Surface water as well as affecting the surface chemistry of silica also plays a key role in biomolecule adsorption as will be discussed later in this review.[162] As might be anticipated, the different kinds of silanols (vicinal, geminal, or interacting) and OH densities depend on the polymorph, the crystallographic plane, and the treatment that the material has received.[162] It is important to note that any fractured crystalline surface will be hydrophilic as reaction of newly created surfaces with water in the environment leads to the creation of silanol groups. Details on the material-dependent networks of silanol groupings and the different surface hydrogen bonded networks that form are provided by Rimola et al.[162] Although we note that quartz is reported as being stable, in the context of this article, we have to remember that in this instance, stable refers to a constancy of structure in an aqueous medium, in the presence of ions and organic molecules.

A further indicator of likely activity of different silica phases is surface energy, which can be calculated from experimental measures of surface area and enthalpy of solution. For amorphous silica of zero water content (i.e., the energy of the pure siloxane surface, assuming that all silanol groups had been condensed) at 23 °C was found to be 259 ± 3 mJ/m^2,[163] whereas the surface energy for a completely hydrated surface (or the energy of pure silanol surface) at the same temperature (23 °C) was calculated to be 129 ± 8 mJ/m^2.[163] The surface energies for quartz ranged from 510 to 2300 mJ/m^2, showing a great diversity in behavior[163] which will be manifest in considerations of how biomolecules will interact with the various materials. It should be noted that cristobalite and tridymite have been very little studied.

Hydrophilic and hydrophobic properties of a crystalline silica surface can be modified, for example, by simply heating the crystalline silica. For example, thermal treatment of cristobalite (up to 1300 °C) has shown the loss of cytotoxicity due to removal of surface radicals and conversion of silanols to siloxane bridges.[162,164] Alternatively, grinding crystalline silicas (i.e., cristobalite and quartz) may produce surface radicals, which would increase surface hydrophilicity; however, this can be suppressed by grinding in the presence of water.[165]

An important factor affecting interaction of silica with biomolecules is the charge that it carries by virtue of the presence of siloxide groups on the surface of the material. A typical approach to measure this is to make zeta-potential measurements. This method can be used for both free-flowing particles and surfaces, suspended in a liquid medium. The extent of charge depends on the nature of the silica particles or the synthesis methodology followed.[126,166,167] For example, SiNPs synthesized by the Stöber method, with size from 28 to 500 nm, have shown an increase in negative surface charge as the particle size increased, being from −27 to −43 mV (ξ pH 7.4), respectively.[168] In brief, the measurement of zeta potential depends on temperature, pH, conductivity (ionic strength), and solvent (viscosity).[169] As recently documented by Smith and co-workers,[170] any small change in these parameters can have a significant effect on the zeta potential values; hence, for comparing and studying biomolecule–surface interactions, it is imperative to use the same solution conditions as the ones used at the time of zeta potential measurement of the mineral alone. Unless such information is given in a publication, zeta potential values are not meaningful and make comparison between data sets impossible.[170] Further, it has been proven that the wettability of silica can be modified by simply varying the electrolyte concentration.[171] Knowing this, one should fully characterize the surface being explored under the precise conditions chosen for any binding studies in order to understand how biomolecules might interact with the mineral phase. It is also important that the experimentalist (and theorist) understands the effect of ions present in the reaction medium on the behavior of the mineral being studied; we will return to this matter many more times throughout this article. Although in this section of the review we are talking specifically about silica, the principles of the approach apply equally to all other materials.

Silica and its interface with water is a material that has been extensively studied by computational approaches. Butenuth et al., in 2012, and Emami et al., in 2014, provide comparisons of a number of force fields for silica developed from the mid 1980s onward, and a review of Mishra et al., in 2017, compares force fields for cementitious materials including those related to silica.[172−174] What is important here is that the approaches used to validate the various force fields are given, although they do vary from one force field to another. Early force fields often assumed overly ionic Si−O bonds, and surface models containing functional groups such as silanol (SiOH) and siloxide (SiO⁻) were not feasible.[173] Subsequent models introduced covalent bonds and more broadly applicable energy expressions, as described in the contributions including those of Butenuth et al., in 2012, and Emami et al., in 2014.[172,173] However, issues with poor representation of stoichiometry, including correct valencies, maintenance of structure throughout a simulation, and the matching of computed surface properties to experimentally derived values, occur. Issues to do with unrealistic atom charges, bond rigidity, defining surface chemical features, and the choice of water model to use (in terms of complexity of terms used to account for bonding and structure) are all common. As understanding of the material and computational approaches further develop, these problems will cease to be issues, but at present a cautious approach to the reading of the literature is suggested, particularly for experimentalists who are generally not aware of the problems and limitations of the theoretical approaches.

2.3.2. Issue of Surface Contamination.

Although siloxanes, silanol, or hydrogen groups and water molecules are the main constituents of a silica surface, traces of ubiquitous carbon contamination, the so-called "adventitious carbon", detectable by X-ray photoelectron spectroscopy (XPS), are present even on the cleanest and purest of samples.[175] It is extremely difficult to ensure removal of this, but ozone has been used to remove adventitious carbon and other ions from a thin (nm thick) layer of silica atop an oxidized silicon wafer.[175] Interestingly, this study had a practical outcome in that removal of unwanted ions from the surface enhanced oil recovery from sandstone reservoirs via interactions between the cleaned surface and the oil present. Further, traces of other elements (i.e., precursors on the surface) could interfere with the measurement of biomolecular interfacial interactions. As an example, Puddu and Perry (2012)[176] using XPS detected traces of nitrogen on silica surfaces which probably arose from the ammonia used in the synthesis process (Stöber method). This level of information on the material being used for biomolecular interaction studies is not always provided, and one can end up making wrong estimates of surface loadings leading to unreasonable models of surface/biomolecule interactions.

An example of experimental techniques used to study (bio)molecular surface interactions, where the issue of surface reproducibility/contamination might be particularly important, is in the use of quartz crystal microbalance (QCM) and surface plasmon resonance (SPR) approaches where commercial sensors are routinely used as delivered. Binding experiments will totally hinge on the surface chemistry of the sensor available/purchased, but manufacturer's details on the characterization of the surfaces vary from vague to nonexistent. How often is it that a researcher is asked to simply try a different sensor when results do not seem to be lining up? Is it that the variation between sensors of the surfaces has more of an effect on binding than the generally expected binding characteristics of the molecule and the material under study? Is this due to differences in molecular level chemistry (i.e., chemical functionality), or is it due to differences in physical structure, perhaps roughness that leads to observable differences in wettability/hydrophilicity, etc? Another important question to consider is, does my material change with time? And if so how? In order to answer these important questions, it is necessary to characterize one's substrate but this will pay dividends in being sure that the experimentally measured data can both be used to propose molecular level mechanisms of interaction and to provide sensible starting points for high level computer simulations. A vast array of surface characterization techniques are available for the scientific community. Later in this article, we compare some of the many characterization techniques that can do just this. The information is summarized in Table 1. Note, this table of methods applies to all materials listed in this review.

2.4. Modifying the Functionality of Silicas

The abundant number of hydroxyl groups on the silica surface allows them to be used for further functionalization, including moieties such as carboxyl,[177] amine,[178,180] methyl,[179,180] phenyl,[181] or thiol[128] groups leading to functionalized silicas. Experimental techniques that allow the observation/characterization of silica surface properties have been summarized recently by Rimola et al.[162] These functional groups can be used to change the particles affinity for specific surfaces or
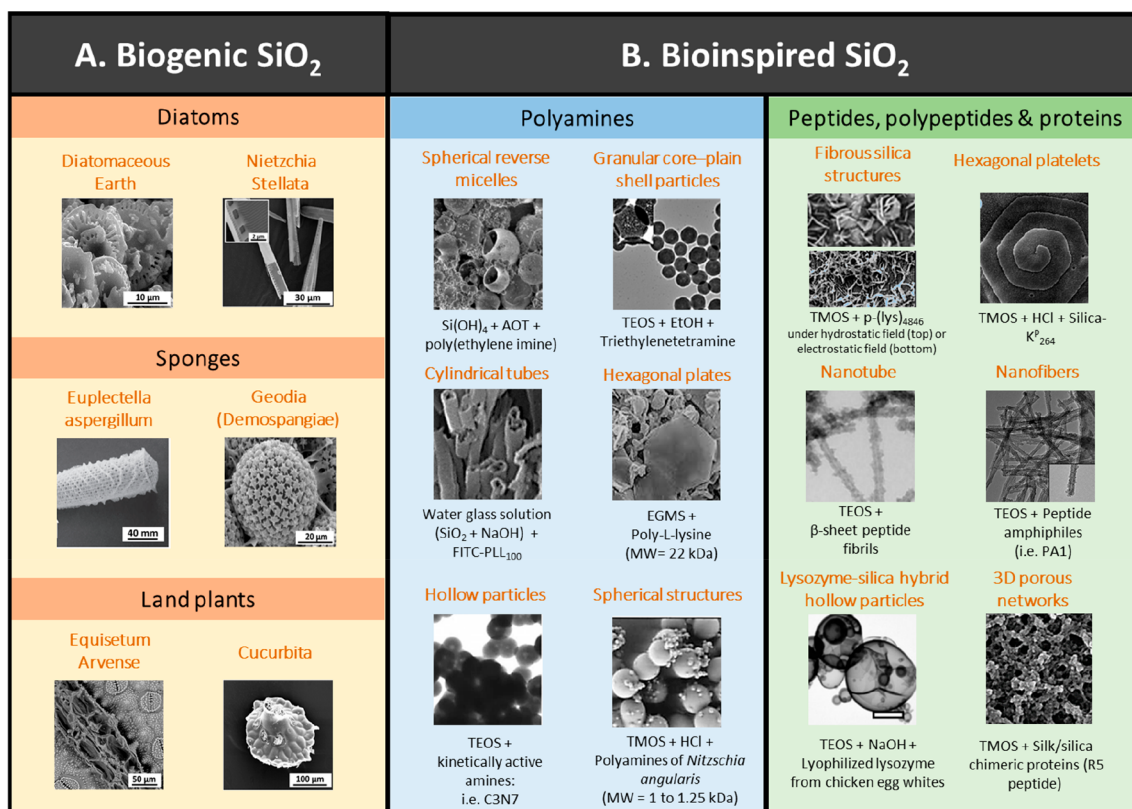
Figure 3. (A) Mineralized living organisms containing biogenic silica skeleton: diatoms, sponges, and land plants reprinted with permission from ref 211. Copyright 2006 Materials Research Society. Reprinted with permission from ref 212. Copyright 2016 MDPI. (B) Synthesized silica structures using a biomimetic approach: All SEM images reprinted with permission from ref 213. Copyright 2011 Elsevier. Granular core−plain shell particles reprinted with permission from ref 212. Copyright 2016 MDPI. Cylindrical tubes reprinted with permission from ref 72. Copyright 2007 Elsevier. Hexagonal plates reprinted with permission from ref 118. Copyright 2005 Royal Society of Chemistry. Hollow particles reprinted with permission from ref 206. Copyright 2008 PNAS. Spherical structures reprinted with permission from ref 203. Copyright 2000 PNAS. Fibrous silica structures reprinted from ref 214. Copyright 2005 American Chemical Society. Hexagonal platelets reprinted from ref 215. Copyright 2006 American Chemical Society. Nanotubes reprinted with permission from ref 216. Copyright 2004 Wiley-VCH. Nanofibers reprinted from ref 217. Copyright 2007 American Chemical Society. Lysozyme-silica hybrid hollow particles reprinted from ref 70. Copyright 2007 American Chemical Society. Three-dimensional Porous networks reprinted from ref 218. Copyright 2010 American Chemical Society.

(bio)molecules by, for example, covalent bonding, electrostatic interaction, and/or hydrogen bonding.[168,180] Metals such as Cr, Mo, and Pd can also be easily attached to a silica support through silanol groups (Si−O−M) with the materials routinely being used as catalysts.[182−184] For the fabrication of surface-modified silica particles, two methods have been generally applied: (i) post modification (or grafting) and (ii) in situ modification (or co-condensation), with the latter route mainly used for aminopropylsilanes since their bifunctional nature quickly induces hydrolysis and condensation of tetraethyl orthosilicate (TEOS) in solution due to the presence of the aminopropyl and alkoxysilane groups. A factor that is not often considered is the extent of coverage possible and/or attained with the assumption often being that addition of excess of a surface functionalizing agent will lead to complete coverage. This is not the case as recent results by Sola-Rabada et al.[180] have shown. The researchers used two different sizes of silica particle (28 and 210 nm diameter) and different concentrations of two functionalizing agents [methyltriethoxysilane and aminopropyltriethoxysilane (both at 10 mM and 500 mM)]. They were able to show that for the smallest particles, a higher level of 3-aminopropyl functionality was possible, while a higher degree of methyl group functionality was found on the

larger particles. In both cases, coverage, as measured by XPS, was far from a monolayer.

Considerable interest in amine-functionalized silica surfaces has developed as their nucleophilic nature make them good candidates for solid base catalysts or to act as linkers between silica and biomolecules (i.e., DNA, enzymes, polypeptides) and/or metals. Although we discuss the applications of silica/biomolecule interactions in the section below, the huge effect that functionalization has on the potential for moderating interaction/new applications is considered separately here. As examples of applications, amino-functionalized silica surfaces have been used to immobilize catalytically active transition metals in applications such as wastewater treatment[185] and in gene delivery,[128,186−188] among others. In more detail, Bharali et al. demonstrated by in vivo studies that the presence of positively charged amino groups on the silica surface (ORMOSIL NPs) improved binding with plasmid DNA (negatively charged), thereby, facilitating its delivery inside neuronal-like cells without damaging brain tissue.[186] For drug-release applications, functionalization of mesoporous silica nanoparticles (MSNs) with amine groups generates good carriers for controlled release.[187,188] Through particle function-alization with alkyl groups protruding from the surface, the hydrophobic character of a particle's surface can be

increased.[179] Biosilica such as that extractable from Mexican giant horsetail can also provide an effective support for enzyme immobilization.[115]

Methyl-functionalized silica surfaces are attractive for industrial applications due to their abrasion resistance[189] and antisticking or self-cleaning properties.[190] The hydrophobic/hydrophilic character of silica materials is also of high importance for application in wastewater treatment.[185] The functionalization of tissue culture polystyrene (TCP) with silica has also been studied for biomedical applications. For example, generating a silica surface upon TCP and applying it as a platform for subsequent functionalization using a fluorinated alkoxysilane has been shown to produce a material with a differential adsorption profile of serum factors derived from cell culture media, producing better control of cancer cell (i.e., human mammary epithelial) aggregation-disaggregation events in vitro,[191] a reaction platform that has enormous potential as a replacement to 3d-culture methods and the use of animal models to study cancer metastasis. Similarly, studies using an amino-propyl functionalized silica material showed that an appropriate surface chemistry (i.e., hydrophilic or superhydrophobic silica film) could facilitate the loss of a mesenchymal cell subpopulation from a mixed mesenchymal/epithelial cancer cell population which could be used to isolate specific cancer cell types for further experimentation to improve understanding of the disease and study possible cures without the need for animal studies.[192] In the area of in vivo assays, SiNPs have also been functionalized with dye molecules to generate, for example, fluorescent silica NPs in order to study biological processes and conduct cell imaging assays.[193−195] A study carried out by Ha et al. showed that fluorescent SiNPs can increase thermal, photochemical, and pH stabilities as well as its biocompatibility for in vivo assays.[196] Other types of doped-silica particles include magnetic SiNPs that can be employed for drug/gene delivery systems,[197−199] biolabeled for magnetic resonance imaging (MRI),[198−200] and bioseparation.[201]

In almost all cases described, little attention is paid to understanding the extent of functionalization and its influence on the properties of the materials generated. Moving forward, provision of such information would greatly benefit the whole community and could lead to additional high value applications for silica.

2.5. SiO₂-Biomolecule Interactions and Applications

This section deals with silica formed in nature, silica formed in the presence of biomolecules, studies of silica biomolecule interactions and applications that make use of silica-biomolecule interactions.

2.5.1. Silica Formed in Nature. The supreme example of silica-biomolecule interactions leading to functional objects, silicification, occurs in unicellular organisms, including diatoms, radiolaria, and synurophytes as well as multicellular sponges and higher plants.[112,114,115,202,211] For many of these organisms, the silica structures serve as the organism's skeleton which accounts for the majority of their body mass.[202] Diatoms, for example, exhibit intricate cell wall patterns in the nano- to micrometer range composed of hydrated, amorphous silica mass[202] (Figure 3A). Evidence for genetic influence over the production of diatom silica cell walls (termed *frustules*) came from observations that the patterning of these structures is species-specific and is precisely replicated in diatom progeny.[202] Since this discovery, biosilica producers

have become extensively studied in order to understand biosilicification processes since this could provide the principles of controlled nanostructure fabrication under conditions that are much milder than those used in traditional material-processing techniques. Important insights into diatom biosilicification have been made by isolating and characterizing specific biomolecules entrapped within the amorphous silica of the frustule [i.e., long-chain polyamines (LCPAs)[203] and cationic polypeptides termed silaffins].[204] Both silica-associated biomolecules have been demonstrated to accelerate silica formation from a silicic acid solution in vitro, though the path by which they do this is not understood.[203,204] Silaffins contain a large number of phosphorylated serine residues and post-translationally modified lysines, which carry oligo-propylene-amine-functionalized side chains.[205] Sumper and Kröger in 2004 proposed a mechanism by which cationic molecules and hydrogen-bonding polymers (hydroxyl amino acids: serine and tyrosine) can interact with anionic silica and neutral silanol groups, respectively, thereby inducing silica condensation.[202] Later studies showed that the silica precipitation process is affected by either the polyamine structure and/or amino acid composition.[206−209] Highly acidic phosphopeptides, termed silacidins, have also been identified from the diatom shell of *Thalassoria pseudonana*, and their role in silica precipitation demonstrated in in vitro studies, though again,[209] little is really known about when and where the molecules associated with the mineral act. Additional insight into the mineralization process has been gained from another silicifying organism, the sponge *Tethya aurantia*, where proteins termed silicateins, present in silicified spicules have been shown to catalyze silica formation from tetraethoxysilane in vitro,[210] though clearly this is not the reaction environment found in nature. Inspired by nature, studies on the effect of biomolecules such as amino acids, polypeptides, oligo-peptides, and polyamines on mineral formation have arisen in materials science and have also served for the fabrication of silica materials with intricate structures (Figure 3B).

2.5.2. Mimetic Studies to Understand Biosilicification. The biomolecules isolated from silicifying organisms are very large and complicated, and scientists have identified smaller components of these molecules that might be used in model studies to generate further understanding of both the role of these biomolecules in regulating silica formation and in their direct pattern of interaction with the surface of the mineral phase.

Extensive studies have been performed on a 19-mer peptide identified as part of silaffin Sil-1A₁, termed R5 (SSKKSGSYS-GSKGSKRRIL) in part due to its ability to precipitate silica in the laboratory at neutral pH;[204] and remarkably, the RRIL motif was shown to be essential for silica precipitation in vitro.[71] These early studies, although not stated as such, actually study the effect of R5 on the coagulation process as the amount of silica harvestable after a certain reaction time was used as a proxy for catalysis of the process. There have been considerable advances in the sophistication of both experimental and computational studies of R5- silica interaction studies as well as its use in developing new composite materials. As examples, recent studies coupling specific ¹³C and ¹⁵N labeling of individual amino acids with NMR analysis have suggested the involvement of the lysine at the N terminus in silica binding, and a vibrational spectroscopy approach coupled with molecular dynamics simulations suggests that all of the peptide interacts with the forming silica phase.[219,220] Clearly
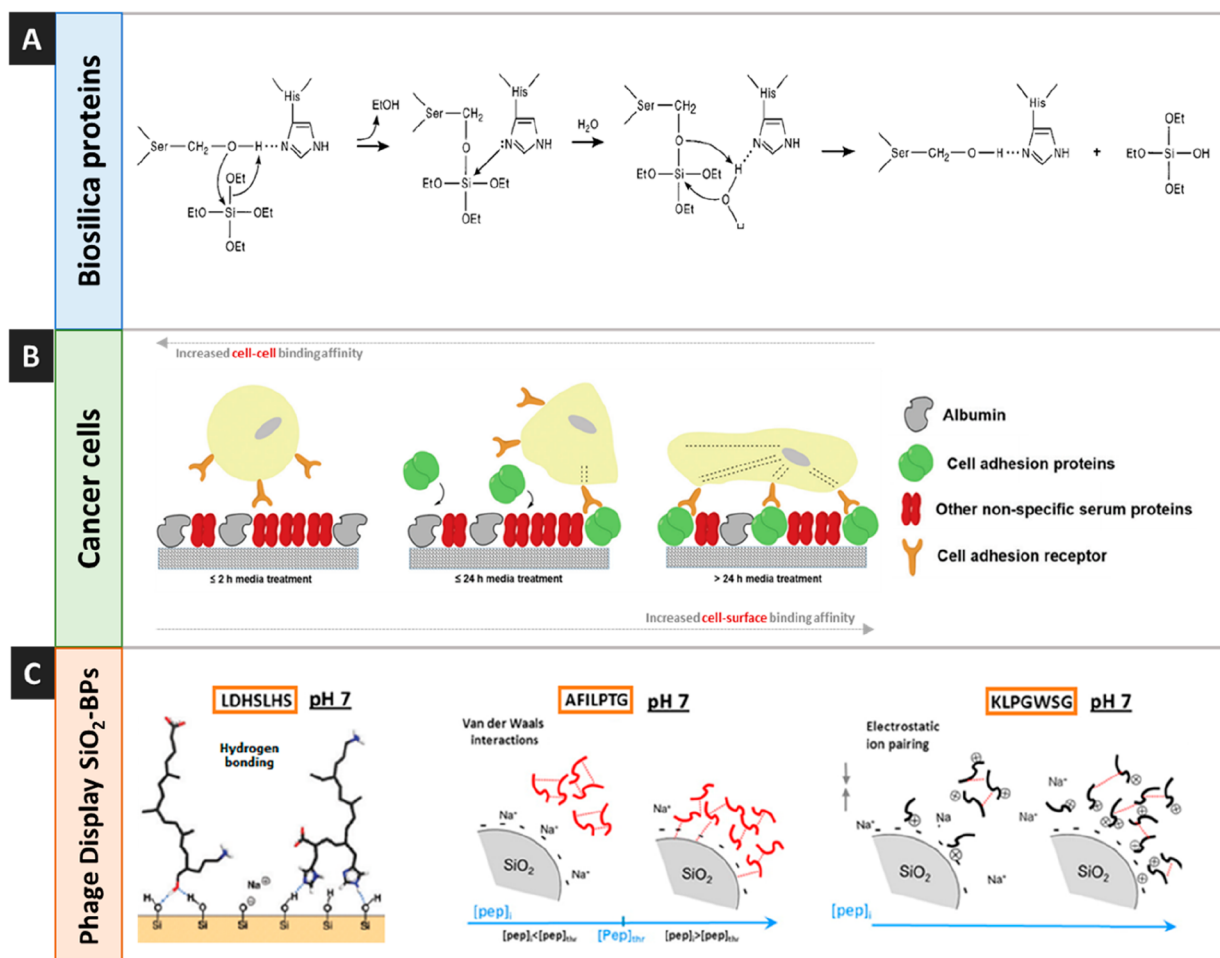
Figure 4. (A) Mechanism proposed for alkoxysilane catalytic hydrolysis by silicatein active sites (serine and histidine) reprinted with permission from ref 235. Copyright 1999 Wiley-VCH. (B) Competitive protein exchange occurring upon the fluoro-silica during cell culture in serum supplemented medium reprinted with permission from ref 191. Copyright 2014 Royal Society of Chemistry. (C) Type of interactions occurring at the silica−peptide interface of phage displayed peptides reprinted from refs 154 and 176. Copyright 2012 American Chemical Society.

the analytical approach used leads to models of peptide-mineral interaction that currently appear incompatible.

Researchers have explored the role of post-translational modification including the role of serine phosphorylation, as well as trimethylation and alkylamine addition to lysine for synthetic constructs of the R5 peptide,[221] though rationale for the choice of position for the point mutations was not given and will most likely have affected the behavior of the molecule in its ability to precipitate/interact with silica. The experimentalists' choice of position for serine phosphorylation has further influenced molecular dynamics studies of silica silaffin interactions as will be described in section 2.6.2 below. The series of modified silaffins were further modified by incorporation of a cysteine residue at the N-terminus to allow further fundamental study by techniques such as SPR as well as application in the nanotechnology field. The additional of the cysteine residue at the N-terminus would allow ready interaction of the peptide with a range of surface materials, including gold though it should be realized that it too could play a role in determining the conformation of the peptide and its surface recognition.[221]

The R5 peptide has shown potential for use in regenerative medicine in the form of chimeric silk silica composites.[218,222−228] By varying the presence and location of the R5 peptide cross-linked to the silk protein, it was shown that

the free N-terminus of the R5 domain induced controlled deposition of silica particles as well as causing cellular differentiation via activation of specific integrins leading to expression of the transcription factor Runx2, which is responsible for osteoblast differention genes.[227] Here, a combination of materials chemistry approaches and molecular biology studies guided by molecular modeling were able to propose a molecular mechanism to explain the observed behavior.

In studies of smaller fragments of the R5 peptide, researchers have shown that variations in the isolated KXXK domains could influence the amount of precipitatable silica (used as a proxy for interaction) but also significantly change the morphology of the silica precipitated.[208] Specifically, silica formation in the presence of the KASK peptide motif lead to the formation of silica spheres of hundreds of nanometres together with what was described in the publication as "grainy" silica structures.[208] In reality, what this means is that the surface of the "grainy" silica appeared rough to the eye when viewed in the electron microscope. In contrast, synthesis in the presence of the KAAK peptide led to silica spheres (∼100 nm) being mainly formed.

If we now consider a further decrease in complexity of the biomolecule structure, here a single amino acid, lysine, or polymers of the same, polylysine (PLL), we find evidence that

even the amino acid alone can catalyze silica formation and growth at near-neutral pH, and remarkably, silica morphology modification, from spheres to hexagonal plates, occurred by increasing the degree of polymerization (DP) of PLL.[229,230] According to Coradin and Livage, the presence of amino acids such as serine, lysine, proline, and aspartic acid or polypeptides of these amino acids favors silicic acid condensation via hydrogen bonding and electrostatic interactions, with polypeptides showing a stronger catalytic effect.[231] In general, positively charged peptides are strongly attracted to anionic silica surfaces, and further, polar groups in peptides can attach to silanol or siloxide groups by hydrogen bonding, ion-dipole, dipole-dipole and van-der-Waals interactions.[154] Interaction of silica with peptides not having cationic groups is driven by nonelectrostatic interactions and, commonly, requires a higher threshold concentration for adsorption. Adsorption studies have shown that the binding event is also governed by the bulk pH of the solution.[154,176,232] For example, a study carried by Meng and co-workers demonstrated that glycine can be adsorbed onto silica surfaces at a wide pH range (from 2 to 10) not only due to simple surface charge compensation but local interactions.[232] The authors pointed out that although electrostatic interactions were more likely to happen between pH 4 and 9, these interactions would be practically nonexistent at pH 2 due to the glycinium cation being in contact with an almost neutral silica surface. Further, adsorption of glycine reached its maximum at pH 6 where hydrogen bonding was suggested due to shifts in $-NH_3^+$ vibration bands as observed by vibrational spectroscopy.[232] Perry and co-workers showed that small changes on the silica surface (i.e., low degree of functional groups) can significantly modulate binding interactions at the silica−peptide interface.[97,154,168,176] Further, the level of functionalization can induce a change in the adsorption mechanisms involved.[180] Although the adsorption process highly depends on the nature/chemistry of the solid surface, other factors such as binding/kinetic energies and/or orientation/conformation of the peptide also play an important role in peptide adsorption.[180,214,233,234] It should be realized, however, that in many of the published studies, full information on extent of binding, surface characteristics, and conformational attributes of both phases are usually not reported on or are unknown.

2.5.3. Interaction of Biomolecules with Silica. The growing applications of silica with chemically attached peptides or biomolecules in nanomedicine has driven researchers to focus on increasing their understanding of how peptides or biomolecules bind to silica, the type of interactions, and the mechanisms involved. In Figure 4 are shown a range of proposed interaction mechanisms involved at the silica−biomolecule interface. Note that, example A shows interactions of a biomolecule during mineralization, and hence, how this biomolecule can be used to grow silica from solution, whereas, examples B and C show how the silica surface is recognized by biomolecules. For example, Zhou et al. proposed a mechanism by which silicatein-α (70% of the silicatein filament obtained from sponges) catalyzes the hydrolysis of alkoxysilanes at neutral pH via an acid/base reaction through the activity of the serine and histidine side chains, specifically, between the hydroxyl group of serine-26 and the imidazole side group of histidine-165 (Figure 4A).[235] Due to the high structural homology of silicatein-α to the hydrolytic enzyme, cathepsin L; this reaction was based on the mechanism of peptide bond hydrolysis by the analogous well-known protease cathepsin-

L.[235] It should be noted that at the time of writing this article, there was still no crystal structure available of a native silicatein, so the precise nature of the active site is still hypothesized rather than a direct reality. Nicklin and co-workers studied the absorption of serum proteins to specific fluorinated silica surfaces.[191] They demonstrated that fluorinated silica surfaces (FS) provide the necessary environment to selectively adsorb serum proteins from the medium, which, were further able to disrupt cellular adhesion and promote cellular aggregation (Figure 4B). Moreover, the capacity of the FS surface to support cellular adherence was seen to increase with culture time. The properties of the functionalized surface facilitate the study of cancer cell (mammary cell line) aggregation and disaggregation as a single dynamic process in vitro, as the cells biological response toward the material changes in tandem with the surface properties.

In a different approach to identifying biomolecules that might interact with/moderate the behavior of silicas, phage display has identified a number of peptides that bind to silica. It should be noted that a majority of studies provide very little information on the material being studied either in the patent literature or the scientific literature. Thus, it is often very difficult to know the precise nature of the material panned against. In a study where the properties of the silica substrate were very well-characterized and reported (aqueous synthesis route, size, surface area, porosity, surface OH concentration, surface charge), the effect of peptides of different charge at neutral pH (in phosphate buffered saline) have been studied at the aqueous silica interface (Figure 4C).[154,176] These peptides, KLPGWSG (positively charged), AFILPTG (neutral), and LDHSLHS (negatively charged), showcase electrostatic/hydrophobic interactions and hydrogen bonding at the aqueous silica interface. The researchers were able to follow the binding in detail and demonstrated that there is a competition between peptide-peptide interactions and peptide-surface interactions, particularly at low concentrations of peptide, where peptide self-assembly is more favored than silica-peptide interaction.[154,176] Further investigations with these peptides and fully characterized silica particles have shown a switch in peptide adsorption behavior depending on the level of amine group functionalization.[180]

In contrast, other studies, for example the excellent NMR study of a Ti-binding peptide and mutants on silica (and titania), do not provide much information on the substrate used.[236] In this particular study, fumed silica was used as target material, but apart from particle size and surface area, no information on the surface properties of the material was provided. It is likely that the unexpected binding of the peptide to silica involving a number of hydrophobic amino acids came about due to the inherent hydrophobic character of the silica particles.

To date, many studies concerning silica-biomolecule adsorption mechanisms have been reported and are summarized in reviews such as Slocik and Naik (peptide binding mechanisms on nanoparticle surfaces),[65] Tamerler and Sarikaya (molecular biomimetics using genetically engineered peptides),[237] Dickerson et al. (protein- and peptide-directed inorganic material synthesis),[56] Lambert et al. (amino acid adsorption on mineral surfaces),[238] Rimola et al. (computational modeling of silica-biomolecule interactions),[162] Heinz and Ramezani (simulation studies and recognition mechanisms of biomolecules),[239] and Costa et al. (fundamental theoretical
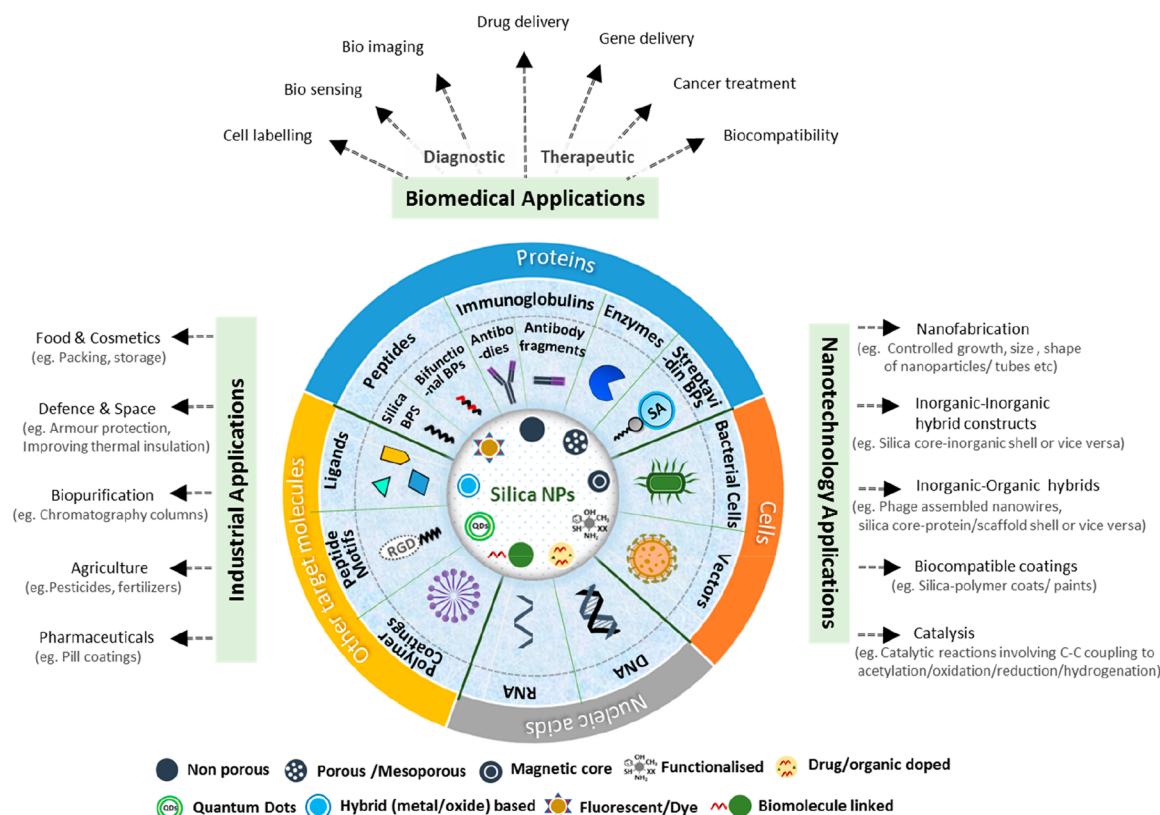
Figure 5. Schematic representation of Silica-biomolecule/cell interactions and their applications.

and experimental approaches to understand biomolecule-biomaterial interactions).[240]

2.5.4. Applications of Silica-Biomolecule Interactions. To date, a wide range of SiNPs has been generated and their physical, chemical, and functional properties tuned either by directing silica nanoparticle formation directly or by modifying them with inorganic or organic molecules. The molecules reported to bind with silica NPs include proteins (silica BPs, antibodies or antibody fragments, enzymes, and streptavidin or avidin BPs),[176,241−245] nucleic acids (DNA or RNA),[246,247] other targeting molecules (ligands and peptide motifs),[248,249] as well as cells (bacterial or viral).[250−252] Continued research efforts by scientists have led to silica being a key material in the design of novel bionanostructures, further broadening its application from nanotechnology to biomedical and further industrial fields as shown schematically in Figure 5. A review of applications and latest patents of solid material BPs have been recently reported by Thota and Perry.[241]

To illustrate the wide diversity of applications, four examples are highlighted below and images associated with materials and their particular application shown in Figure 6. These examples were chosen to show the potential of silica to be used as (i) a drug delivery system (Figure 6A), (ii) biotemplate (Figure 6B), and (iii) solid support for biomolecule immobilization (Figure 6, panels C and D). The use of silica in combination with R5-silk protein constructs for bone and dental repair has already been mentioned above in section 2.5.2.

Tang et al., Figure 6A, reported the therapeutic use of mesoporous SiNPs as a potential drug delivering agent involving a variety of pharmaceutical drugs (ibuprofen, doxorubicin, and docetaxel), therapeutic genes (plasmid DNA, antisense oligonucleotides, and siRNA), and therapeutic

protein cytochrome C.[253] Altintoprak et al., Figure 6B, reported a controlled silica biomineralization process involving selective exposure of lysine amino groups on genetically engineered tobacco mosaic virus templates, chemically conjugating the synthetic peptides and the subsequent final coating with silica.[252] Jin and co-workers (Figure 6C) synthesized a DNA-silica complex able to (i) condense DNA through the positively charged quaternary ammonium group of N-trimethoxysilylpropyl-N,N,N-trimethylammonium chloride (TMAPS) and (ii) stabilize silica mineralization by co-condensing with the silica source, in this case TEOS. Further, the formation of various DNA liquid crystals was achieved by varying DNA concentration and the TMAPS/DNA molar ratio, which allowed control of the DNA interaxial separation.[247] Luckarift et al., in Figure 6D, reported a method for preparation of a solid support for immobilization of the enzyme butyrylcholinesterase. For this, a prepacked column with agarose beads was charged with cobalt(II) ions for the attachment of the His-tag R5 peptide. Afterward, TMOS solution together with the enzyme were added to the system and silica nanospheres precipitated onto the peptide bound to the column, subsequently, immobilizing the enzyme. These silica-immobilized enzyme reactor columns were used as a model liquid chromatography system to effectively screen cholinesterase inhibitors.[254]

Although there has been a steady rise in applications of silica equipped with different biomolecules, the understanding of how these biomolecules interact with silica NPs in vitro, in vivo, and in silico is still unclear. Further, the silica used is mainly amorphous, and there are not many techniques that provide atomic resolution or accurate structural information on such systems, especially when interacting with biomolecules.[162]
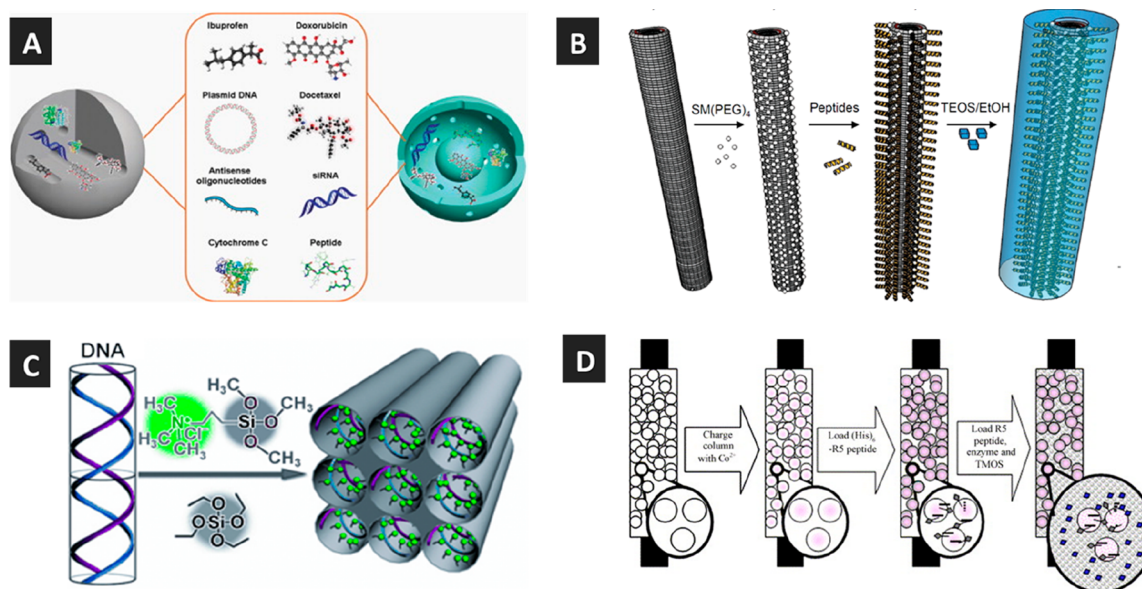
Figure 6. Examples of specific applications of silica-biomolecule attachment: (A) mesoporous SiNPs acting as delivery vehicles carrying potential drugs, peptides and proteins reprinted with permission from ref 253. Copyright 2012 Wiley-VCH. (B) controlled silica biomineralisation process using peptide equipped TMV (tobacco mosaic virus) as templates reprinted with permission from ref 252. Copyright 2015 Beilstein-Institut. (C) Silica mineralization induced by DNA liquid crystals reprinted with permission from ref 247. Copyright 2009 Wiley-VCH. (D) Enzyme immobilization in silica nanospheres via attaching to cobalt-coated resin by affinity binding where agarose beads (empty oval), Co^{2+} coated agarose beads (white oval with red dots), his-tagged peptide (blue kite with string shape), enzyme (blue kite shape), and silica nanospheres (gray sphere array). Reprinted with permission from ref 254. Copyright 2006 Elsevier.

2.6. Techniques Directly Probing SiO$_2$-Biomolecules Interactions

A SiO$_2$-biomolecule interactions have been investigated by a wide range of experimental and theoretical techniques. In this section, some of the most recent (and innovative) studies are discussed together with the techniques that have contributed to our understanding of these interactions; however, as silica is one of the most studied metal oxides worldwide, readers should be aware that many other excellent studies in this field showing the potential of a specific technique or in combination with others have been reported. For example, a summary of significant experimental studies involving interactions between small biomolecules and silica with the corresponding techniques used can be found in Rimola et al in 2013.[162] Again we remind our readers of the importance of understanding the behavior of their material under the same conditions used for binding studies.

2.6.1. Experimental Techniques for the Study of Silica-Biomolecule Interactions.
To study interactions of peptide-peptide/protein-peptide, phage-inorganic materials, the combinatorial phage display technique has been widely used to identify silica-binding peptides, epitopes, and small antibodies from large pools of binders.[56,61,64,154,176,255,256] Further, several groups have applied these phage displayed peptides as molecular linkers to link nanoparticle and biomolecules (i.e., peptides, proteins, enzymes, antigens, antibodies, etc.)[257−261] as well as to direct the synthesis and construction of complex nanoshaped materials.[108,261−266]

Despite the fact that the popularity for using combinatorial display techniques for recognizing unique peptides having high affinity for target materials including silica have grown rapidly, the precision of molecular recognition for inorganic materials is still challenging due to their binding to nonspecific targets or limited understanding of the properties and changes occurring during silica-peptide interfacial studies. This gap in knowledge has forced the scientific community to look for better analytical techniques to understand silica interactions with biomolecules in both solution and the solid state. As an example of the approach, Sarikaya and co-workers reported a peptide-enabled coassembly strategy for developing hierarchical multimaterial nanosurfaces such as quantum dot arrays (QD) and further monitored their specific binding mechanism/affinities using SPR, QCM, and AFM.[265,267−271] Further, in a simultaneous assembly of material BPs to a gold-silica substrate, a quartz silica binding QBP1 (PPPWLPYMPPWS) and a gold binding AuBP2 (WALRRSIRRQSY) peptide showed high affinity to their specific material surfaces as measured by SPR (i.e., SBPs-silica and AuBPs-gold).[272] Moreover QCM was used to measure the thickness of the very thin silica film coating ($\sim$5 nm) onto the Au substrate, and AFM showed specific morphologies of the final material depending on the peptides used. This study further showed that the combination of both materials permitted the design of biologically viable probe specific materials and provided a detailed description of the materials formed.[272]

Other groups have reported the ability of the SPR technique to detect silica or silver-coated plasmonic nanostructures tagged with immunoglobulin G (IgG), which further helped in recognizing early cancer stages and associated biomolecules even at low analyte concentrations.[273] It should be noted that thermodynamic studies of peptide adsorption on silica is little explored compared to studies on gold[274] or silver surfaces using SPR.[273] Part of the problem is in the generation of sensors whose surface chemistry remains stable for long enough during measurement. QCM is another technique that has been used to investigate binding kinetics, including energy dissipation and affinity interactions present between silica (sensor chip) and biomolecules passing over the sensor. The biomolecules reported on so far include amino acids,[275] small

penta or hexa peptides,[255,276,277] longer peptides,[278] human IgG, and hexameric peptide ligand (HWRGWV). In the study using HWRGWW, the short peptide ligand was immobilized on the surface of silica-coated QCM sensors using polyethylene glycol as a solvent with a surface density of ~0.8 chains nm^{-2} reported to result in an increased surface accessibility and allowing a proper orientation of the peptide to IgG.[279]

In a different type of study, Xu et al. have reported on the adsorption behavior of poly(diallyldimethylammonium chloride) (PDADMAC) at the water interface for Laponite (synthetic-layered silicate manufactured from naturally occurring inorganic mineral sources) and Ludox (colloidal silica).[280] This very detailed study revealed the effect of SiNPs shape on absorption: in fact the Laponite material consisting of disklike-shaped nanoparticles (1 nm thick and ~25 nm diameter) showed stronger absorption than the Ludox sample which comprises spheres (20 nm diameter). It was proposed that the shape of Laponite NPs allowed arrangement into a more favorable orientation during the adsorption process, forming a more dense and rigid film/adsorbed layer. It is important to mention that Laponite NPs are not only composed of silica but also other ions with empirical formula [$Na_{0.7}Si_8Mg_{5.5}Li_{0.3}O_{20}(OH)_4$], thus, the two suspensions will present different ionic strength which has been shown to highly affect the conformation of PDADMAC and the type of interactions that can take place.[281] Further, the fact that Laponite comes from a natural source, a hierarchical structure is expected and with it different porosity and surface area values.[282] Of interest, Karpovich et al. showed a NMR relaxometry approach that could be used to measure the surface area of materials directly in suspension.[283]

Often studies employing combinations of techniques are particularly valuable. For example, in a study using a combination of atomic force microscopy (AFM), transmission electron microscopy (TEM), and dynamic light scattering (DLS), Ozaki and co-workers developed a site-specific process for precipitating silica using silica BPs combined with peptide nucleic acids (PNAs) in which the PNA sequence could act as a binding module for a complementary DNA sequence.[246] Here, AFM showed the formation of long chains and unique dumbbell-shaped silica nanospheres as a result of site-specific silica biomineralisation on DNA sites. In addition, transmission electron microscope (TEM) and dynamic light scattering (DLS) analysis revealed that the control of nanoparticles depended on the number of silica binding peptide-PNA conjugates attached to the DNA molecule.[246] Furthermore, Thyparambil et al. functionalized an AFM tip with an oligopeptide and obtained thermodynamic data arising from peptide adsorption on quartz and fused glass.[284]

In a particularly nice study by Bharti and co-workers, they reported the use of cryo-transmission electron microscopy (Cryo-TEM) and small-angle X-ray scattering (SAXS) were used as tools to study the structural properties of bridged silica aggregates directed by the electrostatic adsorption of the globular protein lysozyme as a function of pH ranging from 3 to 11.[285] What is important is that by using cryo methods, the authors could closely approximate to the "real" experimental conditions, and additionally, a theoretical/mathematical model was also used to explain the experimental findings of the interacting particles. Tomczak and co-workers using circular dichroism (CD) demonstrated that modification of silica morphology from spheres to hexagonal plates in the presence

of PLL (polylysine) was due the α-helical secondary structure adopted by PLL at DP > 100, as opposed to random coil for PLL with DP < 100.[229] In another study, ultraviolet circular dichroism (UV-CD) and dynamic light scattering (DLS) have been used as tools to study the effect of surface properties of two different types of SiNPs synthesized either by pyrolytic or colloidal processes in water and in PBS at pH 7.4, respectively.[286] In this study, the surface hydrophobicity/hydrophilicity was found to affect the amount of BSA adsorbed onto the silica NPs and also gave evidence for the formation of a protein hard corona (monolayered or multilayered) when bovine serum albumin was adsorbed.[286]

For studies of peptide silica interaction, fluorescence-based assays using fluorophores and dyes have been used to quantify peptide concentrations in solution. The method (by measurement of the difference in the amount of material remaining in solution) is commonly employed to quantify the amount of peptide adsorbed on amorphous silica NPs of different size and/or functionalities.[154,168,176] By using fluorescamine assays, researchers have shown that simply by changing the silica surface properties and solution pH, the peptide adsorption mechanism can be modified.[168,176] In a particular series of studies, the adsorption isotherms of peptides KLPGWSG (positively charged), AFILPTG (neutral), and LDHSLHS (negatively charged) were used to show the role of electrostatic/hydrophobic interactions and hydrogen bonding at the aqueous silica interface (Figure 4C). Further, the role of hydrophobic interactions in peptide binding at pH 7.4 was provided by a combination of desorption studies and thermal methods, i.e., ITC, to specifically measure the strength of interaction.[180]

Fluorescence-based assays have also been used to study the biosilicification process using the fluorescent dye, 2-(4-pyridyl)-5-((4-(2-dimethylaminoethylaminocarbamoyl)methyl)phenyl) oxazole (PDMPO).[287,288] The response of the "silicaphilic" fluorescence to different environments such as solvent and pH has been recently probed using fluorescence spectroscopy as well as UV−vis, further supported by computational data, dynamic light scattering, and zeta potential measurements to understand the PDMPO-silica interaction. The data show that pH affects charged states of the molecule, particularly in the presence of silica, and modified the mode of attachment, with both single-point (low anisotropy) or multipoint modes (high anisotropy) modes of attachment being possible.[289]

NMR, used to analyze samples both in solution and in the solid state is a technique which is finding application in the study of silica-biomolecule interactions both to understand the fundamentals of biosilicification and in the development of biomedically relevant materials. A few examples to illustrate the information obtainable are described. Solid state NMR has been used to show how a collagen-like peptide (H−(Gly-Pro-Hyp)$_3$−OH) was directly immobilized onto carboxylated mesoporous silica particles (COOH/SBA-15).[290] Note, these experiments were carried out under anhydrous conditions which may well have modified any water/biomolecule/surface interactions. With this in mind when considering the results obtained, the ^{15}N spectral signal was found to be shifted to a higher resonant frequency (70−95 ppm) when the peptide was covalently attached to the bioactive silica material.[290] Shifts of magnetic resonance frequencies have also been associated with possible intermolecular interactions (i.e., hydrogen bonding) as reported by Lopes et al. in 2009.[291] In this study, the

chemical shift (δ) of the bulk zwitterionic forms of glycine and its polymorphs (α-, β-, and γ-glycine) was of the same order; hence, glycine was suggested to be hydrogen-bonded to the silica surface instead of covalently bonded as this would have given rise to much larger chemical shifts.[291] Making further use of the NMR technique, Geiger and co-workers studied the formation of biosilica in vitro directed by the PL12 (KAAKLFKPKASK) peptide in the presence of a phosphate buffer.[292] Here, they used solution NMR (for free PL12 peptide) and two-dimensional (2D) dynamic nuclear polarization enhanced solid state NMR (silica-bound PL12 peptide) to understand the secondary structure and conformational changes of the peptide. The free PL12 peptide showed random coil conformation in solution at the eighth position (proline), while it gets adapted to a somewhat extended (6th position Phe) and compact helical structure (11th position Ser) when embedded inside silica, showing more or less variability in interaction of its hydroxyl groups with the surface of silica.[292] Should these latter studies have been performed in the presence of an aqueous phase, which would better reflect in vivo biosilicification conditions, it is possible that different results in terms of binding pattern would have been observed. Nonetheless, they give helpful hints as to the most likely functional groups interacting with the mineral phase and provide a strong steer in the design of further experiments, using both experimental and computational strategies.

With the advance of sophisticated pulse technqiues in solid state NMR and specific ^{13}C and ^{15}N labeling of the lysine closest to the N terminus in R5 (SSKKSGSYSGSKGSKRRIL) REDOR ssNMR which is able to measure internuclear distances has been used to investigate the role of an N-terminus lysine in R5 silica recognition at the atomic level.[219] The use of labeling helped in recognition of the importance of this specific lysine in binding of the peptide to silica, but given that the polypeptide in nature is described as being heavily post-translationally modified with polyamine units, then the specifics of binding measured only relate to the peptide and not to the biomolecule as would be found in vivo.[293] As the authors themselves point out, it is also possible that additional labeling of other lysine residues might identify further silica interaction points within the polypeptide. It should be noted that the use of interface-specific vibrational spectroscopy in combination with molecular dynamics simulations came to a different conclusion,[220] with the whole sequence proposed to interact with silica leading to a fully intercalated peptide.

Researchers are also starting to use solid-state NMR measurements coupled with computational (MD) studies.[294] The use of heavily ^{29}Si labeled materials is improving the sensitivity of such measurements, and provided the nature of the silica generated in the presence of a particular biomolecule (or used for binding) is understood, then good agreement between experiment and theory can be obtained. This approach is one which will see greater adoption in the future provided researchers can access labeled materials.

Raman-based spectroscopic tools (i.e., Raman, SERS, TERS) have attracted much attention in the past decade for the characterization of biomolecules (i.e., peptides, proteins, DNA) and metal-based compounds such as silica and gold.[295−297] What is important to note is that this technique can be used to study samples in aqueous media unlike in infrared spectroscopy where the signals from water vibrations minimally interfere with signals from the biomolecule or mineral. Moreover, these techniques have been extended from probing inorganic material-peptide/protein interactions[295] to study catalytic reactions[297] and chemical imaging of live cells.[296] Note that, since SERS enhancement is based on the oscillation frequency of the electron plasma, only plasmonic nanostructures (i.e., VO, Mo, Au, etc.) are suitable. Therefore, Raman-based SERS spectroscopic techniques have not been yet considered as potential tools to study biomolecule interactions on a silica surface itself but can be used on a metallic surface such as Au with a thin silica coating layer.[296]

X-ray diffraction (XRD) has been used for the identification and characterization of adsorbed amino acid crystals on the silica surface, as is the case of glycine/SiO_2 surface[232,291] and glutamic acid/SiO_2 surface.[298] Although, bulk amino acid crystals can nowadays be identified by using single-crystal XRD, not many studies involving aa-silica interactions have considered the use of XRD techniques due, in principle, to amorphous silica being the surface of study in many cases. Of interest is the fact that it was only several years ago when the last amino acid structure (L-lysine) has been determined using XRD by Williams et al., thereby completing the set of 20 amino acid crystal structures 75 years on since the first amino acid structure was determined.[299]

2.6.2. Computational Techniques for the Study of Silica-Biomolecule Interactions.

Although many in vitro tools have been employed to study silica−biomolecule interfaces, understanding specific molecular recognition and mineral assembly is still challenging using current technologies. Therefore, computational studies have been used to support the engineering of silica-based materials as they are able to provide atomic level information including computed binding free energies, NMR chemical shifts, vibrational frequencies, and electrostatic potentials maps.[300] The caveats provided in the section on studies of silica surfaces are particularly important to consider when reading literature in this area as it is only relatively recently that differences in speciation of the silica surface have been overtly acknowledged.[173,294,301] We now give a few examples of typical studies presented in the literature with other studies on silica and the silica−water interface being described in section 2.3.

Molecular dynamics simulation studies have been used to great effect to understand the likely structure of the chemically unmodified diatom silaffin peptide R5 in the presence of silica and to explore the role of phosphorylation on binding to silica under both neutral and slightly acidic pH conditions.[220,301] Experimental validation of the observations made provide further validation to the simulation approach.[220]

The study by Sprenger et al. in 2018[301] uses the best available force fields for all of the components, defined surfaces for the mineral phase, and advanced conformational sampling and shows that both pH and the extent of post-translational modification affect biomolecule conformation and mode of interaction.[173,301] Specifically, the results suggest that silica and R5 can interact through a number of amino acid side chain residues in an extended conformation at pH ca. 7 with surface sodium ions helping to bridge between the mineral and biomolecule phases. At lower pH values (ca. 5) and in the presence of phosphate group(s), the interaction is more dependent on hydrogen bonding between the surface and the biomolecule mediated by water. The authors used the (100) face of crystalline quartz/>200 nm diameter silica particle as their model of the surface, which carries different levels of ionization at different pH values. It would be interesting to explore if the pattern of ionization has an effect on binding.

Additionally, for an amorphous silica as formed in nature, a wider range of Si−O bond distances and bond angles (Si−O−Si and O−Si−O) would be present than are found in quartz. Would this have an effect on binding? This is as yet unknown. An advantage of the computational approach is the ability to explore many compositional variants of a peptide sequence without having to worry about the difficulty in synthesis of particular sequences. It will be interesting to see if the position of the phosphate group which could be found attached to serine residues at positions 1, 2, 5, 7, 9, 11, and 14 (already explored) can be used to tune the physicochemical properties of the peptide and its mineral binding properties.

We now consider studies on peptides isolated by phage display. Studies on quartz and quartz binding peptides by Oren and co-workers showed that strong quartz SiO_2-BPs always had at least one of Pro, Leu, and Trp residues in direct surface contact.[267,268] Further investigation on quartz SiO_2-BPs showed that the secondary structure characteristics of the peptides was different between strong or weak binders and suggested that the strong binders involve nonpolar, neutral residues, whereas the weak binders contain polar and charged residues.[302] In this study, the use of advanced sampling approaches such as replica-exchange molecular dynamics (REMD) also revealed that interpeptide interactions are also key in peptide-surface interactions.[302] Most recent studies on quartz SiO_2−BPs have employed replica exchange with solvent tempering (REST) as an alternative approach to REMD-based simulations due to a higher maximization of the conformational sampling of peptides adsorbed at the aqueous interface.[303]

At the other extreme in terms of studies on individual amino acids, Rimola et al. demonstrated by computed adsorption energies that amino acids containing side chains with either polar or large aliphatic groups have the most favorable interaction energies toward hydroxylated amorphous silica and suggested hydrogen bonds and London dispersive interactions as the main driving force.[304]

Recent computational studies using molecular dynamics simulations with the CHARMM-INTERFACE force field showed that adsorption of charged peptides (i.e., KLPGWSG and LDHSLHS) is highly influenced by the working pH.[39,173] In contrast, no significant difference was observed for neutral peptides (i.e., AFILPTG), which were more weakly attached by hydrogen bonds and hydrophobic interactions.[39,173] Moreover, the amount of peptide adsorbed onto the silica surface was shown to be influenced by the particle size, being higher for larger particles due to the larger silica surface ionization.[39,154] These quantitative predictions of peptide-silica binding as a function of pH and particle size were comparable and in accordance with experimental measurements (i.e., fluorescamine assay).[39,154] The good agreement between simulation and experimentation was largely due to a clear understanding of the surface exposed to the biomolecules. In the published study, a range of different surface chemistries were simulated,[173] which could be related to the behavior of the silica under different pH regimes. However, an issue that was not addressed was the fact that the surfaces simulated were still based on a regular or "crystalline" arrangement of silica, which is not found experimentally for any amorphous silica. Where there was not full agreement[39] between simulation and experimental binding data, this may suggest that surface features, including defect structures, may play a role in

determining the binding of peptides to such surfaces. New models are needed to progress the field.

Although great advances have been made in the mechanisms concerning silica-biomolecule interactions, the control of selective recognition of biomolecules is still unclear and is a challenge for applications including the fabrication of drug delivery systems and new catalysts, among others. Furthermore, much scientific attention is needed to increase our limited fundamental understanding of silica-biomolecule interactions as opposed to focusing on an application-oriented advancement approach. A comprehensive understanding of the solution behavior of biomolecules and silica in isolation and in partnership is needed and will ultimately lead to the further development of biomolecule-based silica materials with improved biocompatibility, solubility, or functionality.

2.7. Toxicology of SiO$_2$

Silica is, at ambient temperature and pH, slightly soluble in water and an environmentally inert substance with no known harmful degradation products. However, some important studies on silica toxicology have been reported.[111,305−307] A contribution of particular note is a recent review from the Hoet laboratory where they provide a detailed update on the toxicology of amorphous silica particles.[308] In particular, they consider the differences in response between silicas generated by thermal routes versus those generated by aqueous routes. The cytotoxicity of SiNPs on cells is dependent on the amount of material used, time of exposure to the cells, and size of the nanoparticles, where smaller particles (<20 nm) show higher toxicity.[307,309] Note that surface area also plays an important role in the toxicity of nanosized silica particles.[309] Crystalline silica such as quartz have shown toxicological effects when interacting with biological systems,[120] and a higher pulmonary toxic effect has been associated with surface activity rather than particle size.[310]

Although NPs have been considered potential risk for health with special reference to the respiratory system (i.e., lungs),[119] the dissolution rate of SiNPs have been shown to be more rapid than the precipitation rate,[311] therefore, its dissolution and elimination in biological systems (i.e., in lungs) can be expected.[111] Further, due to the absence of lipophilic character of the SiNPs and the ability of organisms to eliminate absorbed SiO_2 constituents, bioaccumulation is not expected.[111] Surface modifications of nanoparticles, in general, can change cytotoxicity of a material itself, modifying physicochemical properties and, therefore, the way they may interact or travel through biological systems. For example, addition of surface functionalities such as amine groups onto SiNPs, give rise to different surface charge values, which must be considered for toxicity and tissue distribution profiles.[119] It should be remembered that the surface properties of a material and, hence, its toxicity can be affected by its thermal and/or environmental history. As an example of how to reduce toxicity, heat treatment of cristobalite (up to 1300 °C) shows a loss of cytotoxicity which is proposed to be due to removal of surface radicals and conversion of silanols to siloxane bridges.[164] An example of a treatment that might lead to increased toxicity is the grinding of crystalline silicas (i.e., cristobalite and quartz) that may produce surface radicals, which would increase surface hydrophilicity and potentially toxicity; however, it is proposed that this can be suppressed by grinding in the presence of water.[165]

The addition of biomolecules on the surface of nanoparticles of silica, although studied in terms of interactions (see section above) is a topic that has been little explored in terms of moderation of toxicity. It is clear, however, that if biomolecules reside on the surface for any significant period then they will moderate the surface chemistry and solubility of particles and further affect the ability of proteins, etc. occurring in the natural environment to interact with the particles themselves and thus moderate their biological fate. This is an area of science that remains ripe for exploration.

3. TiO$_2$

3.1. Overview of TiO$_2$

Titanium oxide (TiO$_2$) is a common oxide found in nature in titanium-containing ores. The principal natural source of TiO$_2$ is ilmenite (FeTiO$_3$), a mineral containing 40−60% TiO$_2$. TiO$_2$ in pure form occurs naturally as rutile, anatase, brookite, and the rare **TiO$_2$-B**. Other forms exist at high pressures and can be obtained via artificial synthetic methods [i.e., TiO$_2$ (H), TiO$_2$ (R) etc.].[312−317] Every year, at least 4.5 million tons of TiO$_2$ are produced worldwide from mined sources.[318] The main extraction methods are the chloride and sulfate processes.[318] The chloride process produces only the rutile form of TiO$_2$. It is a cleaner, more cost-efficient approach compared to the sulfate process and accounts for 60% of total TiO$_2$ production.[318]

TiO$_2$ is a wide band gap semiconductor (3.2 eV for anatase, 3.0 eV for rutile) with attractive technological applications. Due to its high refractive index and brightness, TiO$_2$ is the most commonly used white pigment.[319] TiO$_2$ in coarse form (grain size in the micrometer range) provides whiteness and opacity to a variety of everyday products, from paint[320] to plastics,[321] cosmetics,[322] and food (where food grade TiO$_2$ materials are labeled as E171).[323]

The discovery of the photocatalytic splitting of water on a TiO$_2$ electrode under ultraviolet (UV) light[324] in 1972, initiated an escalation in scientific research aimed at the optimization of TiO$_2$ as a photoactive catalyst, which continues to this day. As a photoactive material, TiO$_2$ is used in environmental remediation, solar fuels, and photovoltaics, and its photoinduced wettability properties are exploited in the coatings industry.[325−327] TiO$_2$ NPs are known to be more effective as a photocatalyst compared to bulk powders,[328] and they exhibit higher photoactivity compared to macrocrystalline semiconductor particles.[329] In the biomedical field, it finds application as an antibacterial and as a cancer treatment;[330,331] however, the mechanism underpinning its photobiological activity is not well-understood.

Advancement of the technologies listed above relies on the development of purpose-built materials or synthetic strategies that allow for specific functionalities such as high surface area. A range of TiO$_2$ nanomaterials such as nanoparticles, nanorods, and nanotubes, that can form complex three-dimensional (3D) architectures, are accessible via a variety of processes, including liquid-based routes,[332−337] solid state routes,[338,339] metal−organic chemical vapor deposition,[340] electrophoretic deposition,[341] radio frequency (RF) thermal plasma,[342] and laser ablation.[343] However, the nanoscale control of morphology/topology and the rational design of complex architectures still represents a considerable challenge, hence biomimetic approaches represent appealing and promising alternatives to advance the field.

3.2. TiO$_2$ Properties and Traditional Synthetic Methods

Of the three main TiO$_2$ crystal structures: anatase, brookite, and rutile, brookite is the least studied, due to the more laborious synthesis required and the difficulty in obtaining it in pure form.[344] Rutile is the most thermodynamically stable phase, while anatase is metastable at ambient pressure and temperature. However, most sol−gel and aerosol syntheses yield anatase as the main product. Anatase has been found to be the thermodynamically favored phase for crystals up to 14 nm in size.[345] Transition from anatase to rutile is dependent on temperature, impurities, and reaction conditions. Anatase TiO$_2$ nanocrystals with ultrahigh surface area can be produced using a solvothermal synthesis method.[346] Hence, depending on the synthesis route used, different forms of TiO$_2$ can be produced. Another stable form of TiO$_2$ is the monoclinic TiO$_2$−B, which is very rare in nature, though interestingly it has been reported as one of the possible crystalline products in biomolecule-assisted titania mineralization, as discussed later.

Liquid phase processing is favored for the chemical synthesis of TiO$_2$ NPs as it generates homogeneous products, gives good stoichiometry control, develops complex and varied shapes, and can be used to prepare composite materials, all without the requirement for expensive equipment.[347] The most common liquid-based routes to produce TiO$_2$ include sol−gel,[332] solvothermal,[333,334] and hydrothermal processes.[335−337] Liquid-based routes are based on the hydroxylation/condensation reaction of a titanium precursor, usually TiCl$_4$ or Ti tetra alkoxides such as titanium isopropoxide in the presence of water. Variation in synthesis parameters such as pH, temperature, solvent polarity, nature of the precursor, and the presence of acidic or basic catalysts allows fine-tuning of the final product's properties.[348−350]

As an example, for the sol−gel method, a very popular process for preparing TiO$_2$, nanomaterials in irregular aggregate form or spheres can be obtained. The materials are usually amorphous and are converted to a crystalline phase via aging or calcination. This approach requires an extra preparation step when material deposition to support materials is needed. An important parameter in sol−gel synthesis is the water-to-precursor ratio, which must be carefully controlled to obtain products with defined homogeneous properties. For example, an increased water to precursor molar ratio produces smaller particles.[351] A change in the reaction solution temperature or pH is also capable of influencing final nanoparticle size.[348−350] While synthetic strategies and conditions of reaction are commonly reported in detail in the literature, authors often fail to comment on yields or the efficiency of the synthetic procedures performed which has resulted in a lack of knowledge regarding possible side reactions or inhibitory processes occurring during synthesis.

In the hydrothermal approach, extreme pressures and temperatures in solution enable direct synthesis of TiO$_2$ of high crystallinity. This approach is also used to facilitate transition of TiO$_2$ crystallinity from one phase to another (e.g., from a mixture to pure rutile).[352] Modulation of reaction time gives access to nanotubes, nanoplates, and nanobelts.[353,354] The hydrothermal approach also allows for a direct deposition method (e.g., in the growth of TiO$_2$ nanotubes on FTO glass).[355] Some disadvantages include lengthy reaction times, costly reagents, and carbon impurities or the possible formation of trititanate as a byproduct.[353,354]

In bioinspired approaches, where mineralization reactions occur in water, or buffered aqueous solutions, the fast rate of
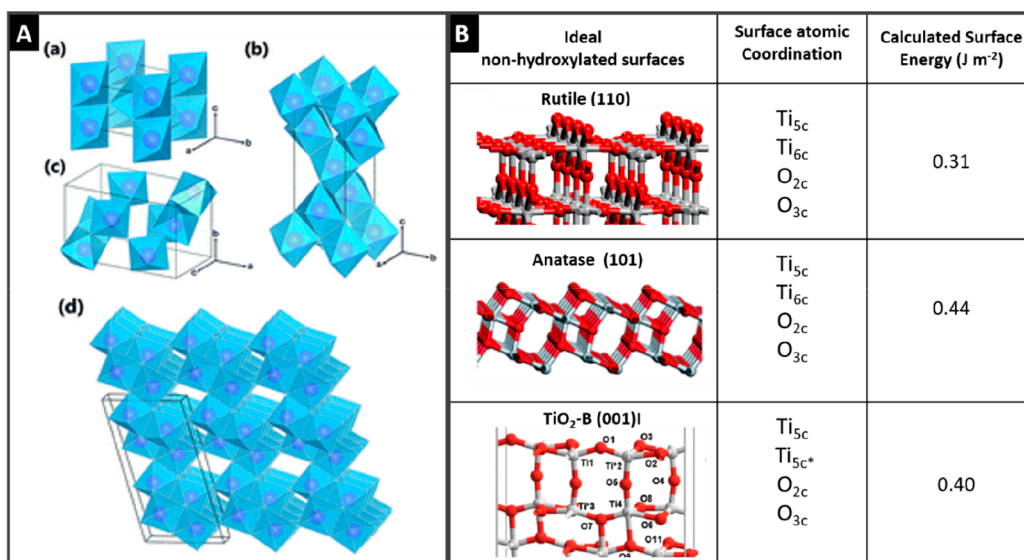
Figure 7. (A) Crystal structures of TiO$_2$ polymorphs: (a) rutile, (b) anatase, (c) brookite, and (d) TiO$_2$-B. Reprinted with permission from ref 361. Copyright 2015 Royal Society of Chemistry. (B) Surface representation, surface atomic coordination, and calculated energy values for lowest energy surfaces of TiO$_2$ polymorphs relevant to bioinorganic interfaces. Rutile surface adapted with permission from ref 362. Copyright 2016 IOP. Anatase surface representation adapted from ref 357. Copyright 2014 American Chemical Society. TiO$_2$-B-I surface adapted from ref 363. Copyright 2009 American Chemical Society. Energies are calculated after relaxation by the PBE method.[357,359]

hydrolysis/condensation of traditional precursors does not allow any control over the formation of the precipitate. We will discuss later how this has limited the choice of precursor for the synthesis of titania to an aqueous stable titanium complex in the majority of biomimetic studies.

3.3. Surface Chemistry of TiO$_2$

TiO$_2$ is the best-characterized metal oxide surface, and a wealth of knowledge is available on its atomic surface structure, water interface, and adsorption of small molecules from experimental and theoretical studies. For comprehensive information on titania bulk and surface chemistry, we refer the reader to the reviews by Diebold and Bourikas.[356,357] Herein, we will focus on the structures and properties relevant to the inorganic/biomolecule interface.

3.3.1. Bulk and Surface Structures. In the four natural crystalline forms of titania: anatase (tetragonal $I4_1/amd$), brookite (orthorhombic $Pbca$), rutile (tetragonal $P4_2/mnm$), and the rarer TiO$_2$−B (monoclinic $C2/m$), the Ti^{4+} atom is surrounded by 6 O^{2-} ions in a distorted octahedral geometry. The four different bulk structures are given by the different stacking of the octahedra and are reported in Figure 7.

Anatase, rutile, and monoclinic TiO$_2$-B have been reported by biomolecule-assisted synthesis.[56,358] Brookite to date has been obtained only in traces in mixed phase precipitates.[25] Figure 7B shows the most stable crystal surfaces exposed in each polymorph. Surface characterization has been performed by XRD on a truncated mineral;[356] however, most of the data concerning exposed crystal surfaces derive from computational studies. The most stable surface of all is the rutile (110), which is also the best characterized due to large availability of pristine mineral crystals.[356] The important role of the (110) surface will be extensively discussed in section 3.6. The anatase (101) surface has received extensive investigation in the past decade, while information is very limited for TiO$_2$-B.[359] In the case of anatase, it is worth mentioning that while the (101) facet is the most exposed in naturally occurring minerals, the (001) facet is

the one most commonly expressed in synthetic samples and has been associated with high catalytic activity.[360]

All surfaces expose 5-fold and 6-fold coordinated titanium atoms, indicated by Ti$_{5c}$ and Ti$_{6c}$, respectively, and 2-fold- and 3-fold-coordinated oxygen anions, indicated by O$_{2c}$ and O$_{3c}$, respectively. O$_{2c}$ are often indicated as bridging oxygens and O$_{3c}$ as terminal oxygens. In the TiO$_2$-B (001)-I surface, the most stable of the two possible surface terminations of TiO$_2$-B (001), there are two types of 5-fold coordinated titanium cations.

3.3.2. Surface Hydroxylation and Charge. Images in Figure 7B refer to nonhydroxylated ideal surfaces, which correspond to the bulk mineral structure cleaved at the corresponding plane, populated by unprotonated bridging oxygens O$_{2c}$. However, the surface of TiO$_2$ can react immediately with water molecules in either aqueous solution or moist air, and hydroxyl groups are formed. Surface relaxation in contact with an aqueous solution at room temperature leads to negligible spatial rearrangement, as suggested by modeling studies and evidenced by XRD data.[364]

The surface hydroxyl group density of TiO$_2$ is considered to play a significant role in photocatalytic processes and has a fundamental role in biomolecule adsorption.[365] On a macroscopic scale, TiO$_2$ is considered to be an amphoteric oxide, reacting with strong bases to form titanate salts or strong acids to form titanium(IV) salts. At an atomic level, this behavior derives from the presence of basic terminal OH groups and acidic bridged OH and terminal OH species. XRD analysis of a perfect rutile (110) surface showed the presence of both terminal and bridging oxygens above the surface plane of Ti and O atoms and a layer of adsorbed water molecules above the surface plane.[366] On nonideal samples (i.e., synthetic nanoparticles), experimental methods used for determination of the surface chemistry include thermogravimetric analysis, Fourier-transform infrared spectroscopy, and X-ray photoelectron spectroscopy. Surface hydroxylation varies from 0.3 to 10 OH/nm^2, depending on the synthetic method. Hydroxyl-

enriched particles with OH density of 12 OH/nm^2 have been obtained by alkaline hydrogen peroxide treatment.[367] A high hydroxylation degree has been associated with good water dispersibility,[367] while DFT calculations suggest a change in electronic structure in highly hydroxylated TiO$_2$ resulting in improved photocatalytic activity.[368]

In the computational community, nonhydroxylated surfaces are often associated with an associative water binding mode (Figure 8A), while for the hydroxylated surface, the water
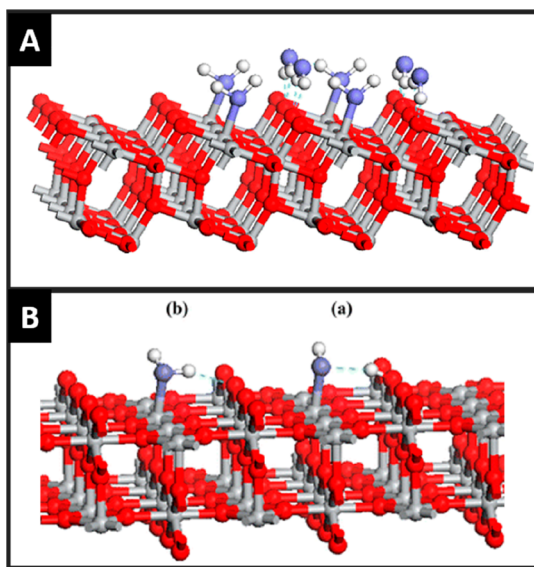

Figure 8. (A) Representation of local structure of water molecules absorbed molecularly and through hydrogen bonds on anatase (101) ideal surface. (B) Representation of (a) dissociative water adsorption and (b) associative water adsorption on a rutile (110) ideal surface. Modified from ref 357. Copyright 2014 American Chemical Society.

molecules in the terminal sites dissociate to form protonated bridging oxygens and terminal hydroxyl surface species (Figure 8B).[357] The point of zero charge (pH$_{pzc}$) of titania has been found to be insensitive to crystallinity, with an average value of 5.9 at 25 °C,[369] and thus a negative surface protonation-induced charge develops at any pH above this point. Surface charge is size-dependent, with a shift in IEP at higher pH for TiO$_2$ with decreasing size (i.e., pzc was pH 6.3 for 12 nm particles, whereas it was 8.4 for 3.5 nm particles).[370] This behavior is similar to that observed for silica particles.[168]

At an atomic level, it is difficult to characterize empirically the hydroxylation equilibrium and its pH dependency. Useful insight comes from the application of models such as the MUlti SIte Complexation Model (MUSIC).[371] This model describes the hydroxylation equilibria of discrete reactions such as the adsorption of hydroxyl groups at surface Ti atoms and the protonation of bridging oxygen atoms. The application of the MUSIC model extended by Köppen and Langel[372] for a (100) rutile surface leads to a surface charge density of 0.25, −0.18, and −0.35 C/m^2, pH values 4.0, 7.4, and 9.0, respectively. This pH-dependent behavior is important to the discussion of biomolecule interactions with the TiO$_2$ surface.

3.3.3. Water/Inorganic Interface. The water structure and mode of binding (i.e., associative or dissociative) on titania has been a matter of controversy for decades. The general agreement is that, on ideal surfaces, water dissociation is not an energetically favorable process except at the early stages of

water binding simulated by low water vapor pressure. If spontaneous dissociation of water is to occur, oxygen vacancies in the material are necessary. When considering biomolecule interactions, up to four layers of water are proposed to be involved in the binding dynamics.[357] The water interface on both rutile (110) and anatase (101) consists of ordered water molecules coordinating on Ti$_{5C}$ and forming hydrogen bonds to O$_{2C}$ in the first monolayer. In the second monolayer, water molecules interact via H bonding with O$_{2C}$, while a third monolayer interacts with the first two layers via a network of H bonds. X-ray measurements have not indicated the presence of ordered water beyond the hydration layer located at 3.8 Å,[357] and water recovers its bulk structure and properties at 15 Å from the rutile (110) surface.[373] To the best of our knowledge, studies on water multilayers on TiO$_2$-B have not been reported.

3.3.4. Outlook for Application at the Bioinorganic Interface. In summary, the study of biomolecule/inorganic interactions should be facilitated in the case of titania with respect to its well-characterized aqueous interfaces, in particular rutile (110) and to a lesser extent anatase (101). Comparatively, there is much less information on brookite and especially TiO$_2$-B. However, we must note that in titania-biomolecule interaction studies, there is a general lack of characterization of the inorganic material. As an example of what is typically reported in the literature, adsorption studies in solution for noncovalently attached species, such as lysine, onto TiO$_2$ was found to be similar for both amorphous and crystalline titania films though the precise form of titania was not described.[374] It must be noted that TiO$_2$ films and powders derived from bioinspired approaches commonly include amorphous material or are polycrystalline. Further, additional anatase terminations such as anatase (001) might be important due to their higher reactivity coupled with lower stability.[356] For these reasons, it is important that less common crystal structures of titania are studied and their aqueous interfaces characterized.

3.4. TiO$_2$-Biomolecule Interactions and Applications

The study of interactions between TiO$_2$ and biomolecules, such as peptides and proteins, at both the fundamental level and in the generation of composite materials has become more prominent in the past decade as researchers gain the knowledge to develop new technological applications involving the interface between titania and biomolecules. For example, biomolecules can be aligned and placed on prefabricated inorganic patterns via aptamers for use in bioelectronics, biosensors, micrototal analysis systems (TAS), biochemistry, drug delivery systems, and bioavailable implants.[375] Also, the introduction of biomolecules into TiO$_2$ synthesis is proving to be an attractive step forward from traditional methods, resulting in the modification of properties such as phase distribution, size, shape, and surface roughness of TiO$_2$.[376,377] Use of biomolecules such as amino acids, peptides, and proteins to assist with TiO$_2$ mineralization are reviewed in this contribution, with emphasis on the role of the biomolecule and the precise nature of its interaction with the growing mineral. A review of the literature has highlighted an issue with the nature of the commonly used titania precursor, especially in the presence of salts in the reaction environment, which we try to clarify.

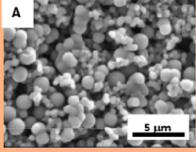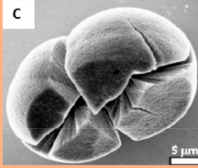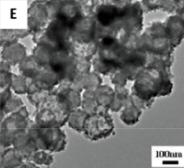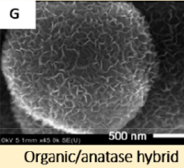**3.4.1. Biomimetic Synthesis of TiO$_2$: Role of the Precursor and Reaction Environment.** *3.4.1.1. Precursor.*
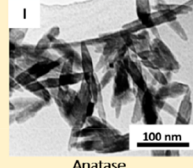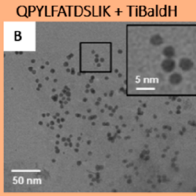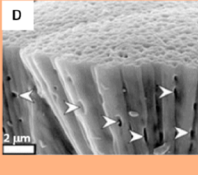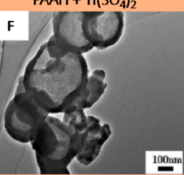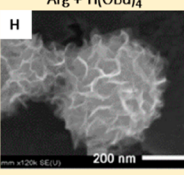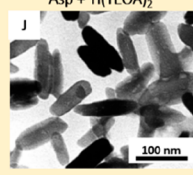
Figure 9. Titania morphologies accessible via biomimetic and bioinspired approaches. Precursor and biomolecule used are summarized above the images; crystalline form is stated below images. (A) Spherical particles/aggregates. SEM image reprinted from ref 376. Copyright 2007 American Chemical Society. (B) Monodisperse NPs from ref 86. Copyright 2013 American Chemical Society. (C−D) Hierarchical structures, SEM images modified with permission from ref 358. Copyright 2006 Wiley-VCH. (E−H) Hollow structures reprinted with permission from ref 25. Copyright 2013 RSC. Also reprinted with permission from ref 36. Copyright 2011 Wiley-VCH. (I and J) Nanorods, modified with permission from ref 383. Copyright 2004 Royal Society of Chemistry.

As with traditional synthesis approaches, modifications in biomimetic reaction conditions can lead to dramatic changes in the reaction mechanism and resulting products. Traditional hydrolysis/condensation of Ti precursors requires either pyrolytic decomposition or alkali/acidic catalysis. Molecules such as silicateins, when used in biomimetic synthesis require roughly physiological conditions for the biomolecule to retain activity; this means working in aqueous solution, at room temperature, and circumneutral pH. An additional constraint is that conditions have to be compatible with a titania precursor that can condense under these experimental conditions. So called traditional precursors, like alkoxides and $TiCl_4$, hydrolyze too quickly in these conditions, so researchers have shifted their attention toward pH neutral carboxylate Ti complexes, in particular, the commercially available titanium(IV) bis-(ammonium lactato)dihydroxide (TiBALDH).

The chemistry of oxo-carboxylate complexes, including TiBALDH was reviewed by Kessler in 2013.[378] Kessler provides detailed structural characterization of TiBALDH in the solid and aqueous phase, reporting the actual molecular structure as obtained by X-ray crystallography to be $(NH_4)_8Ti_4O_4(lactate)_8 \times 4H_2O$. This is rather more complex than that reported by chemical suppliers and remarkably does not contain any Ti−OH bonds, often used in mechanistic explanations of the potential catalytic properties of biomolecules. More importantly, this work also evidences the following coordination equilibrium in the aqueous phase, where $Ti(lactate)_3^{2−}$ coexists with uniform lactate-capped TiO_2 anatase nanoparticles around 3 nm in diameter. Evidence for the presence of the particles comes from DLS, with lactate capping confirmed by NMR NOESY experiments.[378]

$$3[Ti_4O_4(lactate)_8]^{8-} + 8NH_4^+$$
$$\leftrightarrow 8[Ti(lactate)_3]^{2-} + 4TiO_2 + 8NH_3 + 4H_2O$$
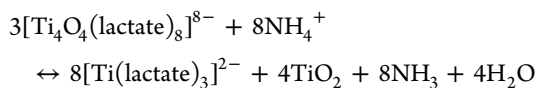
Due to the particle size being below 5 nm, the particles are too small for observation of the Tyndall effect, and their dispersions look clear to the naked eye. Aggregation of such particles can be achieved by addition of polyelectrolytes. BSA[379] and smaller biomolecules,[376] and bioinspired molecules including Polyamines,[26] peptide sequences isolated by combinatorial methods,[56] peptide motifs from proteins,[380] and their sequence permutations[63] were all claimed to catalyze the hydrolysis/condensation reaction at neutral pH and at room temperature to yield amorphous or crystalline TiO_2 from a TiBALDH. In view of this relatively recent insight on TiBALDH structure and nanoparticle equilibrium, it is important that any study claiming hydrolytic properties of biomolecules should be treated with caution, unless direct evidence is clearly provided by experimental observations or when another precursor is used as in the examples discussed in the next section.

3.4.1.2. Reaction Environment. A spatially constrained environment has been observed to influence the final TiO_2 phase obtained. For example, biomineralization experiments performed with peptide CHKKPSKSC in solution were found to form amorphous TiO_2; when expressed in protein cage nanoarchitectures, pure rutile was formed.[381] Similarly, rutile was obtained using the putative silica producing protein silaffin rSilC;[358] however, the use of the silaffin-derived peptide R5 leads to amorphous spherical agglomerates similar to those obtained with natural polyamines and reported in Figure 9A. Buffers are used to keep pH constant during reactions, especially phosphate buffers. It is notable that many studies that carry out mineral formation reactions in the presence of buffer lead to the formation of Ti-phosphate materials, rather than pure TiO_2.[26,56,86] Phosphate ion incorporation in the final precipitates has been evidenced by EDAX analysis with the electron microscope.

3.4.2. Biomimetic Synthesis of TiO_2: Role of the Biomolecule. TiO_2 is considered a nonessential inorganic

material for life, although recent publications discuss its potential role in life in that some organisms can incorporate titanium from their surrounding aqueous environment into biomineralized structures. For example, diatoms cultured in the presence of a water-soluble titanium precursor, led to metabolic incorporation of titanium in their frustules.[382] Although no direct evidence of TiO_2 formation is reported, photocatalytic antibacterial activity was observed for Ti-enriched diatoms.

It is not surprising that the first attempts to biomimetically produce TiO_2 involved the use of the putative silica-producing proteins: silicatein[55] and silaffins.[358] In the attempt to rationalize the role of the biomolecule in the mineralization process, and thus tailor material properties, structurally simpler biomolecules have been studied, including peptides and individual amino acids. The use of these systems has led to the preparation of a range of titania-based materials of different morphologies. However, little progress has been made in the fundamental understanding of the mineralization process, and little or no insight is normally provided about the mechanistic aspects responsible for mineral formation and/or crystal phase control. When a mechanistic explanation is attempted, it is described in terms of the ability of the biomolecule to catalyze hydrolysis–condensation reactions and/or its templating ability, especially when the biomolecule is capable of self-assembly in the reaction environment. There also appears to be little appreciation of the difference between catalysis of a molecular process as opposed to coagulation leading to material formation. Some relevant examples of TiO_2 morphologies are shown in Figure 9 and are discussed below. Little control over morphology was achieved when either protein, polyamine, or peptides were used in biomimetic conditions, leading to a range of amorphous particles in agglomerate form, represented by the spermidine-assisted precipitates shown in Figure 9A. An exception was the titania binding peptide Ti1(QPYLFATDSLIK) which led to precipitation of monodisperse anatase and TiO_2-B particles of 5 nm diameter (Figure 9B). A remarkable result was the formation of a hierarchical structure of crystalline rutile (Figure 9, panels C and D) under ambient temperature and neutral pH using the recombinant silaffin rSilC.[358]

Molecules with a high pI (i.e., a large net positive charge) can induce and control mineralization of complex titania structures. For example, polyamines were shown to produce hollow spherical structures under biomimetic conditions (Figure 9, panels E and F).[25] In this study, XPS was used to investigate the effect of different polyamine protonation/deprotonation states on both the crystalline phase and morphology development over time. The polyamines were claimed to self-assemble in solution, with droplets acting as spherical templates for titania mineralization, in a similar fashion to what has been observed in silica formation.[206] However, contrary to the silica study, no direct evidence was provided for the formation of these droplets.

Individual amino acids have been used as additives in traditional sol–gel or hydrothermal synthesis. In these studies, the experimental conditions are not those expected for a "biomimetic" synthesis as extreme pH and relatively high temperatures are used. Nevertheless, these "bioinspired" studies provide useful insights into the potential control that surface recognition and direct adsorption of biomolecules can have on crystal growth. As an example, hollow spheres were obtained using Lys and Arg through a solvothermal reaction

(Figure 9, panels G and H),[36] through a mechanism similar to that proposed for polyamines discussed above. Interestingly, lysine and arginine show different degrees of control over the morphology of a particle surface (Figure 9, panels G and H). Another example of bioinspired synthesis is reported by Sugimoto and Kanie.[383] They show a drastic change in the aspect ratio of anatase nanorods when Asp and Glu are used in a modified sol–gel method (Figure 9, panels I and J). It was speculated that amino acid adsorption to specific crystal facets was responsible for such a change. Optimisation of amino acid concentration was found to be crucial for morphology control as at high concentrations adsorption on TiO_2 surfaces could hinder controlled crystal growth resulting in roughened polycrystalline particles. Amino acids were shown to influence which crystalline phase formed, with Gly, Glu, Asp, and Ser able to stabilize anatase and polycrystalline materials being obtained in the absence of amino acids.[384]

Several peptide sequences have been identified in the literature as good binders for titania, using mainly single crystal rutile of (100), (110), and (001) orientation, as substrates.[56,86] A clear correlation between enrichment in basic amino acids like Lys, Arg, and His and TiO_2 precipitation activity was observed. The presence of Arg was found to be essential in several mineralization studies. For example, in a biomineralization attempt from a water-soluble precursor, only Arg-tagged hybrid silicatein induced TiO_2 deposition on their filaments, whereas nontagged silicatein remained undecorated.[385] The mechanistic explanation was limited to electrostatic interactions with the titania precursor. In studies that use peptides, mineralization activity was also correlated to the overall positive charge of the sequences used; however, a high precipitation activity has been observed in designed sequences of overall low charge.[386] For these low charge sequences, an interesting catalytic mechanism involving a serine-histidine motif was proposed to bring the peptide and precursor together via electrostatic interactions, but again the model had limited supporting evidence.

To advance understanding of the molecular requirements when designing new peptides for mineral formation, computational (molecular dynamics) simulations have been used. Results suggest that specific conformations and an alternation of hydrophilic and hydrophobic amino acids as in the peptide (Leu-Lys)$_8$ constitutes an effective configuration for TiO_2 mineralization.[387] More examples on how computational studies can complement experiments and contribute to our understanding of the bioinorganic interface will be reported later in section 3.6.2.

To summarize, comparing materials obtained by biomimetic methods and materials generated by traditional synthesis approaches: in traditional synthesis approaches, transition from anatase to rutile is seen at a wide range of temperatures (400–600 °C) depending on other synthesis conditions; however, using a biomimetic approach it is possible to synthesize rutile at low temperature[387] and to retard the anatase to rutile phase transition to temperature up to 800 °C.[380] Nature's ability to produce complex biominerals with precision and consistency remains unrivaled by any artificial process. To date, the most impressive outcome of studies into biomineralized titania structures is that of Kröger and co-workers, with their hierarchical rutile structures formed in the presence of silaffins. A range of morphologies are accessible from biomimetic methods, including particles in the nano and macro range as well as hollow NPs. Despite these achievements, the fine-
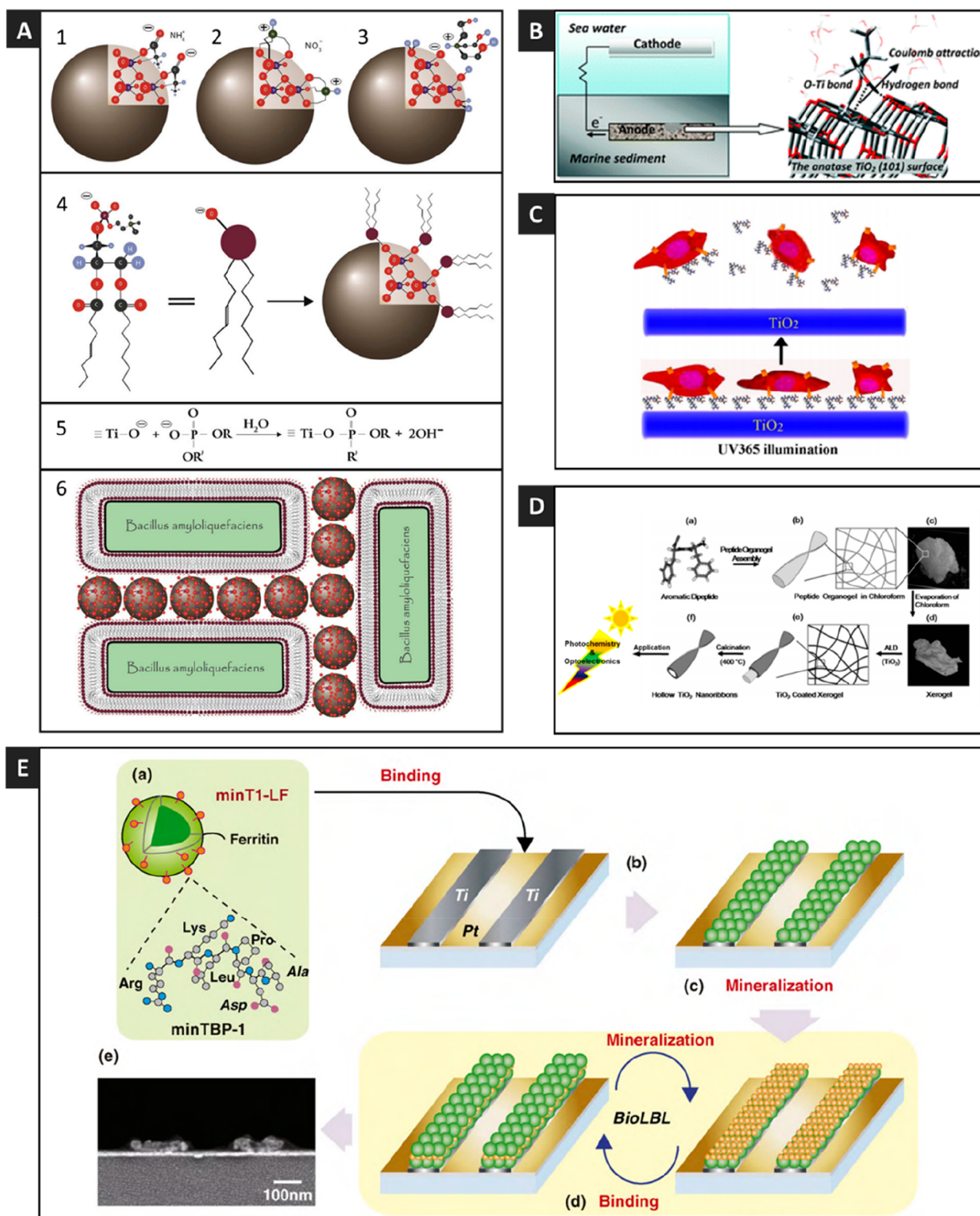
Figure 10. Examples of applications driven by titania-biomolecule interactions. (A) Selective bacterial growth adapted with permission from ref 83. Copyright 2015 Nature Publishing Group. (B) Anode in benthic microbial fuel cell (MFCs) adapted with permission from ref 395. Copyright 2014 Royal Society of Chemistry. (C) Light-induced cell detachment reprinted with permission from ref 84. Copyright 2016 Elsevier. (D) Synthesis of highly entangled hollow TiO_2 nanoribbons for photochemistry and optoelectronics adapted with permission from ref 377. Copyright 2009 Royal Society of Chemistry. (E) Biomimetic layer-by-layer (BioLBL) reprinted from ref 85. Copyright 2007 American Chemical Society.

tuning of structure, morphology, size, and crystallinity is currently far less controllable than for materials generated using traditional synthetic paths. Unfortunately, due to the small yields produced (reaction scale has been very small in biomimetic as compared to traditional methods, limited by biomolecule availability), a comprehensive characterization of the biomineralized titania is not always possible. To evaluate catalytic properties and mechanistic aspects of the process, studies should focus on mineralization using well-characterized hydrolytically stable complexes other than TiBALDH.

3.4.3. Binding Studies of Biomolecules with TiO$_2$.

The mechanisms of interaction at the inorganic/biomolecule aqueous interface underpins most of the applications of TiO$_2$ in nanomedicine and other biological fields. As an example, rationalization of the mechanism guiding molecular recognition is fundamental to understanding biocompatibility and osseointegration of orthopedic implants and can open new opportunities for direct mineral formation. Important work on the identification of surface binding motifs on titania (similarly to silica) is based on combinatorial methods (e.g., biopanning using phage display libraries). Phage-displayed peptides are often claimed to be able to identify specific surfaces via some sort of molecular recognition. However, some sequences show some level of promiscuity,[255] binding to more than one surface or even more than one material. Therefore, binding affinity must be confirmed and quantified. This is often achieved by QCM-D as done by Sano and Shiba for the RKLPDA motif and Puddu and co-workers[86] for sequences Ti-1 (QPYL-FATDSLIK) and Ti-2 (GHTHYHAVRTQT). A good indicator for the validity of the combinatorial approach is that binding studies confirm the affinity of the panning experiment. However, there is a general inconsistency in the materials used to select the binding peptides and those used for the peptide binding tests. So, for the examples mentioned above, the material panned against was described as titanium particles and a commercial titania powder sample, respectively, and the binding properties were characterized on titanium sensors. In both studies, it is assumed the surface of titanium sensor is covered by a TiO$_2$ layer, but no surface characterization data is provided. It is well-accepted from experimental and simulation studies that charged amino acids (i.e., Arg, Lys, Asp, Glu) and to a lesser extent polar amino acids (i.e., Ser, Thr, Asn, Gln, Tyr) display the greatest amount of adsorption to TiO$_2$, whereas hydrophobic residues (i.e., Val, Leu, Ile, Phe) exhibit negligible to zero binding affinity.[87] Yet, the affinity of biomolecules containing a range of classes of amino acids to TiO$_2$ is much less clear and more information on the influence of biomolecule conformation, competing interactions, the role of water and buffer molecules is required.

We now consider the interaction between TiO$_2$ and other biomolecules such as DNA. A noteworthy study with potentially historical implications was carried out by Cleaves and colleagues who proposed roles for several nucleic acid functional groups (including sugar hydroxyl groups, the phosphate group, and extra cyclic functional groups on the bases) in binding. Their results suggest a novel preferred orientation for the monomers on rutile surfaces.[30] The adsorption of small nucleic acid components (nucleotides, nucleosides, and their nitrogenous base components) on various minerals such as rutile is of interest from the standpoint of geochemical markers for life and may have some relevance to the origin of a primordial RNA world.[388]

3.5. Applications of Biomolecule-TiO$_2$ Interactions

When considering examples of applications driven by titania-biomolecule interactions, several investigations have focused on the interaction of various biomolecules, including oligonucleotides with TiO$_2$ surfaces for implant, scaffold, sensor, detoxification, and drug delivery applications.[389] Most research in the area utilizes biomolecules attached to the surface of titania, and in most cases, the success of the application itself is dependent on TiO$_2$-biomolecule interactions. This is a distinct area of research in that molecular scale interactions involve preformed titania. One specific example is a cleavage process which targets proline groups within peptides and proteins using light-generated radicals from a TiO$_2$ surface.[390] This process has the potential to be highly selective, inexpensive, rapid, and tuneable, and is considered an encouraging alternative approach to proteolytic enzymes or chemical agents which typically require a second reagent to discontinue cleavage.[390] In another example, TiO$_2$ nanotubes (TNs) were immobilized with horseradish peroxidase to create a novel photoactive material for photo-electrochemical biosensing of H$_2$O$_2$.[391] This strategy has pioneered applications of nanotubular TiO$_2$ in visible light activated photoelectrochemical biosensing.

In biomedical applications, anatase was shown to be a better osteoconductive polymorph than rutile and brookite.[392,393] It was recently reported that a layer of 3D rutile nanorods on titanium improves osteointegration and bone formation capacity.[394]

Anatase NPs produced from the TiBALDH precursor and using the patented "Captigel" method have been used to support the growth of beneficial rhizobacteria in the colonization of the roots of oilseed rape, Figure 10A.[83] The charges on the nanoparticles allow formation of inner sphere complexes with phospholipids, thus titania NPs were able assist bacterial growth via the formation of clusters (Figure 10, A1–A5), resulting in increased bacteria adhesion at the plant root and associated protection against fungal pathogens.[83] Anatase TiO$_2$ (101) surface selectivity for laevo- serine (L-Ser) has been investigated in detail by the DFTB-D method to design bacteria-friendly anodes for unmediated benthic microbial fuel cells (MFCs), Figure 10B.[395] This paper is interesting in that it uses a theoretical approach to characterize the energetic aspects of adsorption to support design of an anode with a specific application.

In a highly cited paper with implications for the development of advanced tissue engineering, arginine−glycine−aspartic acid peptide (RGD) was immobilized via simple physical adsorption to TiO$_2$ nanodot films to produce an efficient light-induced cell detachment method for cell harvesting, Figure 10C.[84]

We conclude this section with some examples of advanced functional materials prepared by a biomimetic approach. Figure 10D shows how the templating effect of self-assembling diphenylalanine in combination with atomic layer deposition can form highly entangled hollow TiO$_2$ nanoribbons with potential applications in photochemistry and optoelectronics.[377] An interesting cytocompatible process for cell-surface deposition of anatase thin films on chlorella cells was achieved using the peptide sequence (RKK)$_4$D$_8$ and TiBALDH. This process retains cell viability and metabolic activity and increased their tolerance to thermal stress.[396] Finally, we mention the biomimetic layer-by-layer (BioLBL) approach developed by Sano and colleagues.[37,397,398] This research is important as it shows a successful example of how a biomimetic approach can assist in overcoming technological issues in traditional methods, in this specific case, interlayer diffusion in heterogeneous structure obtained by layer-by-layer deposition. BioLBL uses engineered ferritin nanoparticles decorated with sequence RKLPDA (TBP) as building blocks (Figure 10E). TBP was identified as both a good binder and able to mediate the mineralization of materials including titania, silica, and silver.[399] The bifunctionality of TBP allows binding to a Ti nanopattern on a Pt substrate and
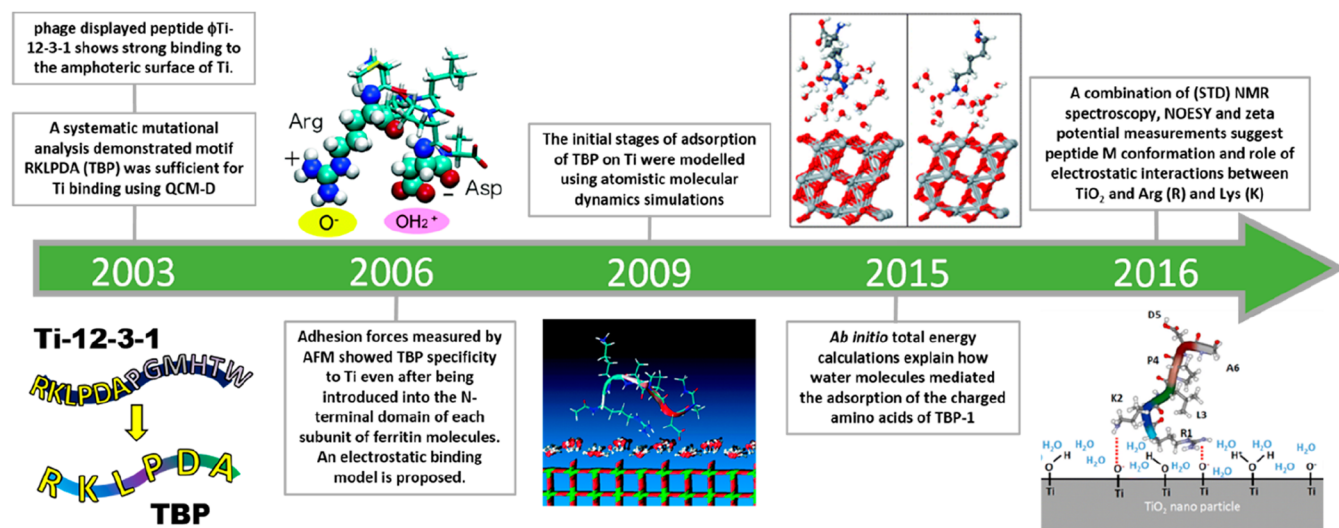
Figure 11. An example of research pathway to understanding biomolecule−surface interactions using a combination of multiexperimental and theoretical approaches. (Left to right) Adapted from ref 63. Copyright 2003 American Chemical Society. Reprinted from ref 375. Copyright 2006 American Chemical Society. Reprinted from ref 400. Copyright 2009 American Chemical Society. Reprinted with permission from ref 404. Copyright 2015 Royal Society of Chemistry. Reprinted from ref 403. Copyright 2016 American Chemical Society.

mineralization of titania on the outer surface of the nanoparticle. The binding and mineralization cycles can be repeated to achieve controlled growth of homogeneous or heterogeneous multilayered structures. The presence of ferritin allows for sufficient segregation between layers and thus minimizes interlayer diffusion.

3.6. Techniques Directly Probing TiO₂-Biomolecule Interactions

Interactions between peptides and titania have been analyzed by using various high-profile experimental tools including QCM-D, SPR, CD, etc. and complemented by computational studies (MD and DFT). A range of information including binding affinity and selectivity, kinetics, and thermodynamics involving surface coverage and biomolecule conformation have all been derived. A combined approach of multiple experimental and theoretical approaches is necessary if we want to progress in our understanding of the biomolecule/titania interface. To illustrate such a research pathway for a biomolecule-metal oxide system involving both experimental and theoretical work, we discuss some of the milestones in the study of the pioneering titanium-binding peptide sequence TBP (RKLPDA) (Figure 11).

The process started with the identification and study of phage harboring peptide ϕTi-12-3-1, with sequence RKLPDAPGMHTW and subsequent identification of RKLPDA as the motif responsible for the binding properties.[63] The qualitative binding mechanism proposed initially by Sano and Shiba involves the concomitant electrostatic interaction of the positively charged side chain of Arg1 and the negatively charged side chain of Asp5 to the amphoteric TiO₂ surface; however, no hard experimental evidence supported this binding model.[63] This promoted further experimental studies on TBP-binding specificity and the role of its primary structure. Hayashi et al.[375] used atomic force microscopy (AFM) to study the role of amino acid residues in binding using TBP and its mutations fused to ferritins. Sequences obtained by replacing Arg1, Lys2, and Pro4 in TBP with Ala were found to be weaker binders to TiO₂; the authors therefore concluded that the geometric configuration of

charged residues affects the binding strength. Molecular dynamic simulations were used to characterize the initial stages of TBP adsorption to the titania−water interface and the role of water layers in surface recognition.[400,401] Simulation shows how anchoring to the surface occurs via the Arg R1 residue, with contributions from positively charged Lys K2 and, in part, the negatively charged Asp D5.[401] This result is consistent with the experimental results on alanine substitution.[402] Recent NMR experiments confirm the importance of conformation rigidity provided by proline (as suggested by Sano) but proposed an M-shaped conformation upon binding (rather than C shape observed upon TBP binding on silica)[236] and indicate that Arg R1 and Lys K2 residues interact with the titania aqueous interface.[403]

It is evident from the above example that given the complexity of the bioinorganic interface, our understanding is being continuously revised and refined as new, more detailed information becomes available from experimental and/or theoretical studies. The main experimental and computational contributions that have advanced our understanding of binding affinity and selectivity, with emphasis on quantitative and kinetic studies and biomolecule mode of adsorption, are discussed in sections 3.6.1 and 3.6.2, respectively.

3.6.1. Experimental Studies of Surface Interaction. QCM-D is a powerful technique to follow and quantify surface binding and is often used to test the binding affinity of candidates suggested by biopanning experiments. Several binding peptides have been studied on Ti sensors. These sensors are generated by physical vapor deposition of titanium onto a quartz disc. The resulting material is polycrystalline[402,405,406] with a surface roughness (before analysis) of 1.7 ± 0.2 nm, though we are not aware of any studies that explore the surface after analysis. It is assumed that the surface of Ti in these sensors is covered by a charged amphoteric oxide film composed of amorphous and nonstoichiometric TiO₂, as previously mentioned,[369] though most publications do not either characterize the QCM-D surfaces and/or do not think to consider the difference important. Further, sensors are replaced on a regular basis as binding is found to decrease with usage,

suggesting that the surface deteriorates with time but again this is not usually reported.

As an example, the kinetic adsorption of peptide Ti-1 (QPYLFATDSLIK) and Ti-2 (GHTHYHAVRTQT) were investigated.[86] Ti-1 shows lower affinity to the titanium sensor and a more gradual adsorption than does Ti-2. This difference in adsorption kinetics was attributed to possible differences in the binding forces, which based on the peptide's primary structures are assumed to be mainly electrostatic for Ti-1, and with a strong H-bonding contribution for Ti-2. Kojima combined reflectometric interference spectroscopy (RIfS) with QCM-D to quantitatively analyze adsorption and solvation of proteins and lipid vesicles on the TiO$_2$ surface. The surface was prepared by anodization of a titanium support, with controlled thickness. This elegant approach showed how QCM-D alone can overestimate the amount of absorbate.[407]

The main experimental technique to study biomolecule conformation in solution and conformational changes in the presence of a mineral surface is CD spectroscopy.[408,409] Changes in secondary structure were revealed in the case of proteins, for example, trypsin, when exposed to TiO$_2$ and linked to the loss of enzymatic activity.[409] In the case of peptide/mineral interactions, CD spectroscopy provides less information about actual conformational change but can still be used to probe interactions in solution. As an example, in the presence of a Ti precursor, shifts or reduction in peak intensities were shown in the cases of Ti-1 and Ti-2 peptides. While such small changes suggest an interaction, it is difficult to relate them to the molecular structure or binding mechanism.[86]

Changes in protein structure upon interaction with surfaces are also investigated by reflectance Fourier transform infrared spectroscopy (ATR-FTIR) as peak shifts or changes in the amide I/amide II ratio indicate changes in structural conformation).[410,411] As an example ATR-FTIR in combination with thermogravimetric analysis enabled characterization of surface coverage on a TiO$_2$ surface.[410] With the use of this approach, it was shown that BSA unfolds in the presence of TiO$_2$, permitting more effective surface binding via electrostatic interactions. However, conformational changes are better understood when complementing experimental data with computational studies, as discussed in section 3.6.2.

Mirau et al. developed high-resolution NMR methods, including NOESY and saturation transfer difference (STD), to study the 3D structure of peptides, including TBP (RKLPDA) adsorbed on fumed silica and titania P25 NPs.[236] Both conformation and orientation of TBP on titania were obtained and unexpectedly were the same as those adopted on fumed silica.[236] A C-shaped conformation for TBP upon binding was proposed; however, little insight on the interactions between peptide and titania or consideration of the titania surface properties are provided. More recently, STD NMR in conjunction with zeta potential measurements were used to characterize the TBP-TiO$_2$ interactions, and the structure and dynamic nature of TBP bound to TiO$_2$ nanoparticles in solution was determined.[403] In accordance with the STD data and zeta potential measurement, the N-terminus acts as a binding anchor with residues Arg1 and Lys2 interacting directly with the negatively charged surface by electrostatic forces. TBP structure upon binding is proposed to be M shaped.[403] In comparison with previously suggested binding models for TBP, this is the first one that takes into account the surface charge speciation derived from experimental data.

3.6.2. Computational Studies of Surface Interactions.
Computational simulations have been used to explore the biomolecule−TiO$_2$ interface. Zapol and Curtiss reviewed literature up to 2007 on the theoretical studies of the interaction of various biomolecules with the anatase and rutile forms of TiO$_2$, relevant to functionalization of TiO$_2$ NPs for applications in catalysis, solar energy, sensors.[412] When simulating the biomolecule/inorganic interface, it is important to consider plausible models of the inorganic surface and the biomolecule in the presence of liquid water. Many computational studies focus on ultrahigh vacuo behavior, which is clearly a nonrealistic representation of the biomolecule/ mineral interface, or use an ideal rutile (110) etc., which does not reflect the chemical complexity of the exposed surface as discussed in section 3.3.[356] The use of realistic surface models and force fields can drastically improve the reliability of molecular dynamics simulations to complement or even predict experimental data, as shown by Emami et al. in the case of silica.[39] We start our discussion providing some examples of research that uses or develops appropriate and validated force fields.

3.6.2.1. Force Fields and Models. To allow for molecular dynamic simulation, the interaction potentials of all species involved must be known or represented by a model. Models that describe the inorganic surface must be validated by comparison with well-characterized physical properties. A remarkable contribution to the understanding of the atomic scale of the rutile (110) aqueous interfacial region and electrical double layer was that of Predota and collaborators who in a series of contributions developed a reliable force field for rutile (110) surfaces applicable to the study of biomolecules.[366,373,413] The development of this force field was elegantly supported by a range of in situ X-ray crystal truncation rod (CTR) measurements of rutile (110) single-crystal surfaces in liquid water at room temperature. Predota's force field is at the center of subsequent variations used in several simulation studies of the (110) rutile surface.[87,400]

A force field to model Ti/TiO$_x$/water interfaces has been developed by Schneider and Ciacchi.[414] This model takes into account the oxidation and hydration reactions of titanium surfaces as discussed in section 3.3 and is developed to match Ti isoelectric point and surface charge consistently with typical experimental values at neutral pH and low ionic strength.[415]

A biomolecule is generally described by well-established force fields such as AMBER[401] or CHARMM.[416] The aqueous solution should include liquid water and dissolved ions. Common models for liquid water are TIP3P and SPC/E, which do not consider water dissociation. This is generally considered appropriate for studies on an ideal surface, as H$_2$O dissociation is unlikely to occur unless on surface defects, as described in section 3.3. However, we need to keep in mind that many real titania/biomolecule interfaces do not use ideal surfaces but amorphous or polycrystalline surfaces with defects; hence, in these systems, water dissociation could be a better representation of the early stages of water adsorption. To the best of our knowledge, a dissociative water model applicable to large computations in the presence of electrolytes is not currently available, thus associative models represent a reasonable compromise between the accurate description of the physical properties of bulk water and their electrolytes and computational efficiency.[373] A simplified force field for simulating amorphous TiO$_2$ nanoparticles, rather than
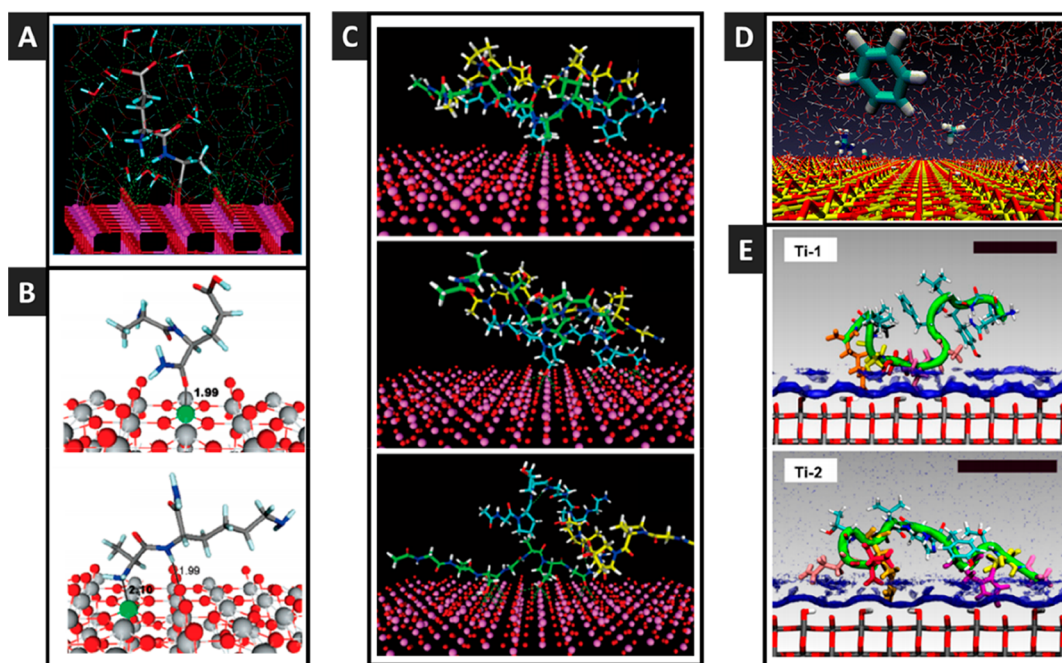
Figure 12. Examples of simulation snapshot of biomolecules on rutile (110) titania surfaces (A) representative structure of the Ala-Glu + water complex reprinted from ref 364. Copyright 2006 American Chemical Society. (B) Dipeptides L-Ala-L-Glu (top) and L-Ala-L-Lys (bottom) reprinted from ref 418. Copyright 2008 American Chemical Society. (C) Binding dynamic of triple helical segment reprinted from ref 419. Copyright 2007 American Chemical Society. (D) Amino acid analogues reprinted from ref 416. Copyright 2014 American Chemical Society. (E) Ti-1 and Ti-2, predicted from the REST-only simulations scale bars: 1 nm. Reprinted from ref 87. Copyright 2016 American Chemical Society.

crystalline surfaces, was recently developed by Luan et al. and applied to the study of biomolecule adsorption.[417]

Experimental work is often carried out at high ionic concentration, and this should be taken into account when correlating simulation results with experimental work.[402] While the potential for the inclusion of ions compatible with different liquid water models is available,[373] most works do not include their contribution or do not use them at concentrations comparable to real life experiments. There is therefore a lack of understanding on the effect of high ion concentrations at the biomolecule/TiO$_2$ interface. Further, it must be noted that comprehensive pH-resolved surface models for titania surfaces have not yet become available.[239]

3.6.2.2. Adsorption Conformation and Mechanism of Interaction. Atomistic molecular dynamic simulations complemented by ab initio calculations can provide important geometrical information, such as atom surface distance, peptide backbone, and side chain geometries upon binding.

The use of simple dipeptides has provided important insight on binding anchoring points onto the TiO$_2$ rutile (110) surface. Figure 12A shows an early report using a MD simulation to indicate that the C-terminal polar group provides an anchor to the surface with a bidentate interaction involving both carboxyl oxygens and two adjacent undercoordinated Ti atoms.[364] In another study, classical MD simulations in conjunction with XPS suggest carbonyl oxygens and nitrogen atoms as most probable surface contact points (Figure 12B).[418]

The dynamics of biomolecule conformational changes upon binding were elegantly simulated for a type I collagen triple helical segment comprising 21 amino acids.[419] A clear disruption of the otherwise stable secondary structure in solution, upon binding to rutile (110), was suggested in a classical MD simulation study as shown in Figure 12C.[419] The binding mechanism involves hydroxyproline and proline

residues through a combination of Ti–O coordination and hydrogen-bond interactions, resulting in strong adsorption of the peptide to the TiO$_2$ surface.

Calculations of the binding free energy of various amino acid side chains at the negatively charged aqueous rutile (110) interface suggest that charged amino acid analogues have a stronger affinity for a TiO$_2$ surface compared to uncharged amino acid analogues.[416] Uncharged amino acid analogues display weak or repulsive interactions with TiO$_2$, the interactions between polar residues may be cumulative and therefore may contribute to their adhesion to TiO$_2$ (Figure 12D).

The role of water at the interface has been suggested to have a crucial role in binding events at the interface. Acidic and charged residues were shown to bind to titania indirectly via interactions with the water layers at the interface, as opposed to the titania surface itself.[400,420] Water activity was found to influence peptide surface interaction, with adsorbed water layers playing an intermediary role by creating hydrogen bonds with hydrophilic peptide groups.[364] Local water density was found to vary on a rough surface and found to favor the binding of peptide sequences of appropriate hydrophilic/hydrophobic motifs capable of matching these changes.[401] Concerning the binding mechanism, enthalpic versus entropic modes of binding were suggested for two titania-binding peptides Ti-1 (QPYLFATDSLIK) and Ti-2 (GHTHYHAVRTQT).[87] These peptides were shown to have similar binding affinity as measured by QCM; however, replica exchange molecular dynamics (REST-MD) suggested dramatically different modes of binding,[87] Figure 12E. The degree and distribution of residue-surface contact support a binding model where Ti-1 without the presence of a strong anchor residue is an entropically driven binder. On the other hand, Ti-2 which features a high number of periodically spaced anchor residues
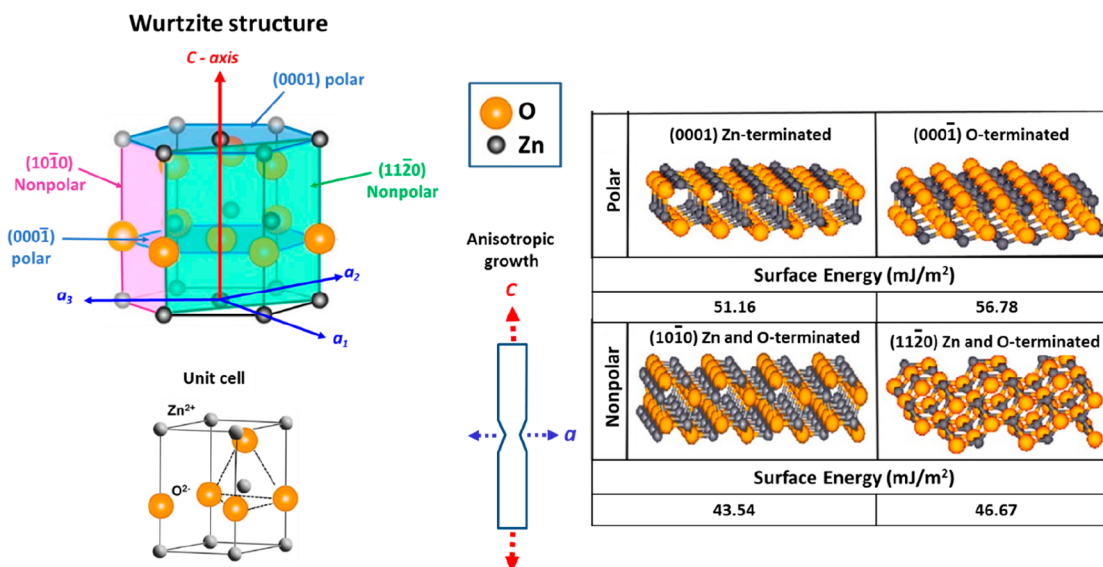
AA

Figure 13. Models of ZnO crystals showing the spatial arrangement of oxygen and zinc atoms forming the Wurtzite crystal structure, anisotropic growth of ZnO along the *c* axis forming rods, and the properties, including surface energies of four low-index ZnO crystal planes. The model of the unit cell of ZnO was adapted with permission from ref 464. Copyright 2012 Elsevier. The model of the Wurtzite crystal structure and the surface energies of the four low-index ZnO crystal planes were adapted with permission from ref 464. Copyright 2012 Elsevier. Note: $(10\bar{2}0)$ and $(11\bar{2}0)$ when expressed in the more conventional 3 digit Miller indices sometimes used in publications are equivalent to the (100) and (110) planes. Examples of both are found in the literature.

along the chain length can be described as an enthalpically driven binder.[87]

3.6.3. Summary. In summary, despite years of study, TiO_2 remains a relevant and exciting material from a surface science perspective. Despite being a nonbiogenic mineral, biomolecule-titania interactions have pivotal roles in a wide range of technological and biomedical applications. Much progress in understanding TiO_2-biomolecule interactions has been made; however, further fundamental knowledge is still required if we are to truly understand and exploit the MO—biomolecule interface. Compared with other oxides, titania surface chemistry and the aqueous interface is well-characterized with substantial experimental and theoretical research available on the most stable surface terminations. This knowledge is not always taken into account when considering interactions with biomolecules, thus limiting advancement of our understanding. This is for both the generation of novel forms of the mineral and for exploiting the surface chemistry by the binding of molecules directly to the surface. Substantial progress in determining surface structures from first-principles has been achieved through theoretical studies (i.e., DFT). The combination of theoretical studies with experimental studies is allowing more realistic representations of the interactions of biomolecules including molecules such as water with the surface of TiO_2.

3.7. Toxicology of TiO_2

In the past decade there has been a rapid growth in publications regarding the safety of TiO_2. TiO_2 particles were originally considered to possess low toxicity,[421] but this general consensus was contested after lung tumors were discovered in rats exposed for two years to high concentrations of fine TiO_2 particles.[422] This revelation caused The International Agency for Research on Cancer to swiftly class TiO_2 as a Group 2B carcinogen (possibly carcinogenic to humans); however, this move has since been questioned as it emerged that the observed tumorigenic effect may have been

attributed to lung overload instead of the specific carcinogenicity of fine TiO_2.[421,423]

Further studies have shown that NPs of TiO_2 possess physiochemical properties that affect their biological behavior, and thus potentially these nanoscopic particles offer a greater safety concern compared to larger particles.[424−426] Since interest in this material has grown significantly over recent years, the research community has begun to realize what was once regarded as a benign material with low toxicity may not be the case with many credible sources of information highlighting potential toxicity.[424−426]

Today, articles connected with the safety of TiO_2 particles are frequently published, as many research groups explore this important topic.[427−429] The exposure to TiO_2 NPs can be in the form of aerosols, suspensions, or emulsions. To exert toxicity, titania must be able to enter the organism, via inhalation or ingestion. Once in the organism, it has been shown how NPs can migrate and accumulate in other organs, although these studies were carried out on mice and rat models and at concentrations much higher than those encountered in the workplace or daily life.[430] As nanosized TiO_2 is thought to exert greater toxicity due to the increased surface area,[430] the presence of biomolecules on the TiO_2 surface will increase particle size and potentially reduce toxicity.[431]

The use of thin films of good mechanical quality should highly reduce the risk of exposure. Though there is no definitive answer on the topic of the long-term safety of particles at this time, future research into this area may ultimately provide answers to this question.

The toxicity of TiO_2 nanoparticles has potential to be harnessed for the good by the photoinduced toxicity of TiO_2 being exploited for medical and clinical purposes. TiO_2 coated surfaces have been shown to inhibit bacterial growth[331] or be active in photodynamic and sonodynamic therapy of cancer.[330]

4. ZnO

4.1. Introduction to ZnO

Zinc oxide (ZnO) is a II to VI compound semiconductor with a wide direct band gap of ~3.4 eV and a comparatively large exciton binding energy of ~60 meV at room temperature (300 K).[432,433] Naturally occurring ZnO, known as zincite is ordinarily found with impurities including manganese and other elements giving it a yellow or red appearance.[434] Early uses of ZnO date as far back as the Bronze Age where it was produced as a byproduct of copper ore smelting and used for wound healing.[435] For many centuries, its major application was in the production of brass, an alloy of copper and zinc.[435] In the last century, interest in this material has grown rapidly with the discovery of its useful piezoelectric properties.[436] Improvements in synthetic ZnO growth processes has also led to a rise in research, particularly for electrical and optoelectronic applications.[437,438] Emerging technological use includes the making of field emitters, varistors, piezoelectric devices, acoustic wave devices, solar cells, photocatalysts, and transparent conducting materials.[78,439,440] In its polycrystalline form, ZnO has been used as an additive in paint pigmentation, as a lubricant and in the manufacture of rubber.[441,442] Despite debates about the toxicity of ZnO, as will be discussed in this review, it remains an attractive material for biomedical applications.[77,443,444] In the pharmaceutical and cosmetic industry, ZnO nanoparticles (ZnO NPs) are used as an additive for sunscreen or facial powders as they reflect and scatter UV light without damaging human skin.[445] ZnO NPs have also been investigated for use by the food industry in surface coatings and packaging because of its antimicrobial activity.[446,447] Other developing biomedical applications generating attention in recent years is the use of ZnO NPs for drug delivery, gene delivery, cancer therapy, biosensing, and biomedical imaging.[77,444,448,449]

4.2. ZnO Synthesis Methods and Properties

The most common methods to synthesize ZnO nanostructures are either vapor routes (usually at high temperatures, from 500−1500 °C) or solution routes (typically at temperatures below 200 °C). Commonly used vapor route techniques are vapor phase transport,[450−452] physical vapor deposition,[453,454] and chemical vapor deposition.[455−457] Frequently used solution routes are hydrothermal methods,[458] chemical bath deposition (CBD),[459] spray pyrolysis,[460] electrophoresis,[461,462] and microwave-assisted thermal decomposition.[463] Depending on the synthesis process used, three crystal forms of ZnO can be formed; rock salt which requires relatively high pressure for its formation, zinc blende which can only be synthesized using cubic substrates, and the wurtzite structure which is the thermodynamically stable phase synthesized under ambient reaction conditions.[438,459]

When biomimetic synthesis strategies are used, ZnO typically crystallizes in the wurtzite form; Figure 13 shows hexagonal symmetry, a space group $C6mc$ and lattice parameters a = 0.325 and c = 0.521 nm giving it a c/a ratio of 1.60, which is close to the elementary translation vectors of an ideal hexagonal unit cell (c/a = 1.633).[432,433] The wurtzite structure consists of tetrahedrally coordinated ions where one Zn^{2+} ion is surrounded by four O^{2-} ions and vice versa forming alternating planes that are stacked along the c axis, resulting in a structure with no central symmetry.[464,466] Crystal morphology is controlled by a combination of energetic and kinetic factors. Characteristically, using solution synthesis methods that employ alkoxides or various simple salts as precursors without additives, elongated hexagonal crystals having both polar and nonpolar planes are formed, Figure 13.[18,27,459,467,468] The most common basal planes are the positively charged (0001) Zn-terminated and the negatively charged (000$\bar{1}$) O-terminated polar planes.[459,469,470] The more thermodynamically stable nonpolar planes such as the (10$\bar{1}$0) and (11$\bar{2}$0) planes contain both Zn and O species.[459] The oppositely charged (0001) and (000$\bar{1}$) polar planes result in a dipole moment across a crystal and have higher surface energy than the nonpolar surfaces; therefore, to lower the free energy of the system, incoming precursor ions favorably adsorb to the polar planes resulting in anisotropic crystal growth along the c axis with the formation of elongated hexagonal crystals.[18,27,467] With the use of solution synthesis methods, one- (1D), two-, and three-dimensional ZnO structures have been formed. 1D ZnO structures have the most abundant and diverse configurations including rods,[33,471,472] plates,[33] disks,[27] needles,[473] tubes,[474] rings,[27,475] belts,[476] wires,[476] prisms,[477] pyramids,[478,479] flowers,[479,480] and spheres.[481] Remarkably, further morphology modification including the formation of mesoporous structures with enhanced surface area has been achieved in a controlled fashion using biomolecules such as amino acid and peptides.[32,33,43,80] What is clear from the extensive literature on this material is that the vast morphological landscape reflects the relative energies of the various crystal faces expressed/allowed to grow. The system is a good one to study in that small changes in reaction conditions manifest themselves in directly observable differences. However, this factor also causes problems in terms of reproducibility and in the understanding of which specific change in the reaction medium has led to the observed effect. This will be discussed in detail further on in this review in the section, Techniques Directly Probing ZnO-Biomolecule Interactions. It is incredibly important to the community that full details of experimental protocols are reported so that others can extend a particular area of research.

4.3. Surface Chemistry of ZnO

Characterization of the surface in relation to the liquid phase is very important as physicochemical properties of the surface directly influence interaction with other chemical species including biomolecules. The surface of ZnO has been studied using experimental, theoretical, and computational techniques such as low energy electron diffraction (LEED), X-ray photoelectron spectroscopy (XPS), X-ray emission spectroscopy (XES), scanning tunneling microscopy (STM), and density functional theory (DFT).[482−484] STM has been particularly useful for structural characterization of ZnO surfaces at the atomic scale.[482,483] For example, using STM microscopy, the surface of the (0001) plane has been found to be rough with triangular step edges, small terraces, holes, and islands, whereas the (10$\bar{1}$0) plane has been described as a surface with a well-defined flat (small roughness) terrace step structure associated with ZnO dimers that are elongated and aligned along the (0001) or ($\bar{1}$2$\bar{1}$0) direction.[482−484] The adsorption (physisorption and chemisorption) of solvent molecules on the surface of ZnO has also been of considerable research interest.[485,486] For example, in water, the surface of ZnO is hydrolyzed forming hydroxide layers which, depending on solution pH, become charged by reacting with either H^+ or OH^- ions due to the surface amphoteric nature of ZnO and $Zn(OH)_2$.[485] Characterization of the surface in relation to the

liquid phase is crucial as it will directly influence interaction with other chemical species including biomolecules. Understanding the surface properties and surface terminations is essential for the atomistic understanding of binding behavior as well as being able to compare data between experimental studies and simulations. Therefore, we highlight what is known regarding the surface properties of ZnO, focusing on the influence of an aqueous environment.

The investigation of the facet specific interaction of H_2O with ZnO started in the early 1980s.[487] Researchers studying various stable ZnO faces found different water surface interaction patterns including complete or partial dissociation of water which generated different kinds of hydroxyl groups, water adsorption, and indicators of the formation of H_2O bilayers and multilayers.[484] Variations in these patterns obtained from experimental and computational approaches indicate that the H_2O/ZnO interface is very complicated. Even more challenging is that disputes and differences persist in computational approaches used to study ZnO surfaces, whether in vacuum or a more realistic aqueous environment. Computational methods that have been used to study ZnO surface include MD, density functional theory based tight binding (DFTB) density functional theory (DFT), and reactive force field (ReaxFF). Herein, we will discuss some studies where these computational methods have been used and thought to result in conclusions that complement/support experimental studies.

4.3.1. Nonpolar ZnO Surface in an Aqueous Environment. As previously mentioned, the ideal $(10\bar{1}0)$ ZnO surface (as well as the $(11\bar{2}0)$ facet) is terminated with both zinc and oxygen atoms and is therefore nonpolar and stable in contrast to the polar surfaces. The surfaces possess the same periodicity as the bulk crystal.[487] The $(10\bar{1}0)$ surface comprises ZnO dimers that are partially coordinately unsaturated and can act as Lewis acid or base sites. The unsaturated linkages are tilted from the surface with the oxygen atom being on the outside.[488,489] The characteristic structure appears as a series of rows separated by trenches along the $(11\bar{2}0)$ direction.[482]

The interaction of H_2O with the ZnO $(10\bar{1}0)$ surface has also been extensively investigated by quantum chemistry calculations (DFT)[490] where a surface pattern with (2×1) periodicity under a monolayer of water was identified. This result was in good agreement with previous STM investigations.[491] The (2×1) superstructure led to the formation of a strongly bound hydrogen-bonding network, while molecular adsorption was preferred at lower water coverage.[492] For all studies discussed below, unless otherwise stated, the (2×1) superstructure is referred to. In another study, MD simulations applying a reactive relatively recently developed force field (ReaxFF) was used to study the monolayer coverage adsorption of water on flat and stepped ZnO $(10\bar{1}0)$ surfaces at three different temperatures.[493] This study also confirmed the occurrence of an equilibrium between molecularly and dissociatively adsorbed water on the $(10\bar{1}0)$ surface.[493] ReaxFF force field is designed to simulate the breaking and formation of bonds during dynamics and has only recently been adapted to model interactions between ZnO surfaces and water molecules.[493] The accuracy of ReaxFF is often disputed as it attempts to simulate complicated electronic effects using simple potential energy functions.[494] Although many questions remain about the different computational approaches used, the current disagreements are certainly a vital healthy step toward developing accurate simulations of complex surfaces like ZnO

and subsequently precise modeling of ZnO-biomolecule interactions.

High-resolution electron energy loss spectroscopy (HREELS) and thermal desorption spectroscopy (TDS) studies of water interaction with the mixed-terminated ZnO $(10\bar{1}0)$ surface at ambient conditions also provide evidence for the development of a well-defined superstructure based on the partial dissociation of water molecules. This observation was confirmed by infrared data which show the water-induced O—H stretching modes at 3193 and 3709 cm^{-1} as well as the peak at 3677 cm^{-1} arising from the OH species. The red shift indicates strong hydrogen-bonding interactions of H_2O to neighboring adsorbate molecules as well as the surface oxygen atoms that are responsible for the partial dissociation of water molecules on the perfect ZnO $(10\bar{1}0)$ surface.[495]

The hydroxyl groups on mixed-terminated ZnO $(10\bar{1}0)$ surfaces have been studied by infrared spectroscopy where partial dissociation of water was observed leading to coexisting H_2O ($\sim$3150 and 3687 cm^{-1}) and OH species (3672 cm^{-1}). Furthermore, isolated OH species (3639 and 3656 cm^{-1}) could be identified for the mixed-terminated ZnO $(10\bar{1}0)$ surface. The interaction of H_2O with surface defects was suggested to yield hydroxyl groups (or O—H$\cdots$O species) (3564 and 3448 cm^{-1}).[496] In contrast to the 50% dissociated water model for monolayer structure, an alternate model of a fully dissociated (1×1) monolayer has been proposed based on results from synchrotron-based ambient pressure X-ray photoelectron spectroscopy (APXPS).[497]

In other studies on the same crystal face combining STM and DFT, most H_2O molecules were found to be in the half-dissociated (2×1) superstructure, which is the lowest-energy configuration. However, the authors also identified the coexistence of an energetically, almost degenerate, configuration which corresponds to a fully molecular water monolayer. A continuous switching between these two states via a dynamical process of association and dissociation was suggested to occur.[498] It is clear from the literature that even for this purportedly stable surface, there is still some disagreement as to the exact nature of the ZnO—water interface. Clearly this has huge implications for how we approach the development of models to use in our studies of biomolecule- material interaction from both the design and execution of experiments and computational simulations. Particularly for the latter, a bad choice of surface/water construct will lead to very different outcomes.

4.3.2. Polar ZnO Surface in an Aqueous Environment. In comparison to the ZnO (1010) surface, the polar stable surfaces of ZnO are less well-studied. These surfaces are very important in bioinspired ZnO materials. The stability of such surfaces is problematic as the atomic configurations and associated electronic structure of the surface very much depend on the preparation techniques and conditions.[499] The (0001)-Zn and (0001)-O surfaces may be viewed as planes of Zn and O, respectively, that are coordinatively unsaturated and present dangling bonds at the surface. Due to partially filled energy levels, a surface perpendicular dipole moment is developed, creating surfaces which are expected to be unstable and prone to reconstructions.[489,500] Stabilization of the surface has been proposed to occur through the creation of metallic surface states,[519] geometric reconstruction,[482,483] randomly distributed vacancies,[501] impurity atoms in the surface layers, or the presence of charged adsorbates.[484,489] The conditions used to prepare and observe the material itself will almost certainly
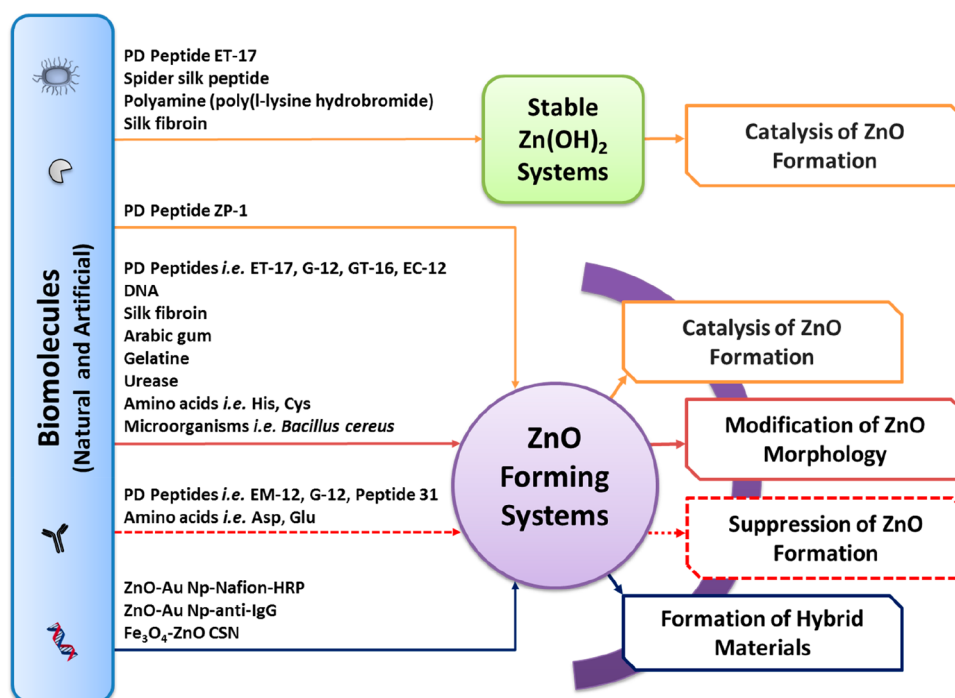
Figure 14. Examples of the effects of biomolecules on ZnO and stable $Zn(OH)_2$ forming systems: (i) catalysis of ZnO formation by phage display (PD) identified peptide ET-17, ET-17 fused to collagen triple helix, spider silk peptide,[523] polyamine, ZP-1 (GAMHLPWHMGTL), and silk fibroin.[525] (ii) Modification of ZnO morphology by PD peptides (ET-17, G-12, GT-16, and EC-12), DNA,[508] silk fibroin, arabic gum, gelatin,[535−537] urease,[509] amino acids, and microorganisms. (iii) Suppression of ZnO formation by PD peptides and amino acids,[43] and (iv) formation of hybrid materials such as ZnO-Au NPs-Nafion-horseradish peroxidase (HRP)-modified glass carbon electrode nanocomposite,[538] Au Np-anti-immunoglobulin G (IgG) conjugates,[544] and Fe_3O_4-ZnO core−shell nanoparticles (CSN).[76]

affect the surface structure and lead to some of the variability in surface structures reported.

Examples of methods used to characterize the unstable surfaces include UHV scanning tunneling microscopy where nanosized islands with a size-dependent shape and triangular holes with single-height steps were identified with corresponding ab initio calculations predicting triangular-shaped reconstructions over a wide range of oxygen and hydrogen chemical potentials.[502] The reconstruction was proposed to be electrostatically driven with the overall decrease of the surface Zn concentration stabilizing this polar surface. There is even a report of a particular amount of charge transfer needed to stabilize the polar surface [$\delta = (1-2u)Z \approx Z/4$].[489] In addition to triangular phases, a coexisting (1×1) surface reconstruction has also been observed.[503] Moreover, if the surface charge can be reduced by $1/3$ (which is more than the estimated reduction of 25% from a classical ionic model) then the electrostatic instability of polar ZnO surfaces can be eliminated.

The surface/H_2O interface is important as water is involved in many reactions, for example as a reactant, solvent, or contaminant.[504] A recent review by Costa et al., in 2016, on the adsorption of amino acids and peptides on metals and oxides in an aqueous environment highlights the importance of water molecules on the surface chemistry, the adsorbed chemical form, and its distribution on the surface.[505] A complementary computational study exploring the adsorption of selected amino acids on bare and hydrated (one to two hydration layers) ZnO ($10\bar{1}0$) surfaces showed that the calculated binding energies are strongly affected by the presence or absence of this hydration layer.[506] Clearly these outcomes are important for us to consider as we develop our

understanding of the ZnO biomolecule interface, whether it be through computational or experimental approaches, and is an area of research that requires further development. In section 4.5, we will discuss in further detail techniques that have been used to probe interactions between biomolecules and ZnO. First, we highlight the developing technologies exploiting ZnO-biomolecule interactions to underline why it is indeed important to further develop understanding of their interfacial interaction processes.

4.4. ZnO-Biomolecule Interactions and Applications

Realization of the potential applications of metal oxides like ZnO depends on control over its physicochemical properties, which in turn is directly influenced by the synthesis process. This section highlights the growing use of biomolecules in synthesis to control growth and physicochemical properties as well as advancements in applications that exploit ZnO-biomolecule interactions.

4.4.1. Biomolecules Used for ZnO Synthesis. Some of the biomolecules used in ZnO synthesis include gelatin, polyethylene glycol (PEG),[28,507] DNA,[508] silk, albumen, urease,[509] amino acids,[32,43,510] peptides, polyamines, cyclodextrin,[511] egg-shell membranes,[512] palm olein,[513] arabic gum,[514,515] bacteria,[516,517] and viruses.[518−520] As shown in Figure 14, these biomolecules do not only interact with ZnO and form hybrid materials but also influence, in some instances, $Zn(OH)_2$ and ZnO forming systems either by catalyzing ZnO formation,[80,521−525] causing the stabilization of intermediate phases thereby inhibiting ZnO formation[43,526−528] and/or by, in some cases, also modifying ZnO morphology.[32,33,80,509,514,522,525,526,529−531] Artificial ZnO-binding peptides (ZnO-BPs) identified using either CSD or
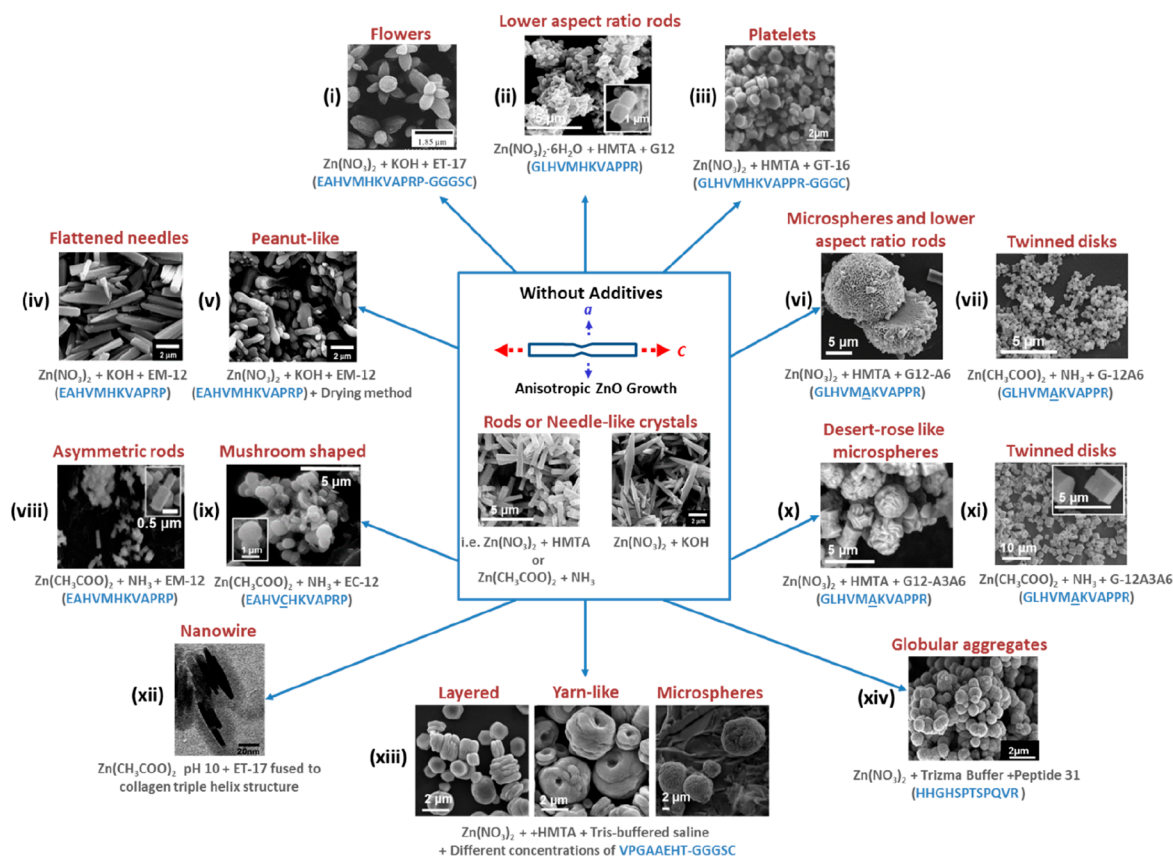
Figure 15. Effect of biomolecules on ZnO morphology. (Central) ZnO rods formed without additives. Left central image reprinted from ref 527. Copyright 2015 American Chemical Society. Right central image reprinted with permission from ref 539. Copyright 2011 Elsevier. Radial SEM/TEM images showing reported modifications of ZnO morphology using ZnO binding peptides (ZnO-BPs) in different hydrothermal synthesis methods; (i) flowers reprinted with permission from ref 80. Copyright 2005 John Wiley & Sons, Inc. (ii) Low aspect ratio rods reprinted from ref 527. Copyright 2015 American Chemical Society. (iii) Platelets reprinted with permission from ref 33. Copyright 2009 Elsevier. (iv) Flattened needles reprinted with permission from ref 539. Copyright 2011 Elsevier. (v) Peanutlike structures reprinted with permission from ref 539. Copyright 2011 Elsevier. (vi) Microspheres and lower aspect ratio rods reprinted from ref 527. Copyright 2015 American Chemical Society. (vii) Twinned disks reprinted from ref 527. Copyright 2015 American Chemical Society. (viii) Asymmetric rods reprinted with permission from ref 539. Copyright 2011 Elsevier. (ix) Mushroom-shaped reprinted with permission from ref 539. Copyright 2011 Elsevier. (x) Desert-rose like microspheres reprinted from ref 527. Copyright 2015 American Chemical Society. (xi) Twinned disks reprinted from ref 527. Copyright 2015 American Chemical Society. (xii) Nanowire reprinted with permission from ref 522. Copyright 2009 Royal Society of Chemistry. (xiii) Layered, yarnlike, and microsphere structures reprinted with permission from ref 529. Copyright 2015 Springer. (xiv) Globular aggregates reprinted from ref 526. 2012 Open access Journal.

PD libraries have particularly shown great potential and versatility in their ability to affect ZnO formation. There is growing interest in understanding ZnO-ZnO-BP interaction mechanisms, the consequences of such interactions, and possible applications that can be developed exploiting such interactions.[33,44,81,526-528,532-534]

Reports of ZnO morphology modification where ZnO-BPs have been incorporated in syntheses include the formation of lower (in comparison to the aspect ratio of ZnO rods formed without peptide) aspect ratio ZnO rods and platelets when G-12 (GLHVMHKVAPPR),[33,44] its derivative GT-16 (GLHVMHKVAPPR-GGGSC),[33,44] EM-12 (EAHVMHK-VAPRP),[80] and certain postselection-modified alanine mutants of G-12[527] were incorporated in the ZnO synthesis under specific growth conditions. Peptide-directed aspect ratio reduction of ZnO rods was also observed when dipeptides from the EM-12 sequence [i.e., $M_5 H_6$ (dipeptide of methionine and histidine found at position 5 and 6 in EM-12 sequence) and $H_6 K_7$ (dipeptide of histidine and lysine found at position 6 and 7 in EM-12 sequence)] suppressed

growth of ZnO along the (0001) direction even more than EM-12 when used in ZnO synthesis.[539]

Interestingly, aside from affecting aspect ratio reduction of ZnO rods through capping, other different morphologies of ZnO have also been formed in the presence of ZnO-BPs. ZnO synthesis with ET-17 (EAHVMHVAPRP-GGGSC), a derivative of EM-12, produced flowerlike ZnO microparticles[80] and when fused to a collagen triple helix structure, ET-17 was able to template the growth of monodisperse single crystalline ZnO nanowires. Other reported peptide influenced ZnO morphologies are peanutlike structures with EM-12, spheres obtained using HHGHSPTSPQVR peptide, G-12 alanine mutants [G-12A6 (GLHVM**A**KVAPPR) and G-12A3A6 (GL**A**VM**A**KVAPPR)],[527] a VPGAAEHT-GGGSC peptide,[529] mushroom-shaped crystals using EC-12 (EAHV**C**HKVAPRP),[528] and yarnlike shapes using the VPGAAEHT-GGGSC peptide.[529] Strikingly, in two of the above studies, this change from aspect ratio reduction of rods to the formation of different morphologies under the same ZnO growth conditions (reaction precursor, temperature, and peptide concentration)
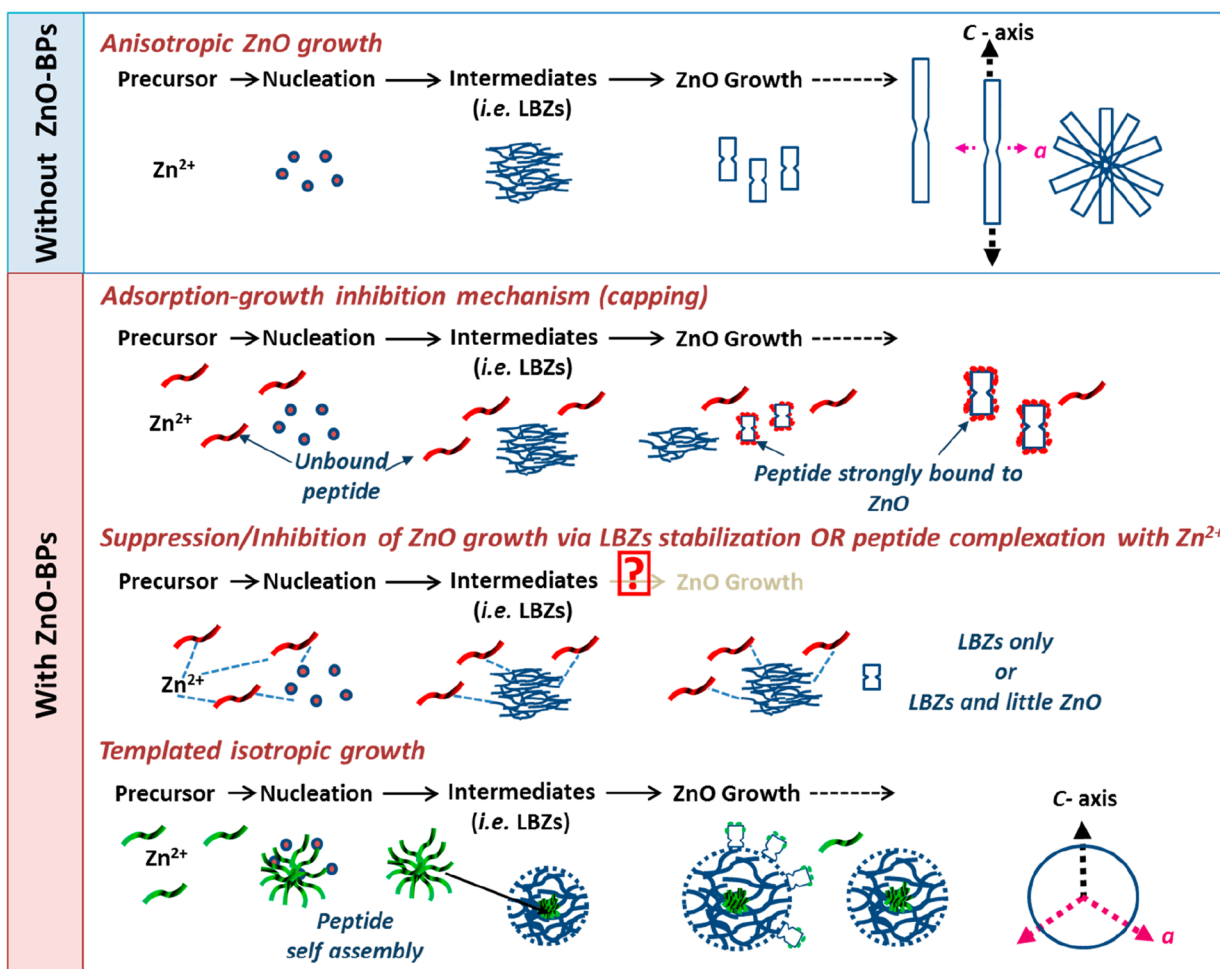
Figure 16. Illustration of reported mechanisms through which ZnO-BPs influence ZnO growth process and modify morphology. Adapted with permission from ref 527. Copyright 2015 American Chemical Society.

was attributed to a single point mutation of a peptide sequence.[527,528] Specifically, the formation of spheres required the substitution of histidine with alanine at position 6 in the G-12 sequence, and formation of mushroom-shaped crystals required the substitution of methionine with cysteine at position 5 in the EM-12 sequence.[527,528] Figure 15 illustrates some of these ZnO morphologies formed using ZnO-BPs. Note, the precise effect of these mutations on the conformation of the peptide, and hence, the relative orientation of potential functional groups has not been explored.

Also reported in literature is the ability to fine-tune the morphology and size of ZnO particles by varying the relative concentration of a given peptide sequence. With increasing peptide concentration, rods of lower aspect ratio can be obtained. In some instances, with the same peptide at higher peptide concentrations the anisotropic growth habit of ZnO crystals can be completely altered to form spheres, templating through concentration-dependent formation of peptide–peptide interactions. In one study, this change from rods to spheres has been shown to be associated with a change from single crystals at lower peptide concentration to polycrystalline particles at higher peptide concentrations.[529] The different morphologies reported are peptide directed but are also influenced by the ZnO solution synthesis systems used, which vary in the precursor used and growth conditions.[527,528,539]

The synthesis system used dictates the solid phases formed from the early stages of nucleation, the formation of intermediates including layered basic zinc salts (LBZs), and ZnO crystal growth. Peptides can interact with these solid phases and consequently modify the ZnO growth process and morphology.[527,528,540] This explains why across the different research groups studying these peptides, different morphologies have been reported for a single peptide incorporated as an additive in ZnO synthesis as different synthesis systems have been used. As small changes in reaction conditions in ZnO synthesis manifest themselves in directly observable differences, it is crucial that every step be described in detail. For example, how was mixing of reagents carried out, with or without stirring, for how long (only as the precursor was mixed with the base or throughout the synthesis)? Often reports in literature provide insufficient information which does not allow repetition of the precise conditions used, a situation which needs to be rectified in the future.

As examples of the variety of structures that can be formed, even with a single peptide, ZnO spheres have been reported with G-12A6 peptide using a $Zn(NO_3)_2 \cdot 6H_2O$-HMTA system, whereas only aspect ratio reduction of ZnO rods and LBZs stabilization (with increased G-12A6 concentration) was observed using a $Zn(CH_3COO)_2$-NH_3 system.[527] Needles with flattened edges and peanutlike structures were synthesized in the presence of EM-12 using a $Zn(NO_3)_2$-KOH system,

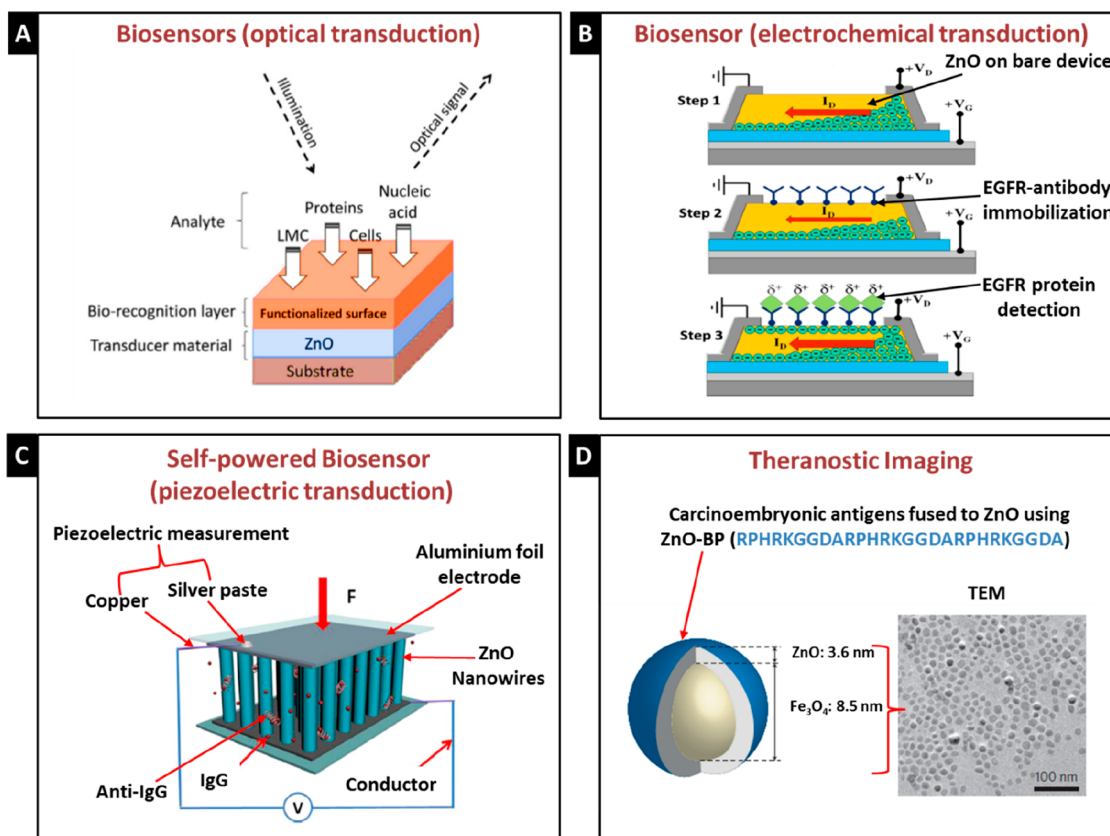**Figure 17.** Examples of developing technologies exploiting ZnO-biomolecule interactions. (A) Schematic of biosensors based on optical transduction reprinted with permission from ref 79. Copyright 2016 Elsevier. (B) Image of a biosensor based on electrochemical transduction. Adapted with permission from ref 547. Copyright 2011 American Institute of Physics. (C) Illustration of self-powered biosensor adapted with permission from ref 544. Copyright 2014 Elsevier. (D) Illustration of Fe_3O_4-ZnO CSN developed for diagnostics and therapy. Adapted with permission from ref 76. Copyright 2011 Macmillan Publishers Limited.

while aspect ratio reduction of asymmetric twinned crystals to untwinned crystals and stabilization of LBZs was reported with an increase in the concentration of EM-12 when using a $Zn(CH_3COO)_2$-NH_3 system.[528] From information currently in the public domain, the mechanisms through which ZnO-BPs modify ZnO growth and morphology that have been validated with direct experimental evidence include: (i) adsorption growth inhibition mechanism (capping), (ii) peptide templating of unusual ZnO morphologies such as isotropic growth of crystals into spheres,[526,527,529] (iii) peptide suppression/inhibition of ZnO growth by stabilization of intermediate LBZs,[527,528] and (iv) peptide complexation with Zn^{2+} ions in solution delaying the growth of ZnO crystals,[43,528] all illustrated in Figure 16. These mechanisms can occur separately or in combination depending on the peptide sequence, peptide concentration, and the synthesis system used.

4.4.2. Applications of ZnO-Biomolecule Constructs. From the many reports on the formation of novel and diverse ZnO structures using biomolecules, it is clear that (i) biomolecules are significant tools for the controlled, reproducible, and predictable modification of the physicochemical properties of ZnO and (ii) detailed studies can be carried out to understand the biomolecule-directed ZnO formation mechanisms. However, more research is needed to demonstrate how we can design a biomolecule to obtain ZnO structure of specific properties (i.e., morphology and crystallinity) and how biomolecule surface functionalization

can impact on the applications of the material. Both areas of research are needed to encourage the wider use of biomolecules in synthesis to further expand and develop the potential industrial, biomedical, and nanotechnological applications of ZnO. Additional research is needed to compare the physical (i.e., conductivity/electronic/optical) properties of the numerous ZnO structures synthesized using biomolecules as this information is seldom reported by scientists exploring the effects of the biomolecules on the composite constructs generated.

In general, defect-free single crystalline ZnO is preferable for piezoelectric and optoelectronic applications, while polycrystalline ZnO is acceptable for gas sensing and photocatalysis.[529] An example of the modification of ZnO optical properties using biomolecules in synthesis is the enhanced green photoluminescence for materials synthesized in the presence of spider silk peptides that could potentially be directly used as biosensors or in optoelectronic devices.[523] Similarly, use of a ZnO-BP, VPGAAEHT was shown to alter both green and blue emissions of ZnO particles synthesized with the peptide by affecting surface and interstitial defects.[529] Photoluminescence-based biosensors making use of biomolecule inorganic interfaces have also been developed to detect biomolecules such as glucose,[541] Avidin-horseradish peroxidase,[542] and cells for example in the detection of Salmonella antigen.[543] A recent review by Tereshchenko and co-workers covers the latest advancements in ZnO and ZnO-metal (Au and Ag) nanocomposite biosensors based on the most developed optical

methods of detection [fluorescence, photoluminescence, surface enhanced Raman spectroscopy (SERS), and surface plasmon resonance (SPR)].[79] Biomolecules including low molecular weight biological compounds (i.e., dopamine, urea, riboflavin), nucleic acids [i.e., DNA and ribonucleic acid (RNA)], proteins, and cells are some of the most common analytes that have been studied, and these have been targeted using biorecognition layers that are immobilized onto a ZnO surface, Figure 17A.[79]

Other ZnO biosensor devices have been designed with signal output based on electrochemical and piezoelectric[544−546] transduction, Figure 17 (panels B and C). An example of a biosensor based on electrochemical transduction is the design of a ZnO-gold nanoparticle (Au NP)-Nafion-horseradish peroxidase (HRP)-modified glass carbon (GC) electrode.[538] The nanohybrid ZnO-Au NP-Nafion-film was able to facilitate direct electron transfer (DET) between HRP and the GC electrode to reduce and detect hydrogen peroxide (H_2O_2).[538] In another example, a highly selective and sensitive ZnO-based thin film transistor immunosensor was designed to bind to epidermal growth factor receptor (EGFR) for potential application in the diagnosis and treatment of cancer, Figure 17B.[547] A ZnO thin film surface was functionalized with primary monoclonal antibodies that bind to EGFR. The antibody−antigen reaction was detected as it caused measurable channel carrier modulation. A major development in ZnO applications is the resourceful concept of coupling the properties of ZnO (e.g., its piezoelectric properties) to a direct application such as a nanosensor through a single physical process, thereby generating remarkable nanosystems that are self-powered. This has been realized in the design of a ZnO biosensor whose piezoelectric output is dependent on the adsorption of Immunoglobulin G (IgG). In this development, ZnO nanowires were vertically deposited on a substrate and assembled into a device with an electrode to measure piezoelectric output, Figure 17B. Au NP anti-immunoglobulin (Au Np-anti-IgG) conjugates were then immobilized onto the surface of the ZnO nanowires to detect IgG molecules. The measured piezoelectric output decreased with the increase in adsorption of IgG.[544]

4.4.3. Applications of ZnO Fused with Other Materials.

Fusing ZnO particles with biomolecules can also directly impart additional functionality. Depending on the nature of the biomolecule and its intended use, the biomolecule can either be used to cap the ZnO particles or ZnO can be used to encapsulate the biomolecule. In one study, demonstrating the former, ZnO was used to coat abiogenic iron oxide nanoparticles (Fe_3O_4 NPs) to generate core−shell nanoparticles (CSN), Figure 17D.[76] The Fe_3O_4-ZnO CSN were developed for dendritic cell (DC)-based cancer immunotherapy because NPs with a high surface area can be used as efficient carriers to deliver target antigens (Ags) to DC but more particularly, the Fe_3O_4 NPs can be imaged in vivo using magnetic resonance imaging (MRI).[76] Carcinoembryonic Ags were fused to the Fe_3O_4-ZnO NPs using a ZnO-BP (RPHRKGGDA in a triplicate tandem repeat; RPHPK being the ZnO binding motif while GGDA was the linker), and their delivery into dendritic cells was monitored using MRI and confocal microscopy. The immune response and survival of mice immunized with the NP-Ag complex containing dendritic cells was found to be greatly boosted in comparison to the controls.[76] Similarly, *Bombyx mori* silk-fibroin peptides have been used to template the synthesis of

cobalt (Co)-doped ZnO particles.[548] The doping of ZnO with Co ions increased the magnetic properties of the ZnO particles through formation of intrinsic defects, that is oxygen vacancies and Zn interstitials, which are thought to mediate exchange coupling of Co spins. The capping of the Co-doped ZnO particles with silk-fibroin peptides promoted cell adhesion and proliferation in comparison to uncapped particles and further enhanced the ferromagnetic properties of the Co-doped ZnO particles possibly by promoting the uptake of more Co ions into the ZnO structure.[548] For diagnostic purposes, ZnO NPs capped with saccharides (glucose, sucrose, starch, and alginic acid) have been impregnated into cellulose fiber sheets and used to immobilize anibodies.[549] The presence of ZnO greatly modified the physical properties of the cellulose sheets increasing tensile strength, opacity, and smoothness and decreased the porosity of the sheets in comparison to unmodified sheets. Impregnation of the cellulose sheets with the saccharide-capped ZnO also improved antibody immobilization on their surface, which is a prerequisite for the fabrication of biosensing or bioactive papers. The sheets were also successfully used to detect blood types using blood antibodies and furthermore were shown to possess antimicrobial properties due to the presence of ZnO.[549]

For its biocompatible and antibiotic properties, ZnO has been used to encapsulate and passivate other inorganic NPs and molecules including biomolecules that have additional functionalities required for biomedical applications, but which may be toxic, immunogenic, or unstable in different environments (in vivo or in vitro) if unprotected. For example, fluorescent magnetosomes encapsulated in ZnO have successfully been generated.[81] Magnetosomes are in themselves naturally occurring CSN as they are surrounded by a membrane consisting of phospholipids and proteins. Through fusion to abundant membrane polypeptides like MamC, magnetosomes can be functionalized with moieties such as antibodies, enzymes, and fluorophores for various biotechnological uses. In an example study by Borg and co-workers, a fusion protein of MamC, enhanced green fluorescent protein (EGFP) and the PD identified ZnO-BP 31 with sequence HHGHSPTSPQVR was expressed on magnetosome membranes which were then coated with ZnO.[105] Such hybrid magnetic semiconductor particles may have biotechnological applications in magnetic bioseparation, imaging and drug targeting. For a more detailed discussion on the use of ZnO nanomaterials for biomedical applications, we recommend a review by Zhang and co-workers that summarizes ZnO use in biomedical imaging, drug delivery, gene delivery, and biosensing.[77]

4.5. Techniques Directly Probing ZnO-Biomolecule Interactions

As already discussed in section 4.3, knowledge concerning the surface chemistry of ZnO is incredibly important in understanding how biomolecules might interact with surface species present for any techniques being used to obtain surface specific detail. We now consider the varied approaches that have been used by both experimentalists and computational scientists in the study of ZnO in the presence of biomolecules.

4.5.1. Experimental Techniques Probing ZnO-Biomolecule Interactions.

4.5.1.1. Combinatorial Methods. Efforts continue to be made to identify the principles through which biomolecules interact with ZnO. It is well-understood that the coordination of Zn^{2+} with proteins plays an important

role for the structural stability and functionality of proteins in living organisms as evidenced in metalloproteins such as metallothionine and zinc fingers in DNA-binding proteins.[550−552] The complexation of proteins with Zn^{2+} is thought to occur using specific side chain functionalities of amino acids, namely, sulfur atoms of cysteine and methionine, nitrogen atoms of histidine, and oxygen atoms of aspartic acid and glutamic acid.[533,534] In the study of ZnO-biomolecule interactions, the interaction of combinatorially identified ZnO-BPs peptides with ZnO has been of particular research interest, and some of the key outcomes reported in the literature will be discussed herein. The first indication of which amino acids may be important for the interaction of ZnO-BPs with ZnO can be deduced by noting which amino acids are enriched and which are depleted in the PD or CSD peptide pool. However, a detailed inspection of the peptide pool reveals that there are some limitations to this reasoning. Basic amino acids, particularly histidine are prevalent in most of the peptide sequences that interact with ZnO identified using PD. Nonetheless, as some of the sequences identified to bind to ZnO do not have histidine residues (i.e., QWGWNMPLVEAQ and MKPDKAIRLDLL identified by Rothenstein's group[81] and QNTATAVSRLSP by Umetsu and group[80]), other amino acids may also play significant roles in the interaction or in sequence alignment/conformation. Bacteriophages also preferentially express some amino acids and not others (e.g., cysteine which may be absent in PD identified peptides but may in actuality be important for interaction of peptides with the target surface).[528] This has necessitated the development of other complementary selection methods for material binding peptides and studies to understand the specificity of their interaction with target substrates as described below. Various experimental, theoretical, and computational methods have been used and are being developed further with the aim of achieving a detailed understanding of biomolecule−ZnO interfacial interactions at the molecular level.

4.5.1.2. Spectroscopic Methods. Fluorescence spectroscopy based adsorption assays have been used to study the adsorption of ZnO-BPs to ZnO.[533,534] Yokoo and colleagues fused the EM-12 peptide to the *N*-terminus of green fluorescent protein (GFP) and allowed the tagged peptide to interact with the ZnO particles to quantify the amount of bound peptide. This process was similarly carried out for truncations of the peptide sequence (i.e., GFP-EAHV and GFP-EAHVMHK). Adsorption isotherms were measured at different temperatures and thermodynamic parameters estimated using the Van't Hoff equations. Changes in the Gibbs free energy values (ΔG) for the adsorption of the GFP tagged peptides were estimated to lie between −7.17 and −8.37 kcal/mol. The observed interaction was determined to be enthalpy driven with the main contribution from enthalpy change (ΔH) values.[534] The interaction was mainly attributed to hydrogen bonding and electrostatic interactions through charged resides of the peptide. However, studying truncations of EM-12 demonstrated that the specificity and affinity of the interactions was also influenced by specific recognition of the alignment of the sequence and the peptides conformation by the ZnO surfaces.[534] Where tags are used in interaction studies, whether for detection and quantification (as in the above study using ZnO with fused GFP) or studies with methods requiring immobilization of biomolecules onto surfaces (such as the used of poly histidine tags fused at the C- or N-terminus or biotinylation of proteins for SPR), several questions remain.

For example, what is the effect of such tags on the structure of the biomolecule being studied, does it matter if the tag is fused to the C- or N-terminus, and how does the presence of a tag influence the measured outcomes? It is certainly an advantage to have a method utilizing a peptide/protein of interest with intrinsic fluorescence, but this is not always the case.

In another fluorescence spectroscopy based study, the imidazolium cations of histidine residues in positions 3 and 6 of the EM-12 sequence were suggested to be important for the interaction of the peptide to ZnO.[533] "Hot spot" regions for the adsorption of EM-12 peptide to ZnO were identified to be HVMHKV and HKVAPR by fluorescence-based adsorption studies using peptides generated by stepwise truncations of the EM-12 sequence.[533] Labeled peptides of different concentrations were allowed to interact with ZnO particles then the mixture was centrifuged to be able to quantify unabsorbed peptide in the supernatant. The binding constant and the maximum amount of adsorbed peptide was determined for EM-12, specific truncations of EM-12, and alanine mutants of the truncated sequences. All of the sequences were labeled using fluorescein isothiocyanate (FITC) and used in adsorption studies with ZnO and other metal oxide [zirconium dioxide (ZnO_2), tin oxide (SnO_2), and aluminum oxide (Al_2O_3)] particles. There was clear specific peptide adsorption to the ZnO particles and not the other metal oxides. Comparing the binding constants (K_a), HVMHKV ($K_a = 5.6 \times 10^3$ M^{-1}) and HKVAPR ($K_a = 7.7 \times 10^3$ M^{-1}) peptides had lower K_a for ZnO particles than the original EM-12 sequence ($K_a = 2.7 \times 10^4$ M^{-1}). However, substitution of histidine and cysteine amino acids into certain positions in the truncated sequences (i.e., H$\underline{C}$VA$\underline{H}$R, $K_a = 9.8 \times 10^6$ M^{-1}) increased the K_a of the sequences for ZnO.[533] Note, a problem with this approach is that it does not account for the change in conformational space available for the truncated peptides compared to the original, longer sequence.

XPS is another spectroscopy-based technique that has been used to probe interactions between ZnO and peptides. As previously mentioned, the incorporation of GT-16 in ZnO synthesis had been shown experimentally to decrease the aspect ratio of ZnO crystals much more than with the G-12 peptide to form ZnO platelets.[33] The plane specific adsorption behavior of GT-16 peptide was further studied using single crystalline (0001) and (10$\overline{1}$0) ZnO films deposited onto silicon wafers using the atomic layer deposition (ALD) technique.[44] A solution-based method and XPS was then used to study the adsorption of G-12 and GT-16 onto the individual ZnO planes. Both G-12 and GT-16 adsorbed to both crystal planes, but GT-16 was found to adsorb more selectively to the (0001) plane.[44] The flexible spacer in GT-16 peptide between histidine and cysteine was thought to have facilitated the plane specificity of GT-16 to the (0001) plane of ZnO that has the highest density of zinc atoms compared to other planes of ZnO.[44,541]

^{1}H NMR spectroscopy has been used to determine the binding affinity of two PD identified ZnO-BPs (HSSHHQPKGTNP and HHGHSPTSPQVR) for ZnO particles.[81] The binding affinities were obtained by determining the line broadening effects during interaction of the peptides with different concentrations of ZnO and assuming a 1:1 binding model. The affinity of both ZnO-binding peptides to the substrate at pH 7.5 were determined in the nanomolar range with a K_D value of 10 ± 3 nM for HHGHSPTSPQVR peptide and K_D = 260 ± 160 nM for HSSHHQPKGTNP

peptide. Therefore, the authors deduced that the HHGHSP-TSPQVR peptide was the stronger binder for the ZnO substrate used.[81] On detailed inspection of the literature, we have noted that particularly in kinetic and thermodynamic studies of abiotic–biotic interactions,[81,553–556] there are uncertainties in the selection and use of binding models to appropriately represent interaction processes such that it is not uncommon for assumptions to be made and the simplest binding models selected. Going forward, is the best approach to develop additional models specific to the materials and interactions in question or should the rationale for selection of theoretical models used to interpret data be standardized? The use of different models makes it difficult to compare findings among different research groups, whereas the use of standardized models may be viewed as simplistic, not representative, or accurate.

FTIR spectroscopy has also been used to provide evidence of the adsorption of biomolecules such as amino acids,[557] peptides,[44,527,528] and bacterial surface biomolecules[558] onto ZnO. IR spectral changes are observed for ZnO with biomolecules adsorbed compared to pure ZnO. Also alterations of the IR spectra of a pure biomolecule when it is adsorbed to ZnO may give information on moieties important for interaction. Raman spectroscopy has similarly been used to identify interaction moieties of biomolecules, for example, the amino acid cysteine[557] and adenosine triphosphate (ATP) with ZnO nanostructures.[559] In the study with ATP, Raman shifts in adenine modes were observed when ATP was bound to ZnO under acidic environments. The interaction was attributed to complexation of the nitrogen (N_7) atom of adenine to Zn^{2+}. A Raman shift was also observed for the NH_2 group of adenine which was shown to facilitate hydrogen bonding with water molecules and ionization of phosphate groups which also bind to ZnO.[559] The spectroscopy approaches are not without their own limitations but do offer the possibility for approaching a more detailed understanding of atomic scale interactions based on changes to the vibrational signatures of the molecules/materials alone and in combination, this has yet to be achieved and will require significant investment from computational studies at the quantum level.

4.5.1.3. Nonspectroscopic Methods; X-ray Diffraction (XRD). Using HR-XRD with a synchrotron source, a study by Brif and co-workers showed that some amino acids can be incorporated into the ZnO lattice, particularly, the amino acids cysteine and selenocysteine.[560] Subsequently, this study showed that the incorporation of the amino acids led to a change in the optical and paramagnetic properties of the material as well as the crystal morphology. Particularly, the incorporation of cysteine into the ZnO lattice gave rise to the formation of ZnO spherical crystals instead of the rods formed without additive.[560] In another recent study using XRD, ZnO lattice strain modification was observed when EC-12 peptide was added in a ZnO solution synthesis method.[528] This could have occurred either by the peptide being incorporated into the crystal lattice of ZnO or due to the adsorption of EC-12 onto the ZnO surface. This was also attributed to the presence of cysteine in the sequence as modification in ZnO lattice strain was not observed with the EM-12 peptide, which has M_5 in the sequence instead of C_5, though no attempt was made to understand the role of conformation on the observed interactions.[528] In other studies where there was a different synthesis method from the study with EC-12, no lattice strain modification was observed when ZnO-BPs such as G-12 and

GT-16 (which also has cysteine in the sequence at position 16) were adsorbed to ZnO formed in their presence.[527] In these studies, thermal gravimetric analysis (TGA) was used to substantiate the coprecipitation of peptides with ZnO by determination of the additional weight loss for samples prepared in the presence of biomolecules in comparison to materials prepared in the absence of the biomolecule.[44,527,528] The data suggest that parameters such as synthesis conditions, precursors used, and amino acid position in the sequence may also influence the ability of certain amino acids and peptides to modify crystal lattice strain (and hence optical/electrical properties) and should be explored in a systematic manner.

4.5.1.4. Nonspectroscopic Methods; Isothermal Titration Calorimetry (ITC). ITC has been used to directly probe the thermodynamic changes that occur during the interaction of ZnO-BPs with ZnO.[76,553] In a study where ZnO-BPs were used to link a NP (Fe_3O_4-ZnO)-Ag complex, ITC was used to determine the binding affinity of the ZnO-BPs to the ZnO-coated NPs.[76] A comparison of the affinity of RPHRKGGDA (1 × ZnO-BP) and its triplicate tandem repeat (3 × ZnO-BP) for the NPs was carried out using ITC. The 3 × ZnO-BP ($K_a = 1.4 \times 10^6$ M^{-1}) had about twice higher affinity for the NPs than the 1 × ZnO-BP ($K_a = 6.9 \times 10^5$ M^{-1}) and were therefore selected for complexation with the Ag.[76] Note, no attempt was made to account for changes to binding caused by conformational changes induced by the extended peptide sequence. The interaction of different ZnO structures (rods and platelets) with G-12, GT-16, and selected alanine mutants of G-12 has also been monitored using ITC.[553] Interactions were found to be favorable having high adsorption affinity values and ΔG values between −6 and −8.5 kcal/mol.[553] The values obtained using ITC were similar to those reported for the adsorption of fluorescent-tagged EM-12 (and truncations of the sequence) to ZnO.[534] However, ITC is a direct measure of heat change and a faster method to probe thermodynamic parameters of interaction without the requirement for labeling or carrying out experiments at different concentrations and temperatures to estimate thermodynamic parameters.

As with all techniques, the use of ITC has limitations and challenges. Data interpretation and deconvolution of individual events (i.e., conformational change, displacement of water molecules, van der Waals interactions, electrostatic interactions, hydrogen bonding, or hydrophobic interactions) contributing to the global heat change measured in ITC is not always straightforward and cannot always be described at the atomic level.[561,562] In many cases, the models available for fitting ITC data may not match the system being studied.[561–563] Complementary approaches are therefore important to facilitate interpretation of findings. Moreover, development of new ways to analyze and interpret data is a much needed step forward. An example is one recent study probing the interaction of ZnO NPs with different catechol (CAT) derivatives [*tert*-butyl group (tertCAT), hydrogen (pyroCAT), aromatic ring (naphCAT), ester group (ester-CAT), and nitro group (nitroCAT)].[563] UV/vis and FTIR analysis confirmed that all the different CAT molecules were chemisorbed to the ZnO NPs irrespective of their functionalities. ITC and a mass-based method were then used to determine the heat released during the interaction and to obtain adsorption isotherms, respectively. This is an example of a study where the authors deemed the Langmuir model to be an oversimplification of the underlying adsorption mechanism for adsorption isotherms and were unable to fit their ITC data

using the available models (especially for interactions where no plateau in the heat released was obtained). The authors proposed a new approach of data analysis, combining both heat- and mass-based methods to determine the binding enthalpy per amount of bound molecule without any fitting model. This was done by dividing the heat release measured using ITC by the amount of bound molecules determined from the adsorption isotherm.[563] This enabled them to unambiguously order the interactions of the different CAT functionalities by their binding enthalpies to the surface of the ZnO NPs.[563]

4.5.1.5. Combined Experimental Approaches. As each experimental technique has limitations, complementary use of experimental methods enables users to obtain more useful information and to better understand the system being studied. For example, in ZnO synthesis studies incorporating peptides, the use of different characterization techniques in combination (i.e., SEM, TEM, AFM, ICP-OES, XRD, FTIR, XPS, TGA, and ITC) has enabled understanding of the ZnO growth process and interaction with peptides.[33,44,81,526–528,532–534] This has resulted in certain amino acids being identified as playing important roles in the adsorption of peptides to ZnO or in the stabilization of intermediates like LBZs. For instance, in a study using a $Zn(NO_3)_2$-HMTA hydrothermal reaction, Gerstel et al. demonstrated that the presence of aspartic acid, glutamic acid, and their corresponding dipeptides produced LBZs as opposed to the expected ZnO.[43] This was achieved using XPS, AFM, SEM, XRD, FTIR, and zeta potential measurements.[43] Using a $Zn(NO_3)_2$-NaOH hydrothermal reaction followed by characterization using a combination of techniques (XRD, SEM, FTIR, TGA, and XPS), it was also shown that the presence of peptides with different isoelectric points (in the acid, basic, and neutral range) results in the formation LBZs as a metastable phase during the precipitation process.[526] Therein, it was suggested that negatively charged peptides may be intercalated easily in metastable LBZs.[526] More recently, in agreement with findings reported by Okochi and co-workers,[533] studies using a $Zn(NO_3)_2 \cdot 6H_2O$-HMTA and a $Zn(CH_3COO)_2$-NH_3 system demonstrated the specific roles of histidine and cysteine within ZnO-BPs in interaction with ZnO and also in stabilization of LBZs formed during ZnO formation.[527,528] This was also achieved using a number of characterization methods (FTIR, XRD, SEM, TGA, and XPS) in combination.

4.5.2. Theoretical and Computational Approaches to Study ZnO-Biomolecule Interactions. To understand how biomolecules are able to specifically bind to ZnO surfaces, theoretical and computational tools such as MD simulations, density-functional tight-binding theory (DFTB), and DFT have been employed.[12,44,465,486,564–567] There is particular interest to develop theoretical and computational approaches because they enable one to theoretically investigate the behavior of complex systems at a molecular level, further than can presently be achieved experimentally.[568–572] In particular, it is possible to explore interactions on a range of well-defined surfaces but there are limitations using MD approaches in that a fully validated ZnO-biomolecule force field is not yet available.

In one exemplar study, MD simulations were used to provide an explanation as to the experimentally observed predominant binding of IgG to the $(10\bar{1}0)$ plane of ZnO. This was in a study probing the adsorption of IgG to four low-index crystal surfaces of ZnO [(0001), $(000\bar{1})$ $(10\bar{1}0)$ and

$(11\bar{2}0)$].[465] Using AFM imaging, IgG was seen to predominantly bind to the $(10\bar{1}0)$ plane in comparison to the other three planes examined. This unusual behavior was explained using Monte Carlo MD simulations and was attributed to the spatial location and distribution of amino acids in the protein that strongly interact with ZnO, thereby affecting their availability for interaction.[465] The particular amino acids thought to strongly interact with ZnO planes had been determined from a previous MD simulation study of interactions of the ZnO planes with twenty-two different amino acids.[486] There, the amino acids identified to have high binding energies (BEs) for the Zn-terminated (0001) surface in water were tyrosine and tryptophan, whereas for the $(10\bar{1}0)$ surface, asparagine, tryptophan, and histidine had the highest BEs in water.[486]

Using a different approach, Muthukumara developed a theoretical model based on effective interfacial energies to understand the morphology modification of ZnO using the GT-16 peptide.[541] An adsorption-nucleation model was used to make theoretical predictions of relative growth rates of ZnO crystal planes in the presence of GT-16.[541] This theoretical approach was viewed as a simpler alternative to molecular modeling. The theoretical findings were validated using aspect ratio measurements from experimental findings reported by Tomczak and colleagues,[33,541] which were in agreement. In subsequent studies carried out in-house, Monte Carlo MD simulations were used to further the understanding of the experimentally observed differences in the adsorption behavior of G-12 and GT-16 peptides to ZnO planes.[44] The aim was to determine calculated energetics of interaction (adsorption energy, E_{ads}) and to predict possible binding moieties of G-12 and GT-16 to the ZnO planes [(0001) and $(10\bar{1}0)$].[44] Stable configurations of G-12 and GT-16 were simulated in water by MD then exposed to ZnO surfaces in vacuum.[44] The adsorption of both peptides to ZnO planes was seen to be energetically favorable.[44] For both peptides, a lower E_{ads} was observed for the (0001) ZnO plane compared to the $(10\bar{1}0)$ plane. Interestingly, the E_{ads} of GT-16 to the (0001) plane of ZnO was much lower than E_{ads} to the $(10\bar{1}0)$ plane (an interplane E_{ads} difference of 288 kJ mol^{-1}), greater than the interplane E_{ads} of G-12 peptide (a difference of 100 kJ mol^{-1}).[44] The computation approach, though simplistic, was in complete agreement with experimental data showing the plane specificity of GT-16 to the (0001) plane of ZnO and provided plausible explanations for the adsorption phenomenon observed. These computational studies were a first step toward understanding the complexity of the thermodynamic changes occurring during the interaction of G-12 and GT-16 peptides with ZnO, which was later studied experimentally using ITC (previously discussed in the experimental techniques section of ZnO).[553] Though the ITC studies were carried out using whole ZnO crystals (rods and platelets), the interaction with both G-12 and GT-16 was still observed to be favorable.[553]

Other strategies such as computational alanine scanning mutagenesis have also been developed which in combination with experimental alanine mutations of sequences may, for example, enable one to elucidate the roles (involved directly in interaction or influence conformation or structure stability) of functional groups of a biomolecule.[63,436,527,570,573,574] There, however, still remain great challenges and debates on the accuracy of simulations of complex surfaces like ZnO such as the need for developing more representative force fields and a

reasonable number of adjustable parameters.[566] It is important to emphasize that an accurately representative computational modeling approach should describe the chemical and physical interactions between all components in the system and accurately balance all these interactions.[568,572,575−577] For accurate simulations, much progress is still needed to validate and better design methods that appropriately describe the molecular and atomic level details of biomolecules interacting with the surface of ZnO while also describing the material's surface features and the influence of the medium in which the simulation is performed. Nevertheless, computational tools undoubtedly have great potential to improve and accelerate our understanding of biomolecule-inorganic interactions.[39,173,240,578]

4.5.3. Summary. The studies discussed above do not exhaustively cover all the techniques/methods that have been used to probe ZnO-biomolecule interactions but demonstrate that the understanding of interactions has greatly been advanced using appropriately selected experimental and computational tools. Complementary use of experimental and computational techniques to study ZnO-biomolecule interactions will lead to further development in experimental design and facilitate data interpretation. With continued improvements in instrumentation, methodology, and theoretical models, realization of applications utilizing ZnO-biomolecule interactions is within reach. We expect that research on ZnO-biomolecule interactions will continue to flourish over the next decade, attracting new interdisciplinary contributors to bridge the research gaps.

4.6. Toxicology of ZnO

Though the development of ZnO for biomedical applications has generated much excitement over the years, uncertainties exist in relation to its toxicological effects and the stability of particles, particularly at the nanosize scale. Various toxicological studies have shown that ultrafine nanoparticles pose a serious hazard to human organs like lungs,[579] skin,[580] and to the environment (ecotoxicity).[581,582] If released into the environment, ZnO may be harmful because Zn^{2+} ions form on dissolution in aqueous media,[444,583,584] with the toxicity of ZnO NPs being mediated by reactive oxygen species (ROS).[585] The uptake of Zn^{2+} ions and of nanoparticle fragments by biological cells is thought to raise the level of intracellular Zn^{2+} that is connected with the formation of harmful ROS species.[586−588] The photocatalytic activity of ZnO NPs is also a cause for concern as it might promote additional generation of ROS.[585] In contrast, other studies have argued that dissolution of ZnO can be favorable (biocompatible and biodegradable), as dissolved Zn^{2+} ions can be adsorbed in the body and used as a source of zinc ions for naturally occurring hydrolytic enzymes.[589] Despite these disagreements, there are commercial products already in use that contain ZnO nanoparticles like sunscreens and cosmetics;[443,445] here >80% of the industrial manufacturing is used for cosmetics and ~14% for paints.[590]

One review analyzed and compared reported toxicological response of individual species to ZnO NPs, based on median L(E)C50 (median lethal dose/half-maximal effective concentration) values for organisms and median MIC (minimum inhibitory concentration) for bacteria.[591] Where comparisons were carried out regardless of the material properties, ZnO NPs were thought to be most toxic toward algae (<0.1 mg/L), followed by crustaceans, fish, then bacterium *Vibrio fischeri*,

and protozoa.[591] The sensitivity of planktonic microalgae to zinc is important as they are a key component of the food chain in aquatic ecosystems and influence water quality.[591] Where it was possible to analyze toxicity of ZnO with respect to the size of NPs, the median size of ZnO used to derive median L(E)C50 values in mammalian cells or median MIC values in bacteria was determined to be 55 and 20 nm, respectively.[591] Interestingly, other studies of IC50 (growth inhibition) have shown a range of zinc concentrations from <1 mg/L to several hundred milligrams per liter even within the same *Escherichia coli* species, potentially related to the impact of particle size on the antibacterial activity of ZnO.[585]

There are several causes for variability in toxicological reports making it challenging to directly compare findings. For instance, for a clearer understanding of the toxicological effects of ZnO, detailed characterization and description of the properties (size, shape, surface functionalization) of materials used in toxicological studies should be specified in reports. It is important to highlight that the majority of ZnO toxicity studies have been performed using bare nanoparticles, whereas the existing applications in sunscreens for example, usually utilize surfaces that have been modified. Effects of functionalization of ZnO surfaces for applications (including those utilizing biomolecule-ZnO interactions) should be taken into account in toxicological studies[588,592] and is an area of research that should be developed further.

While ZnO growth conditions largely determine its properties, the effects of postgrowth treatment should also be considered. This is in relation to dissolution, aging, and changes such as aggregation that may be caused by storage conditions or environment: the influence of exposure to environmental conditions (temperature, humidity, pH, and light), exposure to natural organic matter in the environment, and the influence of exposure time.[588,593,594] ZnO is sensitive to water and surface adsorption of ambient gases which can result in great changes to its properties especially for nanostructures which have a large surface to volume area.[588] Reported examples include the modification of ZnO polar surfaces in air by the formation of nanomounds resulting in zinc vacancy formation in their surroundings[595] and humidity (in ambient air)-induced modification of ZnO nanocrystal growth and crystallinity.[596]

Similarly, another factor that may influence the variability observed in analysis and toxicology reports is the different media used in the toxicity tests. The toxicity mechanism is specifically influenced by the chemistry of the medium in which exposure occurs (e.g., pH, temperature, organic matter, and presence of anions). The modeling of environmental concentrations is challenging because of a lack of empirical data, especially due to processes that influence the environmental concentrations such as dissolution, agglomeration, degradation, and complexation allow a quantitative understanding that is far from complete.[597,598] All in all, toxicity has similarly been observed with other materials like TiO_2,[599,600] which is also valued for its existing and potential applications. Research to develop biomedical applications of ZnO continues in parallel with increasingly developing debate and research on the toxicological and environmental effects of such materials.

5. GeO$_2$

5.1. Overview of GeO$_2$

Germanium, previously one of the most important components of integrated circuits, is an ideal candidate for the preparation of complementary metal-oxide-semiconductors (CMOS)[601−603] due to its hole and electron mobilities being four and two times higher than silicon.[602] Germanium dioxide, GeO$_2$, has a band gap of 5 eV, higher than other transparent conductive oxides, thus making this material suitable for the development of luminescent devices operating from the ultraviolet to the near-infrared range.[604] GeO$_2$ has also been used in catalysis and infrared optics due to its high linear coefficient of thermal expansion.[605,606] Highly mesoporous aerogels of pure GeO$_2$ have also been prepared that show high thermal stability.[607] However, probably the most attractive property of GeO$_2$ is its refractive index, which at 1.7 is greater than for SiO$_2$ (1.455)[608] and makes germania an ideal candidate for optical fibers[609,610] either alone or as a composite with SiO$_2$.[611] The intrinsic properties of Ge and GeO$_2$ have permitted its use in optoelectronics, biological imaging, and lithium ion batteries as reviewed by Vaughn and Schaak.[612] Their review focuses on synthetic methodological routes to the material and the role that size and shape control play in determining the final material's properties and applications.[612]

In nature, germanium is found as a trace element within other minerals such as silica.[613] Though it is not known to have any biological role, Ge has been found in natural water systems at the part per trillion range and is incorporated in siliceous organisms forming part of their biogenic opal.[613] This is thought to be largely due to the chemical similarities between Ge and Si atoms. As an example, the simultaneous and competing SiO$_2$−GeO$_2$ condensation process has been studied in siliceous sponges and diatoms, which have the ability to incorporate inorganic Ge in their siliceous skeleton. As a model, the sponge, *Suberites Domuncula* when grown in the presence of germanic acid showed inhibition of growth with the spicules containing a GeO$_2$ and SiO$_2$ coprecipitated material, Figure 18. This effect was observed regardless of
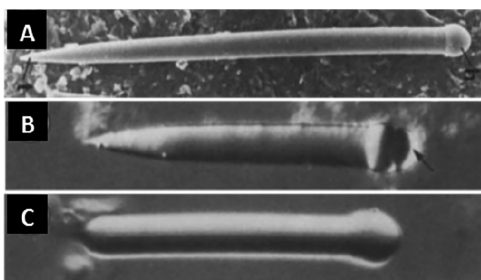

Figure 18. *Suberites Domuncula* sponge spicules formed in 0.36 mM silicic acid (A, control), in a Ge/Si ratio of 0.01 (B), and spicules grown in silicic acid for 20 days and then transferred into a Ge/Si ratio of 0.1 (C). The magnification of the images is ×730. Images reprinted with permission from ref 614. Copyright 1985 John Wiley & Sons, Inc.

whether the germanium was added before the start of spicule formation or once the spicules had started to grow.[614] Azam and co-workers suggested that incorporation of germanium in another living species, albeit a single cellular organism (diatom), required some cell wall silicification to have occurred before any germanium could be incorporated into the silicified

cell wall (known as the frustule in diatoms).[615] Thus, despite the similarities and affinity of these two materials, GeO$_2$ precipitation in nature does not seem to be incorporated in the same way as SiO$_2$ and, consequently, the role of biomolecules and proteins on GeO$_2$ synthesis is also expected to be different.

5.2. Surface Chemistry of GeO$_2$

As with silica, germania exists in amorphous and crystalline phases.[616] Three forms of GeO$_2$ exist at room temperature and atmospheric pressure, a vitreous form and two crystalline forms, namely, trigonal-hexagonal (α-quartz-like, Figure 19A), and tetragonal (rutilelike). For vitreous and hexagonal germania, the coordination number of Ge^{4+} is 4, whereas tetragonal Ge^{4+} has a coordination number of 6. The hexagonal form, which is the metastable polymorph,[616] is called the "soluble" form as it dissolves in water. The tetragonal form is chemically inert and practically insoluble in water.[617,618] Further, the hexagonal form has piezoelectric properties not present in the rutilelike form.[619] The most common form of crystalline GeO$_2$ as reported in the literature, and especially in biomimetic approaches, is hexagonal GeO$_2$ with a cubelike morphology.[89,90,94,95,620,621]

The surface chemistry and reactivity of GeO$_2$ in respect to SiO$_2$ is less well-known as it has not been studied as widely both theoretically or experimentally. The most significant surfaces of α-quartz-like GeO$_2$ are (001), (100), and (101), Figure 19B;[619] these are also the most studied surfaces of isomorphous α-quartz SiO$_2$. There are two possible terminations for the germania (100) surface, which are named (100)α and (100)β, Figure 19B. The α version corresponds to the β structure without the top dense surface; it is less highly packed and the most energetically stable.[619] The (001) surface has a top layer of oxygen and a sublayer of germanium. This surface is known to be highly reactive when compared to its analogous SiO$_2$ surface.[162]

To reach an understanding of how crystalline GeO$_2$ nanoparticles are formed, the BFDH method (suggested by Bravais, Freidel, Donnay, and Harker) and the HP model (proposed by Hartman and Perdok) have been applied.[94,622,623] Results suggest that the ideal morphology of hexagonal GeO$_2$ involves two hexagonal pyramids at the edges and a hexagonal prism in the middle, Figure 19C, i. However, in most syntheses performed under mild conditions, cubelike particles are observed which can be explained by the theoretical models described above. The models explain that crystal faces with the lowest attachment energies are the most prominent during crystal growth. For GeO$_2$, the crystal planes with the highest atomic density are ($1\bar{1}1$), (101), (011), (010), ($01\bar{1}$), ($10\bar{1}$), ($1\bar{1}\bar{1}$), and ($1\bar{1}0$) and grow at a slower rate than the rest, leading to the bipyramidal shape, Figure 19C, i.[620] As the crystal continues growing, the crystal planes (011), ($1\bar{1}\bar{1}$), and ($10\bar{1}$), with higher attachment energy, grow at a lower rate, resulting in cubelike-shaped particles, Figure 19C, ii, iii, and iv.[620,622,623]

Despite their chemical analogy and proximity in the periodic table, there are remarkable differences between SiO$_2$ and GeO$_2$. As an example, the electronic structure and optical properties of a GeO$_2$ continuous random network were studied by computational methods and compared to their silicon counterpart.[608] The calculated bond length of Si−O (1.631 Å) was found to be shorter than Ge−O (1.790 Å), and angles of SiO$_2$ were closer to a perfect tetrahedral than for GeO$_2$. The
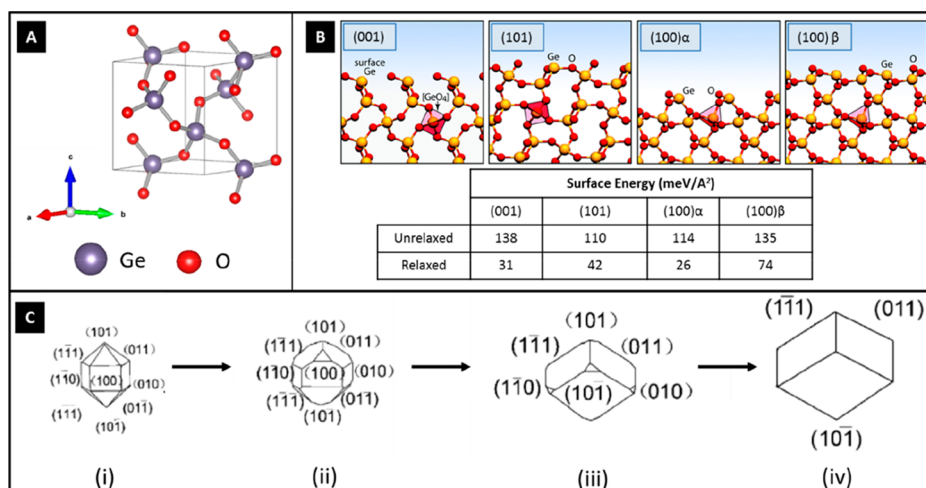
Figure 19. (A) Crystalline unit cell for α-quartzlike trigonal-hexagonal GeO_2 (space group $P3_121$) drawn using VESTA software[138] and the COD reference 9007477.[139] (B) Models of unrelaxed quartz-type GeO_2 surfaces (space group $P3_121$) with computed surface energies for unrelaxed (cleaved) and relaxed (reconstructed, $T = 0$ K) structures. Image adapted with permission from ref 619. Copyright 2014 Royal Society of Chemistry. (C) Scheme of the particle growth of hexagonal GeO_2. Crystals scheme reprinted with permission from ref 620. Copyright 2008 Elsevier.
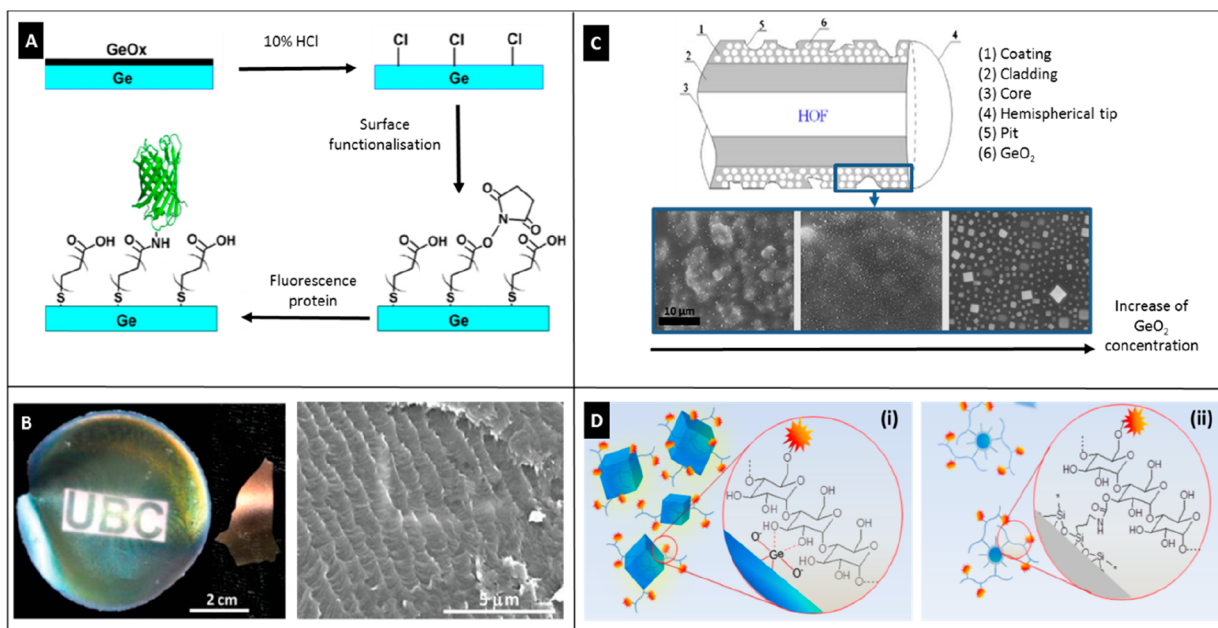
Figure 20. (A) Scheme of the GeO_2 surface modification for immobilization of green fluorescence protein. Image adapted with permission from ref 626. Copyright 2014 Elsevier. (B) Chiral nematic cellulose nanocrystals-GeO_2 films and the SEM micrograph of the fracture cross sections of the GeO_2/CNC composite. Images reprinted from ref 96 and information added. Copyright 2015 RSC. (C) Chitosan-SiO_2-GeO_2 hollow optical fiber and SEM images of the GeO_2 coating at different concentrations of germania.[627] (D) Polysaccharide-coated (i) GeO_2 and (ii) GeO_2-SiO_2. Image extracted with permission from ref 91. Copyright 2016 Springer.

bond order (strength of a bond between atoms) was also found to be higher for silica than that of germania.[608] Solubility in water is a further key property that differentiates SiO_2 and GeO_2 and varies according to particle size, crystallinity, and precursor used to generate the metalloid oxide.[113,617] This is a critical parameter as it determines the synthetic routes that can be used to form the material and its final applications. At room temperature, silica glass is soluble in water at a maximum concentration of 2.5 mM,[113] whereas germania is soluble at as high a concentration as 49.6 mM for amorphous materials and 43.3 mM for hexagonal crystals.[617]

This high solubility of germania strictly limits its synthesis and application in aqueous media, and is one of the main reasons why the synthesis of GeO_2 (from germanium alkoxide) is often performed in a mixture of water and alcohol.[89,90,607,624] The alcohol fraction facilitates the miscibility of the precursor in the aqueous media and reduces the solubility of the formed GeO_2, while water is still available for hydrolysis of the precursor. As an exception, tetragonal GeO_2 can be synthesized in aqueous media even at low concentrations as it is insoluble in water.[617] As can be expected, the reactivity of germania precursors in water is also different to that for silica. Germanium alkoxides are known to hydrolyze into germanic

acid, Ge(OH)$_4$, and subsequently condense as germanium dioxide, GeO$_2$, through a sol−gel process in a similar way to silica formation from alkoxysilanes,[113] although germanium alkoxides are known to hydrolyze much faster than their Si analogues.[94,625]

When using components such as biomolecules to direct materials formation, in addition to the potential effect of alcohol on the biomolecules themselves, the fast hydrolysis/ condensation reactions of Ge compounds may reduce the potential interaction time between germania precursors or hydrolysis species with the biomolecules. This suggests that control of biomolecules over particle growth may be more limited. Care is required when choosing both the medium in which the experiment is conducted and the time scale of the experiment in order to allow interaction of the various components (biomolecules, solvent molecules, and Ge-precursors/hydrolysis species) to occur. It is also important that the effect of the reaction medium on the behavior of the biomolecule is considered, as this may have a dramatic effect on biomolecule conformation, aggregation, exposed charges etc., all of which will impact on any potential mineral biomolecule interactions.

5.3. Bioinspired GeO$_2$ Based Materials, Synthesis, and Applications

5.3.1. Biopolymers as Directing/Templating Agents.
There have been some investigations that have explored the possibility of combining GeO$_2$ with biomolecules. In an investigation aiming at future applications in bioelectronics and biosensors, a Ge substrate semiconductor coated with a GeO$_2$ top layer was chemically functionalized in order to cross-link biomolecules on its surface.[626] The binding was shown by cross-linking a green fluorescent protein (GFP) onto the surface, Figure 20A, and this approach opens up a wide range of applications in bioelectronics using different types of biological molecules. Taking advantage of the unique properties of GeO$_2$, this mineral has been combined with high performance biopolymers such as cellulose,[96] pectin, or chitosan[627] to produce new materials with enhanced properties. For example, the synthesis of photonic films was achieved by combining cellulose nanocrystals (CNCs) with GeO$_2$ leading to composites with potential application in chiral separation, enantioselective adsorption, or catalysis.[96] In this study, CNCs added to GeO$_2$ in the form of an acqueous crystalline suspension were able to keep their chiral nematic properties even as a dry film. Furthermore, the use of polar organic solvents such as *N,N*-dimethylformamide (DMF) promoted the formation of lyotropic-chiral-nematic phases. In an alternative synthetic approach, CNCs have also been used as a template for amorphous GeO$_2$ condensation in a water/DMF solution with DMF serving as a drying control additive to reduce the hydrolysis and condensation kinetics of the germanium alkoxide precursor,[96] as previously used in a silica sol−gel synthesis.[628] Freestanding, transparent, and crack-free films of CNC/GeO$_2$ could be obtained, Figure 20B,[96] that could be calcined to yield porous germanium-based films. Pectin, a biopolymer commonly used as a gelling and stabilizing agent in the food industry, when combined with germania generates a biocompatible biodegradable material with antibacterial properties though little seems to be understood about how the two phases mix at the molecular level nor the specific role that each phase plays in the antibacterial properties observed.[629]

Germanium oxide and silica share common chemical properties which have inspired scientists to combine these materials using biomolecules to direct mineral deposition. As an example, formation of GeO$_2$ and SiO$_2$ in the presence of chitosan led to an efficient coating of hollow optical fibers that have been used for cell immobilization.[627] The characteristics of the GeO$_2$ coating of the fiber and the resulting luminescence properties were tuned according to the light transmission mode by simply changing the concentration of germania used in the synthesis, Figure 20C. Increasing the concentration of germania used in the preparation led to higher mineral coverage of the fiber by larger, crystals leading to a rougher surface, though a full understanding of the processes involved is not currently available. In a further study, the coated fibers were used for the production of hydrogen by cultivated photosynthetic bacteria.[630] The qualities of this biofilm photobioreactor were attributed to the provided nutrition, good luminescent properties, and roughness of the SiO$_2$− GeO$_2$-chitosan coating, allowing an adequate stabilization of the H$_2$-producing cells. Moreover, cells adhered to the coated fibers showed a normal size and formation of colonies, therefore demonstrating the biocompatibility and nontoxicity of the coating.[630] Another example of carbohydrates interacting with GeO$_2$, Lobaz et al., in 2016, reported that polysaccharides adsorbed on the growing germania crystal planes caused a morphology change on GeO$_2$ particles and reduced growth rate, leading to smaller particles and a higher number of nucleation sites, Figure 20D.[91] This effect on the nucleation and growth of GeO$_2$ particles was only observed for some of the polysaccharides studied. The proposed application of such materials is in the area of biological track and image applications where the results of the studies performed to date hint at the presence of specificity in the interaction between germania and biomolecules structures.

In another biomimetic approach focused on the optical properties of Ge and GeO$_2$, photonic crystals have been synthesized from GeO$_2$ by biotemplating using butterfly wings and GeO$_2$ liquid-phase deposition.[631] This combination of materials is interesting in that butterfly wings consist of a periodically repeating structure combining high and low refraction index regions, and Ge is a semiconductor with the highest refractive index, thus combinations of the two components have promising potential for applications requiring light propagation. The synthetic process consisted in the dissolution of germania powder in basic media with further GeO$_2$ condensation occurring under acidic conditions in the presence of activated butterfly wings, rich in chitin, as a template.[631] A sintering process was then applied to remove the organic template, leading to hexagonal GeO$_2$, which replicated the microstructure of the original butterfly wings. Finally, germania was reduced to Ge to obtain photonic crystals of high refractive index.[631]

In the research area of porous materials, mesoporous organo-germano-silicates with activated carboxylic groups were synthesized using fatty acids with potential use as enzyme-binder substrates. Calcination of the hybrid materials resulted in mesoporous amorphous silica and crystalline germania mixed oxides (Si−O−Ge−O−Si).[632]

Interest in GeO$_2$ has also developed from the biological point of view, where the aim is to understand the influence of microorganisms on mineral synthesis. The discovery of GeO$_2$ crystals templated by bacteria is suggested to have great potential in the sensor technology sector.[633] As an example,
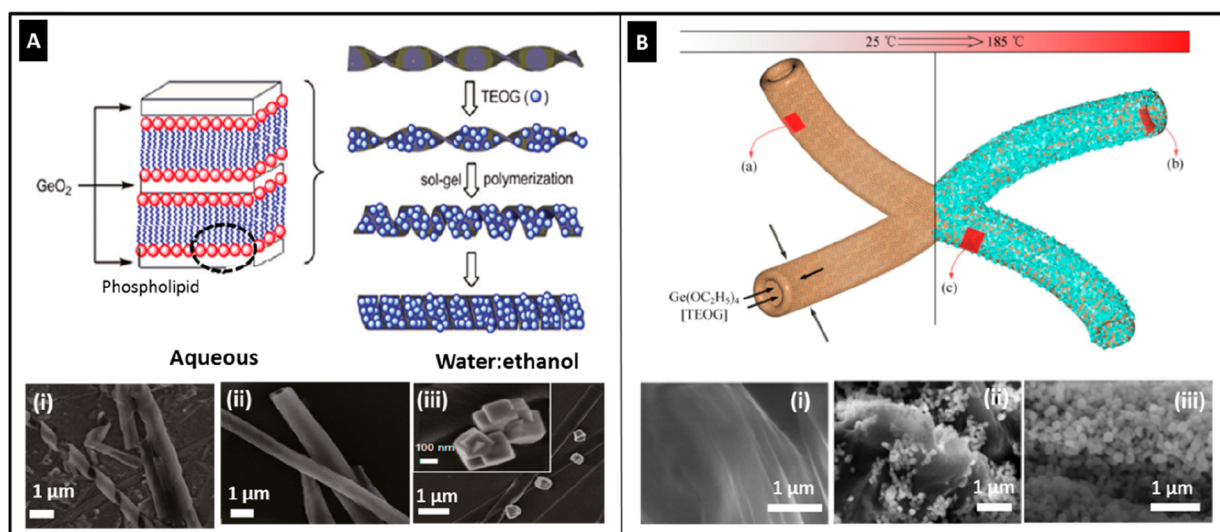
Figure 21. (A) Scheme of the assembly of lipids and germania, resulting in a (i, ii) GeO$_2$ coating of lipid tubules and (iii) further GeO$_2$ crystal formation through a sol−gel condensation on the previously coated lipids. Scheme and microscopy images adapted with permission from ref 624. Copyright 2009 American Chemical Society. (B) Scheme of the hydrothermal synthesis of GeO$_2$ nanocrystals on chitin fibers and SEM micrographs of the (i) chitin surface and (ii, iii) GeO$_2$ nanoparticles formed on different areas of the chitin fibers upon heating at 185 °C. Figure adapted with permission from ref 90. Copyright 2015 Springer.

biocrystals were grown from a Ge surface in the presence of *Pseuodomonas syzygii* bacteria submitted to a flow of water and UV light that allowed oxidation of Ge into GeO$_2$, where the bacteria served as nucleation sites for square GeO$_2$ crystals.[633]

One of the critical parameters for determining the interaction between metal oxides (or its precursor) and biomolecules is the surface charge. Several studies suggest that anionic germanate species resulting from an hydrolyzed precursor can interact with cationic groups like poly(allylamine hydrochloride),[97] phospholipids,[624] or chitin,[90] leading to precipitates of germania. As an example, tubular lipid structures coated with GeO$_2$ were obtained by the coassembly of aqueous TEOG (germanium(IV) ethoxide) with diacetylene phospholipid chains.[624] The adsorption of germania on the lipid surface was suggested to occur due to electrostatic interaction between anionic germanate species and positively charged phospholipids together with the mild acid catalysis provided by the lipids, leading to the neutralized species forming a thin film. A similar experiment performed with TEOS instead of TEOG resulted in a much lower yield of SiO$_2$, which was ascribed to the slower hydrolysis of the silica precursor in the absence of a catalyst. Further, GeO$_2$ crystals were formed by sol−gel reaction in a water:ethanol system on the previously germania coated lipids, Figure 21A.[624] In another example of biomolecule-induced germania synthesis, α-quitin from marine sponges served as biomimetic inspiration to hydrothermally prepare hexagonal germania-chitin composites of improved photoluminescence properties from TEOG. High temperatures applied were feasible due to the high thermal resistance of chitin, on which crystalline GeO$_2$ NPs grew and remained bound to the organic compound also after ultrasound treatment, Figure 21B.[90]

5.3.2. Peptides and Amino Acids As Directing/Templating Agents. Dickerson and co-workers identified a series of 21 peptides that could specifically recognize germania using biopanning.[634] Investigations related to the synthesis of germania in the presence of peptides suggested that some peptide-germania interactions may enhance the formation of

the mineral as analyzed by the increased yield of germania in the form of fine interconnected aggregated amorphous particles.[634] However, it should be noted that no assessment of the quantity of peptide incorporated/associated with the mineral phase was made, thus the extent of actual mineral formation remains unknown. The promotion of germania formation was stated to relate to the presence of amino acid functionality like hydroxyl or imidazole in the isolated sequences which we well know can only be part of the story. Following on from the identification of peptides with binding potential for germania, applications of individual peptides were explored. Hollow GeO$_2$ spheres of ca. 600 nm diameter were formed in the presence of an amphiphilic peptide able to form micelles in solution, suggesting templated particle growth.[92] One of the germania binding peptides identified, Ge34 (TGHQSPGAYAAH), was further used to functionalize gold particles and condense amorphous GeO$_2$ onto the gold phase with calcination of the biomaterial, resulting in crystalline rutilelike germania.[635] In this case, interaction between the peptide and germania was suggested to occur through the available deprotonated amine groups of the amino acid residues and germania at basic conditions (pH 9). The same research group synthesized biomimetic Ge34-germania mesoporous nanospheres to control the growth of embedded magnetic alloy CoPt nanoparticles of a size range of 8−9 nm diameter using calcined germania as a template.[636] The authors reported that the size range of these magnetic nanoparticles generated possible application in the biotechnology field as magnetic carriers for drug targeting. In a further study, the versatility of Ge34-germania materials was also shown by entrapping an enzyme (invertase) during synthesis, thereby improving the stability of the enzyme against temperature and pH.[637]

A different peptide sequence, Ge28 (HATGTHGLSLSH), also identified by biopanning[634] to bind to germania specifically, when used in our studies, at least for the conditions explored, showed no catalytic enhancement or morphological effect on the synthesis of hexagonal GeO$_2$. This suggested that
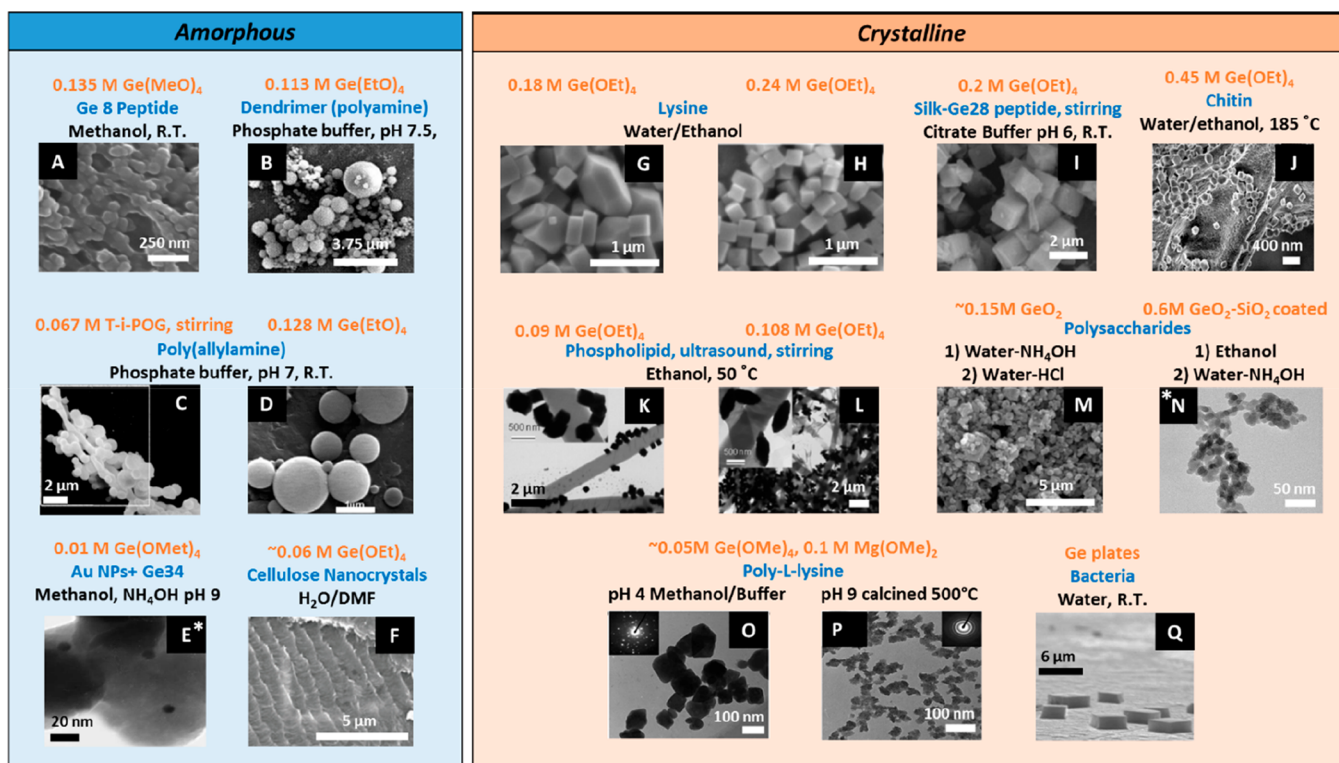
Figure 22. SEM and TEM micrographs from amorphous and crystalline GeO₂ synthesized in the presence of different molecules: (A) Ge8 peptide. Reprinted from ref 634. Copyright 2004 Royal Society of Chemistry. B) Dendrimer, reprinted with permission from ref 93. Copyright 2008 Royal Society of Chemistry. (C and D) Poly(allylamine) reprinted with permission from ref 97. Copyright 2005 Elsevier. (E) Au NPs and Ge34 peptide, reprinted with permission from ref 635. Copyright 2006 Elsevier. (F) Cellulose nanocrystals, reprinted with permission from ref 96. Copyright 2015 RSC. (G and H) Lysine, reprinted from ref 95. Copyright 2007 American Chemical Society. (I) Silk and Silk-peptide chimera, reprinted with permission from ref 621. Copyright 2014 Royal Society of Chemistry. (J) Chitin, reprinted with permission from ref 90. Copyright 2015 Springer. (K and L) Phospholipid, reprinted from ref 624. Copyright 2009 American Chemical Society. (M and N) Polysaccharides, reprinted with permission from ref 91. Copyright 2016 Springer. (O and P) Poly-L-lysine, reprinted with permission from ref 89. Copyright 2009 SAGE Publishing. (Q) Bacteria, reprinted with permission from ref 633. Copyright 2014 MDPI. Concentration values were obtained from the referenced literature or calculated from the described aliquots. The germania precursors used include germanium(IV) methoxide, Ge(MeO)₄; germanium(IV) ethoxide, Ge(OEt)₄; germanium(IV) isopropoxide, T-i-POG; GeO₂ powder and germanium plates, Ge.

despite the presence of hydroxyl and histidine functionalities, both thought to be involved in mineral surface recognition, catalysis of mineral precipitation required more than GeO₂ peptide binding affinity. We can speculate that these missing features could be related to specific peptide conformation or the presence of hydrophilic/hydrophobic domains. Perhaps surprisingly, the same Ge28 peptide induced the formation of bigger crystals when cross-linked to silk proteins under the same media conditions, exhibiting a different effect than that of the silk protein itself.[621] These experimental results support the hypothesis that peptide conformation in solution and in the presence of the mineral phases is a key parameter in enhancing and controlling mineral formation.

Despite its affinity for Ge surfaces, another Ge BP named Ge 8 (SLKMPHWPHLLP) was used to form Ag⁰ through binding to Ag⁺ in the presence of HEPES buffer [4-(2-hydroxyethyl)-1-piperazineethanesulfonic acid] and exposed to light, acting as a reduction inducer.[638] This peptide showed specificity for silver, but it was not able to induce the formation of inorganic nanoparticles such as ZnO or TiO₂. By applying electrochemical analysis, it was suggested that the formation of Ag⁰ depended on the Ag⁺: Ge 8 peptide ratio, with a ratio of 3 to 1 being optimum. Mutagenic sequences of peptide Ge 8 revealed that histidines were involved in the peptide to Ag⁺ binding; however, the Ag⁰ NPs formation depended on the presence of

methionine and tryptophan, presumably also by binding to silver. In this particular study, it was also shown that both specific amino acids and sequence order influence NPs synthesis. Furthermore, Ge 8 was able to control morphology, leading to the formation of spherical Ag NPs when the peptide was free in solution or nanowires when the peptide was immobilized on a surface.[638] Although the influence of specific amino acids on the alkoxide hydrolysis/condensation mechanism is still not clear, there is evidence that these biomolecules have a catalytic effect on the nucleation of mineral oxides.[88]

5.3.3. Approaches to Control GeO₂ Morphology and Crystallinity. Germania crystallization is dependent on germania concentration[95,639] and also on the nature of the precursor.[93] In fact, the size of amorphous GeO₂ particles was also found to depend on precursor concentration.[635] Precipitation of crystalline GeO₂ from TEOG in an aqueous system was found to take place at concentrations around 0.06 M, being close to its solubility limit (0.05 M). The incorporation of lysine in the solution resulted in a delay on germania crystallization, requiring more than a 2-fold increase of the GeO₂ concentration (0.14 M) for mineralization to occur. For those samples, the coexistence of amorphous and crystalline particles was found.[95]

The crystal growth of hexagonal GeO₂ evolves from a hexagonal to cubelike morphology, as described above.[620,623]

Variations on GeO_2 nucleation and final particle morphology has been previously achieved by different methods using biomolecules. The size, distribution, and morphology of germania particles, and other metalloid oxides, are known to be key parameters that control the chemical and physical properties of the resulting materials; therefore, there is much interest in finding synthetic routes that are able to tune nanoparticle growth. Avanzato and co-workers, associated the formation of cube-shape germania-magnesia nanocomposites to a slowing down effect during the condensation at low pH, in the presence of poly-L-lysine.[89] Germania nanocube formation has been also attributed to an H^+ etching effect in the presence of a surfactant related to fatty acids.[89,623] By means of varying media composition such as pH, water:surfactant ratio, and nature of the oil phase, Wu et al., achieved changes in the morphology of crystalline hexagonal germania nanoparticles.[623]

The use of biomolecules has shown a vast potential to tune the size and the morphology of germania in a simple process such as varying the concentration of a biomolecule (i.e., phospholipid).[624] Figure 22 shows a summary of the morphology diversity for amorphous and crystalline GeO_2 particles obtained in the presence of biomolecules. From these images, one can make a series of deductions based on key parameters influencing particle growth such as additive nature, concentration (precursor and additives), and media conditions. For example, the synthesis at concentrations lower than 0.14 M leads to amorphous GeO_2, Figure 22 (panels A–F)[93,97,634,635] unless heat is applied, Figure 22 (panels K and L).[624] The stirring process during the synthesis has been shown to lead to a morphological elongation effect on amorphous GeO_2 particles, Figure 22C;[97] however, this does not apply for crystalline materials, Figure 22I.[621] The use of templating biomolecules that are able to form microemulsions, such as polyamines, leads to the formation of well-defined dispersed GeO_2 spherical particles, Figure 22 (panels B and D).[93,97] Slight variations in precursor concentration and the presence of biomolecules has been shown to produce crystalline NPs of different morphologies, Figure 22 (panels G and H).[95,635] Generally, germanium alkoxides are used as precursor molecules for directing GeO_2 condensation in the presence of biomolecules; however, the element itself, Ge has also been used to prepare crystalline GeO_2 using bacteria as the templating element, Figure 22Q.[633]

The solvent, nature of the buffer, and the pH of the reaction solution is known to determine morphology and size of metalloid oxide particles. Since the solubility of germanate ions and GeO_2 is lower in ethanol than in water, nucleation in ethanol precedes particle growth and ripening, resulting in highly crystalline particles of smaller size than would be generated in water, Figure 22 (panels M and N).[91] The presence of phosphate buffer has been found to increase the particle size of dendrimer-templated GeO_2, thought to be due to cations in the buffer (Na^+) neutralizing surface charge on nanoparticles and allowing extended growth.[93] In one of our previous studies, the presence of bis-tris propane/citric acid buffer in a protein system increased GeO_2 particle size when compared to an analogous water system, leading to cubelike particles of up to 1.4 μm by a nontemplated synthetic path (as no significant organic content was found within the particles). However, the yield of GeO_2 precipitation decreased considerably, which could be the result of a low condensation rate due to biomolecule charge neutralization or capping effect of the buffer.[621] In both studies, one can suggest that the resulting

increase in particle size could be a consequence of a slower mineral condensation rate. The media pH also influenced the size and shape of GeO_2-Mg nanocomposites synthesized in the presence of poly-L-lysine, being rhombic cubic shaped and bigger at lower pH and small spheres at higher pH, Figure 22 (panels O and P).[89]

5.4. Techniques Directly Probing GeO₂-Biomolecule Interactions

To date, the biomolecule−GeO_2 interface remains largely unknown with few studies reported in the literature. A series of investigations discussed above simply describes how biomolecules are able to induce or template germania precipitation and to a limited extent, control its properties. The focus on these studies is on confirming and quantifying the inclusion of organic matter (i.e., the biomolecule) in the precipitates as evidence of an interaction, with limited effort devoted to understanding interfacial interactions.

The presence of GeO_2-protein composites has been demonstrated by Fourier transform infrared spectroscopy (FTIR), where both inorganic (Ge−O−Ge) and organic components (C=O stretch and N−H bend of amide groups of protein) were measurable for a range of peptide-germania and silk protein-germania composites.[621] In a FTIR study of chitin-GeO_2 nanocomposites, it was suggested that both species were interconnected by H-bonding, as observed from the O−H and C−OH vibration shift of chitin-related spectroscopic bands.[90] FTIR has also been used to identify the formation of pectin germania composites.[629] The absence of specific bands arising from C=O components of carboxyl groups in pectin on interaction with the mineral phase suggested direct carboxyl-mineral interaction.

Thermogravimetric analyses has also been used to provide evidence of the entrapment of peptide and silk composites within the mineral matrix, where organic matter was degraded between 200 and 600 °C.[621] Electrospray mass spectrometry (ESI-MS) has been used to study the complexation of GeO_2-lysine, with the incorporated lysine being suggested as the reason for a delayed nucleation of germania crystals as observed by small- and wide-angle X-ray scattering (SWAXS).[95]

Compared to silica and titania, computational models describing the GeO_2 surface and its aqueous interface are less developed. Early studies of the interface between a GeO_2 surface, the protein encephalin, and water molecules has been studied by molecular dynamic simulations in silico, though the results should be treated with some caution as even until now there is no established force field for germania, and neither were the experiments performed under a conformational sampling strategy that scientists working in this field would deem acceptable. Nonetheless, the results of the study showed that an hydrophilic surface of germania strongly interacted with hydrogen atoms of water, resulting in repulsion of the polar side of the protein by water molecules and that, when the protein approached the germania surface from the nonpolar side, water showed no repulsive forces.[640] These observations may provide hints as to a possible mechanism of interaction that should be explored further.

It is clear that much remains to be explored at the germania−biomolecule interface before we can confidently predict the likely effect that a particular biomolecule will have on the development of the mineral phase alone or in concert with other abiotic−biotic materials.

5.5. Toxicology of GeO$_2$

To date there are few studies in this area with some suggesting that germania is nontoxic while others suggest that the oxide has limited cytotoxicity. Note that with Ge, the element is able to substitute up to a few percent in silica structures with no harmful effect as seen in examples of biosilicifed structures formed in the presence of soluble germanium species.[614] Biocompatibility and nontoxicity of SiO$_2$-GeO$_2$-chitosan-coated optical fibers for a photosynthetic bacterium (*Rhodopseudomonas palustris* CQK 01) has been shown.[630] It was found that bacteria were able to adhere to coated fibers containing crystalline GeO$_2$, showing a normal size and formation of many colonies. This cell proliferation was not observed for uncoated fibers made of quartz glass, showing the difference in toxicity between the different oxides or forms of the oxide.[630]

Composites of pectin and germania show antibacterial activity against *E. coli*. This effect was suggested to be due to the release of germanium-containing species into the medium and their transport across cell membranes with deposition on cell organelles inhibiting intracellular transport and nutrition.[629] In this study, the germanium-containing species (precise identity unknown) were clearly acting as a toxic agent to the cells.

A study on Chinese hamster ovary cells reported that GeO$_2$ has limited cytotoxicity (80% of cells survived even at 22 mM GeO$_2$) and is not genotoxic. The cytotoxicity was measured by a cell density determination method (SRB assay), and the genotoxicity was analyzed by micronuclei assay. However, germanium oxide was able to block cell progression at a specific phase (G2/M) due to the reduced activity of a protein involved in the cell cycle regulation (Cdk1). The cell arrest effect increased as GeO$_2$ concentration increased up to 5 mM and then decreased for concentrations greater than 5 mM.[641]

Clearly, this remains an area where very little has been explored concerning the effect of particle size, composition, and surface chemistry whether or not these effects are modulated by the presence of biomolecules.

6. MO-BIOMOLECULE INTERACTIONS: BENEFITS AND PROBLEMS WITH CURRENT ANALYSIS APPROACHES

This review has demonstrated that combining MOs with biomolecules creates novel materials with a unique range of possibilities, yet to be fully explored and exploited. Biomolecules have proven to be smart and versatile tools with great potential in controlling the synthesis, structure, and/ or function of MOs. Thus, their continued use in developing applications that utilize the MO–biomolecule interface as well as further studies to understand and master the fundamentals of interaction is crucial to fully exploit the materials generated. Undoubtedly, interactions at MO–biomolecule interfaces are complex and can vary drastically depending on the intrinsic properties of the biomolecule, the physicochemical features of the MO surface, and the environment in which they are found as shown in Figure 23. It has also been suggested that the specific recognition of materials by biomolecules such as short peptide sequences is mediated from the sensing of the local changes in the H$_2$O density at the solid/liquid interface at the molecular level.[401] Furthermore, several studies indicate the importance of the precise structure of the water layers in proximity of the interface for adhesion.[642–645] Therefore,
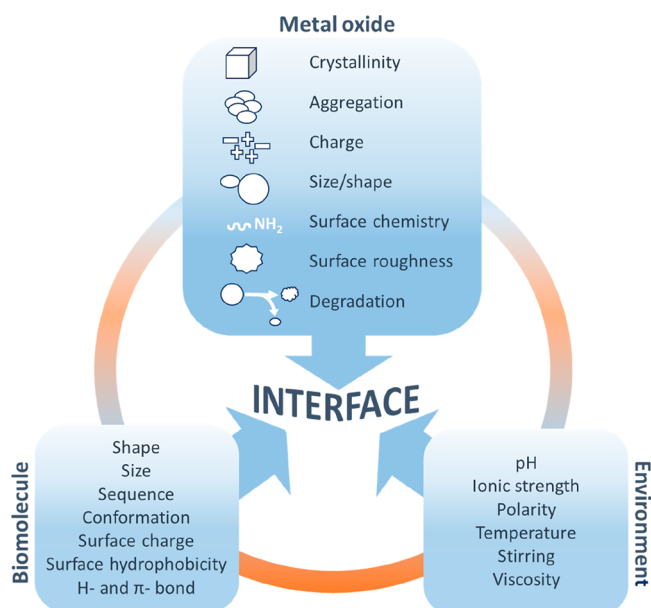

Figure 23. Scheme showing variables that affect interactions at MO–biomolecule interfaces: the intrinsic properties of the biomolecule, the physicochemical features of the MO surface, and the environment/ media conditions.

before carrying out interaction studies, a question should be asked as to what exactly the biomolecule will recognize on the MO surface? First, a thorough characterization of the MO surface and the biomolecule should be carried out, and the effects of the surrounding media should be taken into account. It is surprising how few reported studies fully characterize the materials being used, making comparisons and reproducibility difficult across different research groups. Progress demands that much more rigorous characterization of materials is performed and more detailed descriptions of experimental procedures are provided in the literature.

Nonetheless, experimental techniques and computational tools that have been used to investigate and characterize MO-biomolecule interactions have significantly contributed toward enhancing our understanding. This has been achieved through determination of binding selectivity,[65,154,168,239] surface coverage,[63,168,286,398,402] kinetic, and thermodynamic changes during interaction[87,553] and elucidation of biomolecule conformation when unbound/free and surface bound.[214,286,646–648] As a guide, Table 1 is a summary evaluation of key techniques that have been used to study interactions of biomolecules with ZnO, TiO$_2$, SiO$_2$, and GeO$_2$, where a description of the principle of the method, information that can be obtained, and factors to consider when using the techniques are given alongside examples of studies that have used the techniques. As these techniques have different fundamental principles and measurement modes, they will therefore have different advantages and disadvantages associated with their use. Thorough evaluation is required to identify the appropriate areas of application of these techniques depending on the MO (or other material) and biomolecule being studied.

6.1. Detection and Quantification of Biomolecules Adsorbed to MOs

As shown in Table 1, a number of methods are used for the detection and quantification of biomolecules adsorbed on and within MOs. For example, FTIR, RAMAN, NMR, TGA, XPS,

Table 1. Techniques for the Study of the Oxide−Biomolecule Interface

Technique	Method/Principle	Information	Considerations	Ref
UV/Vis	▪ Measurement of the attenuation of a beam of light (UV/vis range) after it is adsorbed by or reflected from a sample ▪ Change in electromagnetic absorption at specific wavelength	▪ Crystal defects, grafted labelled biomolecules, complexation of non-precipitated MO precursor for biomolecule catalytic activity ▪ Adsorption kinetic studies and protein quantification *i.e.* using Bradford assay	▪ Solution based technique. ▪ Fast & non-invasive ▪ Low sensitivity ▪ Not selective (if several components absorb at the same wavelength)	91,93,409,658, 659,694-697
FTIR	▪ Measurement of change in frequencies due to molecules absorbing light in the infra-red region of the electromagnetic spectrum ▪ A samples infrared spectrum of absorption and emission is obtained ▪ Different accessories can be used (*i.e.* Attenuated Total Reflection (ATR), transmission, specular reflection and diffuse reflectance)	▪ Sample identification; Observed frequencies are characteristic of a specific molecular structure ▪ Quantitative analysis to determine amounts of additives or contaminants ▪ Kinetic analysis by observing the growth or decay of infrared absorptions ▪ Peak deconvolution can be carried out to identify changes in bonding or determine secondary structure of a protein/ peptide	▪ Short analysis time ▪ Small sample required for analysis ▪ Highly sensitive giving qualitative data ▪ FTIR simultaneously collects high spectral resolution data over a wide spectral range ▪ Possible overlapping peaks which may limit interpretation ▪ The wavelength scale is calibrated by a laser beam of known wavelength that passes through the interferometer which is more stable and accurate compared to dispersive instruments.	31,44,73,90,93, 154,214,410,52 7,528,557,558, 621,646,698,69 9
Raman, SERS, TERS	▪ Detection of inelastic scattering of monochromatic light by a sample	▪ Gives chemical and structural information ▪ Probes MO-biomolecule interactions if they are located near binding site/ exposed to a different microenvironment (i.e. biomolecule conformational changes upon binding) ▪ Quantification	▪ SERS limited to plasmonic structures (*i.e.* Au, Mo) and only thin layer of non-plasmonic surface can be added (*i.e.* SiO₂, Al₂O₃) ▪ Raman has no interference from absorption of water molecules	295- 297,439,553,55 7,559,699-702
CD	▪ Difference between the absorption of left-handed and right-handed circular polarised light that takes place in chiral chromophore molecules.	▪ Conformational changes (i.e. α-helical, random coil) ▪ Chirality	▪ Fast & highly sensitive (< 0.1 mg for proteins) ▪ Solution based technique ▪ Some buffer incompatibility (i.e. phosphate, sulphate) ▪ Only for chiral molecules (i.e. polypeptides and proteins) ▪ Low structural resolution ▪ Low sensitivity to structural changes	86,96,180,229, 286,409,658,66 0,694,703-707
DLS	▪ Changes in the light scattered by particles in Brownian motion	▪ Determine size of biomolecules and MO particles and aggregates ▪ Formation of complexes *i.e.* soft and hard biomolecule corona complexes with MO can be measured	▪ Simple and fast ▪ Only for particles in the submicron region ▪ Viscosity dependence ▪ Lower resolving power (i.e. polydisperse sample) ▪ Scattering from large particles can mask detection of smaller particles in mixtures.	31,91,246,286, 378,411,557,70 6,708-711
Zeta potential	▪ Gives the electrokinetic potential difference between the dispersion medium and the stationary fluid layer around the dispersed particle/ droplet under measure.	▪ Biomolecule detection & quantification ▪ Surface coverage ▪ Indirect determination of K_B ▪ Adsorption Isotherm ▪ Determination of hard and soft corona ▪ Determination of protein conformation	▪ Solution (pH dependent) based technique ▪ Probe may be required to label biomolecule and/or MO ▪ Buffer restrictions	176,557,656,65 9,708,712-715
Fluorescence	▪ Intrinsic fluorescence (i.e. protein fluorescence predominantly from tryptophan) ▪ labelling using fluorescent molecules to aid the detection of a biomolecule and/ or MO	▪ Biomolecule detection ▪ Probing stability of biomolecules ▪ Probing conformational changes ▪ Live cell localization of biomolecules (in vivo studies)	▪ Solution based technique ▪ Where a probe is required to label biomolecule and/or MO this may influence their properties and their interaction	716-721
Photo-Luminescence Spectroscopy	▪ Light emission by matter as a consequence of the absorption of photons at a particular wavelength and emitted.	▪ Quantification of adsorbed biomolecule ▪ Determination of surface coverage	▪ Contamination can quench the photoluminescence	523,529,557,69 4
Mass Spectrometry	▪ MALDI TOF MS - Pulsed UV laser strikes a matrix of small organic molecules which adsorb UV light	▪ Detects & characterises mixtures of biomolecules i.e. peptides, lipids, nucleotides, saccharides	▪ Versatile technique best suited to study biomolecules due to its "soft ionisation" technique	654,722-726

Table 1. continued

Technique	Method/Principle	Information	Considerations	Ref
	and are energetically ablated from the sample surface, converting analytes into gaseous form (Ionisation) ■ TOF-SIMS - mass analysis of secondary ions sputtered from a surface bombarded with primary ions ■ TOF is used to separate & detect analyte ions by mass-to-charge ratio	and other organic macromolecules ■ Versatile molecular analysis with ranging applications including surface imaging and ■ depth profiling	■ Organic matrix used to facilitate ionisation ■ Flight-path variation in TOF due to inhomogeneity in the sample surface and variation in the size of the crystal or the matrix compound can cause mass drift ■ Lack of heated injection chamber present in other forms of MS, allows for the analysis of sensitive biomolecules ■ Preparation & storage of solid sample possible ■ TOF-SIMS: lateral resolution of is much higher than that of MALDI-MS imaging	
NMR	■ Shift of magnetic resonance frequency (δ)	■ Determination of K_D ■ Structural information ■ Chemical shift (δ) can be related with type of interactions ■ Distinguishes molecules based on local chemical environment ■ Nuclear Overhauser effect (NOE) may help with biomolecule structure determination, as well as identifying which biomolecules have interacted with MO ■ Can distinguish between a free and bound biomolecule ■ Many complex pulse sequences available	■ The sensitivity of the technique depends on the strength of the magnetic field ■ Non-destructive ■ Solid/Solution state	81,236,290-292,403,705,727,728
QCM-D	■ Changes in oscillation frequency (Δ_f) and dissipation (ΔD) of a quartz crystal disk upon mass loading	■ Δ_f related to adsorbed/desorbed mass/thickness ■ ΔD related to rigidity and softness of adlayer ■ Indirect determination of K_B, ΔH, ΔS, ΔG	■ Label free ■ Sensitive to the nanoscale ■ Kinetics influenced by viscoelastic factors of adsorbing layer ■ Immobilization required ■ Measured mass also includes hydration and entrapment of solvent molecules ■ Requires thin surface that should be evenly distributed	86,87,265,278-280,284,697,722,729,730
ITC	■ Heat of binding	■ Determination of thermodynamic parameters (K_B, ΔH, ΔS, ΔCp, n) by direct measurement of heat change (endothermic/exothermic) as a result of interaction.	■ Solution based technique ■ Label free ■ No immobilization ■ No buffer restrictions ■ Buffer matching of the component in the cells (sample and reference) and syringe is required ■ Few available models for data analysis ■ Dependant on accurate quantification of interacting components (ligand and macromolecule)	29,76,180,553,677,708
SPR	■ Optical technique that detects change in refractive index at the surface of a sensor due to mass adsorbed	■ Real-time quantitative binding affinities and determination of kinetics rate constants: (k_{on}, k_{off}, K_D, and R_{max}) ■ Measure dielectric properties, surface degradation or hydration ■ Biomolecule conformational changes	■ Label free ■ High molecular mass of the ligand required ■ Surface coupled: Immobilization required on a metal film, typically gold	256,270,272,284,731-736
AFM/ SMFS	■ Measures force between a probe and sample ■ Maps the tip-sample interaction	■ Topographic imaging (3D surface profile) ■ Determination of height, friction, and magnetism ■ Measures adhesion forces of biomolecules with MO surface	■ High resolution possible in some cases, ■ Low scanning speed ■ Low resolution ■ Sample treatment not required i.e. metal/carbon coating ■ Usually no charging artefacts in the image ■ Solution based measurements possible	246,265,284,375,402,439,465,649,695,700,713,737-740

Table 1. continued

Technique	Method/Principle	Information	Considerations	Ref
Ellipsometry	• Optical method that records the change in polarization of elliptically polarized light when it reflects on a sample surface. If biomolecule adsorption occurs on a MO surface the associated change in polarization is detected	• From changes in the ellipsometric angles, the refractive index, optical thickness, composition, roughness and crystalline nature of the film can be deduced	• Measures an intensity ratio therefore is less affected by intensity instabilities of the light source or atmospheric absorption • Measurements are not influenced by normal ambient unpolarised stray light • Ellipsometry is considered superior to reflectivity measurements for anisotropic samples	741-743
XPS	• Changes in the binding energy and kinetic energy	• Elemental identification and chemical state of element • Relative composition of the surface	• Solid state • Surface characterization highly sensitive (< 10 nm)	439,527,528,649,654,695,698,700,702,729,740,744
XANES/NEXAFS	• X-ray absorption spectroscopy spectra	• Elemental specificity • Provides information about the molecular organization including order and organization	• Synchrotron radiation • Commonly used adsorption edges: carbon (285 eV), nitrogen (400 eV) or oxygen (530 eV)	745-748
XRD	• Changes in d-spacing values measures the angles and intensities of beams diffracted from incident X-rays by crystalline atoms	• Lattice strain modification caused by biomolecules intercalating in the lattice crystal • Distinguish between crystalline and amorphous materials • Determine changes in d-spacing	• Solid state • Crystalline material can be studied using Wide-angle X-ray Scattering (WAXS) • Amorphous materials can be studied using Small-angle X-ray Scattering (SAXS) • Single-crystal for amino acids?	96,232,298,439,527,528,557,560,621,649,700
TGA and/or DSC	• Sample is continuously weighed as it is heated to temperatures up to 2000 °C. • Various components of the sample are decomposed as the temp increases • The weight % of each resulting mass change is measured	• Provides information about physical phenomena such as vaporization, sublimation, adsorption, desorption • Provides information about chemical phenomena such as chemisorption, dehydration, decomposition, solid-gas reactions	• Solid state thus only quantifies hard corona (tight binding) • Heating can alter the material • A destructive technique	44,91,527,528,621,727,749,750
Gas Adsorption (N$_2$)	• Physical adsorption of gas molecules on a solid surface for the measurement of the specific surface area of MOs	• Specific surface area and the pore size distribution	• Requires sample pre-treatment • Non-destructive solid-state analysis	637,751,752
SEM/TEM/STEM	• High resolution imaging using a finely focused electron beam	• SEM/TEM: Morphology and structural changes upon interaction of MOs and biomolecules	• SEM: Only solid nm to μm scale samples that can withstand high vacuum pressure can be analysed in routine instruments though environmental SEM possible for 'wet' samples	32,33,43,44,70,75,80,214-218,508,510,522,526-529,539,649,659,697,698,718,740

DLS, and zeta potential measurements are techniques that can give concurrent direct information about both organic and inorganic constituents. Their complementary use has been used to probe the MO−biomolecule interface. For instance, when biomolecules like proteins, peptides, or amino acids interact with a MO surface, this may be observed by detection of the amide-I band ($\sim$1700−1600 cm^{-1}) and amide II band ($\sim$1500 and 1600 cm^{-1}) using FTIR.[44,154,411,527,528,621] Furthermore, using FTIR, the secondary structure of proteins, for example, can also be determined and changes (from its native form) may be associated with adsorption events occurring at the MO−biomolecule interface.[214,411] However, this method does not necessarily identify the binding moieties. For example, it was suggested that shifts in −NH$_x$ and CO bands could be due to hydrogen bonding with the surface;[232] however, this was not substantiated until studies were performed on similar samples by NMR[291] and then only for specific peptide oxide pairings. More remains to be done using this combination of techniques.

In contrast, when MO synthesis occurs through the formation of intermediates such that more than one crystalline phase is identified using XRD, XPS may be used to determine the relative ratio of M/O and hence deduce if the final MO product has been achieved.[439,527,528,540,649] With the use of XPS, the presence of biomolecules can be confirmed by observation of, for example, the N 1s region and C 1s region, corresponding to the nitrogen atom of an amino group (BE $\sim$ 399.0 eV) and to the tertiary carbon connected to it (BE $\sim$ 286.5 eV), respectively.[526,528,564] As changes/shifts in the binding energy of an element are indicative of atoms in a different chemical environment, biomolecule interactions with a MO may be identified. However, XPS cannot be used to study specific interaction modes at the interface due to instability of biomolecules in ultra high vacuum conditions. Using XPS to monitor changes in the relative ratios of M/O in precipitates collected at different time points during the synthesis of a MO in the absence and presence of a biomolecule can serve as a tool to identify the effects of the biomolecule during MO formation. As an example, this has been demonstrated in a study where delayed formation of ZnO has been shown to occur in the presence of a specific peptide.[528]

In combination with XPS, Raman has also been used to confirm the strong adsorption of peptide to ZnO by detecting the presence of the amide I band, the amide III ($\sim$1300 cm^{-1}) band, as well as peaks that can be suggested to arise from a specific amino acid in the peptide.[553] In comparison to FTIR, the potential of Raman spectroscopy to study MO-biomolecule

interactions is far from being fully explored. Raman spectra can be used to track changes due to interaction of a MO with a biomolecule; that is, it has been reported that changes in Raman spectra of the aromatic amino acids tyrosine, tryptophan, and phenylalanine can be used to probe protein/peptide-material interactions if they are located near the binding site or exposed to a different microenvironment (protein/peptide conformational changes upon binding).[650] When compared, both Raman and FTIR help to probe different responses of the same normal modes. Since structurally sensitive, normal modes, sampled by the two techniques, become valuable objects for numeric evaluations. This facilitates approaching a solution of the inverse problem—anticipation of a structural function using Fourier Transformed responses from such.[651] This is an area of research that is ripe for development as access to high power computing facilities becomes more widely available and experimentalists and theorists better understand the potential of combining experiment with simulation to drive advances in understanding how biomolecules can interface with materials.[39,154] Both Raman and FTIR have advantages and disadvantages associated with their use (i.e., fluorescence from samples like SiO$_2$ may interfere with the ability to take Raman spectra, which is not an issue with FTIR).[652] On the other hand, FTIR is sensitive to polar bonds, especially OH stretching in water which can interfere with spectra of hydrated samples and is not an issue with Raman.[652,653]

In some of the above-mentioned studies where adsorbed biomolecules have been identified using combinations of FTIR, Raman, and XPS, TGA has been used to quantify the amount of a biomolecule adsorbed to the MO precipitate.[44,527,528] Additionally, during synthesis, DLS can be used to obtain information on particle growth and the size of any initial droplets or aggregates of the biomolecule that may serve as a template for the MO/biomolecule composite.[91] One can compare the hydrodynamic radius of the individual components and the composite to have a first understanding of the hybrid synthesis path (i.e., templating). This can later be confirmed by analyzing the organic composition of the composite by TGA analysis.[527,528,540] A limitation of DLS to measure crystal growth is that hydrodynamic radius refers to a spherical model, hence, is significant only if materials have spherical or nearly spherical shape.

Fluorescence-based labeling techniques such as fluorescence spectroscopy[91,168,176,533,534] and confocal microscopy[186,654,655] have also been widely used for detection and/or quantification of biomolecules. Exceptionally, live cell protein detection and its localization can be determined by FRET microscopy imaging.[648] Studies have similarly shown that much more information can be generated for a fuller understanding of events occurring during MO formation when fluorescence-based labeling techniques are used in combination with other techniques. For example, fluorescamine assays have been used to quantify biomolecule adsorption on MO surfaces generating adsorption isotherms that can be used to determine biomolecule affinity and surface coverage.[176,180] Zeta potential measurements carried out in parallel may yield additional information such as surface charge/peptide pI which can be used to predict possible binding mechanisms.[31,89,154,176,180,656] The fluorescence lifetime behavior of amino acids in protein has been related to conformational changes, as is the case of tryptophan adsorbed on a hydrophobic Teflon surface where its shortened fluorescence lifetime was associated with an increase of α helix content on binding.[657] However, the same trend was not observed on hydrophilic SiO$_2$ surfaces (fluorescence lifetime unchanged with variation in α helix content).[657] CD spectroscopy has also been used to obtain more conformational information on the secondary and tertiary state of biomolecules including proteins and peptides.[180,409,647,658−660]

6.2. Real Time Monitoring of MO-Biomolecule Interactions

Techniques that allow for real-time monitoring of MO-biomolecule interactions include QCM-D, SPR, AFM, ITC, and fluorescence-based adsorption assays.

QCM-D is an established technique for probing abiotic−biotic interaction processes such as MOs and biomolecules as has been demonstrated in various studies with TiO$_2$[86,87] and SiO$_2$.[265,278−280,284] Limited stability of ZnO films in an aqueous environment has currently precluded its use in the study of ZnO biomolecule interactions. Experimental information obtained using QCM-D such as adsorbed/desorbed mass/thickness, rigidity, or softness of an adlayer, and possible determination of orientation of adsorbed biomolecules can be used to investigate the mechanism behind specific MO-biomolecule interactions. Information from QCM-D can also be used to indirectly determine values of K_B, ΔH, ΔS, and ΔG as well as physical parameters such as density, viscosity, or storage modulus. It is important to note that in QCM-D, the measured mass coupled to a MO surface includes added mass due to biomolecule hydration and entrapment of solvent molecules.[661,662] This issue can be circumvented by using a complementary method like SPR that can be used to differentiate the measured mass adsorbed during MO-biomolecule interaction due to hydration and not the biomolecule. SPR is, however, limited to materials that can be deposited as nanoscale-thick films (about 100 nm thick or less) on a biosensor substrate coated with gold. For example, the adsorption of peptides to gold-alkanethiol self-assembled monolayer (SAM) surfaces has been studied using SPR.[663] In this study, the standard state adsorption free energy was determined from adsorption isotherms and the use of the Langmuir model characterizing peptide adsorbed as a function of concentration.[663]

The use of AFM has greatly advanced beyond high-resolution imaging to directly probe biomolecular interactions.[664] AFM-based single molecule force spectroscopy (SMFS) allows one to directly access the interactions between biomolecules and different material interfaces ranging from surfaces (including MOs) to soft biosubstrates.[665−667] The biomolecules are tethered to the AFM cantilever via a chemical functionalization procedure, commonly including a silanization step and the usage of PEG linkers.[668] The binding free energies of the biomolecules to MO substrates can be estimated by means of measurements performed at variable loading rates.[669] The curves of binding force as a function of the loading rate can be fitted via kinetic models, from which the binding free energy values can be extracted.[670,671] Investigated biomolecules range from single amino acids to whole proteins.[498,672] Additionally, AFM tips can be functionalized with oligonucleotides with sequences engineered to display specific affinities toward analytes. The measured adhesion forces between the functionalized tips and generally passive substrates (including MO surfaces) change when in the presence or absence of the molecules of interest. With this method, molecules at concentrations $\leq$ 100 pM can be detected.[673]

The stability of the substrate during AFM measurement is essential for reliable results since changes in surface roughness may have an influence on the measured binding forces. Further challenges in this field include overcoming issues to do with understanding precisely how the conformation of a molecule is affected by the coupling procedures, how the molecule of interest recognizes the surface, and further, there are current issues to do with poor reproducibility of results, the ability to automate the process to reduce operator bias, as well as development of better models appropriate to the complex samples that are being studied. In combination, SPR and AFM have been used to obtain biomolecule surface adsorption free energies.[284] Note, AFM requires a macroscopically flat MO surface, which does not have to be as thin and evenly distributed as is required for SPR and even more so for QCM-D. An AFM method has been developed to estimate $\Delta G°_{ads}$ for biomolecule adsorption to materials including MOs that cannot be easily formed into thin films.[284] Strong correlation between desorption forces (F_{des}) obtained using a standardized AFM method and $\Delta G°_{ads}$ determined using SPR have been reported.[284]

ITC, as a method to measure energy changes during binding has evolved from its conventional use to study biomolecular recognition reactions into diverse areas of interest including its development to study interactions between biomolecules and inorganic nanoparticles including MOs.[553,674−677] The main advantages of using ITC over other more established techniques used to study the interaction of biomolecules and MOs (i.e., SPR, QCM-D, XPS, NMR, and fluorescence-based adsorption isotherms) is that it is a direct measure of molar enthalpy, thus it is able to determine all thermodynamic parameters (ΔH, ΔS, K_A, and ΔG) from a single experiment (experiments do not need to be carried out at different concentrations or temperatures to derive thermodynamic parameters).[678−680] ITC can also be used to study interactions of biomolecules with MOs in their bulk or particulate form, whereas techniques like QCM-D, SPR, and AFM require the immobilization of MOs on a surface. Additionally, ITC also does not require labeling of an interaction component as is needed for fluorescence-based adsorption assays. Nonetheless, like any other technique, the use of ITC has challenges such as difficulty in data interpretation (i.e., definition of the binding sites on the biomolecule and the MO surface).[561,562] It has been proposed that when studying interactions between biomolecules and particles (including MOs) using ITC, the effective concentration of surface sites on the particles available for interaction can be estimated from equilibrium adsorption isotherm measurements (AI) and the BET-determined surface area of the particles.[681,682] Such combinations of ITC and equilibrium adsorption isotherm measurements can facilitate interpretation by separating the adsorption free energy change into discrete entropic and enthalpic contributions.[683]

It is however important to note that there may be discrepancies between the surface sites that are accessible to small gaseous molecules such as nitrogen used in BET experiments compared to the size of interacting biomolecules being studied.[681] Equally, quantification of the maximum number of biomolecule interaction sites (N_{max}) per unit surface area of the particles and correlating adsorption isotherm measurements to ITC measurements is not applicable in instances where multilayer adsorption occurs with global heat effects produced, as there is no clear distinction between heat change due to biomolecule-MO surface interaction and biomolecule−biomolecule interaction.[553,674−677] It is also important to note that in adsorption isotherm measurements, if centrifugation is used to separate the supernatant containing unbound biomolecules from the pellet containing particles with adsorbed biomolecules, then this may perturb the peptide-nanoparticle complex, leading to inaccurate quantification of bound and free biomolecules. Nevertheless, the application of ITC to measure abiotic−biotic interactions continues to be developed. Improvements in ITC analysis methods are needed (i.e., to generate mathematical models that are more representative of the interaction process or to determine new ways to interpret data even without fitting models as proposed by Lin and co-workers in 2017).[563] The use of complementary techniques to kinetically/thermodynamically characterize MO-biomolecule interactions will also drive improvements in ITC data analysis and interpretation.

6.3. Importance of Complementary Use of Techniques

The importance of complementary use of a range of experimental and computational methods has been highlighted throughout the review. There is no single technique developed that is able to obtain all the information necessary to fully characterize MO-biomolecule interactions. Every instrument has its detection limits which influence the findings. For example, to elucidate if biomolecules are entrapped within the bulk of the MO or on the surface, techniques such as XPS and FTIR can be applied. However, very few published studies use these methods appropriately to describe the surface of a material under the conditions where interactions occur, and yet it is at the very surface that biomolecules and ions present in the reaction medium and water itself will compete for adsorption sites on the mineral surface. XPS and FTIR, as well as having different detection limits, the complementary techniques of XPS, and attenuated total reflectance FTIR (FTIR-ATR) provide data at different distances into the surface of a sample. XPS (detection limit 0.1−1 atomic %) reveals the surface atomic composition of a material at the few nanometer scale range (3−10 nm).[684] Further, this technique can allow one to analyze the composition at different depths within this range. FTIR (detection limit of 0.1−1 wt %) can also be used to compare the surface chemistry of certain materials; it can analyze a specimen at a depth of a few microns.[685] In the case of biomolecules entrapped in a thick coating of MO, only the inorganic fraction would be detected by this approach. However, the data obtained could then be compared to information acquired by conventional FTIR analysis, where the IR beam is absorbed/transmitted through the sample. In the analysis of samples containing multiple phases, for example where MO synthesis occurs through the formation of intermediates that are mixed with the final MO product, detection of specific materials may vary with different techniques. For example, in a study reporting the presence of intermediates in synthesized ZnO precipitates, the organic components were quantifiable using TGA.[540] However, using XRD, such minor phases may not be detected if the amount is below the lower detection limit of the instrument which is about 1−2 wt %.[686,687] Further, these phases might be especially difficult to detect if the minor intermediate component is less crystalline than the major crystalline MO phase. In a study on ZnO, the occurrence and identification of the intermediate phases could be clearly confirmed when FTIR was used alongside many other methods.[540] This is in part, as stated above, in comparison to XRD (detection limit of about

1−2 wt %), FT-IR has a lower detection limit of 0.1−1 wt %.[688]

As discussed in other sections of this review, combinatorial techniques including phage display and cell surface display methods have played an important role in the identification of artificial biomolecules that bind to MOs with peptide sequences being identified that can interact with, and in some cases, control the morphology of MOs. However, many researchers have come to the realization that these approaches have their own biases in either intrinsic biases from the biological systems being used[62,689] or from the choice of components used in the screening procedure.[176,690,691] Therefore, advancements in peptide design may lie in the development of newer complementary random and rational approaches.[62,65,689,690,692] Alternative rational approaches include random mutations of sequences to investigate the significance of specific sequence alignment, conformation, and resulting effects on binding potency during interaction with target substrates.[527,573,693]

Theoretical methods (computational modeling and bioinformatics) are increasingly being applied for a selection of biomolecules that can strongly interact with MOs.[87,418] Moreover, it is becoming common to combine experimental characterization of MO-biomolecule interactions with theoretical studies to validate the modes of surface binding as well as provide more detailed understanding of possible interaction at the atomic scale, which is not accessible through practical experimental means.[87,418] The current challenges and debates on the accuracy of simulations of MO-biomolecule interactions, the need for representative force fields, and determination of an agreeable number of adjustable parameters is the platform that will lead to a standardization of the approaches taken in computational studies. When achieved, computational studies will accelerate our understanding of MO-biomolecule interactions. More is discussed in relation to this area in the section on Remaining Grand Challenges and Take Home Messages.

Complementary use of the range of experimental and computational methods discussed above would clearly enable users to obtain more useful information. It is expected that challenges may be faced in standardizing experimental conditions for a comparative study with different techniques (i.e., the working principles or limitations of techniques may prevent studies being carried out under identical conditions for direct comparison). However, researchers should strive to obtain data and interpret their findings based on information from as many complementary methods/techniques as is possible. From the exemplar MOs discussed in this review, it is clear that much more research has been carried out for some MOs like SiO_2, TiO_2, and ZnO with biomolecules in comparison to studies with GeO_2. Many of the methods/techniques that have been successfully used to build an understanding of interactions of biomolecules with the more extensively studied MOs are transferable to the less explored MOs like GeO_2 that have useful related and unique properties yet to be realized/exploited.

7. EMERGING TRENDS AND FUTURE OUTLOOK

We conclude by discussing some remarkable advances in other fields that may transform or shape our understanding and application of MO-biomolecule interactions. These examples demonstrate how biomimetic approaches are contributing to deliver new technologies.

7.1. Additive Manufacturing (AM)/ 3D Printing

Additive manufacturing (AM)/3D printing, which is the assembly of structures in three dimensions by adding materials layer by layer, is completely transforming the world of materials engineering and manufacturing.[753,754] Its application has extended from design in industries such as automotive and aerospace to diverse areas such as biomedical engineering.[755,756] There is no doubt that advancements in AM will have countless implications on society from the economic through political and environmental impacts.[757,758] Sophisticated computer-aided design enables superior flexibility and versatility to fabricate complex 3D structures which could not be realized using conventional manufacturing methods.[755] Pertinent to this review, AM engineers are employing biomimetic strategies to design intricate 3D printed constructs with an aim of creating materials with superior properties (i.e., strength and lightweight structures) and functionality.[759−762] There is also great interest and effort in the improvement of AM techniques to exploit an increasing variety of materials. Although synthetic polymers are the most utilized material in AM, natural polymers (biomolecules) (i.e., proteins, polysaccharides, and polynucleotides)[763,764] are progressively being utilized in 3D printing. Other materials that have also been used in AM methods include metals[765,766] (e.g., aluminum and bronze)[767,768] and metal oxides (e.g., SiO_2, TiO_2, Cu_2O, and ZnO).[768,769]

The growing interest in creating new composite materials is being realized through the convergence of AM with nanotechnology and biomedical engineering technologies with further expansion in the use of 3D printing. Biomedical applications of 3D printing include tissue engineering of devices such as medical implants and surgical guides as well as the fabrication of delivery systems that can act as carriers for cells or biomolecules that include drugs, growth factors, or antibiotics.[758,763,770] The use of biomolecules in biomedical engineering has the advantage that natural polymers are highly similar to the materials found in the native environment of host tissues, thus biological interactions could be strongly enhanced. At present, however, the principle limitations of the use of natural polymers are their high cost and inferior 3D printability.[763] A comprehensive review on the use of natural polymers in 3D printing is provided by Carrow and co-workers.[764]

In the merging of AM with nanotechnology, the addition of nanomaterials such as quantum dots, nanowires, metals, and carbon nanotubes to printable matrices made from materials such as polymers has the potential to expand the capabilities of nanocomposite 3D printed materials by taking advantage of the unique properties of nanomaterials.[754] If we now think of extending these ideas in the context of this review, we can ask, what is the potential for the development of technologies using 3D printing methods that exploit metal oxide-biomolecule interactions? Approaches may include the delivery of biomolecules by 3D printed scaffolds that have metal oxides incorporated for imaging or controlled biomolecule release. This would require the development of 3D printing approaches able to incorporate biomolecules during the printing process. The printing of scaffolds with encapsulated metal oxide micro- or nanostructures that can be carriers of biomolecules would need to be carried out using "greener" synthesis/fabrication conditions without thermal, radiative, or harsh chemical treatments.

Currently, 3D bioprinting techniques are being developed which have the potential to recruit biomolecules and cells during the printing process.[758,763,770,771] This general approach, albeit without the need for 3D printing was shown for growth factor/cell mixtures embedded in silica-alginate spheres back in 2011[772] but has more recently been demonstrated with the use of 3D printing for a multidimensional organized system using synthetic polymers [i.e., polymer poly(lactic-coglycolic acid) microspheres encapsulated with growth factors and embedded inside a scaffold made of polycaprolactone microfibers].[773] Complete exploitation of such mixed component systems will require careful characterization using orthogonal techniques to understand the effect of the interface on the behavior/functionality of the different components. This will require advances in materials characterization methods and techniques. It will be exciting to see how these emerging technologies will contribute to our understanding of interactions between metal oxides and biomolecules and influence the development of applications employing these interactions. There is no doubt that with continued improvements in the capabilities of 3D printing techniques such as resolution (to the molecular level or lower nanometer scale), speed, and compatibility with mixed components while maintaining functionality, the applications utilizing 3D printing will increase.

7.2. Synthetic Biology and Systems Biology

Another evolving area of research that is revolutionizing our understanding of biomolecules and their functionality is synthetic biology, which brings together the expertise of engineers and biologists to design/engineer novel artificial biomolecular components, networks, or pathways.[774,775] The approach is to apply circuit analogies of established frameworks used in electrical engineering with an end goal of achieving cellular control.[776−778] The method entails reprograming of organisms in a logical approach using standardized components termed biological circuitry (i.e., genes, proteins, cells, viruses, biological pathways, and biochemical reactions).[774,775] Using a synthetic biology approach, the behavior of organisms can be extended or modified to perform new tasks. For example, among the first synthetic gene networks designed and constructed is the genetic toggle switch which is an artificial gene regulatory network in *Escherichia coli*.[777] More recent advancements in synthetic gene circuit engineering including prokaryotic and mammalian gene regulation have been discussed in a review by Bashor and Collins.[779]

Like synthetic biology, systems biology which has been coined to refer to computational and mathematical modeling of biomolecular systems, focuses on characterization and understanding of the functionality of systems in their entirety rather than focusing on individual components.[780,781] This will allow elucidation of complex and integrated biological systems such as metabolic steady state and function, supramolecular functional properties like the cell cycle, the understanding of multifactorial diseases, and will advance other fields of research such as biotechnology.[782] For this to be achieved, significant progress in our understanding of computational sciences (i.e., the design of methods based on definite design principles and simulations as well as the development and implementation of databases), genomics, improvements in measurement technologies, and integration of these with existing knowledge will be required.[781]

Artificially engineered products of synthetic biology designed with insights from systems biology may achieve functionalities that far surpass those of biomolecules, eventually replacing them with much cheaper options. Nonetheless, where integration of cellular systems and materials is desired then a clear understanding of the forces at play between the various components, whether they be at the chemical, biochemical, or cellular level will all benefit from molecular level understanding of interactions occurring between inanimate (abiotic) and living (biotic) materials. Advances in our understanding will power the development of new applications for the betterment of the world and its ever-expanding population.

8. REMAINING GRAND CHALLENGES AND TAKE HOME MESSAGES

As we conclude, we note that much has been learned from interaction studies of MOs with biomolecules especially using relatively simple biomolecules, including amino acids and short genetically engineered peptides which in themselves offer a vast library of possibilities that can be studied. Ultimately, the knowledge gained may be transferred beyond biomolecular recognition to the design of cheaper and more stable small organic molecules with properties suitable for the design of MOs and hybrid functional MO-biomolecule conjugates.

This review provides insight into the current state of research in this field and may ultimately facilitate and provide guidance to new research strategies in the scientific community. We finish with a description of some of the remaining grand challenges in the field and provide some "take home messages" for those either entering into or already working in the field which we hope will lead to reduced ambiguity in terms of data reporting and interpretation.

There are many similarities between the materials discussed in this review article and, as such, there are common issues that need to be addressed before the field can move forward. These include (a) techniques for the specific study of the interface, including the ability to measure time-dependent changes for both the mineral phase and the inherently disordered biomolecules themselves; (b) the role of interfacial water and ions next to surfaces; and (c) the development of appropriate force-fields and simulation environments that mimic "real" life.

The aqueous−mineral interface plays an important role in (bio)molecule−surface interactions, but the development of a full understanding of the physical/chemical events occurring at the aqueous interface requires both a qualitative and quantitative description of the surface characteristics/properties that, in the case of amorphous silica, can be challenging due to the limited techniques that can be used to explore its structure at an atomic level.[162]

An even greater challenge has become to understand and characterize interfacial water, as, for example, it is difficult to distinguish between silica-biomolecule, silica-water, or biomolecule-water amalgams from the resulting interaction forces.[783] In this respect, third-order two-color ultrafast infrared nonlinear spectroscopy, established specifically for application to intermolecular structural analysis at complex biointerfaces,[784] demonstrates promise for unique resolving power to describe both the structure and intermolecular relations at complex disordered interfaces on the subpicosecond time scale. In this respect, it is important to notice that one-dimensional second-order Sum-Frequency Generation

(SFG) spectroscopy reveals a wealth of information on the nature of aqueous states associated with interfaces such as titania, one of the many metal oxides discussed in this review.[785] As one-dimensional bulk-specific linear infrared spectroscopy can be extended to two-dimensional third-order absorption spectroscopy to correlate different interatomic displacements in the bulk, so one-dimensional surface-specific second-order SFG spectroscopy can be extended to two-dimensional fourth-order SFG spectroscopy to correlate interatomic displacements at surfaces. Recently, actively phased controlled fourth-order SFG spectroscopy was reported for the first time.[786] Should these tools become more widely available then their application will be invaluable for advancing our understanding of biotic−abiotic interfaces. Further, optical infrared and Raman spectroscopies are particularly valuable in applications to disordered interfaces and their use, in combination with advanced quantum chemical calculation (see below for more details), should be developed further.

Many of the biomolecules that are used in studies of MOx-biomolecule interactions are short peptides identified from phage display that have no inherent particular secondary structure which causes great problems in characterization both of the peptides alone and in the presence of a mineral phase. Researchers who have shown that oligomers of specific binding peptides[270] (e.g., a quartz binding peptide oligomer binds better than the peptide themselves) may be simply seeing the effect of organization of the longer polypeptides into secondary structural motifs, leading to enhanced interaction, rather than an effect of the original sequence itself as has been proposed. It is possible that MOx-biomolecule binding will lead to increased organization, but as yet this is a little explored area with techniques needing to be developed that are amenable to study these composite systems using conditions (aqueous) that correctly replicate what is found during binding/mineralization.

Although, there has been great progress in the development of theoretical and computational methods, there is still great challenges to modeling interactions at the aqueous interface. Recently, Ozboyaci et al., in 2016, published a review of achievements and challenges for modeling and simulation of biomolecule−surface interactions in which a large number of the examples given refer to the MOx studied in this manuscript.[787] Similarly, a review by Knecht and Walsh, in 2017, describes in detail advances that have been made in computational approaches to examine nanoparticle biointerfaces.[109] In particular, they point out issues to do with the modeling of the inherently disordered short peptide sequences and the fact that the propensity of a peptide to bind via noncovalent interactions is not simply a sum of the binding strengths of individual residues. This problem not only exists for small peptides but also for disordered proteins and proteins containing both ordered and disordered segments. Very recent research by the Shaw group, in 2018,[788] and a review by Huang and Mackerell, also in 2018,[789] have shown that a number of common force fields used to study protein biophysics are not able to cope with disordered structures.[788,789] In proteins, this situation arises when the primary sequence contains a large number of hydrophilic (charged and polar) amino acids and reduced numbers of nonpolar residues that normally drive hydrophobic core formation.[789] In the case of small peptides interacting with inorganic materials, the situation is further compounded in that there is little possibility for the small peptides to form specific secondary structural motifs, that is

unless water (and ions) are excluded from the interface. The solution to this problem involves modifications of the force field used. For intrinsically disordered proteins, several approaches have been suggested. In the case of the nonpolarizable *a99SB-disp* model described by Shaw and co-workers,[788] this involved modifications to the water model (TIP4P-D), small changes in backbone torsion corrections and a change in strength of a backbone O−H Lennard-Jones pair.[790] An alternative solution has been proposed by Song and co-workers, in 2017, who generated improved force fields (*ff14IDPSFF*) by correcting the backbone dihedral distribution for all 20 amino acids.[791] Interestingly, their force field worked well with traditional TiP3P water and was tested against small proteins and a range of 9 mer peptides as might be encountered in studies of peptide-mineral interactions. What is clear is that in new computational studies of biomolecules at interfaces, one should consider using these types of advanced force fields to get better conformational sampling of the biomolecular species. The computational data so obtained should be supported by experimental measurement of biomolecule structure using NMR wherever possible. A further issue that has to be addressed is the relatively flat conformation space adopted by such molecules such that sampling methods need to be adopted that obtain information on a representative conformational ensemble as one would measure in an experiment.

Careful thought and planning of the protocol is needed to accurately capture this structural complexity in any simulation. A range of simulation approaches are discussed in the review by Walsh and Knecht.[109] Studies on silica and titania are well-represented, but studies on zinc oxide and germania although similar in scope have not been studied or as well-reported up to now. For all, there is still a need to model both the bulk and the surface of a material as well its interface with water, ions, and biomolecules. Force fields and parameter sets that better match the experiment are being developed, but even these have limitations. As an example, a force-field such as the CHARMM-INTERFACE FF[792] has been developed, but at present, its application to the study of silica (and other mineral) peptide interactions still uses as its mineral structure extracts of a regularly ordered material which is a far cry from reality. New approaches are needed that appropriately allow for the amorphous hydroxylated surface of all MO$_x$, including defect structures and different degrees of hydroxylation and charge. It should be noted, however, that independent validation of another factor in biomolecule-mineral interactions which has been shown to be important is curvature,[214] and yet for the MO$_x$ of interest in this review, this has not yet been explored. Studies on small metal clusters of Pd are known,[693] and as computing power further increases, similar atomistic studies should be performed on MO$_x$ clusters and nanoparticles. An alternative computational approach that consider groups of atoms as a single point, the so-called coarse graining approach, yields information at the same resolution as experimental AFM studies, and more studies that link these two techniques should be encouraged as these approaches generate complementary information that will enhance our understanding of the abiotic−biotic interface. At the other distance extreme, the use of quantum chemical calculation, for example, density functional theory (DFT) approaches coupled with vibrational or electronic spectroscopies, could provide a direct link between an experimental observable (an infrared or Raman spectrum of a biomolecule-mineral construct) and an

understanding of structure at the atomic scale. In all instances, the role of interfacial water and ions must be considered carefully.

Since the recent report on stabilization of a robust technological bit,[793] 10^7-10^8 faster quantum computing may be a realistic prospect within 5 years. This would offer high-quality hybrid QM/MM,[794] static DFT[795] and dynamic quantum approaches as the Carr-Parrinello approach[796] or similar,[797] to assist in the structural analysis of large (thousands of atoms) bioinorganic systems. This is essential whenever the lack of order (symmetry) and the range of sizes reduce the ability of X-ray and NMR techniques to probe structure. If such is the case, structural properties and thermodynamical properties may be extracted and discussed using vibrational spectral properties. This requires modeling of vibrational normal modes at inorganic interfaces to test and narrow down according to experimental results. Recent efforts in combining classical simulations and static DFT techniques[798] indicate the sensitivity of calculated properties to structural variances of a mineral phase. It is obvious that such effects would become of great significance when at metallic surfaces. In this respect, it is specifically instructive to work on the development and characterization of metallic surfaces to be considered as reference standards. This would allow planning computational studies either on properly reproduced representative surfaces or on engineered surfaces of interest to match the situation as in experiment.

8.1. Take Home Messages

For experimental studies, we have to make efforts to ensure that (a) All components of a reaction system are characterized and reported to help reproducibility and repeatability of published work. This should include the most thorough possible description of the mineral phase and its physical-chemical state (whether that be particulate or "flat" surfaces, or commercial sensors, or commercial minerals/powders), the biomolecule itself, and the medium in which experiments are conducted. (b) The processing history and effect of time on the properties of the mineral substrate (before and during measurement time) have to be documented to facilitate post research recapitulation. (c) A new generation of binding models need to be developed. Ideally, such would provide student friendly universal platforms for kinetic simulations under possible hierarchies of time and physical dimensions, including coexistence and competition of dynamic scenarios where possible stochastic, diffusive, and/or intermediate events would play roles in defining structural ensembles in systems with interfaces of complex topology. There is a need to further develop and standardize the rationale for selection of theoretical models used to interpret data as well as the need to develop additional models specific to the materials in question. (d) Initiatives on new methodological protocols are suggested to declare possible toxicity and/or physiological-medical implications. These should be stored at the level of a dedicated national service whenever a new biocomposite material is developed and reported. The initiative is of particular urgency as new classes of active and genetically driven biohybrid materials are about to emerge. This is where genetically modified life-forms may be engineered to induce large scale assembling or decomposition according to the encrypted switch on/off mechanisms.[799] We must consider the possibility of unexpected interspecies genetic drift for such materials. (e) Scientists that approach the investigation of

MO−biomolecule interfaces from a theoretical perspective must ensure that simulations are built using models that can represent "real" interfacial events (e.g., water content, presence of salts, etc.). The development of new and validated force fields is necessary, especially in the case of less studied MO. Advances in computational power promises progress in representation of biomolecules of increasing complexity.

AUTHOR INFORMATION

Corresponding Author

*E-mail: carole.perry@ntu.ac.uk.

ORCID

Carole C. Perry: 0000-0003-1517-468X

Author Contributions

‖M.J.L., A.S.-R., and E.B. contributed equally to this work.

Notes

The authors declare no competing financial interest.

Biographies

Marion J. Limo graduated with a BSc in Biochemistry (2007) from the University of Nairobi, Kenya. She subsequently received the degrees MSc Biotechnology (2009), distinction and Ph.D. in Chemistry (2014) from Nottingham Trent University (NTU) UK. Her Ph.D. contributed toward an understanding of peptide-inorganic interactions. She continued to work in the Biomolecular and Materials Interface Research Group at NTU as a Postdoctoral Researcher (2014−2016). Marion is currently working as a Biophysical Analyst in the Interface and Surface Analysis Centre (ISAC), School of Pharmacy, at the University of Nottingham, where she supports commercial, industrial, and research operations. Her research interests probe the relationship between material/biomolecule structure and function, and the extension of fundamental principles to the advancement of a broad spectrum of applications in biotechnology, materials chemistry, and product development.

Anna Sola-Rabada graduated in Chemistry (2009) from the Universitat Rovira i Virgili (Spain). She received a Ph.D. (2016) from Nottingham Trent University in the studies of mineral formation and interactions at the mineral−biomolecule interface. Anna was involved in a Newton Fund Institutional Links-CONACYT (Mexico government) and British Council project (NTU and the Universidad Autonoma del Estado de Morelos), exploring enzyme immobilization on biogenic silica extracted from *Equisetum Myriochaetum* for potential use in biomedical applications. Anna worked in the Imaging Science Group at NTU (2016−2018) on an EPSRC multicentre project, "Point-of-Care High Accuracy Fracture Risk Prediction" and on the development of innovative material specific imaging systems for airport security funded by the U.S. Department of Homeland Security. She is currently working on an EPSRC-funded project exploring the role of sequence-specific binding peptides on the physical properties and assembly of microporous metal−organic frameworks (MOFs).

Estefania Boix received her Licenciature in Chemistry from the Universitat Rovira i Virgili in Tarragona, Spain (2009), and Ph.D. in Chemistry of Biomaterials (silica and germania) (2014) as part of a Marie Curie EU Programme between Nottingham Trent University (UK) and the Johannes Gutenberg University of Mainz, Germany, under the supervision of Prof. C. Perry. Estefania continued her research career as a Postdoctoral fellow in Cemef, Sophia-Antipolis (France), working on biobased concrete composites with silica-treated plants (2015). Afterwards, she was awarded a one-year

fellowship for research on cellulose-based hybrid materials at Aalto University in Espoo, Finland (2016). She continued her career as Project Coordinator for the chemical identification of hydrocarbon substances in an association conducting environmental research programmes in Brussels, Belgium (2018). Currently, she works as a Scientist providing technical expertise in the regulatory compliance of substances used in food-contact materials.

Veeranjaneyulu Thota received his BSc in Biotechnology and Chemistry from Acharya Nagarjuna University, India (2007), an MSc in Biotechnology from Bangalore University (2009), a Postgraduate diploma in intellectual property rights law from the National Law School of India University (2010), and a MSc in chemistry with professional practice from Nottingham Trent University (2014). He is currently completing his Ph.D. on "Identifying and Investigating Peptides That Bind to Specific Materials Using Phage Display Methods Together with Their Utilization in Bio-Nanotechnological Applications" at Nottingham Trent University.

Zayd C. Westcott received his integrated Masters Degree in Chemistry from Nottingham Trent University, UK, in 2013, and his Ph.D. on studies at the biotic−abiotic interface with emphasis on peptide interactions with TiO_2 and metal organic frameworks (MOFs) in 2018. Notable achievements include a Japanese Society for the Promotion of Science Fellowship in 2014, when he spent the summer in the laboratory of Professor K. Shiba in Tokyo and a Post Graduate Diploma in research practice in 2017. He is currently working for an office of the UK government.

Valeria Puddu is a senior lecturer in inorganic chemistry at Nottingham Trent University. She obtained a Laurea degree in Chemistry, Cum Laude, from the University of Cagliari, Italy (2004), and a Ph.D. in Chemical Engineering from the University of Nottingham, UK (2008, supervisor Prof G. Li Puma) with a thesis on TiO_2 materials for photocatalysis. In 2009, she joined Nottingham Trent University as a postdoctoral Research Associate in the Biomolecular Materials Interface Research Group, where she worked on interactions at the bioinorganic interface. She was appointed Lecturer at Nottingham Trent University in 2013. Her current research interest is focused on the synthesis of multifunctional photocatalytic materials with specific interest in environmental remediation and energy.

Professor Carole C. Perry is a University Distinguished Professor at Nottingham Trent University. She obtained her B.A. (1982) and DPhil (1985, supervisor Professor R. J. P. Williams, FRS) at Somerville College, Oxford, and was an E.P.A. Brereton-Sherman Junior Research Fellow at St Hilda's College, Oxford (1985−1987), before taking up her first permanent lecturing position at Brunel University in 1987. She moved to Nottingham Trent University in 1993 and was promoted to Professor in 2003. Carole has been department head (2003−2008), served as elected Council member and trustee of the Royal Society of Chemistry (2007−2011) and as chairman of the UK Heads of Chemistry (2009−1011). She has held visiting professorships at Université Pierre et Marie Curie, KIT, MIT, and competitive fellowships at the Weizmann Institute of Science and The Radcliffe Institute of Advanced Study, Harvard University. Carole has extensively published articles and reviews on a range of biological materials related topics. Her current research interests include in vivo and in vitro silicon-biomolecule interactions, composite biomaterials for tissue repair based on silk, aqueous routes to materials and their interactions with peptides, proteins, and cells using both in silico and experimental methods. A recipient of the prestigious Wolfson Research Merit award, Carole was also instrumental in securing two awards from The Higher Education Funding Council for England and Wales, namely Chemistry: the Next Generation and Chemistry for our Future. The legacy of these two projects continues to inspire students across the country to consider a career in science.

REFERENCES

(1) Guo, T.; Yao, M.; Lin, Y.; Nan, C. A Comprehensive Review on Synthesis Methods for Transition-Metal Oxide Nanostructures. *CrystEngComm* **2015**, *17*, 3551−3585.

(2) Nguyen, T.; Do, T. *Size-and Shape-ontrolled Synthesis of Monodisperse Metal Oxide and Mixed Oxide Nanocrystals*; Open Access Publisher: INTECH, 2011.

(3) Devan, R. S.; Patil, R. A.; Lin, J.; Ma, Y. One-Dimensional Metal-Oxide Nanostructures: Recent Developments in Synthesis, Characterization, and Applications. *Adv. Funct. Mater.* **2012**, *22*, 3326−3370.

(4) Lee, J.; Orilall, M. C.; Warren, S. C.; Kamperman, M.; DiSalvo, F. J.; Wiesner, U. Direct Access to Thermally Stable and Highly Crystalline Mesoporous Transition-Metal Oxides with Uniform Pores. *Nat. Mater.* **2008**, *7*, 222−228.

(5) Patil, S. A.; Shinde, D. V.; Patil, D. V.; Tehare, K. K.; Jadhav, V. V.; Lee, J. K.; Mane, R. S.; Shrestha, N. K.; Han, S.; Ahn, D. Y. A Simple, Room Temperature, Solid-state Synthesis Route for Metal Oxide Nanostructures. *J. Mater. Chem. A* **2014**, *2*, 13519−13526.

(6) Daniel, M. C.; Astruc, D. Gold nanoparticles: Assembly, Supramolecular Chemistry, Quantum-Size-Related Properties, and Applications Toward Biology, Catalysis, and Nanotechnology. *Chem. Rev.* **2004**, *104*, 293−346.

(7) Galloway, J. M.; Staniland, S. S. Protein and Peptide Biotemplated Metal and Metal Oxide Nanoparticles and Their Patterning Onto Surfaces. *J. Mater. Chem.* **2012**, *22*, 12423−12434.

(8) Ghosh, P.; Han, G.; De, M.; Kim, C. K.; Rotello, V. M. Gold Nanoparticles in Delivery Applications. *Adv. Drug Delivery Rev.* **2008**, *60*, 1307−1315.

(9) Thakkar, K. N.; Mhatre, S. S.; Parikh, R. Y. Biological Synthesis of Metallic Nanoparticles. *Nanomedicine* **2010**, *6*, 257−262.

(10) Zhang, S. Building From the Bottom Up. *Mater. Today* **2003**, *6*, 20−27.

(11) Niemeyer, C. M. Nanoparticles, Proteins, and Nucleic Acids: Biotechnology Meets Materials Science. *Angew. Chem., Int. Ed.* **2001**, *40*, 4128−4158.

(12) Shimomura, M.; Sawadaishi, T. Bottom-Up Strategy of Materials Fabrication: A New Trend in Nanotechnology of Soft Materials. *Curr. Opin. Colloid Interface Sci.* **2001**, *6*, 11−16.

(13) Mijatovic, D.; Eijkel, J.; Van Den Berg, A. Technologies for Nanofluidic Systems: Top-Down vs. Bottom-Up—a Review. *Lab Chip* **2005**, *5*, 492−500.

(14) Chiu, C.; Ruan, L.; Huang, Y. Biomolecular Specificity Controlled Nanomaterial Synthesis. *Chem. Soc. Rev.* **2013**, *42*, 2512−2527.

(15) Gogolides, E.; Constantoudis, V.; Kokkoris, G.; Kontziampasis, D.; Tsougeni, K.; Boulousis, G.; Vlachopoulou, M.; Tserepi, A. Controlling Roughness: From Etching to Nanotexturing and Plasma-Directed Organization on Organic and Inorganic Materials. *J. Phys. D: Appl. Phys.* **2011**, *44*, 174021.

(16) Oskam, G. Metal Oxide Nanoparticles: Synthesis, Characterization and Application. *J. Sol-Gel Sci. Technol.* **2006**, *37*, 161−164.

(17) Yoshimura, M.; Byrappa, K. Hydrothermal Processing of Materials: Past, Present and Future. *J. Mater. Sci.* **2008**, *43*, 2085−2103.

(18) Baruah, S.; Dutta, J. Hydrothermal Growth of ZnO Nanostructures. *Sci. Technol. Adv. Mater.* **2009**, *10*, 013001.

(19) De Yoreo, J. J.; Vekilov, P. G. Principles of Crystal Nucleation and Growth. *Rev. Mineral. Geochem.* **2003**, *54*, 57−93.

(20) Adschiri, T.; Hakuta, Y.; Arai, K. Hydrothermal Synthesis of Metal Oxide Fine Particles at Supercritical Conditions. *Ind. Eng. Chem. Res.* **2000**, *39*, 4901−4907.

(21) Deravi, L. F.; Swartz, J. D.; Wright, D. W. *The Biomimetic Synthesis of Metal Oxide Nanomaterials*; Wiley-VCH: Weinheim, Germany, 2007.

(22) Titirici, M.; Antonietti, M.; Thomas, A. A Generalized Synthesis of Metal Oxide Hollow Spheres Using a Hydrothermal Approach. *Chem. Mater.* **2006**, *18*, 3808−3812.

(23) Banerjee, S.; Kumar, A.; Devi, P. S. Preparation of Nanoparticles of Oxides by the Citrate-Nitrate Process. *J. Therm. Anal. Calorim.* **2011**, *104*, 859−867.

(24) Costa, M. E. V.; Baptista, J. L. Characteristics of Zinc Oxide Powders Precipitated in the Presence of Alcohols and Amines. *J. Eur. Ceram. Soc.* **1993**, *11*, 275−281.

(25) Yan, Y.; Hao, B.; Wang, X.; Chen, G. Bio-Inspired Synthesis of Titania with Polyamine Induced Morphology and Phase Transformation at Room-Temperature: Insight into the Role of the Protonated Amino Group. *Dalton Trans.* **2013**, *42*, 12179−12184.

(26) Cole, K. E.; Ortiz, A. N.; Schoonen, M. A.; Valentine, A. M. Peptide- and Long-Chain Polyamine-Induced Synthesis of Micro- and Nanostructured Titanium Phosphate and Protein Encapsulation. *Chem. Mater.* **2006**, *18*, 4592−4599.

(27) Peng, Y.; Xu, A.; Deng, B.; Antonietti, M.; Colfen, H. Polymer-Controlled Crystallization of Zinc Oxide Hexagonal Nanorings and Disks. *J. Phys. Chem. B* **2006**, *110*, 2988−2993.

(28) Li, Z.; Xiong, Y.; Xie, Y. Selected-Control Synthesis of ZnO Nanowires and Nanorods via a PEG-Assisted Route. *Inorg. Chem.* **2003**, *42*, 8105−8109.

(29) Louguet, S.; Kumar, A. C.; Sigaud, G.; Duguet, E.; Lecommandoux, S.; Schatz, C. A Physico-Chemical Investigation of Poly (ethylene oxide)-block-poly (L-lysine) Copolymer Adsorption onto Silica Nanoparticles. *J. Colloid Interface Sci.* **2011**, *359*, 413−422.

(30) Cleaves, H. J., II; Jonsson, C. M.; Jonsson, C. L.; Sverjensky, D. A.; Hazen, R. M. Adsorption of Nucleic Acid Components on Rutile (TiO$_2$) Surfaces. *Astrobiology* **2010**, *10*, 311−323.

(31) Pasqui, D.; Golini, L.; Della Giovampaola, C.; Atrei, A.; Barbucci, R. Chemical and Biological Properties of Polysaccharide-Coated Titania Nanoparticles: The Key Role of Proteins. *Biomacromolecules* **2011**, *12*, 1243−1249.

(32) Kim, S. H.; Olson, T. Y.; Satcher, J. H., Jr.; Han, T. Y. Hierarchical ZnO Structures Templated with Amino Acid Based Surfactants. *Microporous Mesoporous Mater.* **2012**, *151*, 64−69.

(33) Tomczak, M. M.; Gupta, M. K.; Drummy, L. F.; Rozenzhak, S. M.; Naik, R. R. Morphological Control and Assembly of Zinc Oxide Using a Biotemplate. *Acta Biomater.* **2009**, *5*, 876−882.

(34) Zhang, X.; Wang, F.; Liu, B.; Kelly, E. Y.; Servos, M. R.; Liu, J. Adsorption of DNA Oligonucleotides by Titanium Dioxide Nanoparticles. *Langmuir* **2014**, *30*, 839−845.

(35) Tong, Z.; Jiang, Y.; Yang, D.; Shi, J.; Zhang, S.; Liu, C.; Jiang, Z. Biomimetic and Bioinspired Synthesis of Titania and Titania-Based Materials. *RSC Adv.* **2014**, *4*, 12388−12403.

(36) Ding, S.; Wang, Y.; Hong, Z.; Lu, X.; Wan, D.; Huang, F. Biomolecule-Assisted Route to Prepare Titania Mesoporous Hollow Structures. *Chem. - Eur. J.* **2011**, *17*, 11535−11541.

(37) Sano, K.; Yoshii, S.; Yamashita, I.; Shiba, K. Aqua Structuralization of a Three-Dimensional Configuration Using Biomolecules. *Nano Lett.* **2007**, *7*, 3200−3202.

(38) Patwardhan, S. V.; Patwardhan, G.; Perry, C. C. Interactions of Biomolecules with Inorganic Materials: Principles, Applications and Future Prospects. *J. Mater. Chem.* **2007**, *17*, 2875−2884.

(39) Emami, F. S.; Puddu, V.; Berry, R. J.; Varshney, V.; Patwardhan, S. V.; Perry, C. C.; Heinz, H. Prediction of Specific Biomolecule Adsorption on Silica Surfaces as a Function of pH and Particle Size. *Chem. Mater.* **2014**, *26*, 5725−5734.

(40) Slocik, J. M.; Naik, R. R. Sequenced Defined Biomolecules for Nanomaterial Synthesis, Functionalization, and Assembly. *Curr. Opin. Biotechnol.* **2017**, *46*, 7−13.

(41) Gupta, A.; Wells, S. Surface-Modified Superparamagnetic Nanoparticles for Drug Delivery: Preparation, Characterization, and Cytotoxicity studies. *IEEE Transactions on Nanobioscience* **2004**, *3*, 66−73.

(42) Byl, C.; Gloter, A.; Baltaze, J. P.; Bérardan, D.; Dragoe, N. Influence of Structural Isomerism of Amino Acid on the Crystal Growth of ZnO Nanoparticles Synthetized by Polyol Methods. *J. Sol-Gel Sci. Technol.* **2017**, *83*, 296−307.

(43) Gerstel, P.; Lipowsky, P.; Durupthy, O.; Hoffmann, R. C.; Bellina, P.; Bill, J.; Aldinger, F. Deposition of Zinc Oxide and Layered Basic Zinc Salts from Aqueous Solutions Containing Amino Acids and Dipeptides. *J. Ceram. Soc. Jpn.* **2006**, *114*, 911−917.

(44) Liang, M.; Deschaume, O.; Patwardhan, S. V.; Perry, C. C. Direct Evidence of ZnO Morphology Modification via the Selective Adsorption of ZnO-Binding Peptides. *J. Mater. Chem.* **2011**, *21*, 80−89.

(45) Slocik, J. M.; Stone, M. O.; Naik, R. R. Synthesis of Gold Nanoparticles Using Multifunctional Peptides. *Small* **2005**, *1*, 1048−1052.

(46) Bazylinski, D. A.; Frankel, R. B.; Heywood, B. R.; Mann, S.; King, J. W.; Donaghay, P. L.; Hanson, A. K. Controlled Biomineralization of Magnetite (Fe(inf3)O(inf4)) and Greigite (Fe(inf3)S(inf4)) in a Magnetotactic Bacterium. *Appl. Environ. Microbiol.* **1995**, *61*, 3232−3239.

(47) Kröger, N.; Sandhage, K. H. From Diatom Biomolecules to Bioinspired Syntheses of Silica-and Titania-Based Materials. *MRS Bull.* **2010**, *35*, 122−126.

(48) Mann, S.; Perry, C. C.; Williams, R. J.; Fyfe, C. A.; Gobbi, G. C.; Kennedy, G. J. The Characterisation of the Nature of Silica in Biological Systems. *J. Chem. Soc., Chem. Commun.* **1983**, *0*, 168−170.

(49) Perry, C. C.; Keeling-Tucker, T. Biosilicification: The Role of the Organic Matrix in Structure Control. *JBIC, J. Biol. Inorg. Chem.* **2000**, *5*, 537−550.

(50) Gotliv, B.; Kessler, N.; Sumerel, J. L.; Morse, D. E.; Tuross, N.; Addadi, L.; Weiner, S. Asprich: A Novel Aspartic Acid-Rich Protein Family from the Prismatic Shell Matrix of the Bivalve Atrina rigida. *ChemBioChem* **2005**, *6*, 304−314.

(51) Kaplan, D. L. Mollusc Shell Structures: Novel Design Strategies for Synthetic Materials. *Curr. Opin. Solid State Mater. Sci.* **1998**, *3*, 232−236.

(52) Marin, F.; Luquet, G. Unusually Acidic Proteins in Biomineralization. In *Handbook of Biomineralization: Biological Aspects and Structure Formation*; Bäuerlein, E., Ed.; Wiley, 2007; pp 273−290.

(53) Sarashina, I.; Endo, K. Primary Structure of a Soluble Matrix Protein of Scallop Shell: Implications for Calcium Carbonate Biomineralization. *Am. Mineral.* **1998**, *83*, 1510−1515.

(54) Bäeuerlein, E.; Behrens, P.; Mann, S. *Handbook of Biomineralization: Biomimetic and bioinspired chemistry*; Wiley-VCH Verlag: Weinheim, Germany, 2007.

(55) Sumerel, J.; Yang, W.; Kisailus, D.; Weaver, J.; Choi, J.; Morse, D. Biocatalytically Templated Synthesis of Titanium Dioxide. *Chem. Mater.* **2003**, *15*, 4804−4809.

(56) Dickerson, M. B.; Sandhage, K. H.; Naik, R. R. Protein- and Peptide-Directed Syntheses of Inorganic Materials. *Chem. Rev.* **2008**, *108*, 4935−4978.

(57) Weiner, S. Biomineralization: A Structural Perspective. *J. Struct. Biol.* **2008**, *163*, 229−234.

(58) Perry, C. C.; Patwardhan, S. V.; Deschaume, O. From Biominerals to Biomaterials: The Role of Biomolecule-Mineral Interactions. *Biochem. Soc. Trans.* **2009**, *37*, 687−691.

(59) Grünberg, K.; Müller, E. C.; Otto, A.; Reszka, R.; Linder, D.; Kube, M.; Reinhardt, R.; Schüler, D. Biochemical and Proteomic Analysis of the Magnetosome Membrane in *Magnetospirillum gryphiswaldense*. *Appl. Environ. Microbiol.* **2004**, *70*, 1040−1050.

(60) Müller, W. E. G.; Krasko, A.; Le Pennec, G.; Schröder, H. C. Biochemistry and Cell Biology of Silica Formation in Sponges. *Microsc. Res. Tech.* **2003**, *62*, 368−377.

(61) Naik, R. R.; Brott, L. L.; Clarson, S. J.; Stone, M. O. Silica-Precipitating Peptides Isolated from a Combinatorial Phage Display Peptide Library. *J. Nanosci. Nanotechnol.* **2002**, *2*, 95−100.

(62) Sarikaya, M.; Tamerler, C.; Jen, A. K.; Schulten, K.; Baneyx, F. Molecular Biomimetics: Nanotechnology Through Biology. *Nat. Mater.* **2003**, *2*, 577−585.

(63) Sano, K.; Shiba, K. A Hexapeptide Motif that Electrostatically Binds to the Surface of Titanium. *J. Am. Chem. Soc.* **2003**, *125*, 14234−14235.

(64) Eteshola, E.; Brillson, L. J.; Lee, S. C. Selection and Characteristics of Peptides That Bind Thermally Grown Silicon Dioxide Films. *Biomol. Eng.* **2005**, *22*, 201−204.

(65) Slocik, J. M.; Naik, R. R. Probing Peptide−Nanomaterial Interactions. *Chem. Soc. Rev.* **2010**, *39*, 3454−3463.

(66) Ramezani-Dakhel, H.; Ruan, L.; Huang, Y.; Heinz, H. Molecular Mechanism of Specific Recognition of Cubic Pt Nanocrystals by Peptides and of the Concentration-Dependent Formation from Seed Crystals. *Adv. Funct. Mater.* **2015**, *25*, 1374−1384.

(67) Ramezani-Dakhel, H.; Bedford, N. M.; Woehl, T. J.; Knecht, M. R.; Naik, R. R.; Heinz, H. Nature of Peptide Wrapping Onto Metal Nanoparticle Catalysts and Driving Forces for Size Control. *Nanoscale* **2017**, *9*, 8401−8409.

(68) Walsh, T. R. Pathways to Structure-Property Relationships of Peptide-Materials Interfaces: Challenges in Predicting Molecular Structures. *Acc. Chem. Res.* **2017**, *50*, 1617−1624.

(69) Coradin, T.; Livage, J. Aqueous Silicates in Biological Sol-Gel Applications: New Perspectives for Old Precursors. *Acc. Chem. Res.* **2007**, *40*, 819−826.

(70) Shiomi, T.; Tsunoda, T.; Kawai, A.; Mizukami, F.; Sakaguchi, K. Biomimetic Synthesis of Lysozyme-Silica Hybrid Hollow Particles Using Sonochemical Treatment: Influence of pH and Lysozyme Concentration on Morphology. *Chem. Mater.* **2007**, *19*, 4486−4493.

(71) Knecht, M. R.; Wright, D. W. Functional Analysis of the Biomimetic Silica Precipitating Activity of the R5 Peptide from Cylindrotheca fusiformis. *Chem. Commun.* **2003**, *0*, 3038−3039.

(72) Gautier, C.; Lopez, P. J.; Livage, J.; Coradin, T. Influence of Poly-L-lysine on the Biomimetic Growth of Silica Tubes in Confined Media. *J. Colloid Interface Sci.* **2007**, *309*, 44−48.

(73) Wang, S.; Ge, X.; Xue, J.; Fan, H.; Mu, L.; Li, Y.; Xu, H.; Lu, J. R. Mechanistic Processes Underlying Biomimetic Synthesis of Silica Nanotubes From Self-Assembled Ultrashort Peptide Templates. *Chem. Mater.* **2011**, *23*, 2466−2474.

(74) Noll, F.; Sumper, M.; Hampp, N. Nanostructure of Diatom Silica Surfaces and of Biomimetic Analogues. *Nano Lett.* **2002**, *2*, 91−95.

(75) Jackson, E.; Ferrari, M.; Cuestas-Ayllon, C.; Fernández-Pacheco, R.; Perez-Carvajal, J.; de la Fuente; Jesús, M.; Grazú, V.; Betancor, L. Protein-Templated Biomimetic Silica Nanoparticles. *Langmuir* **2015**, *31*, 3687−3695.

(76) Cho, N.; Cheong, T.; Min, J. H.; Wu, J. H.; Lee, S. J.; Kim, D.; Yang, J.; Kim, S.; Kim, Y. K.; Seong, S. A Multifunctional Core-Shell Nanoparticle for Dendritic Cell-Based Cancer Immunotherapy. *Nat. Nanotechnol.* **2011**, *6*, 675−682.

(77) Zhang, Y.; Nayak, T. R.; Hong, H.; Cai, W. Biomedical Applications of Zinc Oxide Nanomaterials. *Curr. Mol. Med.* **2013**, *13*, 1633−1645.

(78) Zhang, Y.; Ram, M. K.; Stefanakos, E. K.; Goswami, D. Y. Synthesis, Characterization, and Applications of ZnO anowires. *J. Nanomater.* **2012**, *2012*, 1−22.

(79) Tereshchenko, A.; Bechelany, M.; Viter, R.; Khranovskyy, V.; Smyntyna, V.; Starodub, N.; Yakimova, R. Optical Biosensors Based on ZnO Nanostructures: Advantages and Perspectives. A Review. *Sens. Actuators, B* **2016**, *229*, 664−677.

(80) Umetsu, M.; Mizuta, M.; Tsumoto, K.; Ohara, S.; Takami, S.; Watanabe, H.; Kumagai, I.; Adschiri, T. Bioassisted Room-Temperature Immobilization and Mineralization of Zinc Oxide—The Structural Ordering of ZnO Nanoparticles into a Flower-Type Morphology. *Adv. Mater.* **2005**, *17*, 2571−2575.

(81) Rothenstein, D.; Claasen, B.; Omiecienski, B.; Lammel, P.; Bill, J. Isolation of ZnO-Binding 12-mer Peptides and Determination of their Binding Epitopes by NMR Spectroscopy. *J. Am. Chem. Soc.* **2012**, *134*, 12547−12556.

(82) Bhat, S. S.; Qurashi, A.; Khanday, F. A. ZnO Nanostructures Based Biosensors for Cancer and Infectious Disease Applications: Perspectives, Prospects and Promises. *TrAC, Trends Anal. Chem.* **2017**, *86*, 1−13.

(83) Palmqvist, N. G. M.; Bejai, S.; Meijer, J.; Seisenbaeva, G. A.; Kessler, V. G. Nano Titania Aided Clustering and Adhesion of Beneficial Bacteria to Plant Roots to Enhance Crop Growth and Stress Management. *Sci. Rep.* **2015**, *5*, 10146.

(84) Cheng, K.; Wang, T.; Yu, M.; Wan, H.; Lin, J.; Weng, W.; Wang, H. Effects of RGD Immobilization on Light-Induced Cell Sheet Detachment from TiO₂ Nanodots Films. *Mater. Sci. Eng., C* **2016**, *63*, 240−246.

(85) Shiba, K. Exploitation of Peptide Motif Sequences and their Use in Nanobiotechnology. *Curr. Opin. Biotechnol.* **2010**, *21*, 412−425.

(86) Puddu, V.; Slocik, J. M.; Naik, R. R.; Perry, C. C. Titania Binding Peptides as Templates in the Biomimetic Synthesis of Stable Titania Nanosols: Insight into the Role of Buffers in Peptide-Mediated Mineralization. *Langmuir* **2013**, *29*, 9464−9472.

(87) Sultan, A. M.; Westcott, Z. C.; Hughes, Z. E.; Palafox-Hernandez, J. P.; Giesa, T.; Puddu, V.; Buehler, M. J.; Perry, C. C.; Walsh, T. R. Aqueous Peptide−TiO₂ Interfaces: Isoenergetic Binding via Either Entropically or Enthalpically Driven Mechanisms. *ACS Appl. Mater. Interfaces* **2016**, *8*, 18620−18630.

(88) Fabijanic, K. I.; Regan, M. R.; Banerjee, I. A. Amino Acid Catalyzed Biomimetic Preparation of Tin Oxide-Germania Nanocomposites and their Characterization. *J. Nanosci. Nanotechnol.* **2007**, *7*, 2674−82.

(89) Avanzato, C. P.; Follieri, J. M.; Banerjee, I. A.; Fath, K. R. Biomimetic Synthesis and Antibacterial Characteristics of Magnesium Oxide-Germanium dioxide Nanocomposite Powders. *J. Compos. Mater.* **2009**, *43*, 897−910.

(90) Wysokowski, M.; Motylenko, M.; Beyer, J.; Makarova, A.; Stöcker, H.; Walter, J.; Galli, R.; Kaiser, S.; Vyalikh, D.; Bazhenov, V. V.; et al. Extreme Biomimetic Approach for Developing Novel Chitin-GeO₂ Nanocomposites with Photoluminescent Properties. *Nano Res.* **2015**, *8*, 2288−2301.

(91) Lobaz, V.; Rabyk, M.; Panek, J.; Doris, E.; Nallet, F.; Stepanek, P.; Hruby, M. Photoluminescent Polysaccharide-Coated Germanium-(IV) Oxide Nanoparticles. *Colloid Polym. Sci.* **2016**, *294*, 1225.

(92) Dickerson, M. B.; Cai, Y.; Sandhage, K. H.; Naik, R. R.; Stone, M. O. Sequence Specific Morphological Control Over the Formation of Germanium Oxide During Peptide Mediated Synthesis. In *Advances in Bioceramics and Biocomposites: Ceramic Engineering and Science Proceedings*; Mizuno, M., Ed.; John Wiley & Sons, Inc., 2008; pp 25−32.

(93) Sewell, S. L.; Rutledge, R. D.; Wright, D. W. Versatile Biomimetic Dendrimer Templates used in the Formation of TiO₂ and GeO₂. *Dalton Trans* **2008**, *1*, 3857−3857.

(94) Kawai, T.; Usui, Y.; Kon-No, K. Synthesis and Growth Mechanism of GeO₂ particles in AOT Reversed Micelles. *Colloids Surf., A* **1999**, *149*, 39−47.

(95) Davis, T. M.; Snyder, M. A.; Tsapatsis, M. Germania Nanoparticles and Nanocrystals at Room Temperature in Water and Aqueous Lysine Sols. *Langmuir* **2007**, *23*, 12469−72.

(96) Xu, J.; Nguyen, T.; Xie, K.; Hamad, W. Y.; MacLachlan, M. J. Chiral Nematic Porous Germania and Germanium/Carbon Films. *Nanoscale* **2015**, *7*, 13215−23.

(97) Patwardhan, S. V.; Clarson, S. J. Bioinspired Mineralisation: Macromolecule Mediated Synthesis of Amorphous Germania Structures. *Polymer* **2005**, *46*, 4474−4479.

(98) Kisailus, D.; Choi, J.; Weaver, J.; Yang, W.; Morse, D. Enzymatic Synthesis and Nanostructural Control of Gallium Oxide at Low Temperature. *Adv. Mater.* **2005**, *17*, 314−318.

(99) Taş, A. C.; Majewski, P. J.; Aldinger, F. Synthesis of Gallium Oxide Hydroxide Crystals in Aqueous Solutions with or without Urea and Their Calcination Behavior. *J. Am. Ceram. Soc.* **2002**, *85*, 1421−1429.

(100) Laurent, S.; Forge, D.; Port, M.; Roch, A.; Robic, C.; Vander Elst, L.; Muller, R. N. Magnetic Iron Oxide Nanoparticles: Synthesis, Stabilization, Vectorization, Physicochemical Characterizations, and Biological Applications. *Chem. Rev.* **2008**, *108*, 2064−2110.

(101) Kaushik, A.; Khan, R.; Solanki, P. R.; Pandey, P.; Alam, J.; Ahmad, S.; Malhotra, B. D. Iron Oxide Nanoparticles−Chitosan Composite Based Glucose Biosensor. *Biosens. Bioelectron.* **2008**, *24*, 676−683.

(102) Dong, X.; Xu, H.; Wang, X.; Huang, Y.; Chan-Park, M. B.; Zhang, H.; Wang, L.; Huang, W.; Chen, P. 3D Graphene-Cobalt Oxide Electrode for High-Performance Supercapacitor and Enzyme-less Glucose Detection. *ACS Nano* **2012**, *6*, 3206−3213.

(103) Salimi, A.; Hallaj, R.; Soltanian, S. Immobilization of Hemoglobin on Electrodeposited Cobalt-Oxide Nanoparticles: Direct Voltammetry and Electrocatalytic Activity. *Biophys. Chem.* **2007**, *130*, 122−131.

(104) Reardon, P. N.; Chacon, S. S.; Walter, E. D.; Bowden, M. E.; Washton, N. M.; Kleber, M. Abiotic Protein Fragmentation by Manganese Oxide: Implications for a Mechanism to Supply Soil Biota with Oligopeptides. *Environ. Sci. Technol.* **2016**, *50*, 3486−3493.

(105) Borg, S.; Rothenstein, D.; Bill, J.; Schüler, D. Generation of Multishell Magnetic Hybrid Nanoparticles by Encapsulation of Genetically Engineered and Fluorescent Bacterial Magnetosomes with ZnO and SiO_2. *Small* **2015**, *11*, 4209−4217.

(106) Sanchez, C.; Arribart, H.; Giraud Guille, M. M. Biomimetism and Bioinspiration as Tools for the Design of Innovative Materials and Systems. *Nat. Mater.* **2005**, *4*, 277−288.

(107) Sun, T.; Qing, G.; Su, B.; Jiang, L. Functional Biointerface Materials Inspired from Nature. *Chem. Soc. Rev.* **2011**, *40*, 2909−2921.

(108) Tamerler, C.; Kacar, T.; Sahin, D.; Fong, H.; Sarikaya, M. Genetically Engineered Polypeptides for Inorganics: A Utility in Biological Materials Science and Engineering. *Mater. Sci. Eng., C* **2007**, *27*, 558−564.

(109) Walsh, T. R.; Knecht, M. R. Biointerface Structural Effects on the Properties and Applications of Bioinspired Peptide-Based Nanomaterials. *Chem. Rev.* **2017**, *117*, 12641−12704.

(110) Oberdörster, G.; Stone, V.; Donaldson, K. Toxicology of Nanoparticles: A Historical Perspective. *Nanotoxicology* **2007**, *1*, 2−25.

(111) Fruijtier-Pölloth, C. The Toxicological Mode of Action and the Safety of Synthetic Amorphous Silica—A Nanostructured Material. *Toxicology* **2012**, *294*, 61−79.

(112) Lowenstam, H. A.; Weiner, S. *On Biomineralisation*; Oxford University Press: Oxford, 1989.

(113) Iler, R. K. *The Chemistry of Silica: Solubility, Polymerization, Colloid and Surface Properties, and Biochemistry*; Wiley: New York, 1979.

(114) Sola-Rabada, A.; Rinck, J.; Belton, D. J.; Powell, A. K.; Perry, C. C. Isolation of a Wide Range of Minerals from a Thermally Treated Plant: Equisetum arvense, a Mare's Tale. *JBIC, J. Biol. Inorg. Chem.* **2016**, *21*, 101−112.

(115) Sola-Rabada, A.; Sahare, P.; Hickman, G. J.; Vasquez, M.; Canham, L. T.; Perry, C. C.; Agarwal, V. Biogenic Porous Silica and Silicon Sourced from Mexican Giant Horsetail (Equisetum

myriochaetum) and their Application as Supports for Enzyme Immobilization. *Colloids Surf., B* **2018**, *166*, 195−202.

(116) Perry, C. C.; Keeling-Tucker, T. Model Studies of Colloidal Silica Precipitation Using Biosilica Extracts from Equisetum telmateia. *Colloid Polym. Sci.* **2003**, *281*, 652−664.

(117) Poulsen, N.; Kröger, N. A New Molecular Tool for Transgenic Diatoms. *FEBS J.* **2005**, *272*, 3413−3423.

(118) Patwardhan, S. V.; Clarson, S. J.; Perry, C. C. On the Role(s) of Additives in Bioinspired Silicification. *Chem. Commun.* **2005**, *5*, 1113−1121.

(119) De Jong, W. H.; Borm, P. J. Drug Delivery and Nano-particles:Applications and Hazards. *Int. J. Nanomed.* **2008**, *3*, 133−149.

(120) Fubini, B. Surface Chemistry and Quartz Hazard. *Ann. Occup. Hyg.* **1998**, *42*, 521−530.

(121) Kirkland, J.; Truszkowski, F.; Dilks, C.; Engel, G. Superficially Porous Silica Microspheres for Fast High-Performance Liquid Chromatography of Macromolecules. *J. Chromatogr. A* **2000**, *890*, 3−13.

(122) Unger, K.; Jilge, O.; Kinkel, J.; Hearn, M. Evaluation of Advanced Silica Packings for the Separation of Biopolymers by High-Performance Liquid Chromatography II. Performance of Non-Porous Monodisperse 1.5-μm Silica Beads in the Separation of Proteins by Reversed-Phase Gradient Elution High-Performance Liquid Chroma-tography. *J. Chromatogr. A* **1986**, *359*, 61−72.

(123) Girelli, A. M.; Mattei, E. Application of Immobilized Enzyme Reactor in On-Line High Performance Liquid Chromatography: A Review. *J. Chromatogr. B: Anal. Technol. Biomed. Life Sci.* **2005**, *819*, 3−16.

(124) Zucca, P.; Sanjust, E. Inorganic Materials as Supports for Covalent Enzyme Immobilization: Methods and Mechanisms. *Molecules* **2014**, *19*, 14139−14194.

(125) Huang, X.; Li, L.; Liu, T.; Hao, N.; Liu, H.; Chen, D.; Tang, F. The Shape Effect of Mesoporous Silica Nanoparticles on Biodis-tribution, Clearance, and Biocompatibility In Vivo. *ACS Nano* **2011**, *5*, 5390−5399.

(126) Wu, S.; Mou, C.; Lin, H. Synthesis of Mesoporous Silica Nanoparticles. *Chem. Soc. Rev.* **2013**, *42*, 3862−3875.

(127) Slowing, I. I.; Wu, C.; Vivero-Escoto, J. L.; Lin, V. S. Mesoporous Silica Nanoparticles for Reducing Hemolytic Activity Towards Mammalian Red Blood Cells. *Small* **2009**, *5*, 57−62.

(128) Yang, P.; Gai, S.; Lin, J. Functionalized Mesoporous Silica Materials for Controlled Drug Delivery. *Chem. Soc. Rev.* **2012**, *41*, 3679−3698.

(129) He, Q.; Zhang, J.; Chen, F.; Guo, L.; Zhu, Z.; Shi, J. An Anti-ROS/Hepatic Fibrosis Drug Delivery System Based on Salvianoli-cAacid B Loaded Mesoporous Silica Nanoparticles. *Biomaterials* **2010**, *31*, 7785−7796.

(130) He, Q.; Zhang, J.; Shi, J.; Zhu, Z.; Zhang, L.; Bu, W.; Guo, L.; Chen, Y. The Effect of PEGylation of Mesoporous Silica Nano-particles on Nonspecific Binding of Serum Proteins and Cellular Responses. *Biomaterials* **2010**, *31*, 1085−1092.

(131) Lin, Y.; Haynes, C. L. Synthesis and Characterization of Biocompatible and Size-Tunable Multifunctional Porous Silica Nanoparticles. *Chem. Mater.* **2009**, *21*, 3979−3986.

(132) Vallet-Regí, M.; Balas, F.; Arcos, D. Mesoporous Materials for Drug Delivery. *Angew. Chem., Int. Ed.* **2007**, *46*, 7548−7558.

(133) Tang, L.; Cheng, J. Nonporous Silica Nanoparticles for Nanomedicine Application. *Nano Today* **2013**, *8*, 290−312.

(134) Kim, T.; Slowing, I. I.; Chung, P.; Lin, V. S. Ordered Mesoporous Polymer− Silica Hybrid Nanoparticles as Vehicles for the Intracellular Controlled Release of Macromolecules. *ACS Nano* **2011**, *5*, 360−366.

(135) Hartono, S. B.; Gu, W.; Kleitz, F.; Liu, J.; He, L.; Middelberg, A. P.; Yu, C.; Lu, G. Q.; Qiao, S. Z. Poly-L-lysine Functionalized Large Pore Cubic Mesostructured Silica Nanoparticles as Biocompat-ible Carriers for Gene Delivery. *ACS Nano* **2012**, *6*, 2104−2117.

(136) Manzano, M.; Vallet-Regí, M. New Developments in Ordered Mesoporous Materials for Drug Delivery. *J. Mater. Chem.* **2010**, *20*, 5593−5604.

(137) Douglas, B. E.; Ho, S. Crystal Structures of Silica and Metal Silicates. In *Structure and Chemistry of Crystalline Solids*; Springer: New York, 2006; pp 233−278.

(138) Momma, K.; Izumi, F. VESTA 3 for Three-Dimensional Visualization of Crystal, Volumetric and Morphology Data. *J. Appl. Crystallogr.* **2011**, *44*, 1272−1276.

(139) Grazulis, S.; Chateigner, D.; Downs, R. T.; Yokochi, A. F. T.; Quiros, M.; Lutterotti, L.; Manakova, E.; Butkus, J.; Moeck, P.; Le Bail, A. Crystallography Open Database - An Open-Access Collection of Crystal Structures. *J. Appl. Crystallogr.* **2009**, *42*, 726−729.

(140) Zhuravlev, L. The Surface Chemistry of Amorphous Silica. Zhuravlev Model. *Colloids Surf., A* **2000**, *173*, 1−38.

(141) Ferrando, N.; Gosalvez, M. A.; Colom, R. J. Evolutionary Continuous Cellular Automaton for the Simulation of Wet Etching of Quartz. *J. Micromech. Microeng.* **2012**, *22*, 025021.

(142) Brinker, C. J.; Scherer, G. W. *Sol-Gel Science:The Physics and Chemistry of Sol-Gel Processing*; Academic Press: London, 1990.

(143) Van Blaaderen, A.; Van Geest, J.; Vrij, A. Monodisperse Colloidal Silica Spheres from Tetraalkoxysilanes: Particle Formation and Growth Mechanism. *J. Colloid Interface Sci.* **1992**, *154*, 481−501.

(144) Stöber, W.; Fink, A.; Bohn, E. Controlled Growth of Monodisperse Silica Spheres in the Micron Size Range. *J. Colloid Interface Sci.* **1968**, *26*, 62−69.

(145) Osseo-Asare, K.; Arriagada, F. Preparation of SiO_2 Nanoparticles in a Non-Ionic Reverse Micellar System. *Colloids Surf.* **1990**, *50*, 321−339.

(146) Karmakar, B.; De, G.; Ganguli, D. Dense Silica Microspheres from Organic and Inorganic Acid Hydrolysis of TEOS. *J. Non-Cryst. Solids* **2000**, *272*, 119−126.

(147) Izutsu, H.; Mizukami, F.; Nair, P. K.; Kiyozumi, Y.; Maeda, K. Preparation and Characterization of Porous Silica Spheres by the Sol−Gel Method in the Presence of Tartaric Acid. *J. Mater. Chem.* **1997**, *7*, 767−771.

(148) Kawaguchi, T.; Ono, K. Spherical Silica Gels Precipitated from Acid Catalyzed TEOS Solutions. *J. Non-Cryst. Solids* **1990**, *121*, 383−388.

(149) De, G.; Karmakar, B.; Ganguli, D. Hydrolysis−Condensation Reactions of TEOS in the Presence of Acetic Acid Leading to the Generation of Glass-Like Silica Microspheres in Solution at Room Temperature. *J. Mater. Chem.* **2000**, *10*, 2289−2293.

(150) Lovingood, D. D.; Owens, J. R.; Seeber, M.; Kornev, K. G.; Luzinov, I. Preparation of Silica Nanoparticles Through Microwave-Assisted Acid-catalysis. *J. Visualized Exp.* **2013**, *82*, No. e51022, DOI: 10.3791/51022.

(151) Vansant, E. F.; Van Der Voort, P.; Vrancken, K. C. *Characterization and Chemical Modification of the Silica Surface*; Elsevier: Amsterdam, 1995.

(152) Yeh, Y.; Creran, B.; Rotello, V. M. Gold Nanoparticles: Preparation, Properties, and Applications in Bionanotechnology. *Nanoscale* **2012**, *4*, 1871−1880.

(153) Grabowsky, S.; Hesse, M. F.; Paulmann, C.; Luger, P.; Beckmann, J. How to Make the Ionic Si− O Bond More Covalent and the Si− O− Si Linkage a Better Acceptor for Hydrogen Bonding. *Inorg. Chem.* **2009**, *48*, 4384−4393.

(154) Patwardhan, S. V.; Emami, F. S.; Berry, R. J.; Jones, S. E.; Naik, R. R.; Deschaume, O.; Heinz, H.; Perry, C. C. Chemistry of Aqueous Silica Nanoparticle Surfaces and the Mechanism of Selective Peptide Adsorption. *J. Am. Chem. Soc.* **2012**, *134*, 6244−6256.

(155) Davydov, V. Y.; Kiselev, A.; Zhuravlev, L. Study of the Surface and Bulk Hydroxyl Groups of Silica by Infra-red pectra and D_2O-Exchange. *Trans. Faraday Soc.* **1964**, *60*, 2254−2264.

(156) Ek, S.; Root, A.; Peussa, M.; Niinistö, L. Determination of the Hydroxyl Group Content in Silica by Thermogravimetry and a Comparison with 1H MAS NMR Results. *Thermochim. Acta* **2001**, *379*, 201−212.

(157) Nicholls, A.; Sharp, K. A.; Honig, B. Protein Folding and Association: Insights from the Interfacial and Thermodynamic Properties of Hydrocarbons. *Proteins: Struct., Funct., Genet.* **1991**, *11*, 281−296.

(158) Ostuni, E.; Grzybowski, B. A.; Mrksich, M.; Roberts, C. S.; Whitesides, G. M. Adsorption of Proteins to Hydrophobic Sites on Mixed Self-Assembled Monolayers. *Langmuir* **2003**, *19*, 1861−1872.

(159) Giovambattista, N.; Lopez, C. F.; Rossky, P. J.; Debenedetti, P. G. Hydrophobicity of Protein Surfaces: Separating Geometry from Chemistry. *Proc. Natl. Acad. Sci. U. S. A.* **2008**, *105*, 2274−2279.

(160) Jass, J.; Tjärnhage, T.; Puu, G. From Liposomes to Supported, Planar Bilayer Structures on Hydrophilic and Hydrophobic Surfaces: an Atomic Force Microscopy Study. *Biophys. J.* **2000**, *79*, 3153−3163.

(161) Shi, B.; Shin, Y. K.; Hassanali, A. A.; Singer, S. J. DNA Binding to the Silica Surface. *J. Phys. Chem. B* **2015**, *119*, 11030−11040.

(162) Rimola, A.; Costa, D.; Sodupe, M.; Lambert, J.; Ugliengo, P. Silica Surface Features and their Role in the Adsorption of Biomolecules: Computational Modeling and Experiments. *Chem. Rev.* **2013**, *113*, 4216−4313.

(163) Brunauer, S.; Kantro, D. L.; Weise, C. H. The Surface Energies of Amorphous Silica and Hydrous Amorphous Silica. *Can. J. Chem.* **1956**, *34*, 1483−1496.

(164) Fubini, B.; Zanetti, G.; Altilia, S.; Tiozzo, R.; Lison, D.; Saffiotti, U. Relationship Between Surface Properties and Cellular Responses to Crystalline Silica: Studies with Heat-Treated Cristobalite. *Chem. Res. Toxicol.* **1999**, *12*, 737−745.

(165) Fubini, B.; Bolis, V.; Cavenago, A.; Volante, M. Physicochemical Properties of Crystalline Silica Dusts and their Possible Implication in Various Biological Responses. *Scand. J. Work, Environ. Health* **1995**, *21*, 9−14.

(166) Barisik, M.; Atalay, S.; Beskok, A.; Qian, S. Size Dependent Surface Charge Properties of Silica Nanoparticles. *J. Phys. Chem. C* **2014**, *118*, 1836−1842.

(167) Behrens, S.; Grier, D. The Charge of Glass and Silica Surfaces. *J. Chem. Phys.* **2001**, *115*, 6716−6721.

(168) Puddu, V.; Perry, C. C. Interactions at the Silica−Peptide Interface: The Influence of Particle Size and Surface Functionality. *Langmuir* **2014**, *30*, 227−233.

(169) Clogston, J. D.; Patri, A. K. Importance of Physicochemical Characterization Prior to Immunological Studies. In *Handbook of Immunological Properties of Engineered Nanomaterials*; Dobrovolskaia, M. A., McNeil, S. E., Eds.; World Scientific Publishing Ltd: Singapore, 2016; pp 25−52.

(170) Smith, M. C.; Crist, R. M.; Clogston, J. D.; McNeil, S. E. Zeta potential: A Case Study of Cationic, Anionic, and Neutral Liposomes. *Anal. Bioanal. Chem.* **2017**, *409*, 5779−5787.

(171) Desmond, J. L.; Juhl, K.; Hassenkam, T.; Stipp, S. L. S.; Walsh, T. R.; Rodger, P. M. Organic-Silica Interactions in Saline: Elucidating the Structural Influence of Calcium in Low-Salinity Enhanced Oil Recovery. *Sci. Rep.* **2017**, *7*, 10944.

(172) Butenuth, A.; Moras, G.; Schneider, J.; Koleini, M.; Köppen, S.; Meißner, R.; Wright, L. B.; Walsh, T. R.; Ciacchi, L. C. *Ab initio* Derived Force-Field Parameters for Molecular Dynamics Simulations of Deprotonated Amorphous-SiO_2/Water Interfaces. *Phys. Status Solidi B* **2012**, *249*, 292−305.

(173) Emami, F. S.; Puddu, V.; Berry, R. J.; Varshney, V.; Patwardhan, S. V.; Perry, C. C.; Heinz, H. Force Field and a Surface Model Database for Silica to Simulate Interfacial Properties in Atomic Resolution. *Chem. Mater.* **2014**, *26*, 2647−2658.

(174) Mishra, R. K.; Mohamed, A. K.; Geissbühler, D.; Manzano, H.; Jamil, T.; Shahsavari, R.; Kalinichev, A. G.; Galmarini, S.; Tao, L.; Heinz, H.; et al. A Force Field Database for Cementitious Materials Including Validations, Applications and Opportunities. *Cem. Concr. Res.* **2017**, *102*, 68−89.

(175) Hassenkam, T.; Mitchell, A. C.; Pedersen, C. S.; Skovbjerg, L. L.; Bovet, N.; Stipp, S. L. S. The Low Salinity Effect Observed on Sandstone Model Surfaces. *Colloids Surf., A* **2012**, *403*, 79−86.

(176) Puddu, V.; Perry, C. C. Peptide Adsorption on Silica Nanoparticles: Evidence of Hydrophobic Interactions. *ACS Nano* **2012**, *6*, 6356−6363.

(177) An, Y.; Chen, M.; Xue, Q.; Liu, W. Preparation and Self-Assembly of Carboxylic Acid-Functionalized Silica. *J. Colloid Interface Sci.* **2007**, *311*, 507−513.

(178) Asenath Smith, E.; Chen, W. How to Prevent the Loss of Surface Functionality Derived from Aminosilanes. *Langmuir* **2008**, *24*, 12405−12409.

(179) Luechinger, M.; Prins, R.; Pirngruber, G. D. Functionalization of Silica Surfaces with Mixtures of 3-Aminopropyl and Methyl Groups. *Microporous Mesoporous Mater.* **2005**, *85*, 111−118.

(180) Sola-Rabada, A.; Michaelis, M.; Oliver, J. D.; Roe, M. J.; Colombi Ciacchi, L.; Heinz, H.; Perry, C. C. Interactions at the Silica−Peptide Interface: Influence of the Extent of Functionalization on the Conformational Ensemble. *Langmuir* **2018**, *34*, 8255−8263.

(181) Wu, Z.; Xiang, H.; Kim, T.; Chun, M.; Lee, K. Surface Properties of Submicrometer Silica Spheres Modified with Aminopropyltriethoxysilane and Phenyltriethoxysilane. *J. Colloid Interface Sci.* **2006**, *304*, 119−124.

(182) Groppo, E.; Lamberti, C.; Bordiga, S.; Spoto, G.; Zecchina, A. The Structure of Active Centers and the Ethylene Polymerization Mechanism on the Cr/SiO$_2$ Catalyst: A Frontier for the Characterization Methods. *Chem. Rev.* **2005**, *105*, 115−184.

(183) Freund, H.; Pacchioni, G. Oxide Ultra-Thin Films on Metals: New Materials for the Design of Supported Metal Catalysts. *Chem. Soc. Rev.* **2008**, *37*, 2224−2242.

(184) Min, B.; Santra, A.; Goodman, D. Understanding Silica-Supported Metal Catalysts: Pd/Silica as a Case Study. *Catal. Today* **2003**, *85*, 113−124.

(185) Aguado, J.; Arsuaga, J. M.; Arencibia, A.; Lindo, M.; Gascón, V. Aqueous Heavy Metals Removal by Adsorption on Amine-Functionalized Mesoporous Silica. *J. Hazard. Mater.* **2009**, *163*, 213−221.

(186) Bharali, D. J.; Klejbor, I.; Stachowiak, E. K.; Dutta, P.; Roy, I.; Kaur, N.; Bergey, E. J.; Prasad, P. N.; Stachowiak, M. K. Organically Modified Silica Nanoparticles: A Nonviral Vector for In Vivo Gene Delivery and Expression in the Brain. *Proc. Natl. Acad. Sci. U. S. A.* **2005**, *102*, 11539−11544.

(187) Manzano, M.; Aina, V.; Arean, C.; Balas, F.; Cauda, V.; Colilla, M.; Delgado, M.; Vallet-Regi, M. Studies on MCM-41 Mesoporous Silica for Drug Delivery: Effect of Particle Morphology and Amine Functionalization. *Chem. Eng. J.* **2008**, *137*, 30−37.

(188) Song, S.; Hidajat, K.; Kawi, S. Functionalized SBA-15 materials as Carriers for Controlled Drug Delivery: Influence of Surface Properties on Matrix-Drug Interactions. *Langmuir* **2005**, *21*, 9568−9575.

(189) Das, I.; Mishra, M. K.; Medda, S. K.; De, G. Durable Superhydrophobic ZnO−SiO$_2$ Films: A New Approach to Enhance the Abrasion Resistant Property of Trimethylsilyl Functionalized SiO$_2$ Nanoparticles on Glass. *RSC Adv.* **2014**, *4*, 54989−54997.

(190) Subhash Latthe, S.; Basavraj Gurav, A.; Shridhar Maruti, C.; Shrikant Vhatkar, R. Recent Progress in Preparation of Superhydrophobic Surfaces: A Review. *J. Surf. Eng. Mater. Adv. Technol.* **2012**, *2*, 76−94.

(191) Nicklin, M.; Rees, R. C.; Pockley, A. G.; Perry, C. C. Development of an Hydrophobic Fluoro-Silica Surface for Studying Homotypic Cancer Cell Aggregation−Disaggregation as a Single Dynamic ProcessI in vitro. *Biomater. Sci.* **2014**, *2*, 1486−1496.

(192) Hickman, G. J.; Rees, R. C.; Boocock, D. J.; Pockley, A. G.; Perry, C. C. Controlling the Dynamics of Cell Transition in Heterogeneous Cultures using Surface Chemistry. *Adv. Healthcare Mater.* **2015**, *4*, 593−601.

(193) Nakamura, M.; Shono, M.; Ishimura, K. Synthesis, Characterization, and Biological Applications of Multifluorescent Silica Nanoparticles. *Anal. Chem.* **2007**, *79*, 6507−6514.

(194) Knopp, D.; Tang, D.; Niessner, R. Review: Bioanalytical Applications of Biomolecule-Functionalized Nanometer-Sized Doped Silica Particles. *Anal. Chim. Acta* **2009**, *647*, 14−30.

(195) Bringley, J. F.; Penner, T. L.; Wang, R.; Harder, J. F.; Harrison, W. J.; Buonemani, L. Silica Nanoparticles Encapsulating Near-Infrared Emissive Cyanine Dyes. *J. Colloid Interface Sci.* **2008**, *320*, 132−139.

(196) Ha, S.; Camalier, C. E.; Beck, G. R., Jr.; Lee, J. New Method to Prepare Very Stable and Biocompatible Fluorescent Silica Nanoparticles. *Chem. Commun.* **2009**, *0*, 2881−2883.

(197) Arruebo, M.; Fernández-Pacheco, R.; Ibarra, M. R.; Santamaría, J. Magnetic Nanoparticles for Drug Delivery. *Nano Today* **2007**, *2*, 22−32.

(198) Lee, J. E.; Lee, N.; Kim, H.; Kim, J.; Choi, S. H.; Kim, J. H.; Kim, T.; Song, I. C.; Park, S. P.; Moon, W. K.; et al. Uniform Mesoporous Dye-Doped Silica Nanoparticles Decorated with Multiple Magnetite Nanocrystals for Simultaneous Enhanced Magnetic Resonance Imaging, Fluorescence Imaging, and Drug Delivery. *J. Am. Chem. Soc.* **2010**, *132*, 552−557.

(199) Sun, C.; Lee, J. S.; Zhang, M. Magnetic Nanoparticles in MR Imaging and Drug Delivery. *Adv. Drug Delivery Rev.* **2008**, *60*, 1252−1265.

(200) Lu, A.; Salabas, E. L.; Schüth, F. Magnetic Nanoparticles: Synthesis, Protection, Functionalization, and Application. *Angew. Chem., Int. Ed.* **2007**, *46*, 1222−1244.

(201) Hola, K.; Markova, Z.; Zoppellaro, G.; Tucek, J.; Zboril, R. Tailored functionalization of Iron Oxide Nanoparticles for MRI, Drug Delivery, Magnetic Separation and Immobilization of Biosubstances. *Biotechnol. Adv.* **2015**, *33*, 1162−1176.

(202) Sumper, M.; Kröger, N. Silica Formation in Diatoms: theFfunction of Long-Chain Polyamines and Silaffins. *J. Mater. Chem.* **2004**, *14*, 2059−2065.

(203) Kröger, N.; Deutzmann, R.; Bergsdorf, C.; Sumper, M. Species-Specific Polyamines from Diatoms Control Silica Morphology. *Proc. Natl. Acad. Sci. U. S. A.* **2000**, *97*, 14133−14138.

(204) Kröger, N.; Deutzmann, R.; Sumper, M. Polycationic Peptides from Diatom Biosilica That Direct Silica Nanosphere Formation. *Science* **1999**, *286*, 1129−1132.

(205) Kröger, N.; Lorenz, S.; Brunner, E.; Sumper, M. Self-Assembly of Highly Phosphorylated Silaffins and Their Function in Biosilica Morphogenesis. *Science* **2002**, *298*, 584−586.

(206) Belton, D. J.; Patwardhan, S. V.; Annenkov, V. V.; Danilovtseva, E. N.; Perry, C. C. From Biosilicification to Tailored Materials: Optimizing Hydrophobic Domains and Resistance to Protonation of Polyamines. *Proc. Natl. Acad. Sci. U. S. A.* **2008**, *105*, 5963−5968.

(207) Bernecker, A.; Ziomkowska, J.; Heitmüller, S.; Wieneke, R.; Geyer, A.; Steinem, C. Formation of Silica Precipitates on Membrane Surfaces in Two and Three Dimensions. *Langmuir* **2010**, *26*, 13422−13428.

(208) Wieneke, R.; Bernecker, A.; Riedel, R.; Sumper, M.; Steinem, C.; Geyer, A. Silica Precipitation with Synthetic Silaffin Peptides. *Org. Biomol. Chem.* **2011**, *9*, 5482−5486.

(209) Wenzl, S.; Hett, R.; Richthammer, P.; Sumper, M. Silacidins: Highly Acidic Phosphopeptides from Diatom Shells Assist in Silica Precipitation In Vitro. *Angew. Chem.* **2008**, *120*, 1753−1756.

(210) Cha, J. N.; Shimizu, K.; Zhou, Y.; Christiansen, S. C.; Chmelka, B. F.; Stucky, G. D.; Morse, D. E. Silicatein Filaments and Subunits from a Marine Sponge Direct the Polymerization of Silica and Silicones *in vitro*. *Proc. Natl. Acad. Sci. U. S. A.* **1999**, *96*, 361−365.

(211) Woesz, A.; Weaver, J. C.; Kazanci, M.; Dauphin, Y.; Aizenberg, J.; Morse, D. E.; Fratzl, P. Micromechanical Properties of Biological Silica in Skeletons of Deep-Sea Sponges. *J. Mater. Res.* **2006**, *21*, 2068−2078.

(212) Masse, S.; Pisera, A.; Laurent, G.; Coradin, T. A Solid State NMR Investigation of Recent Marine Siliceous Sponge Spicules. *Minerals* **2016**, *6*, 21.

(213) Bauer, P.; Elbaum, R.; Weiss, I. M. Calcium and Silicon Mineralization in Land Plants: Transport, Structure and Function. *Plant Sci.* **2011**, *180*, 746−756.

(214) Roach, P.; Farrar, D.; Perry, C. C. Interpretation of Protein Adsorption: Surface-Induced Conformational Changes. *J. Am. Chem. Soc.* **2005**, *127*, 8168−8173.

(215) Bellomo, E. G.; Deming, T. J. Monoliths of Aligned Silica-Polypeptide Hexagonal Platelets. *J. Am. Chem. Soc.* **2006**, *128*, 2276−2279.

(216) Meegan, J. E.; Aggeli, A.; Boden, N.; Brydson, R.; Brown, A. P.; Carrick, L.; Brough, A. R.; Hussain, A.; Ansell, R. J. Designed Self-Assembled β-Sheet Peptide Fibrils as Templates for Silica Nanotubes. *Adv. Funct. Mater.* **2004**, *14*, 31−37.

(217) Yuwono, V. M.; Hartgerink, J. D. Peptide Amphiphile Nanofibers Template and Catalyze Silica Nanotube Formation. *Langmuir* **2007**, *23*, 5033−5038.

(218) Mieszawska, A. J.; Nadkarni, L. D.; Perry, C. C.; Kaplan, D. L. Nanoscale Control of Silica Particle Formation via Silk−Silica Fusion Proteins for Bone Regeneration. *Chem. Mater.* **2010**, *22*, 5780−5785.

(219) Ndao, M.; Goobes, G.; Emani, P. S.; Drobny, G. P. A REDOR ssNMR Investigation of the Role of an N-Terminus Lysine in R5 Silica Recognition. *Langmuir* **2018**, *34*, 8678−8684.

(220) Lutz, H.; Jaeger, V.; Schmüser, L.; Bonn, M.; Pfaendtner, J.; Weidner, T. The Structure of the Diatom Silaffin Peptide R5 within Freestanding Two-Dimensional Biosilica Sheets. *Angew. Chem., Int. Ed.* **2017**, *56*, 8277−8280.

(221) Lechner, C. C.; Becker, C. F. W. Exploring the Effect of Native and Artificial Peptide Modifications on Silaffin Induced Silica Precipitation. *Chem. Sci.* **2012**, *3*, 3500−3504.

(222) Wong Po Foo, C.; Patwardhan, S. V.; Belton, D. J.; Kitchel, B.; Anastasiades, D.; Huang, J.; Naik, R. R.; Perry, C. C.; Kaplan, D. L. Novel Nanocomposites from Spider Silk-Silica Fusion (Chimeric) Proteins. *Proc. Natl. Acad. Sci. U. S. A.* **2006**, *103*, 9428−9433.

(223) Mieszawska, A. J.; Fourligas, N.; Georgakoudi, I.; Ouhib, N. M.; Belton, D. J.; Perry, C. C.; Kaplan, D. L. Osteoinductive Silk−Silica Composite Biomaterials for Bone Regeneration. *Biomaterials* **2010**, *31*, 8902−8910.

(224) Zhou, S.; Huang, W.; Belton, D. J.; Simmons, L. O.; Perry, C. C.; Wang, X.; Kaplan, D. L. Control of Silicification by Genetically Engineered Fusion Proteins: Silk−Silica Binding Peptides. *Acta Biomater.* **2015**, *15*, 173−180.

(225) Belton, D. J.; Mieszawska, A. J.; Currie, H. A.; Kaplan, D. L.; Perry, C. C. Silk−silica composites from Genetically Engineered Chimeric Proteins: Materials Properties Correlate with Silica Condensation Rate and Colloidal Stability of the Proteins in Aqueous Solution. *Langmuir* **2012**, *28*, 4373−4381.

(226) Currie, H. A.; Deschaume, O.; Naik, R. R.; Perry, C. C.; Kaplan, D. L. Genetically Engineered Chimeric Silk-Silver Binding Proteins. *Adv. Funct. Mater.* **2011**, *21*, 2889−2895.

(227) Martín-Moldes, Z.; Ebrahimi, D.; Plowright, R.; Dinjaski, N.; Perry, C. C.; Buehler, M. J.; Kaplan, D. L. Intracellular Pathways Involved in Bone Regeneration Triggered by Recombinant Silk−Silica Chimeras. *Adv. Funct. Mater.* **2018**, *28*, 1702570.

(228) Plowright, R.; Dinjaski, N.; Zhou, S.; Belton, D. J.; Kaplan, D. L.; Perry, C. C. Influence of Silk−Silica Fusion Protein Design on Silica Condensation in vitro and Cellular Calcification. *RSC Adv.* **2016**, *6*, 21776−21788.

(229) Tomczak, M. M.; Glawe, D. D.; Drummy, L. F.; Lawrence, C. G.; Stone, M. O.; Perry, C. C.; Pochan, D. J.; Deming, T. J.; Naik, R. R. Polypeptide-Templated Synthesis of Hexagonal Silica Platelets. *J. Am. Chem. Soc.* **2005**, *127*, 12577−12582.

(230) Patwardhan, S.; Maheshwari, R.; Mukherjee, N.; Kiick, K.; Clarson, S. Conformation and Assembly of Polypeptide Scaffolds in Templating the Synthesis of Silica: An Example of aPpolylysine Macromolecular ″Switch″. *Biomacromolecules* **2006**, *7*, 491−497.

(231) Coradin, T.; Livage, J. Effect of Some Amino Acids and Peptides on Silicic Acid Polymerization. *Colloids Surf., B* **2001**, *21*, 329−336.

(232) Meng, M.; Stievano, L.; Lambert, J. Adsorption and Thermal Condensation Mechanisms of Amino acids on Oxide Supports. 1. Glycine on Silica. *Langmuir* **2004**, *20*, 914−923.

(233) Gray, J. J. The Interaction of Proteins with Solid Surfaces. *Curr. Opin. Struct. Biol.* **2004**, *14*, 110−115.

(234) Rabe, M.; Verdes, D.; Seeger, S. Understanding Protein Adsorption Phenomena at Solid Surfaces. *Adv. Colloid Interface Sci.* **2011**, *162*, 87−106.

(235) Zhou, Y.; Shimizu, K.; Cha, J. N.; Stucky, G. D.; Morse, D. E. Efficient Catalysis of Polysiloxane Synthesis by Silicatein α Requires Specific Hydroxy and Imidazole Functionalities. *Angew. Chem., Int. Ed.* **1999**, *38*, 779−782.

(236) Mirau, P. A.; Naik, R. R.; Gehring, P. Structure of Peptides on Metal Oxide Surfaces Probed by NMR. *J. Am. Chem. Soc.* **2011**, *133*, 18243−18248.

(237) Tamerler, C.; Sarikaya, M. Molecular Biomimetics: Nanotechnology and Bionanotechnology Using Genetically Engineered Peptides. *Philos. Trans. R. Soc., A* **2009**, *367*, 1705−1726.

(238) Lambert, J. Adsorption and Polymerization of Amino Acids on Mineral Surfaces: A Review. *Origins Life Evol. Biospheres* **2008**, *38*, 211−242.

(239) Heinz, H.; Ramezani-Dakhel, H. Simulations of Inorganic−Bioorganic Interfaces to Discover New Materials: Insights, Comparisons to Experiment, Challenges, and Opportunities. *Chem. Soc. Rev.* **2016**, *45*, 412−448.

(240) Costa, D.; Garrain, P.; Baaden, M. Understanding Small Biomolecule-Biomaterial Interactions: A Review of Fundamental Theoretical and Experimental Approaches for Biomolecule Interactions with Inorganic Surfaces. *J. Biomed. Mater. Res., Part A* **2013**, *101*, 1210−1222.

(241) Thota, V.; Perry, C. A Review on Recent Patents and Applications of Inorganic Material Binding Peptides. *Recent Pat. Nanotechnol.* **2017**, *11*, 168−180.

(242) Chang, R. H.; Jang, J.; Wu, K. C. Cellulase Immobilized Mesoporous Silica Nanocatalysts for Efficient Cellulose-to-Glucose Conversion. *Green Chem.* **2011**, *13*, 2844−2850.

(243) Cho, E. J.; Jung, S.; Kim, H. J.; Lee, Y. G.; Nam, K. C.; Lee, H.; Bae, H. Co-immobilization of Three Cellulases on Au-Doped Magnetic Silica Nanoparticles for the Degradation of Cellulose. *Chem. Commun.* **2012**, *48*, 886−888.

(244) Johnson, A. K.; Zawadzka, A. M.; Deobald, L. A.; Crawford, R. L.; Paszczynski, A. J. Novel Method for Immobilization of Enzymes to Magnetic Nanoparticles. *J. Nanopart. Res.* **2008**, *10*, 1009−1025.

(245) Wolny, P. M.; Spatz, J. P.; Richter, R. P. On the Adsorption Behavior of Biotin-Binding Proteins on Gold and Silica. *Langmuir* **2010**, *26*, 1029−1034.

(246) Ozaki, M.; Nagai, K.; Nishiyama, H.; Tsuruoka, T.; Fujii, S.; Endoh, T.; Imai, T.; Tomizaki, K.; Usui, K. Site-Specific Control of Silica Mineralization on DNA Using a Designed Peptide. *Chem. Commun.* **2016**, *52*, 4010−4013.

(247) Jin, C.; Han, L.; Che, S. Synthesis of a DNA-Silica Complex with Rare Two-Dimensional Square p4mm Symmetry. *Angew. Chem., Int. Ed.* **2009**, *48*, 9268−9272.

(248) Shiba, K. Natural and Artificial Peptide Motifs: Their Origins and the Application of Motif-Programming. *Chem. Soc. Rev.* **2010**, *39*, 117−126.

(249) Ikeda, T.; Motomura, K.; Agou, Y.; Ishida, T.; Hirota, R.; Kuroda, A. The Silica-Binding Si-tag Functions as an Affinity Tag Even Under Denaturing Conditions. *Protein Expression Purif.* **2011**, *77*, 173−177.

(250) Royston, E.; Lee, S.; Culver, J. N.; Harris, M. T. Characterization of Silica-Coated Tobacco Mosaic Virus. *J. Colloid Interface Sci.* **2006**, *298*, 706−712.

(251) Abdelhamid, M. A. A.; Motomura, K.; Ikeda, T.; Ishida, T.; Hirota, R.; Kuroda, A. Affinity Purification of Recombinant Proteins using a Novel Silica-Binding Peptide as a Fusion Tag. *Appl. Microbiol. Biotechnol.* **2014**, *98*, 5677−5684.

(252) Altintoprak, K.; Seidenstucker, A.; Welle, A.; Eiben, S.; Atanasova, P.; Stitz, N.; Plettl, A.; Bill, J.; Gliemann, H.; Jeske, H.; et al. Peptide-Equipped Tobacco Mosaic Virus Templates for Selective and Controllable Biomineral Deposition. *Beilstein J. Nanotechnol.* **2015**, *6*, 1399−1412.

(253) Tang, F.; Li, L.; Chen, D. Mesoporous Silica Nanoparticles: Synthesis, Biocompatibility and Drug Delivery. *Adv. Mater.* **2012**, *24*, 1504−1534.

(254) Luckarift, H. R.; Johnson, G. R.; Spain, J. C. Silica-Immobilized Enzyme Reactors;Aapplication to Cholinesterase-Inhibition Studies. *J. Chromatogr. B: Anal. Technol. Biomed. Life Sci.* **2006**, *843*, 310−316.

(255) Chen, H.; Su, X.; Neoh, K.; Choe, W. QCM-D Analysis of Binding Mechanism of Phage Particles Displaying a Constrained Heptapeptide with Specific Affinity to SiO₂ and TiO₂. *Anal. Chem.* **2006**, *78*, 4872−4879.

(256) Seker, U. O.; Demir, H. V. Material Binding Peptides for Nanotechnology. *Molecules* **2011**, *16*, 1426−1451.

(257) Care, A.; Chi, F.; Bergquist, P. L.; Sunna, A. Biofunctionalization of Silica-Coated Magnetic Particles Mediated by a Peptide. *J. Nanopart. Res.* **2014**, *16*, 1−9.

(258) Sunna, A.; Chi, F.; Bergquist, P. L. A Linker Peptide with High Affinity Towards Silica-Containing Materials. *New Biotechnol.* **2013**, *30*, 485−492.

(259) Young, M.; Debbie, W.; Uchida, M.; Douglas, T. Plant Viruses as Biotemplates for Materials and Their Use in Nanotechnology. *Annu. Rev. Phytopathol.* **2008**, *46*, 361−384.

(260) Tran, D.; Chen, C.; Chang, J. Immobilization of Burkholderia sp. Lipase on a Ferric Silica Nanocomposite for Biodiesel Production. *J. Biotechnol.* **2012**, *158*, 112−119.

(261) Care, A.; Bergquist, P. L.; Sunna, A. Solid-Binding Peptides: Smart Tools for Nanobiotechnology. *Trends Biotechnol.* **2015**, *33*, 259−268.

(262) Kramer, R. M.; Li, C.; Carter, D. C.; Stone, M. O.; Naik, R. R. Engineered Protein Cages for Nanomaterial Synthesis. *J. Am. Chem. Soc.* **2004**, *126*, 13282−13286.

(263) Merzlyak, A.; Lee, S. Phage as Templates for Hybrid Materials and Mediators for Nanomaterial Synthesis. *Curr. Opin. Chem. Biol.* **2006**, *10*, 246−252.

(264) Biswas, A.; Bayer, I. S.; Biris, A. S.; Wang, T.; Dervishi, E.; Faupel, F. Advances in Top-Down and Bottom-Up Surface Nanofabrication: Techniques, Applications & Future Prospects. *Adv. Colloid Interface Sci.* **2012**, *170*, 2−27.

(265) Seker, U. O. S.; Zengin, G.; Tamerler, C.; Sarikaya, M.; Demir, H. V. Assembly Kinetics of Nanocrystals via Peptide Hybridization. *Langmuir* **2011**, *27*, 4867−4872.

(266) Lu, J.; Shen, H.; Wu, Z.; Wang, B.; Zhao, D.; He, L. Self-Assembly of Bi-Functional Peptides on Large-Pore Mesoporous Silica Nanoparticles for miRNA Binding and Delivery. *J. Mater. Chem. B* **2015**, *3*, 7653−7657.

(267) Oren, E. E.; Tamerler, C.; Sahin, D.; Hnilova, M.; Seker, U. O.; Sarikaya, M.; Samudrala, R. A Novel Knowledge-Based Approach to Design Inorganic-Binding Peptides. *Bioinformatics* **2007**, *23*, 2816−2822.

(268) Oren, E. E.; Notman, R.; Kim, I. W.; Evans, J. S.; Walsh, T. R.; Samudrala, R.; Tamerler, C.; Sarikaya, M. Probing the Molecular Mechanisms of Quartz-Binding Peptides. *Langmuir* **2010**, *26*, 11003−11009.

(269) Tamerler, C.; Sarikaya, M. Molecular iomimetics: utUilizing Nature's Molecular Ways in Practical Engineering. *Acta Biomater.* **2007**, *3*, 289−299.

(270) Seker, U. O.; Wilson, B.; Sahin, D.; Tamerler, C.; Sarikaya, M. Quantitative Affinity of Genetically Engineered Repeating Polypeptides to Inorganic Surfaces. *Biomacromolecules* **2009**, *10*, 250−257.

(271) Demir, H. V.; Seker, U. O. S.; Zengin, G.; Mutlugun, E.; Sari, E.; Tamerler, C.; Sarikaya, M. Spatially Selective Assembly of Quantum Dot Light Emitters in an LED Using Engineered Peptides. *ACS Nano* **2011**, *5*, 2735−2741.

(272) Hnilova, M.; So, C. R.; Oren, E. E.; Wilson, B. R.; Kacar, T.; Tamerler, C.; Sarikaya, M. Peptide-Directed Co-Assembly of Nanoprobes on Multimaterial Patterned Solid Surfaces. *Soft Matter* **2012**, *8*, 4327−4334.

(273) Paul, S.; Paul, D.; Fern, G. R.; Ray, A. K. Surface Plasmon Resonance Imaging Detection of Silver Nanoparticle-Tagged Immunoglobulin. *J. R. Soc., Interface* **2011**, *8*, 1204−1211.

(274) Wei, Y.; Latour, R. A. Determination of the Adsorption Free Energy for Peptide− Surface Interactions by SPR Spectroscopy. *Langmuir* **2008**, *24*, 6721−6729.

(275) Holinga, G. J.; York, R. L.; Onorato, R. M.; Thompson, C. M.; Webb, N. E.; Yoon, A. P.; Somorjai, G. A. An SFG Study of Interfacial Amino Acids at the Hydrophilic SiO₂ and Hydrophobic Deuterated Polystyrene Surfaces. *J. Am. Chem. Soc.* **2011**, *133*, 6243−6253.

(276) Phillips, D. C.; York, R. L.; Mermut, O.; McCrea, K. R.; Ward, R. S.; Somorjai, G. A. Side Chain, Chain Length, and Sequence Effects on Amphiphilic Peptide Adsorption at Hydrophobic and Hydrophilic Surfaces Studied by Sum-Frequency Generation Vibrational Spectroscopy and Quartz Crystal Microbalance. *J. Phys. Chem. C* **2007**, *111*, 255−261.

(277) Satriano, C.; Fragalà, M. E.; Forte, G.; Santoro, A. M.; La Mendola, D.; Kasemo, B. Surface Adsorption of Fibronectin-Derived Peptide Fragments: The Influence of Electrostatics and Hydrophobicity for Endothelial Cells Adhesion. *Soft Matter* **2012**, *8*, 53−56.

(278) Mermut, O.; Phillips, D. C.; York, R. L.; McCrea, K. R.; Ward, R. S.; Somorjai, G. A. In Situ Adsorption Studies of a 14-Amino acid leucine-lysine Peptide onto Hydrophobic Polystyrene and Hydrophilic Silica Surfaces using Quartz Crystal Microbalance, Atomic Force Microscopy, and Sum Frequency Generation Vibrational Spectroscopy. *J. Am. Chem. Soc.* **2006**, *128*, 3598−3607.

(279) Shen, F.; Rojas, O. J.; Genzer, J.; Gurgel, P. V.; Carbonell, R. G. Affinity Interactions of Human Immunoglobulin G with Short Peptides: Role of Ligand Spacer on Binding, Kinetics, and Mass Transfer. *Anal. Bioanal. Chem.* **2016**, *408*, 1829−1841.

(280) Xu, D.; Hodges, C.; Ding, Y.; Biggs, S.; Brooker, A.; York, D. Adsorption Kinetics of Laponite and Ludox Silica Nanoparticles onto a Deposited Poly(diallyldimethylammonium chloride) Layer Measured by a Quartz Crystal Microbalance and Optical Reflectometry. *Langmuir* **2010**, *26*, 18105−18112.

(281) Adamczyk, Z.; Jamrozy, K.; Batys, P.; Michna, A. Influence of Ionic Strength on Poly(diallyldimethylammonium chloride) Macromolecule Conformations in Electrolyte Solutions. *J. Colloid Interface Sci.* **2014**, *435*, 182−190.

(282) Mourchid, A.; Delville, A.; Lambard, J.; Lecolier, E.; Levitz, P. Phase-Diagram of Colloidal Dispersions of Anisotropic Charged-Particles - Equilibrium Properties, Structure, and Rheology of Laponite Suspensions. *Langmuir* **1995**, *11*, 1942−1950.

(283) Karpovich, A. L.; Vlasova, M. F.; Sapronova, N. I.; Sukharev, V. S.; Ivanov, V. V. Determination of Dimensions of Exfoliating Materials in Aqueous Suspensions. *Methodsx* **2016**, *3*, 19−24.

(284) Thyparambil, A. A.; Wei, Y.; Latour, R. A. Determination of Peptide−Surface Adsorption Free Energy for Material Surfaces Not Conducive to SPR or QCM Using AFM. *Langmuir* **2012**, *28*, 5687−5694.

(285) Bharti, B.; Meissner, J.; Findenegg, G. H. Aggregation of Silica Nanoparticles Directed by Adsorption of Lysozyme. *Langmuir* **2011**, *27*, 9823−9833.

(286) Catalano, F.; Alberto, G.; Ivanchenko, P.; Dovbeshko, G.; Martra, G. Effect of Silica Surface Properties on the Formation of Multilayer or Submonolayer Protein Hard Corona: Albumin Adsorption on Pyrolytic and Colloidal SiO₂ Nanoparticles. *J. Phys. Chem. C* **2015**, *119*, 26493−26505.

(287) Leblanc, K.; Hutchins, D. A. New Applications of a Biogenic Silica Deposition Fluorophore in the Study of Oceanic Diatoms. *Limnol. Oceanogr.: Methods* **2005**, *3*, 462−476.

(288) Shimizu, K.; Del Amo, Y.; Brzezinski, M. A.; Stucky, G. D.; Morse, D. E. A Novel Fluorescent Silica Tracer for Biological Silicification Studies. *Chem. Biol.* **2001**, *8*, 1051−1060.

(289) Parambath, M.; Hanley, Q. S.; Martin-Martinez, F. J.; Giesa, T.; Buehler, M. J.; Perry, C. C. The Nature of the Silicaphilic Fluorescence of PDMPO. *Phys. Chem. Chem. Phys.* **2016**, *18*, 5938−5948.

(290) Werner, M.; Heil, A.; Rothermel, N.; Breitzke, H.; Groszewicz, P.; Thankamony, A.; Gutmann, T.; Buntkowsky, G. Synthesis and Solid State NMR Characterization of Novel Peptide/Silica Hybrid Materials. *Solid State Nucl. Magn. Reson.* **2015**, *72*, 73−78.

(291) Lopes, I.; Piao, L.; Stievano, L.; Lambert, J. Adsorption of Amino Acids on Oxide Supports: a Solid-State NMR Study of Glycine Adsorption on Silica and Alumina. *J. Phys. Chem. C* **2009**, *113*, 18163−18172.

(292) Geiger, Y.; Gottlieb, H. E.; Akbey, U.; Oschkinat, H.; Goobes, G. Studying the Conformation of a Silaffin-Derived Pentalysine Peptide Embedded in Bioinspired Silica using Solution and Dynamic Nuclear Polarization Magic-Angle Spinning NMR. *J. Am. Chem. Soc.* **2016**, *138*, 5561−5567.

(293) Kröger, N.; Deutzmann, R.; Sumper, M. Silica-precipitating Peptides from Diatoms: The Chemical Structure of Silaffin-1A from Cylindrotheca Fusiformis. *J. Biol. Chem.* **2001**, *276*, 26066−26070.

(294) Brückner, S. I.; Donets, S.; Dianat, A.; Bobeth, M.; Gutiérrez, R.; Cuniberti, G.; Brunner, E. Probing Silica-Biomolecule Interactions by Solid-State NMR and Molecular Dynamics Simulations. *Langmuir* **2016**, *32*, 11698−11705.

(295) Wei, F.; Zhang, D.; Halas, N. J.; Hartgerink, J. D. Aromatic Amino Acids Providing Characteristic Motifs in the Raman and SERS Spectroscopy of Peptides. *J. Phys. Chem. B* **2008**, *112*, 9158−9164.

(296) Radziuk, D.; Moehwald, H. Prospects for Plasmonic Hot Spots in Single Molecule SERS Towards the Chemical Imaging of Live Cells. *Phys. Chem. Chem. Phys.* **2015**, *17*, 21072−21093.

(297) Kim, H.; Kosuda, K. M.; Van Duyne, R. P.; Stair, P. C. Resonance Raman and Surface- and Tip-Enhanced Raman Spectroscopy Methods to Study Solid Satalysts and Heterogeneous Catalytic Reactions. *Chem. Soc. Rev.* **2010**, *39*, 4820−4844.

(298) Bouchoucha, M.; Jaber, M.; Onfroy, T.; Lambert, J.; Xue, B. Glutamic Acid Adsorption and Transformations on Silica. *J. Phys. Chem. C* **2011**, *115*, 21813−21825.

(299) Williams, P. A.; Hughes, C. E.; Harris, K. D. L-Lysine: Exploiting Powder X-ray Diffraction to Complete the Set of Crystal Structures of the 20 Directly Encoded Proteinogenic Amino Acids. *Angew. Chem., Int. Ed.* **2015**, *54*, 3973−3977.

(300) Becker, O. M.; MacKerell, A. D., Jr.; Roux, B.; Watanabe, M. *Computational Biochemistry and Biophysics*; CRC Press, 2001.

(301) Sprenger, K. G.; Prakash, A.; Drobny, G.; Pfaendtner, J. Investigating the Role of Phosphorylation in the Binding of Silaffin Peptide R5 to Silica with Molecular Dynamics Simulations. *Langmuir* **2018**, *34*, 1199−1207.

(302) Notman, R.; Oren, E. E.; Tamerler, C.; Sarikaya, M.; Samudrala, R.; Walsh, T. R. Solution Study of Engineered Quartz Binding Peptides Using Replica Exchange Molecular Dynamics. *Biomacromolecules* **2010**, *11*, 3266−3274.

(303) Wright, L. B.; Walsh, T. R. Efficient Conformational Sampling of Peptides Adsorbed Onto Inorganic Surfaces: Insights from a Quartz Binding Peptide. *Phys. Chem. Chem. Phys.* **2013**, *15*, 4715−4726.

(304) Rimola, A.; Sodupe, M.; Ugliengo, P. Affinity Scale for the Interaction of Amino Acids with Silica Surfaces. *J. Phys. Chem. C* **2009**, *113*, 5741−5750.

(305) Lin, W.; Huang, Y.; Zhou, X.; Ma, Y. In vitro Toxicity of Silica Nanoparticles in Human Lung Cancer Cells. *Toxicol. Appl. Pharmacol.* **2006**, *217*, 252−259.

(306) Allison, A. C.; Harington, J. S.; Birbeck, M. An Examination of the Cytotoxic Effects of Silica on Macrophages. *J. Exp. Med.* **1966**, *124*, 141−154.

(307) Kim, I.; Joachim, E.; Choi, H.; Kim, K. Toxicity of Silica Nanoparticles Depends on Size, Dose, and Cell Type. *Nanomedicine* **2015**, *11*, 1407−1416.

(308) Murugadoss, S.; Lison, D.; Godderis, L.; Van den Brule, S.; Mast, J.; Brassinne, F.; Sebaihi, N.; Hoet, P. H. Toxicology of Silica Nanoparticles: An Update. *Arch. Toxicol.* **2017**, *91*, 2967−3010.

(309) Napierska, D.; Thomassen, L. C. J.; Rabolli, V.; Lison, D.; Gonzalez, L.; Kirsch-Volders, M.; Martens, J. A.; Hoet, P. H. Size-Dependent Cytotoxicity of Monodisperse Silica Nanoparticles in Human Endothelial Cells. *Small* **2009**, *5*, 846−853.

(310) Warheit, D. B.; Webb, T. R.; Colvin, V. L.; Reed, K. L.; Sayes, C. R. Pulmonary Bioassay Studies with Nanoscale and Fine-Quartz Particles in Rats: Toxicity is Not Dependent upon Particle Size but on Surface Characteristics. *Toxicol. Sci.* **2007**, *95*, 270−280.

(311) Roelofs, F.; Vogelsberger, W. Dissolution Kinetics of Synthetic Amorphous Silica in Biological-Like Media and its Theoretical Description. *J. Phys. Chem. B* **2004**, *108*, 11308−11316.

(312) Marchand, R.; Brohan, L.; Tournoux, M. TiO$_2$(B) a New Form of Titanium Dioxide and the Potassium Octatitanate K$_2$Ti$_8$O$_{17}$. *Mater. Res. Bull.* **1980**, *15*, 1129−1133.

(313) Latroche, M.; Brohan, L.; Marchand, R.; Tournoux, M. New Hollandite Oxides - TiO$_2$(H) and K$_{0.06}$TiO$_2$. *J. Solid State Chem.* **1989**, *81*, 78−82.

(314) Akimoto, J.; Gotoh, Y.; Oosawa, Y.; Nonose, N.; Kumagai, T.; Aoki, K.; Takei, H. Topotactic Oxidation of Ramsdellite-Type Li$_{0.5}$TiO$_2$, a New Polymorph of Titanium-Dioxide - TiO$_2$(R). *J. Solid State Chem.* **1994**, *113*, 27−36.

(315) Dubrovinskaia, N.; Dubrovinsky, L.; Ahuja, R.; Prokopenko, V.; Dmitriev, V.; Weber, H.; Osorio-Guillen, J.; Johansson, B. Experimental and Theoretical Identification of a New High-Pressure TiO$_2$ Polymorph. *Phys. Rev. Lett.* **2001**, *87*, 275501.

(316) Mattesini, M.; de Almeida, J.; Dubrovinsky, L.; Dubrovinskaia, N.; Johansson, B.; Ahuja, R. High-Pressure and High-Temperature Synthesis of the Cubic TiO$_2$ Polymorph. *Phys. Rev. B: Condens. Matter Mater. Phys.* **2004**, *70*, 212101.

(317) Dubrovinsky, L.; Dubrovinskaia, N.; Swamy, V.; Muscat, J.; Harrison, N.; Ahuja, R.; Holm, B.; Johansson, B. Materials Science - The Hardest Known Oxide. *Nature* **2001**, *410*, 653−654.

(318) Gázquez, M. J.; Bolívar, J. P.; Garcia-Tenorio, R.; Vaca, F. A Review of the Production Cycle of Titanium Dioxide Pigment. *Mater. Sci. Appl.* **2014**, *05*, 441.

(319) Pfaff, G.; Reynders, P. Angle-Dependent Optical Effects Deriving From Submicron Structures of Films and Pigments. *Chem. Rev.* **1999**, *99*, 1963−1981.

(320) Braun, J.; Baidins, A.; Marganski, R. TiO$_2$ Pigment Technology - A Review. *Prog. Org. Coat.* **1992**, *20*, 105−138.

(321) Yuan, S.; Chen, W.; Hu, S. Fabrication of TiO$_2$ Nanoparticles/ Surfactant Polymer Complex Film on Glassy Carbon Electrode and its Application to Sensing Trace Dopamine. *Mater. Sci. Eng., C* **2005**, *25*, 479−485.

(322) Salvador, A.; Pascual-Marti, M.; Adell, J.; Requeni, A.; March, J. Analytical Methodologies for Atomic Spectrometric Determination of Metallic Oxides in UV Sunscreen Creams. *J. Pharm. Biomed. Anal.* **2000**, *22*, 301−306.

(323) Weir, A.; Westerhoff, P.; Fabricius, L.; Hristovski, K.; von Goetz, N. Titanium Dioxide Nanoparticles in Food and Personal Care Products. *Environ. Sci. Technol.* **2012**, *46*, 2242−2250.

(324) Fujishima, A.; Honda, K. Electrochemical Photolysis of Water at a Semiconductor Electrode. *Nature* **1972**, *238*, 37−38.

(325) Hoffmann, M. R.; Martin, S. T.; Choi, W.; Bahnemann, D. W. Environmental Applications of Semiconductor Photocatalysis. *Chem. Rev.* **1995**, *95*, 69−96.

(326) Grätzel, M. Photoelectrochemical Cells. *Nature* **2001**, *414*, 338−344.

(327) Irie, H.; Ping, T. S.; Shibata, T.; Hashimoto, K. Reversible Control of Wettability of a TiO$_2$ Surface by Introducing Surface Roughness. *Electrochem. Solid-State Lett.* **2005**, *8*, D23−D25.

(328) Pouget, E.; Dujardin, E.; Cavalier, A.; Moreac, A.; Valéry, C.; Marchi-Artzner, V.; Weiss, T.; Renault, A.; Paternostre, M.; Artzner, F. Hierarchical Architectures by Synergy Between Dynamical Template Self-Assembly and Biomineralization. *Nat. Mater.* **2007**, *6*, 434−439.

(329) Mills, A.; LeHunte, S. An Overview of Semiconductor Photocatalysis. *J. Photochem. Photobiol., A* **1997**, *108*, 1−35.

(330) You, D. G.; Deepagan, V. G.; Um, W.; Jeon, S.; Son, S.; Chang, H.; Yoon, H. I.; Cho, Y. W.; Swierczewska, M.; Lee, S.; et al.

ROS-Generating TiO$_2$ Nanoparticles for Non-Invasive Sonodynamic Therapy of Cancer. *Sci. Rep.* **2016**, *6*, 23200.

(331) Kubacka, A.; Diez, M. S.; Rojo, D.; Bargiela, R.; Ciordia, S.; Zapico, I.; Albar, J. P.; Barbas, C.; Martins dos Santos, V. A. P.; Fernández-García, M.; et al. Understanding the Antimicrobial Mechanism of TiO$_2$-Based Nanocomposite Films in a Pathogenic Bacterium. *Sci. Rep.* **2015**, *4*, 4134.

(332) Arnal, P.; Corriu, R.; Leclercq, D.; Mutin, P.; Vioux, A. A Solution Chemistry Study of Nonhydrolytic Sol-Gel Routes to Titania. *Chem. Mater.* **1997**, *9*, 694−698.

(333) Kim, C.; Moon, B.; Park, J.; Tae Chung, S.; Son, S. Synthesis of Nanocrystalline TiO$_2$ in Toluene by a Solvothermal Route. *J. Cryst. Growth* **2003**, *254*, 405−410.

(334) Kim, C.; Moon, B.; Park, J.; Choi, B.; Seo, H. Solvothermal Synthesis of Nanocrystalline TiO$_2$ in toluene with Surfactant. *J. Cryst. Growth* **2003**, *257*, 309−315.

(335) Ruiz, A.; Sakai, G.; Cornet, A.; Shimanoe, K.; Morante, J.; Yamazoe, N. Microstructure Control of Thermally Stable TiO$_2$ Obtained by Hydrothermal Process for Gas Sensors. *Sens. Actuators, B* **2004**, *103*, 312−317.

(336) Nian, J.; Teng, H. Hydrothermal Synthesis of Single-Crystalline Anatase TiO$_2$ Nanorods with Nanotubes as the Precursor. *J. Phys. Chem. B* **2006**, *110*, 4193−4198.

(337) Kolen'ko, Y.; Churagulov, B.; Kunst, M.; Mazerolles, L.; Colbeau-Justin, C. Photocatalytic Properties of Titania Powders Prepared by Hydrothermal Method. *Appl. Catal., B* **2004**, *54*, 51−58.

(338) Kim, D.; Hong, H.; Kim, S.; Song, J.; Lee, K. Photocatalytic Behaviors and Structural Characterization of Nanocrystalline Fe-doped TiO$_2$ Synthesized by Mechanical Alloying. *J. Alloys Compd.* **2004**, *375*, 259−264.

(339) Pan, X.; Ma, X. Study on the Milling-Induced Transformation in TiO$_2$ Powder with Different Grain Sizes. *Mater. Lett.* **2004**, *58*, 513−515.

(340) Pradhan, S.; Reucroft, P.; Yang, F.; Dozier, A. Growth of TiO$_2$ Nanorods by Metalorganic Chemical Vapor Deposition. *J. Cryst. Growth* **2003**, *256*, 83−88.

(341) Limmer, S.; Chou, T.; Cao, G. A Study on the Growth of TiO$_2$ Nanorods using Sol Electrophoresis. *J. Mater. Sci.* **2004**, *39*, 895−901.

(342) Oh, S.; Ishigaki, T. Preparation of Pure Rutile and Anatase TiO$_2$ Nanopowders using RF Thermal Plasma. *Thin Solid Films* **2004**, *457*, 186−191.

(343) Matsubara, M.; Yamaki, T.; Itoh, H.; Abe, H.; Asai, K. Preparation of TiO$_2$ Nanoparticles by Pulsed Laser Ablation: Ambient Pressure Dependence of Crystallization. *Jpn. J. Appl. Phys.* **2003**, *42*, L479−L481.

(344) Di Paola, A.; Bellardita, M.; Palmisano, L. Brookite, the Least Known TiO$_2$ Photocatalyst. *Catalysts* **2013**, *3*, 36−73.

(345) Gong, X.; Selloni, A. Reactivity of Anatase TiO$_2$ Nanoparticles: The Role of the Minority (001) Surface. *J. Phys. Chem. B* **2005**, *109*, 19560−19562.

(346) Wahi, R. K.; Liu, Y.; Falkner, J. C.; Colvin, V. L. Solvothermal Synthesis and Characterization of Anatase TiO$_2$ Nanocrystals with Ultrahigh Surface Area. *J. Colloid Interface Sci.* **2006**, *302*, 530−536.

(347) Gupta, S. M.; Tripathi, M. A Review of TiO$_2$ Nanoparticles. *Chin. Sci. Bull.* **2011**, *56*, 1639−1657.

(348) Sugimoto, T.; Zhou, X.; Muramatsu, A. Synthesis of Uniform Anatase TiO$_2$ Nanoparticles by Gel−Sol Method: 3. Formation Process and Size Control. *J. Colloid Interface Sci.* **2003**, *259*, 43−52.

(349) Sugimoto, T.; Zhou, X.; Muramatsu, A. Synthesis of Uniform Anatase TiO$_2$ Nanoparticles by Gel-Sol Method 4. Shape Control. *J. Colloid Interface Sci.* **2003**, *259*, 53−61.

(350) Liao, D. L.; Liao, B. Q. Shape, Size and Photocatalytic Activity Control of TiO$_2$ Nanoparticles with Surfactants. *J. Photochem. Photobiol., A* **2007**, *187*, 363−369.

(351) Mahshid, S.; Askari, M.; Ghamsari, M. S. Synthesis of TiO$_2$ Nanoparticles by Hydrolysis and Peptization of Titanium Isopropoxide Solution. *J. Mater. Process. Technol.* **2007**, *189*, 296−300.

(352) Yan, J.; Feng, S.; Lu, H.; Wang, J.; Zheng, J.; Zhao, J.; Li, L.; Zhu, Z. Alcohol Induced Liquid-Phase Synthesis of Rutile Titania Nanotubes. *Mater. Sci. Eng., B* **2010**, *172*, 114−120.

(353) Kasuga, T.; Hiramatsu, M.; Hoson, A.; Sekino, T.; Niihara, K. Formation of Titanium Oxide Nanotube. *Langmuir* **1998**, *14*, 3160−3163.

(354) Dawson, G.; Chen, W.; Zhang, T.; Chen, Z.; Cheng, X. A Study on the effect of Starting Material phase on the Production of Trititanate Nanotubes. *Solid State Sci.* **2010**, *12*, 2170−2176.

(355) Wu, W.; Lei, B.; Rao, H.; Xu, Y.; Wang, Y.; Su, C.; Kuang, D. Hydrothermal Fabrication of Hierarchically Anatase TiO$_2$ Nanowire arrays on FTO Glass for Dye-sensitized Solar Cells. *Sci. Rep.* **2013**, *3*, 1352.

(356) Diebold, U. The Surface Science of Titanium Dioxide. *Surf. Sci. Rep.* **2003**, *48*, 53−229.

(357) Bourikas, K.; Kordulis, C.; Lycourghiotis, A. Titanium Dioxide (Anatase and Rutile): Surface Chemistry, Liquid−Solid Interface Chemistry, and Scientific Synthesis of Supported Catalysts. *Chem. Rev.* **2014**, *114*, 9754−9823.

(358) Kröger, N.; Dickerson, M. B.; Ahmad, G.; Cai, Y.; Haluska, M. S.; Sandhage, K. H.; Poulsen, N.; Sheppard, V. C. Bioenabled Synthesis of Rutile (TiO$_2$) at Ambient Temperature and Neutral pH. *Angew. Chem., Int. Ed.* **2006**, *45*, 7239−7243.

(359) Vittadini, A.; Casarin, M.; Selloni, A. Hydroxylation of TiO$_2$-B: Insights from Density Functional Calculations. *J. Mater. Chem.* **2010**, *20*, 5871−5877.

(360) Song, S.; Luo, C.; Fu, Q.; Pan, C. Hydrothermal Synthesis of the Novel Rutile-Mixed Anatase TiO2 Nanosheets with Dominant {001} Facets for High Photocatalytic Activity. *RSC Adv.* **2016**, *6*, 84035−84041.

(361) Zhang, Y.; Jiang, Z.; Huang, J.; Lim, L. Y.; Li, W.; Deng, J.; Gong, D.; Tang, Y.; Lai, Y.; Chen, Z. Titanate and Titania Nanostructured Materials for Environmental and Energy Applications: A Review. *RSC Adv.* **2015**, *5*, 79479−79510.

(362) Fronzi, M.; Iwaszuk, A.; Lucid, A.; Nolan, M. Metal Oxide Nanocluster-Modified TiO$_2$ as Solar Activated Photocatalyst Materials. *J. Phys.: Condens. Matter* **2016**, *28*, 074006.

(363) Vittadini, A.; Casarin, M.; Selloni, A. Structure and Stability of TiO$_2$-B Surfaces: A Density Functional Study. *J. Phys. Chem. C* **2009**, *113*, 18973−18977.

(364) Carravetta, V.; Monti, S. Peptide−TiO$_2$ Surface Interaction in Solution by Ab Initio and Molecular Dynamics Simulations. *J. Phys. Chem. B* **2006**, *110*, 6160−6169.

(365) Jo, M.; Yu, J.; Kim, H.; Song, H. J.; Kim, K.; Oh, J.; Choi, S. Titanium Dioxide Nanoparticle-Biomolecule Interactions Influence Oral Absorption. *Nanomaterials* **2016**, *6*, 225.

(366) Zhang, Z.; Fenter, P.; Cheng, L.; Sturchio, N. C.; Bedzyk, M. J.; Předota, M.; Bandura, A.; Kubicki, J. D.; Lvov, S. N.; Cummings, P. T.; et al. Ion Adsorption at the Rutile−Water Interface: Linking Molecular and Macroscopic Properties. *Langmuir* **2004**, *20*, 4954−4969.

(367) Wu, C.; Tu, K.; Deng, J.; Lo, Y.; Wu, C. Markedly Enhanced Surface Hydroxyl Groups of TiO$_2$ Nanoparticles with Superior Water-Dispersibility for Photocatalysis. *Materials* **2017**, *10*, 566.

(368) Zhang, D.; Yang, M.; Dong, S. Hydroxylation of the Rutile TiO$_2$(110) Surface Enhancing its Reducing Power for Photocatalysis. *J. Phys. Chem. C* **2015**, *119*, 1451−1456.

(369) Kosmulski, M. The Significance of the Difference in the Point of Zero Charge Between Rutile and Anatase. *Adv. Colloid Interface Sci.* **2002**, *99*, 255−264.

(370) Holmberg, J. P.; Ahlberg, E.; Bergenholtz, J.; Hassellöv, M.; Abbas, Z. Surface Charge and Interfacial Potential of Titanium Dioxide Nanoparticles: Experimental and Theoretical Investigations. *J. Colloid Interface Sci.* **2013**, *407*, 168−176.

(371) Hiemstra, T.; Venema, P.; Van Riemsdijk, W. H. Intrinsic Proton Affinity of Reactive Surface Groups of Metal (Hydr)oxides: The Bond Valence Principle. *J. Colloid Interface Sci.* **1996**, *184*, 680−692.

(372) Köppen, S.; Langel, W. Simulation of the Interface of (100) Rutile with Aqueous Ionic Solution. *Surf. Sci.* **2006**, *600*, 2040−2050.

(373) Předota, M.; Bandura, A. V.; Cummings, P. T.; Kubicki, J. D.; Wesolowski, D. J.; Chialvo, A. A.; Machesky, M. L. Electric Double Layer at the Rutile (110) Surface. 1. Structure of Surfaces and Interfacial Water from Molecular Dynamics by Use of ab Initio Potentials. *J. Phys. Chem. B* **2004**, *108*, 12049−12060.

(374) Roddick-Lanzilotta, A.; Connor, P.; McQuillan, A. An In Situ Infrared Spectroscopic Study of the Adsorption of Lysine to TiO_2 from an Aqueous Solution. *Langmuir* **1998**, *14*, 6479−6484.

(375) Hayashi, T.; Sano, K.; Shiba, K.; Kumashiro, Y.; Iwahori, K.; Yamashita, I.; Hara, M. Mechanism Underlying Specificity of Proteins Targeting Inorganic Materials. *Nano Lett.* **2006**, *6*, 515−519.

(376) Cole, K. E.; Valentine, A. M. Spermidine and Spermine Catalyze the Formation of Nanostructured Titanium Oxide. *Biomacromolecules* **2007**, *8*, 1641−1647.

(377) Han, T. H.; Oh, J. K.; Park, J. S.; Kwon, S.; Kim, S.; Kim, S. O. Highly Entangled Hollow TiO_2 Nanoribbons Templating Diphenylalanine Assembly. *J. Mater. Chem.* **2009**, *19*, 3512−3516.

(378) Seisenbaeva, G. A.; Daniel, G.; Nedelec, J.; Kessler, V. G. Solution Equilibrium Behind the Room-Temperature Synthesis of Nanocrystalline Titanium Dioxide. *Nanoscale* **2013**, *5*, 3330−3336.

(379) Liu, C.; Yang, D.; Jiao, Y.; Tian, Y.; Wang, Y.; Jiang, Z. Biomimetic Synthesis of TiO_2−SiO_2−Ag Nanocomposites with Enhanced Visible-Light Photocatalytic Activity. *ACS Appl. Mater. Interfaces* **2013**, *5*, 3824−3832.

(380) Sewell, S.; Wright, D. Biomimetic Synthesis of Titanium Dioxide Utilizing the R5 Peptide Derived from Cylindrotheca fusiformis. *Chem. Mater.* **2006**, *18*, 3108−3113.

(381) Choi, N.; Tan, L.; Jang, J.; Um, Y. M.; Yoo, P. J.; Choe, W. The Interplay of Peptide Sequence and Local Structure in TiO_2 Biomineralization. *J. Inorg. Biochem.* **2012**, *115*, 20−27.

(382) Lang, Y.; Monte, F. d.; Rodriguez, B. J.; Dockery, P.; Finn, D. P.; Pandit, A. Integration of TiO_2 into the Diatom Thalassiosira weissflogii During Frustule Synthesis. *Sci. Rep.* **2013**, *3*, 3205.

(383) Kanie, K.; Sugimoto, T. Shape Control of Anatase TiO_2 Nanoparticles by Amino Acids in a Gel−Sol System. *Chem. Commun.* **2004**, 1584−1585.

(384) Durupthy, O.; Bill, J.; Aldinger, F. Bioinspired Synthesis of Crystalline TiO_2: Effect of Amino Acids on Nanoparticles Structure and Shape. *Cryst. Growth Des.* **2007**, *7*, 2696−2704.

(385) Gardères, J.; Elkhooly, T. A.; Link, T.; Markl, J. S.; Müller Werner, E. G.; Renkel, J.; Korzhev, M.; Wiens, M. Self-Assembly and Photocatalytic Activity of Branched Silicatein/Silintaphin Filaments Decorated with Silicatein-Synthesized TiO_2 Nanoparticles. *Bioprocess Biosyst. Eng.* **2016**, *39*, 1477−1486.

(386) Zhao, C.; Yu, L.; Middelberg, A. P. J. Design of Low-Charge Peptide Sequences for High-Yield Formation of Titania Nanoparticles. *RSC Adv.* **2012**, *2*, 1292−1295.

(387) Nonoyama, T.; Kinoshita, T.; Higuchi, M.; Nagata, K.; Tanaka, M.; Sato, K.; Kato, K. TiO_2 Synthesis Inspired by Biomineralization: Control of Morphology, Crystal Phase, and Light-Use Efficiency in a Single Process. *J. Am. Chem. Soc.* **2012**, *134*, 8841−8847.

(388) Senanayake, S. D.; Idriss, H. Photocatalysis and the Origin of Life: Synthesis of Nucleoside Bases From Formamide on $TiO_2(001)$ Single Surfaces. *Proc. Natl. Acad. Sci. U. S. A.* **2006**, *103*, 1194−1198.

(389) Wolf-Brandstetter, C.; Hänchen, V.; Schwenzer, B.; Aeckerle, N.; Schliephake, H.; Scharnweber, D. Application of Lateral and Distance Spacers in an Oligonucleotide Based Immobilization System for Bioactive Molecules onto Titanium Implants. *ACS Appl. Mater. Interfaces* **2016**, *8*, 3755−3764.

(390) Jones, B. J.; Vergne, M. J.; Bunk, D. M.; Locascio, L. E.; Hayes, M. A. Cleavage of Peptides and Proteins Using Light-Generated Radicals From Titanium Dioxide. *Anal. Chem.* **2007**, *79*, 1327−1332.

(391) Chen, D.; Zhang, H.; Li, X.; Li, J. Biofunctional Titania Nanotubes for Visible-Light-Activated Photoelectrochemical Biosensing. *Anal. Chem.* **2010**, *82*, 2253−2261.

(392) Sollazzo, V.; Pezzetti, F.; Scarano, A.; Piattelli, A.; Massari, L.; Brunelli, G.; Carinci, F. Anatase Coating Improves Implant Osseointegration In Vivo. *J. Craniofac. Surg.* **2007**, *18*, 806−810.

(393) He, J.; Zhou, W.; Zhou, X.; Zhong, X.; Zhang, X.; Wan, P.; Zhu, B.; Chen, W. The Anatase Phase of Nanotopography Titania Plays an Important Role on Osteoblast Cell Morphology and Proliferation. *J. Mater. Sci.: Mater. Med.* **2008**, *19*, 3465−3472.

(394) Yu, M.; Lin, Y.; Liu, Y.; Zhou, Y.; Liu, C.; Dong, L.; Cheng, K.; Weng, W.; Wang, H. Enhanced Osteointegration of Hierarchical Structured 3D-Printed Titanium Implants. *ACS Appl. Bio Mater.* **2018**, *1*, 90−99.

(395) Zhao, Y.; Wang, C.; Zhai, Y.; Zhang, R.; Van Hove, M. A. Selective Adsorption of L-Serine Functional Groups on the Anatase $TiO_2(101)$ Surface in Benthic Microbial Fuel Cells. *Phys. Chem. Chem. Phys.* **2014**, *16*, 20806−20817.

(396) Ko, E. H.; Yoon, Y.; Park, J. H.; Yang, S. H.; Hong, D.; Lee, K.-B.; Shon, H. K.; Lee, T. G.; Choi, I. S. Bioinspired, Cytocompatible Mineralization of Silica−Titania Composites: Thermoprotective Nanoshell Formation for Individual Chlorella Cells. *Angew. Chem., Int. Ed.* **2013**, *52*, 12279−12282.

(397) Sano, K.; Sasaki, H.; Shiba, K. Utilization of the Pleiotropy of a Peptidic Aptamer to Fabricate Heterogeneous Nanodot-Containing Multilayer Nanostructures. *J. Am. Chem. Soc.* **2006**, *128*, 1717−1722.

(398) Sano, K.; Shiba, K. Stepwise Accumulation of Layers of Aptamer-Ornamented Ferritins using Biomimetic Layer-by-Layer. *J. Mater. Res.* **2008**, *23*, 3236−3240.

(399) Sano, K.; Sasaki, H.; Shiba, K. Specificity and Biomineralization Activities of Ti-Binding Peptide-1 (TBP-1). *Langmuir* **2005**, *21*, 3090−3095.

(400) Skelton, A. A.; Liang, T.; Walsh, T. R. Interplay of Sequence, Conformation, and Binding at the Peptide-Titania Interface as Mediated by Water. *ACS Appl. Mater. Interfaces* **2009**, *1*, 1482−1491.

(401) Schneider, J.; Colombi Ciacchi, L. Specific Material Recognition by Small Peptides Mediated by the Interfacial Solvent Structure. *J. Am. Chem. Soc.* **2012**, *134*, 2407−2413.

(402) Hayashi, T.; Sano, K.; Shiba, K.; Iwahori, K.; Yamashita, I.; Hara, M. Critical Amino Acid Residues for the Specific Binding of the Ti-Recognizing Recombinant Ferritin with Oxide Surfaces of Titanium and Silicon. *Langmuir* **2009**, *25*, 10901−10906.

(403) Suzuki, Y.; Shindo, H.; Asakura, T. Structure and Dynamic Properties of a Ti-Binding Peptide Bound to TiO_2 Nanoparticles As Accessed by ^1H NMR Spectroscopy. *J. Phys. Chem. B* **2016**, *120*, 4600−4607.

(404) Agosta, L.; Zollo, G.; Arcangeli, C.; Buonocore, F.; Gala, F.; Celino, M. Water Driven Adsorption of Amino Acids on the (101) Anatase TiO_2 Surface: an *ab initio* Study. *Phys. Chem. Chem. Phys.* **2015**, *17*, 1556−1561.

(405) Effah, E.; Bianco, P.; Ducheyne, P. Crystal-Structure of the Surface Oxide Layer on Titanium and its Changes Arising from Immersion. *J. Biomed. Mater. Res.* **1995**, *29*, 73−80.

(406) Vittadini, A.; Selloni, A.; Rotzinger, F.; Grätzel, M. Structure and Energetics of Water Adsorbed at TiO_2 Anatase 101 and 001 Surfaces. *Phys. Rev. Lett.* **1998**, *81*, 2954−2957.

(407) Kojima, T. Combined Reflectometric Interference Spectroscopy and Quartz Crystal Microbalance Detect Differential Adsorption of Lipid Vesicles with Different Phase Transition Temperatures on SiO_2, TiO_2, and Au Surfaces. *Anal. Chem.* **2017**, *89*, 13596−13602.

(408) Yongli, C.; Xiufang, Z.; Yandao, G.; Nanming, Z.; Tingying, Z.; Xinqi, S. Conformational Changes of Fibrinogen Adsorption onto Hydroxyapatite and Titanium Oxide Nanoparticles. *J. Colloid Interface Sci.* **1999**, *214*, 38−45.

(409) Wang, W.; Zhu, R.; Xiao, R.; Liu, H.; Wang, S. The Electrostatic Interactions Between Nano-TiO2 and Trypsin Inhibit the Enzyme Activity and Change the Secondary Structure of Trypsin. *Biol. Trace Elem. Res.* **2011**, *142*, 435−446.

(410) Givens, B. E.; Xu, Z.; Fiegel, J.; Grassian, V. H. Bovine Serum Albumin Adsorption on SiO_2 and TiO_2 Nanoparticle Surfaces at Circumneutral and Acidic pH: A Tale of Two Nano-Bio Surface Interactions. *J. Colloid Interface Sci.* **2017**, *493*, 334−341.

(411) Márquez, A.; Berger, T.; Feinle, A.; Huesing, N.; Himly, M.; Duschl, A.; Diwald, O. Bovine Serum Albumin Adsorption on TiO$_2$ Colloids: The Effect of Particle Agglomeration and Surface Composition. *Langmuir* **2017**, *33*, 2551−2558.

(412) Zapol, P.; Curtiss, L. A. Organic Molecule Adsorption on TiO$_2$ Nanoparticles: A Review of Computational Studies of Surface Interactions. *J. Comput. Theor. Nanosci.* **2007**, *4*, 222−230.

(413) Předota, M.; Zhang, Z.; Fenter, P.; Wesolowski, D. J.; Cummings, P. T. Electric Double Layer at the Rutile (110) Surface. 2. Adsorption of Ions from Molecular Dynamics and X-ray Experiments. *J. Phys. Chem. B* **2004**, *108*, 12061−12072.

(414) Schneider, J.; Ciacchi, L. C. A Classical Potential to Model the Adsorption of Biological Molecules on Oxidized Titanium Surfaces. *J. Chem. Theory Comput.* **2011**, *7*, 473−484.

(415) Schneider, J.; Ciacchi, L. C. First Principles and Classical Modeling of the Oxidized Titanium (0001) Surface. *Surf. Sci.* **2010**, *604*, 1105−1115.

(416) Sultan, A. M.; Hughes, Z. E.; Walsh, T. R. Binding Affinities of Amino Acid Analogues at the Charged Aqueous Titania Interface: Implications for Titania-Binding Peptides. *Langmuir* **2014**, *30*, 13321−13329.

(417) Luan, B.; Huynh, T.; Zhou, R. Simplified TiO$_2$ Force Fields for Studies of its Interaction with Biomolecules. *J. Chem. Phys.* **2015**, *142*, 234102.

(418) Monti, S.; Carravetta, V.; Battocchio, C.; Iucci, G.; Polzonetti, G. Peptide/TiO$_2$ Surface Interaction: A Theoretical and Experimental Study on the Structure of Adsorbed ALA-GLU and ALA-LYS. *Langmuir* **2008**, *24*, 3205−3214.

(419) Monti, S. Molecular Dynamics Simulations of Collagen-Like Peptide Adsorption on Titanium-Based Material Surfaces. *J. Phys. Chem. C* **2007**, *111*, 6086−6094.

(420) Liu, S.; Meng, X.; Perez-Aguilar, J.; Zhou, R. An *In Silico* Study of TiO$_2$ Nanoparticles Interaction with Twenty Standard Amino Acids in Aqueous Solution. *Sci. Rep.* **2016**, *6*, 37761.

(421) Warheit, D. B.; Kreiling, R.; Levy, L. S. Relevance of the Rat Lung Tumor Response to Particle Overload for Human Risk Assessment-Update and Interpretation of New Data Since ILSI 2000. *Toxicology* **2016**, *374*, 42−59.

(422) Lee, K.; Trochimowicz, H.; Reinhardt, C. Pulmonary Response of Rats Exposed to Titanium Dioxide (TiO$_2$) by Inhalation for 2 Years. *Toxicol. Appl. Pharmacol.* **1985**, *79*, 179−192.

(423) Shi, H.; Magaye, R.; Castranova, V.; Zhao, J. Titanium Dioxide Nanoparticles: A Review of Current Toxicological Data. *Part. Fibre Toxicol.* **2013**, *10*, 15.

(424) Zhao, J.; Bowman, L.; Zhang, X.; Vallyathan, V.; Young, S.; Castranova, V.; Ding, M. Titanium Dioxide (TiO$_2$) Nanoparticles Induce JB6 Cell Apoptosis Through Activation of the Caspase-8/Bid and Mitochondrial Pathways. *J. Toxicol. Environ. Health, Part A* **2009**, *72*, 1141−1149.

(425) Fabian, E.; Landsiedel, R.; Ma-Hock, L.; Wiench, K.; Wohlleben, W.; van Ravenzwaay, B. Tissue Distribution and Toxicity of Intravenously Administered Titanium Dioxide Nanoparticles in Rats. *Arch. Toxicol.* **2008**, *82*, 151−157.

(426) Oberdörster, G. Pulmonary Effects of Inhaled Ultrafine Particles. *Int. Arch. Occup. Environ. Health* **2000**, *74*, 1−8.

(427) Vranic, S.; Gosens, I.; Jacobsen, N. R.; Jensen, K. A.; Bokkers, B.; Kermanizadeh, A.; Stone, V.; Baeza-Squiban, A.; Cassee, F. R.; Tran, L.; et al. Impact of Serum as a Dispersion Agent for in vitro and in vivo Toxicological Assessments of TiO$_2$ Nanoparticles. *Arch. Toxicol.* **2017**, *91*, 353−363.

(428) Rizk, M. Z.; Ali, S. A.; Hamed, M. A.; El-Rigal, N. S.; Aly, H. F.; Salah, H. H. Toxicity of Titanium Dioxide Nanoparticles: Effect of Dose and Time on Biochemical Disturbance, Oxidative Stress and Genotoxicity in Mice. *Biomed. Pharmacother.* **2017**, *90*, 466−472.

(429) Hong, F.; Ji, L.; Zhou, Y.; Wang, L. Chronic Nasal Exposure to Nanoparticulate TiO$_2$ Causes Pulmonary Tumorigenesis in Male Mice. *Environ. Toxicol.* **2017**, *32*, 1651−1657.

(430) Lin, X.; Li, J.; Ma, S.; Liu, G.; Yang, K.; Tong, M.; Lin, D. Toxicity of TiO$_2$ Nanoparticles to *Escherichia coli*: Effects of Particle Size, Crystal Phase and Water Chemistry. *PLoS One* **2014**, *9*, No. e110247.

(431) Shakeel, M.; Jabeen, F.; Shabbir, S.; Asghar, M. S.; Khan, M. S.; Chaudhry, A. S. Toxicity of Nano-Titanium Dioxide (TiO$_2$-NP) Through Various Routes of Exposure: a Review. *Biol. Trace Elem. Res.* **2016**, *172*, 1−36.

(432) Norton, D. P.; Heo, Y.; Ivill, M.; Ip, K.; Pearton, S.; Chisholm, M. F.; Steiner, T. ZnO: Growth, Doping & Processing. *Mater. Today* **2004**, *7*, 34−40.

(433) Pearton, S.; Norton, D.; Ip, K.; Heo, Y.; Steiner, T. Recent Progress in Processing and Properties of ZnO. *Prog. Mater. Sci.* **2005**, *50*, 293−340.

(434) Klingshirn, C. ZnO: Material, Physics and Applications. *ChemPhysChem* **2007**, *8*, 782−803.

(435) Ellmer, K.; Klein, A.; Rech, B. *Transparent Conductive Zinc Oxide: Basics and Applications in Thin Film Solar Cells*; Springer Science & Business Media: Berlin, 2007.

(436) Serizawa, T.; Sawada, T.; Matsuno, H. Highly Specific Affinities of Short Peptides Against Synthetic Polymers. *Langmuir* **2007**, *23*, 11127−11133.

(437) Hirai, T.; Harada, Y.; Hashimoto, S.; Itoh, T.; Ohno, N. Luminescence of Excitons in Mesoscopic ZnO Particles. *J. Lumin.* **2005**, *112*, 196−199.

(438) Ozgur, U.; Hofstetter, D.; Morkoc, H. ZnO Devices and Applications: A Review of Current Status and Future Prospects. *Proc. IEEE* **2010**, *98*, 1255−1268.

(439) Ahmed, M. H.; Keyes, T. E.; Byrne, J. A.; Blackledge, C. W.; Hamilton, J. W. Adsorption and Photocatalytic Degradation of Human Serum Albumin on TiO$_2$ and Ag-TiO$_2$ Films. *J. Photochem. Photobiol., A* **2011**, *222*, 123−131.

(440) Xia, Y.; Wang, J.; Chen, R.; Zhou, D.; Xiang, L. A Review on the Fabrication of Hierarchical ZnO Nanostructures for Photo-catalysis Application. *Crystals* **2016**, *6*, 148.

(441) Bunn, C. The Lattice-Dimensions of Zinc Oxide. *Proc. Phys. Soc.* **1935**, *47*, 835.

(442) Moezzi, A.; McDonagh, A. M.; Cortie, M. B. Zinc Oxide Particles: Synthesis, Properties and Applications. *Chem. Eng. J.* **2012**, *185−186*, 1−22.

(443) Brayner, R.; Ferrari-Iliou, R.; Brivois, N.; Djediat, S.; Benedetti, M. F.; Fiévet, F. Toxicological Impact Studies Based on *Escherichia coli* Bacteria in Ultrafine ZnO Nanoparticles Colloidal Medium. *Nano Lett.* **2006**, *6*, 866−870.

(444) Reddy, K. M.; Feris, K.; Bell, J.; Wingett, D. G.; Hanley, C.; Punnoose, A. Selective Toxicity of Zinc Oxide Nanoparticles to Prokaryotic and Eukaryotic Systems. *Appl. Phys. Lett.* **2007**, *90*, 213902.

(445) Nohynek, G. J.; Lademann, J.; Ribaud, C.; Roberts, M. S. Grey Goo on the Skin? Nanotechnology, Cosmetic and Sunscreen Safety. *Crit. Rev. Toxicol.* **2007**, *37*, 251−277.

(446) Tankhiwale, R.; Bajpai, S. Preparation, Characterization and Antibacterial Applications of ZnO-Nanoparticles Coated Polyethylene Films for Food Packaging. *Colloids Surf., B* **2012**, *90*, 16−20.

(447) Espitia, P. J. P.; dos Reis Coimbra, J. S.; de Andrade, N. J.; Cruz, R. S.; Medeiros, E. A. A.; de Fátima Ferreira Soares, N. Zinc Oxide Nanoparticles: Synthesis, Antimicrobial Activity and Food Packaging Applications. *Food Bioprocess Technol.* **2012**, *5*, 1447−1464.

(448) He, D.; He, X.; Yang, X.; Li, H. A Smart ZnO@ Polydopamine-Nucleic Acid Nanosystem for Ultrasensitive Live Cell mRNA Imaging by the Target-Triggered Intracellular Self-Assembly of Active DNAzyme Nanostructures. *Chem. Sci.* **2017**, *8*, 2832−2840.

(449) Shanmugam, N. R.; Muthukumar, S.; Prasad, S. A Review on ZnO-Based Electrical Biosensors for Cardiac Biomarker Detection. *Future Sci. OA* **2017**, *3*, FSO196.

(450) Tang, C. C.; Fan, S. S.; Chapelle, M. L. d. l.; Li, P. Silica-Assisted Catalytic Growth of Oxide and Nitride Nanowires. *Chem. Phys. Lett.* **2001**, *333*, 12−15.

(451) Zhu, Z.; Chen, T.; Gu, Y.; Warren, J.; Osgood, R. Zinc Oxide Nanowires Grown by Vapor-Phase Transport Using Selected Metal Catalysts: A Comparative Study. *Chem. Mater.* **2005**, *17*, 4227−4234.

(452) Miao, L.; Ieda, Y.; Tanemura, S.; Cao, Y. G.; Tanemura, M.; Hayashi, Y.; Toh, S.; Kaneko, K. Synthesis, Microstructure and Photoluminescence of Well-Aligned ZnO Nanorods on Si Substrate. *Sci. Technol. Adv. Mater.* **2007**, *8*, 443−447.

(453) Lim, J.; Kang, C.; Kim, K.; Park, I.; Hwang, D.; Park, S. UV Electroluminescence Emission from ZnO Light-Emitting Diodes Grown by High-Temperature Radiofrequency Sputtering. *Adv. Mater.* **2006**, *18*, 2720−2724.

(454) Lyu, S.; Zhang, Y.; Lee, C.; Ruh, H.; Lee, H. Low-Temperature Growth of ZnO Nanowire Array by a Simple Physical Vapor-Deposition Method. *Chem. Mater.* **2003**, *15*, 3294−3299.

(455) Fay, S.; Kroll, U.; Bucher, C.; Vallat-Sauvain, E.; Shah, A. Low Pressure Chemical Vapour Deposition of ZnO Layers for Thin-Film Solar Cells: Temperature-Induced Morphological Changes. *Sol. Energy Mater. Sol. Cells* **2005**, *86*, 385−397.

(456) Lee, W.; Jeong, M.; Myoung, J. Catalyst-Free Growth of ZnO Nanowires by Metal-Organic Chemical Vapour Deposition (MOCVD) and Thermal Evaporation. *Acta Mater.* **2004**, *52*, 3949−3957.

(457) Sato, H.; Minami, T.; Miyata, T.; Takata, S.; Ishii, M. Transparent Conducting Zno Thin-Films Prepared on Low-Temperature Substrates by Chemical-Vapor-Deposition using $Zn(C_5H_7O_2)_2$. *Thin Solid Films* **1994**, *246*, 65−70.

(458) Yadav, R. S.; Pandey, A. C. Needle-Like ZnO Nanostructure Synthesized by Organic-Free Hydrothermal Process. *Phys. E* **2008**, *40*, 660−663.

(459) Govender, K.; Boyle, D. S.; Kenway, P. B.; O'Brien, P. Understanding the Factors that Govern the Deposition and Morphology of Thin Films of ZnO from Aqueous Solution. *J. Mater. Chem.* **2004**, *14*, 2575−2591.

(460) Krunks, M.; Mellikov, E. Zinc Oxide Thin Films by the Spray Pyrolysis Method. *Thin Solid Films* **1995**, *270*, 33−36.

(461) Yin, X.; Liu, X.; Wang, L.; Liu, B. Electrophoretic Deposition of ZnO Photoanode forPplastic Dye-Sensitized Solar Cells. *Electrochem. Commun.* **2010**, *12*, 1241−1244.

(462) He, H.; Cai, W.; Lin, Y.; Chen, B. Surface Decoration of ZnO Nanorod Arrays by Electrophoresis in the Au Colloidal Solution Prepared by Laser Ablation in Water. *Langmuir* **2010**, *26*, 8925−8932.

(463) Lagashetty, A.; Havanoor, V.; Basavaraja, S.; Balaji, S. D.; Venkataraman, A. Microwave-Assisted Route for Synthesis of Nanosized Metal Oxides. *Sci. Technol. Adv. Mater.* **2007**, *8*, 484−493.

(464) Li, L.; Zhai, T.; Bando, Y.; Golberg, D. Recent Progress of One-Dimensional ZnO Nanostructured Solar Cells. *Nano Energy* **2012**, *1*, 91−106.

(465) Xie, T.; Song, S.; Schwenke, K.; Singh, M.; Gonzalez, L. E.; Del Gado, E.; Hahm, J. Low-Index ZnO Crystal Plane-Specific Binding Behavior of Whole Immunoglobulin G Proteins. *Langmuir* **2015**, *31*, 10493−10499.

(466) Wang, Z. L. Zinc Oxide Nanostructures: Growth, Properties and Applications. *J. Phys.: Condens. Matter* **2004**, *16*, R829−R858.

(467) Xu, S.; Wang, Z. L. One-Dimensional ZnO Nanostructures: Solution Growth and Functional Properties. *Nano Res.* **2011**, *4*, 1013−1098.

(468) Masuda, Y.; Kinoshita, N.; Koumoto, K. Morphology Control of ZnO Crystalline Particles in Aqueous Solution. *Electrochim. Acta* **2007**, *53*, 171−174.

(469) Garcia, S. P.; Semancik, S. Controlling the Morphology of Zinc Oxide Nanorods Crystallized from Aqueous Solutions: The Effect of Crystal Growth Modifiers on Aspect Ratio. *Chem. Mater.* **2007**, *19*, 4016−4022.

(470) Weintraub, B.; Zhou, Z.; Li, Y.; Deng, Y. Solution Synthesis of One-Dimensional ZnO Nanomaterials and their Applications. *Nanoscale* **2010**, *2*, 1573−1587.

(471) Pietruszka, R.; Witkowski, B. S.; Luka, G.; Wachnicki, L.; Gieraltowska, S.; Kopalko, K.; Zielony, E.; Bieganski, P.; Placzek-Popko, E.; Godlewski, M. Photovoltaic Properties of ZnO Nanorods/p-Type Si Heterojunction Structures. *Beilstein J. Nanotechnol.* **2014**, *5*, 173−179.

(472) Liu, B.; Zeng, H. Hydrothermal Synthesis of ZnO Nanorods in the Diameter Regime of 50 nm. *J. Am. Chem. Soc.* **2003**, *125*, 4430−4431.

(473) Wu, X.; Bai, H.; Li, C.; Lu, G.; Shi, G. Controlled One-Step Fabrication of Highly Oriented ZnO Nanoneedle/Nanorods Arrays at Near Room Temperature. *Chem. Commun.* **2006**, *0*, 1655−1657.

(474) Duan, J.; Huang, X.; Wang, E. PEG-Assisted Synthesis of ZnO Nanotubes. *Mater. Lett.* **2006**, *60*, 1918−1921.

(475) Lian, J.; Ding, Z.; Kwong, F.; Ng, D. H. L. Template-Free Hydrothermal Synthesis of Hexagonal ZnO Micro-Cups and Micro-Rings Assembled by Nanoparticles. *CrystEngComm* **2011**, *13*, 4820−4822.

(476) Hu, H.; Huang, X.; Deng, C.; Chen, X.; Qian, Y. Hydrothermal Synthesis of ZnO Nanowires and Nanobelts on a Large Scale. *Mater. Chem. Phys.* **2007**, *106*, 58−62.

(477) Zhang, Z.; Mu, J. Hydrothermal Synthesis of ZnO Nanobundles Controlled by PEO-PPO-PEO Block Copolymers. *J. Colloid Interface Sci.* **2007**, *307*, 79−82.

(478) Zhou, X.; Xie, Z.; Jiang, Z.; Kuang, Q.; Zhang, S.; Xu, T.; Huang, R.; Zheng, L. Formation of ZnO Hexagonal Micro-Pyramids: a Successful Control of the Exposed Polar Surfaces with the Assistance of an Ionic Liquid. *Chem. Commun.* **2005**, *0*, 5572−5574.

(479) Wang, H.; Xie, J.; Yan, K.; Duan, M. Growth Mechanism of Different Morphologies of ZnO Crystals Prepared by Hydrothermal Method. *J. Mater. Sci. Technol.* **2011**, *27*, 153−158.

(480) Su, Y.; Li, J.; Luo, Z.; Lu, B.; Li, P. Microstructure, Growth Process and Enhanced Photocatalytic Activity of Flower-Like ZnO Particles. *RSC Adv.* **2016**, *6*, 7403−7408.

(481) Yin, J.; Gao, F.; Wei, C.; Lu, Q. Water Amount Dependence on Morphologies and Properties of ZnO nanostructures in Double-solvent System. *Sci. Rep.* **2015**, *4*, 3736.

(482) Diebold, U.; Koplitz, L. V.; Dulub, O. Atomic-Scale Properties of Low-Index ZnO Surfaces. *Appl. Surf. Sci.* **2004**, *237*, 336−342.

(483) Dulub, O.; Boatner, L. A.; Diebold, U. STM Study of the Geometric and Electronic Structure of ZnO(0001)-Zn, (000$\bar{1}$)-O, (10$\bar{1}$0), and (11$\bar{2}$0) Surfaces. *Surf. Sci.* **2002**, *519*, 201−217.

(484) Wöll, C. The Chemistry and Physics of Zinc Oxide Surfaces. *Prog. Surf. Sci.* **2007**, *82*, 55−120.

(485) Degen, A.; Kosec, M. Effect of pH and Impurities on the Surface Charge of Zinc Oxide in Aqueous Solution. *J. Eur. Ceram. Soc.* **2000**, *20*, 667−673.

(486) Nawrocki, G.; Cieplak, M. Amino Acids and Proteins at ZnO−Water Interfaces in Molecular Dynamics Simulations. *Phys. Chem. Chem. Phys.* **2013**, *15*, 13628−13636.

(487) Lubinsky, A.; Duke, C.; Chang, S.; Lee, B.; Mark, P. Atomic Geometry of the Low-Index Surfaces of ZnO: LEED Analysis. *J. Vac. Sci. Technol.* **1976**, *13*, 189−192.

(488) Scarano, D.; Spoto, G.; Bordiga, S.; Zecchina, A.; Lamberti, C. Lateral Interactions in CO Adlayers on Prismatic ZnO Faces: a FTIR and HRTEM Study. *Surf. Sci.* **1992**, *276*, 281−298.

(489) Meyer, B.; Marx, D. Density-Functional Study of the Structure and Stability of ZnO Surfaces. *Phys. Rev. B: Condens. Matter Mater. Phys.* **2003**, *67*, 035403.

(490) Meyer, B.; Rabaa, H.; Marx, D. Water Adsorption on ZnO(1010): From Single Molecules to Partially Dissociated Monolayers. *Phys. Chem. Chem. Phys.* **2006**, *8*, 1513−1520.

(491) Meyer, B.; Marx, D.; Dulub, O.; Diebold, U.; Kunat, M.; Langenberg, D.; Wöll, C. Partial Dissociation of Water Leads to Stable Superstructures on the Surface of Zinc Oxide. *Angew. Chem., Int. Ed.* **2004**, *43*, 6641−6645.

(492) große Holthaus, S.; Köppen, S.; Frauenheim, T.; Colombi Ciacchi, L. Atomistic Simulations of the ZnO(1$\bar{2}$10)/Water Interface: A Comparison between First-Principles, Tight-Binding, and Empirical Methods. *J. Chem. Theory Comput.* **2012**, *8*, 4517−4526.

(493) Raymand, D.; van Duin, A. C. T.; Spangberg, D.; Goddard, W. A., III; Hermansson, K. Water Adsorption on Stepped ZnO surfaces from MD Simulation. *Surf. Sci.* **2010**, *604*, 741−752.

(494) Tainter, C. J.; Schatz, G. C. Reactive Force Field Modeling of Zinc Oxide Nanoparticle Formation. *J. Phys. Chem. C* **2016**, *120*, 2950−2961.

(495) Wang, Y.; Muhler, M.; Wöll, C. Spectroscopic Evidence for the Partial Dissociation of H$_2$O on ZnO(1010). *Phys. Chem. Chem. Phys.* **2006**, *8*, 1521−1524.

(496) Noei, H.; Qiu, H.; Wang, Y.; Löffler, E.; Wöll, C.; Muhler, M. The Identification of Hydroxyl Groups on ZnO Nanoparticles by Infrared Spectroscopy. *Phys. Chem. Chem. Phys.* **2008**, *10*, 7092−7097.

(497) Newberg, J. T.; Goodwin, C.; Arble, C.; Khalifa, Y.; Boscoboinik, J. A.; Rani, S. ZnO(1010) Surface Hydroxylation under Ambient Water Vapor. *J. Phys. Chem. B* **2018**, *122*, 472−478.

(498) Puchner, E. M.; Gaub, H. E. Force and Function: Probing Proteins with AFM-Based Force Spectroscopy. *Curr. Opin. Struct. Biol.* **2009**, *19*, 605−614.

(499) Noguera, C. Polar Oxide Surfaces. *J. Phys.: Condens. Matter* **2000**, *12*, R367−R410.

(500) Valtiner, M.; Todorova, M.; Grundmeier, G.; Neugebauer, J. Temperature Stabilized Surface Reconstructions at Polar ZnO(0001). *Phys. Rev. Lett.* **2009**, *103*, 065502.

(501) Kresse, G.; Dulub, O.; Diebold, U. Competing Stabilization Mechanism for the Polar ZnO(0001)-Zn Surface. *Phys. Rev. B: Condens. Matter Mater. Phys.* **2003**, *68*, 245409.

(502) Dulub, O.; Diebold, U.; Kresse, G. Novel Stabilization Mechanism on Polar Surfaces: ZnO(0001)-Zn. *Phys. Rev. Lett.* **2003**, *90*, 016102.

(503) Torbruegge, S.; Ostendorf, F.; Reichling, M. Stabilization of Zinc-Terminated ZnO(0001) by a Modified Surface Stoichiometry. *J. Phys. Chem. C* **2009**, *113*, 4909−4914.

(504) Wang, Y.; Wöll, C. IR Spectroscopic Investigations of Chemical and Photochemical Reactions on Metal Oxides: Bridging the Materials Gap. *Chem. Soc. Rev.* **2017**, *46*, 1875−1932.

(505) Costa, D.; Savio, L.; Pradier, C.-M. Adsorption of Amino Acids and Peptides on Metal and Oxide Surfaces in Water Environment: A Synthetic and Prospective Review. *J. Phys. Chem. B* **2016**, *120*, 7039−7052.

(506) Buonocore, F.; Arcangeli, C.; Gala, F.; Zollo, G.; Celino, M. Adsorption of Modified Arg, Lys, Asp, and Gln to Dry and Hydrated ZnO Surface: A Density Functional Theory Study. *J. Phys. Chem. B* **2015**, *119*, 11791−11797.

(507) Feng, Y.; Zhang, M.; Guo, M.; Wang, X. Studies on the PEG-Assisted Hydrothermal Synthesis and Growth Mechanism of ZnO Microrod and Mesoporous Microsphere Arrays on the Substrate. *Cryst. Growth Des.* **2010**, *10*, 1500−1507.

(508) Cai, A.; Wang, Y.; Xing, S.; Du, L.; Ma, Z. Tuned Morphologies of DNA-Assisted ZnO Struggling Against pH. *Ceram. Int.* **2013**, *39*, 605−609.

(509) De La Rica, R.; Matsui, H. Urease as a Nanoreactor for Growing Crystalline ZnO Nanoshells at Room Temperature. *Angew. Chem., Int. Ed.* **2008**, *47*, 5415−5417.

(510) Wu, Q.; Chen, X.; Zhang, P.; Han, Y.; Chen, X.; Yan, Y.; Li, S. Amino Acid-Assisted Synthesis of ZnO Hierarchical Architectures and their Novel Photocatalytic Activities. *Cryst. Growth Des.* **2008**, *8*, 3010−3018.

(511) Cai, A.; Wang, Y.; Xing, S.; Ma, Z. Cavity of Cyclodextrin, a Useful Tool for the Morphological Control of ZnO Micro/Nanostructures. *Ceram. Int.* **2012**, *38*, 5265−5270.

(512) Dong, Q.; Su, H.; Zhang, C.; Zhang, D.; Guo, Q.; Kiessling, F. Fabrication of Hierarchical ZnO Films with Interwoven Porous Conformations by a Bioinspired Templating Technique. *Chem. Eng. J.* **2008**, *137*, 428−435.

(513) Ramimoghadam, D.; Hussein, M. Z. B.; Taufiq-Yap, Y. H. Synthesis and Characterization of ZnO Nanostructures using Palm Olein as Biotemplate. *Chem. Cent. J.* **2013**, *7*, 71.

(514) Greer, H. F.; Zhou, W.; Liu, M.; Tseng, Y.; Mou, C. The Origin of ZnO Twin Crystals in Bio-Inspired Synthesis. *CrystEngComm* **2012**, *14*, 1247−1255.

(515) Jitianu, M.; Goia, D. V. Zinc Oxide Colloids with Controlled Size, Sshape, and Structure. *J. Colloid Interface Sci.* **2007**, *309*, 78−85.

(516) Hussein, M. Z.; Mustafa, M.; Yahaya, A. H.; Wan Nor Azmin, W. H. Bacillus cereus as a Biotemplating Agent for the Synthesis of Zinc Oxide with Raspberry-and Plate-Like Structures. *J. Inorg. Biochem.* **2009**, *103*, 1145−1150.

(517) Zhou, H.; Fan, T.; Zhang, D. Hydrothermal Synthesis of ZnO Hollow Spheres using Spherobacterium as Biotemplates. *Microporous Mesoporous Mater.* **2007**, *100*, 322−327.

(518) Atanasova, P.; Rothenstein, D.; Schneider, J. J.; Hoffmann, R. C.; Dilfer, S.; Eiben, S.; Wege, C.; Jeske, H.; Bill, J. Virus-Templated Synthesis of ZnO Nanostructures and Formation of Field-Effect Transistors. *Adv. Mater.* **2011**, *23*, 4918−4922.

(519) Fujita, S.; Matsuura, K. Inclusion of Zinc Oxide Nanoparticles into Virus-Like Peptide Nanocapsules Self-Assembled from Viral β-Annulus Peptide. *Nanomaterials* **2014**, *4*, 778−791.

(520) Zelechowska, K.; Karczewska-Golec, J.; Karczewski, J.; Los, M.; Klonkowski, A. M.; Wegrzyn, G.; Golec, P. Phage-Directed Synthesis of Photoluminescent Zinc Oxide Nanoparticles under Benign Conditions. *Bioconjugate Chem.* **2016**, *27*, 1999−2006.

(521) Begum, G.; Manorama, S. V.; Singh, S.; Rana, R. K. Morphology-Controlled Assembly of ZnO Nanostructures: A Bioinspired Method and Visible Luminescence. *Chem. - Eur. J.* **2008**, *14*, 6421−6427.

(522) Bai, H.; Xu, F.; Anjia, L.; Matsui, H. Low Temperature Synthesis of ZnO Nanowires by using a Genetically-Modified Collagen-Like Triple Helix as a Catalytic Template. *Soft Matter* **2009**, *5*, 966−969.

(523) Huang, Z.; Yan, D.; Yang, M.; Liao, X.; Kang, Y.; Yin, G.; Yao, Y.; Hao, B. Preparation and Characterization of the Biomineralized Zinc Oxide Particles in Spider Silk Peptides. *J. Colloid Interface Sci.* **2008**, *325*, 356−362.

(524) Wei, Z.; Maeda, Y.; Matsui, H. Discovery of Catalytic Peptides for Inorganic Nanocrystal Synthesis by a Combinatorial Phage Display Approach. *Angew. Chem.* **2011**, *123*, 10773−10776.

(525) Yan, D.; Yin, G.; Huang, Z.; Yang, M.; Liao, X.; Kang, Y.; Yao, Y.; Hao, B.; Han, D. Characterization and Bacterial Response of Zinc Oxide Particles Prepared by a Biomineralization Process. *J. Phys. Chem. B* **2009**, *113*, 6047−6053.

(526) Baier, J.; Naumburg, T.; Blumenstein, N. J.; Jeurgens, L. P.; Welzel, U.; Do, T. A.; Pleiss, J.; Bill, J. Bio-inspired Mineralization of Zinc Oxide in Presence of ZnO-Binding Peptides. *Biointerface Res. Appl. Chem.* **2012**, *2*, 380−391.

(527) Limo, M. J.; Ramasamy, R.; Perry, C. C. ZnO Binding Peptides: Smart Versatile Tools for Controlled Modification of ZnO Growth Mechanism and Morphology. *Chem. Mater.* **2015**, *27*, 1950−1960.

(528) Sola-Rabada, A.; Liang, M.; Roe, M. J.; Perry, C. C. Peptide-Directed Crystal Growth Modification in the Formation of ZnO. *J. Mater. Chem. B* **2015**, *3*, 3777−3788.

(529) Moon, C. H.; Tousi, M.; Cheeney, J.; Ngo-Duc, T.; Zuo, Z.; Liu, J.; Haberer, E. D. Effects of 8-mer Acidic Peptide Concentration on the Corphology and Photoluminescence of Synthesized ZnO Nanomaterials. *Appl. Phys. A: Mater. Sci. Process.* **2015**, *121*, 757−763.

(530) Manna, J.; Rana, R. K. Oriented Morphogenesis of ZnO Nanostructures from Water-Soluble Zinc Salts under Environmentally Mild Conditions and Their Optical Properties. *Chem. - Eur. J.* **2012**, *18*, 498−506.

(531) Tomizaki, K.; Kubo, S.; Ahn, S.; Satake, M.; Imai, T. Biomimetic Alignment of Zinc Oxide Nanoparticles Along a Peptide Nanofiber. *Langmuir* **2012**, *28*, 13459−13466.

(532) Thai, C. K.; Dai, H.; Sastry, M.; Sarikaya, M.; Schwartz, D. T.; Baneyx, F. Identification and Characterization of Cu$_2$O-and ZnO-Binding Polypeptides by *Escherichia coli* Cell Surface Display: Toward an Understanding of Metal Oxide Binding. *Biotechnol. Bioeng.* **2004**, *87*, 129−137.

(533) Okochi, M.; Sugita, T.; Furusawa, S.; Umetsu, M.; Adschiri, T.; Honda, H. Peptide Array-Based Characterization and Design of ZnO-High Affinity Peptides. *Biotechnol. Bioeng.* **2010**, *106*, 845−851.

(534) Yokoo, N.; Togashi, T.; Umetsu, M.; Tsumoto, K.; Hattori, T.; Nakanishi, T.; Ohara, S.; Takami, S.; Naka, T.; Abe, H.; et al.

Direct and Selective Immobilization of Proteins by Means of an Inorganic Material-Binding Peptide: Discussion on Functionalization in the Elongation to Material-Binding Peptide. *J. Phys. Chem. B* **2010**, *114*, 480−486.

(535) Fang, K.; Wang, Z.; Zhang, M.; Wang, A.; Meng, Z.; Feng, J. Gelatin-Assisted Hydrothermal Synthesis of Single Crystalline Zinc Oxide Nanostars and Their Photocatalytic Properties. *J. Colloid Interface Sci.* **2013**, *402*, 68−74.

(536) Tseng, Y.; Lin, H.; Liu, M.; Chen, Y.; Mou, C. Biomimetic Synthesis of Nacrelike Faceted Mesocrystals of ZnO−Gelatin Composite. *J. Phys. Chem. C* **2009**, *113*, 18053−18061.

(537) Bauermann, L. P.; del Campo, A.; Bill, J.; Aldinger, F. Heterogeneous Nucleation of ZnO Using Gelatin as the Organic Matrix. *Chem. Mater.* **2006**, *18*, 2016−2020.

(538) Xiang, C.; Zou, Y.; Sun, L.; Xu, F. Direct Electrochemistry and Enhanced Electrocatalysis of Horseradish Peroxidase Based on Flowerlike ZnO−Gold Nanoparticle−Nafion Nanocomposite. *Sens. Actuators, B* **2009**, *136*, 158−162.

(539) Togashi, T.; Yokoo, N.; Umetsu, M.; Ohara, S.; Naka, T.; Takami, S.; Abe, H.; Kumagai, I.; Adschiri, T. Material-Binding PeptideAapplication—ZnO Crystal Structure Control by Means of a ZnO-Binding Peptide. *J. Biosci. Bioeng.* **2011**, *111*, 140−145.

(540) Liang, M.; Limo, M. J.; Solo- Rabada, A.; Roe, M.; Perry, C. C. New Insights into the Mechanism of ZnO Formation from Aqueous Solutions of Zinc Acetate and Zinc Nitrate. *Chem. Mater.* **2014**, *26*, 4119−4129.

(541) Muthukumar, M. Theory of Competitive Adsorption-Nucleation in Polypeptide-Mediated Biomineralization. *J. Chem. Phys.* **2009**, *130*, 161101−161105.

(542) Politi, J.; Rea, I.; Dardano, P.; De Stefano, L.; Gioffrè, M. Versatile Synthesis of ZnO Nanowires for Quantitative Optical Sensing of Molecular Biorecognition. *Sens. Actuators, B* **2015**, *220*, 705−711.

(543) Viter, R.; Khranovskyy, V.; Starodub, N.; Ogorodniichuk, Y.; Gevelyuk, S.; Gertnere, Z.; Poletaev, N.; Yakimova, R.; Erts, D.; Smyntyna, V.; et al. Application of Room Temperature Photoluminescence From ZnO Nanorods for Salmonella Detection. *IEEE Sens. J.* **2014**, *14*, 2028−2034.

(544) Zhao, Y.; Deng, P.; Nie, Y.; Wang, P.; Zhang, Y.; Xing, L.; Xue, X. Biomolecule-Adsorption-Dependent Piezoelectric Output of ZnO Nanowire Nanogenerator and its Application as Self-Powered Active Biosensor. *Biosens. Bioelectron.* **2014**, *57*, 269−275.

(545) Wang, Z. L.; Song, J. Piezoelectric Nanogenerators Based on Zinc Oxide Nanowire Arrays. *Science* **2006**, *312*, 242−246.

(546) Xu, S.; Qin, Y.; Xu, C.; Wei, Y.; Yang, R.; Wang, Z. L. Self-Powered Nanowire Devices. *Nat. Nanotechnol.* **2010**, *5*, 366−373.

(547) Reyes, P. I.; Ku, C.; Duan, Z.; Lu, Y.; Solanki, A.; Lee, K. ZnO Thin Film Transistor Immunosensor with High Sensitivity and Selectivity. *Appl. Phys. Lett.* **2011**, *98*, 173702.

(548) Zou, Y.; Huang, Z.; Wang, Y.; Liao, X.; Yin, G.; Gu, J. Synthesis and Cellular Compatibility of Co-Doped ZnO Particles in Silk-Fibroin Peptides. *Colloids Surf., B* **2013**, *102*, 29−36.

(549) Khatri, V.; Halász, K.; Trandafilović, L. V.; Dimitrijević-Branković, S.; Mohanty, P.; Djoković, V.; Csóka, L. ZnO-Modified Cellulose Fiber Sheets for Antibody Immobilization. *Carbohydr. Polym.* **2014**, *109*, 139−147.

(550) Berg, J. M.; Godwin, H. A. Lessons From Zinc-Binding Peptides. *Annu. Rev. Biophys. Biomol. Struct.* **1997**, *26*, 357−371.

(551) Bertini, I. *Biological Inorganic Chemistry: Structure and Reactivity*; University Science Books: VA, 2007.

(552) Dudev, T.; Lim, C. Principles Governing Mg, Ca, and Zn Binding and Selectivity in Proteins. *Chem. Rev.* **2003**, *103*, 773−788.

(553) Limo, M. J.; Perry, C. C. Thermodynamic Study of Interactions Between ZnO and ZnO Binding Peptides Using Isothermal Titration Calorimetry. *Langmuir* **2015**, *31*, 6814−6822.

(554) Freyer, M. W.; Lewis, E. A. Isothermal Titration Calorimetry: Experimental Design, Data Analysis, and Probing Macromolecule/Ligand Binding and Kinetic Interactions. *Methods Cell Biol.* **2008**, *84*, 79−113.

(555) Schmidtchen, F. P. Isothermal Titration Calorimetry in Supramolecular Chemistry. In *Supramolecular Chemistry*; Gale, P. A., Steed, J. W., Eds.; Wiley Online Library, 2012; pp 67−103.

(556) Coppage, R.; Slocik, J. M.; Ramezani-Dakhel, H.; Bedford, N. M.; Heinz, H.; Naik, R. R.; Knecht, M. R. Exploiting Localized Surface Binding Effects to Enhance the Catalytic Reactivity of Peptide-Capped Nanoparticles. *J. Am. Chem. Soc.* **2013**, *135*, 11048−11054.

(557) Sandmann, A.; Kompch, A.; Mackert, V.; Liebscher, C. H.; Winterer, M. Interaction of l-Cysteine with ZnO: Structure, Surface Chemistry, and Optical Properties. *Langmuir* **2015**, *31*, 5701−5711.

(558) Jiang, W.; Yang, K.; Vachet, R. W.; Xing, B. Interaction Between Oxide Nanoparticles and Biomolecules of the Bacterial Cell Envelope as Examined by Infrared Spectroscopy. *Langmuir* **2010**, *26*, 18071−18077.

(559) Bhaumik, A.; Shearin, A.; Delong, R.; Wanekaya, A.; Ghosh, K. Probing the Interaction at the Nano−Bio Interface Using Raman Spectroscopy: ZnO Nanoparticles and Adenosine Triphosphate Biomolecules. *J. Phys. Chem. C* **2014**, *118*, 18631−18639.

(560) Brif, A.; Bloch, L.; Pokroy, B. Bio-Inspired Engineering of a Zinc Oxide/Amino Acid Composite: Synchrotron Microstructure Study. *CrystEngComm* **2014**, *16*, 3268−3273.

(561) Ball, V.; Maechling, C. Isothermal Microcalorimetry to Investigate Non Specific Interactions in Biophysical Chemistry. *Int. J. Mol. Sci.* **2009**, *10*, 3283−3315.

(562) Limo, M. J.; Perry, C. C.; Thyparambil, A.; Wei, Y.; Latour, R. A. Experimental Characterization of Peptide−Surface Interactions. In *Bio-Inspired Nanotechnology*; Knecht, M. R., Walsh, T. R., Eds.; Springer: New York, 2014; pp 37−94.

(563) Lin, W.; Schmidt, J.; Mahler, M.; Schindler, T.; Unruh, T.; Meyer, B.; Peukert, W.; Segets, D. Influence of Tail Groups during Functionalization of ZnO Nanoparticles on Binding Enthalpies and Photoluminescence. *Langmuir* **2017**, *33*, 13581−13589.

(564) Gao, Y.; Traeger, F.; Shekhah, O.; Idriss, H.; Wöll, C. Probing the Interaction of the Amino Acid Alanine with the Surface of ZnO. *J. Colloid Interface Sci.* **2009**, *338*, 16−21.

(565) Shewale, V.; Joshi, P.; Mukhopadhyay, S.; Deshpande, M.; Pandey, R.; Hussain, S.; Karna, S. P. First-Principles Study of Nanoparticle−Biomolecular Interactions: Anchoring of a (ZnO) 12 Cluster on Nucleobases. *J. Phys. Chem. C* **2011**, *115*, 10426−10430.

(566) große Holthaus, S.; Köppen, S.; Frauenheim, T.; Ciacchi, L. C. Molecular Dynamics Simulations of the Amino Acid-ZnO (10−10) Interface: A Comparison Between Density Functional Theory and Density Functional Tight Binding Results. *J. Chem. Phys.* **2014**, *140*, 234707.

(567) Maddahi, P. S.; Shahtahmassebi, N.; Rezaee Roknabadi, M.; Moosavi, F. Site Specific Interaction of Aromatic Amino Acids with ZnO Nanotubes: A Density Functional Approach. *Comput. Theor. Chem.* **2016**, *1086*, 36−44.

(568) Di Felice, R.; Corni, S. Simulation of Peptide−Surface Recognition. *J. Phys. Chem. Lett.* **2011**, *2*, 1510−1519.

(569) Leach, A. R.; Schomburg, D. *Molecular Modelling: Principles and Applications*; Longman: London, 1996.

(570) Pandey, R. B.; Heinz, H.; Feng, J.; Farmer, B. L.; Slocik, J. M.; Drummy, L. F.; Naik, R. R. Adsorption of Peptides (A3, Flg, Pd2, Pd4) on Gold and Palladium Surfaces by a Coarse-Grained Monte Carlo Simulation. *Phys. Chem. Chem. Phys.* **2009**, *11*, 1989−2001.

(571) Sagui, C.; Darden, T. A. Molecular Dynamics Simulations of Biomolecules: Long-Range Electrostatic Effects. *Annu. Rev. Biophys. Biomol. Struct.* **1999**, *28*, 155−179.

(572) Raut, V. P.; Agashe, M. A.; Stuart, S. J.; Latour, R. A. Molecular Dynamics Simulations of Peptide-Surface Interactions. *Langmuir* **2005**, *21*, 1629−1639.

(573) Coppage, R.; Slocik, J. M.; Briggs, B. D.; Frenkel, A. I.; Naik, R. R.; Knecht, M. R. Determining Peptide Sequence Effects That Control the Size, Structure, and Function of Nanoparticles. *ACS Nano* **2012**, *6*, 1625−1636.

(574) Massova, I.; Kollman, P. A. Computational Alanine Scanning to Probe Protein-Protein Interactions: a Novel Approach to Evaluate Binding Free Energies. *J. Am. Chem. Soc.* **1999**, *121*, 8133−8143.

(575) Evans, J. S.; Samudrala, R.; Walsh, T. R.; Oren, E. E.; Tamerler, C. Molecular Design of Inorganic-Binding Polypeptides. *MRS Bull.* **2008**, *33*, 514−518.

(576) Ponder, J. W.; Wu, C.; Ren, P.; Pande, V. S.; Chodera, J. D.; Schnieders, M. J.; Haque, I.; Mobley, D. L.; Lambrecht, D. S.; DiStasio, R. A., Jr Current status of the AMOEBA polarizable force field. *J. Phys. Chem. B* **2010**, *114*, 2549−2564.

(577) Walsh, T. R.; Tomasio, S. d. M. Investigation of the Influence of Surface Defects on Peptide Adsorption Onto Carbon Nanotubes. *Mol. BioSyst.* **2010**, *6*, 1707−1718.

(578) Tang, Z.; Palafox-Hernandez, J. P.; Law, W.; Hughes, Z. E.; Swihart, M. T.; Prasad, P. N.; Knecht, M. R.; Walsh, T. R. Biomolecular Recognition Principles for Bionanocombinatorics: An Integrated Approach To Elucidate Enthalpic and Entropic Factors. *ACS Nano* **2013**, *7*, 9632−9646.

(579) Donaldson, K.; Stone, V.; Clouter, A.; Renwick, L.; MacNee, W. Ultrafine Particles. *Occup. Environ. Med.* **2001**, *58*, 211−216.

(580) Sharma, V.; Shukla, R. K.; Saxena, N.; Parmar, D.; Das, M.; Dhawan, A. DNA Damaging Potential of Zinc Oxide Nanoparticles in Human Epidermal Cells. *Toxicol. Lett.* **2009**, *185*, 211−218.

(581) Kahru, A.; Dubourguier, H. From Ecotoxicology to Nano-ecotoxicology. *Toxicology* **2010**, *269*, 105−119.

(582) Li, L.; Zhou, D.; Peijnenburg, W. J.; van Gestel, C. A.; Jin, S.; Wang, Y.; Wang, P. Toxicity of Zinc Oxide Nanoparticles in the Earthworm, *Eisenia fetida* and Subcellular Fractionation of Zn. *Environ. Int.* **2011**, *37*, 1098−1104.

(583) Xia, T.; Kovochich, M.; Liong, M.; Maedler, L.; Gilbert, B.; Shi, H.; Yeh, J. I.; Zink, J. I.; Nel, A. E. Comparison of the Mechanism of Toxicity of Zinc Oxide and Cerium Oxide Nanoparticles Based on Dissolution and Oxidative Stress Properties. *ACS Nano* **2008**, *2*, 2121−2134.

(584) Michaelis, M.; Fischer, C.; Colombi Ciacchi, L.; Luttge, A. Variability of Zinc Oxide Dissolution Rates. *Environ. Sci. Technol.* **2017**, *51*, 4297−4305.

(585) Ma, H.; Williams, P. L.; Diamond, S. A. Ecotoxicity of Manufactured ZnO Nanoparticles−A Review. *Environ. Pollut.* **2013**, *172*, 76−85.

(586) Song, W.; Zhang, J.; Guo, J.; Zhang, J.; Ding, F.; Li, L.; Sun, Z. Role of the Dissolved Zinc Ion and Reactive Oxygen Species in Cytotoxicity of ZnO Nanoparticles. *Toxicol. Lett.* **2010**, *199*, 389−397.

(587) Li, Q.; Mahendra, S.; Lyon, D. Y.; Brunet, L.; Liga, M. V.; Li, D.; Alvarez, P. J. Antimicrobial Nanomaterials for Water Disinfection and Microbial Control: Potential Applications and Implications. *Water Res.* **2008**, *42*, 4591−4602.

(588) Djurišić, A. B.; Chen, X.; Leung, Y. H.; Man Ching Ng, A. ZnO Nanostructures: Growth, Properties and Applications. *J. Mater. Chem.* **2012**, *22*, 6526−6535.

(589) Zhou, J.; Xu, N. S.; Wang, Z. L. Dissolving Behavior and Stability of ZnO wires in Biofluids: a Study on Biodegradability and Biocompatibility of ZnO Nanostructures. *Adv. Mater.* **2006**, *18*, 2432−2435.

(590) Sun, T. Y.; Gottschalk, F.; Hungerbühler, K.; Nowack, B. Comprehensive Probabilistic Modelling of Environmental Emissions of Engineered Nanomaterials. *Environ. Pollut.* **2014**, *185*, 69−76.

(591) Bondarenko, O.; Juganson, K.; Ivask, A.; Kasemets, K.; Mortimer, M.; Kahru, A. Toxicity of Ag, CuO and ZnO Nanoparticles to Selected Environmentally Relevant Test Organisms and Mammalian Cells In Vitro: a Critical Review. *Arch. Toxicol.* **2013**, *87*, 1181−1200.

(592) Zhou, Y.; Fang, X.; Gong, Y.; Xiao, A.; Xie, Y.; Liu, L.; Cao, Y. The Interactions between ZnO Nanoparticles (NPs) and α-Linolenic Acid (LNA) Complexed to BSA Did Not Influence the Toxicity of ZnO NPs on HepG2 Cells. *Nanomaterials* **2017**, *7*, 91.

(593) Keller, A. A.; Wang, H.; Zhou, D.; Lenihan, H. S.; Cherr, G.; Cardinale, B. J.; Miller, R.; Ji, Z. Stability and Aggregation of Metal Oxide Nanoparticles in Natural Aqueous Matrices. *Environ. Sci. Technol.* **2010**, *44*, 1962−1967.

(594) Müller, K. H.; Kulkarni, J.; Motskin, M.; Goode, A.; Winship, P.; Skepper, J. N.; Ryan, M. P.; Porter, A. E. pH-Dependent Toxicity of High Aspect Ratio ZnO Nanowires in Macrophages due to Intracellular Dissolution. *ACS Nano* **2010**, *4*, 6767−6779.

(595) Merz, T. A.; Doutt, D. R.; Bolton, T.; Dong, Y.; Brillson, L. J. Nanostructure Growth-Induced Defect Formation and Band Bending at ZnO Surfaces. *Surf. Sci.* **2011**, *605*, L20−L23.

(596) Ali, M.; Winterer, M. ZnO Nanocrystals: Surprisingly 'Alive'. *Chem. Mater.* **2010**, *22*, 85−91.

(597) Hendren, C. O.; Lowry, M.; Grieger, K. D.; Money, E. S.; Johnston, J. M.; Wiesner, M. R.; Beaulieu, S. M. Modeling Approaches for Characterizing and Evaluating Environmental Exposure to Engineered Nanomaterials in Support of Risk-Based Decision Making. *Environ. Sci. Technol.* **2013**, *47*, 1190−1205.

(598) Gottschalk, F.; Sun, T.; Nowack, B. Environmental Concentrations of Engineered Nanomaterials: Review of Modeling and Analytical Studies. *Environ. Pollut.* **2013**, *181*, 287−300.

(599) Wilson, M. R.; Lightbody, J. H.; Donaldson, K.; Sales, J.; Stone, V. Interactions Between Ultrafine Particles and Transition Metals *in vivo* and *in vitro*. *Toxicol. Appl. Pharmacol.* **2002**, *184*, 172−179.

(600) Heinlaan, M.; Ivask, A.; Blinova, I.; Dubourguier, H.; Kahru, A. Toxicity of Nanosized and Bulk ZnO, CuO and TiO$_2$ to Bacteria *Vibrio fischeri* and Crustaceans *Daphnia magna* and *Thamnocephalus platyurus*. *Chemosphere* **2008**, *71*, 1308−1316.

(601) Binder, J. F.; Broqvist, P.; Komsa, H.; Pasquarello, A. Germanium Core-Level Shifts at Ge/GeO$_2$ Interfaces Through Hybrid Functionals. *Phys. Rev. B: Condens. Matter Mater. Phys.* **2012**, *85*, 245305−245305.

(602) Sze, S. M. *Physics of Semiconductor Devices*; Wiley: New York, 1998.

(603) Robertson, J.; Wallace, R. M. High-K Materials and Metal Gates for CMOS Applications. *Mater. Sci. Eng., R* **2015**, *88*, 1−41.

(604) Hidalgo, P.; Liberti, E.; Rodríguez-Lazcano, Y.; Méndez, B.; Piqueras, J. GeO$_2$ Nanowires Doped with Optically Active Ions. *J. Phys. Chem. C* **2009**, *113*, 17200−17205.

(605) Simanzhenkov, V.; Wiggers, H.; Roth, P. Properties of Flame Synthesized Germanium Oxide Nanoparticles. *J. Nanosci. Nanotechnol.* **2005**, *5*, 436−41.

(606) Lin, Q.; Bu, X.; Mao, C.; Zhao, X.; Sasan, K.; Feng, P. Mimicking High-Silica Zeolites: Highly Stable Germanium- and Tin-Rich Zeolite-Type Chalcogenides. *J. Am. Chem. Soc.* **2015**, *137*, 6184−6187.

(607) Chen, G.; Chen, B.; Liu, T.; Mei, Y.; Ren, H.; Bi, Y.; Luo, X.; Zhang, L. The Synthesis and Characterization of Germanium Oxide Aerogel. *J. Non-Cryst. Solids* **2012**, *358*, 3322−3326.

(608) Walker, B.; Dharmawardhana, C. C.; Dari, N.; Rulis, P.; Ching, W. Electronic Structure and Optical Properties of Amorphous GeO$_2$ in Comparison to Amorphous SiO$_2$. *J. Non-Cryst. Solids* **2015**, *428*, 176−183.

(609) Maurer, R. D.; Schultz, P. C. U.S. Patent US3884550 A, 1975.

(610) Dianov, E. M.; Mashinsky, V. M. Germania-Based Core Optical Fibers. *J. Lightwave Technol.* **2005**, *23*, 3500−3508.

(611) Costacurta, S.; Malfatti, L.; Kidchob, T.; Takahashi, M.; Mattei, G.; Bello, V.; Maurizio, C.; Innocenzi, P. Self-Assembled Mesoporous Silica-Germania Films. *Chem. Mater.* **2008**, *20*, 3259−3265.

(612) Vaughn, D. D., II; Schaak, R. E. Synthesis, Properties and Applications of Colloidal Germanium and Germanium-Based Nanomaterials. *Chem. Soc. Rev.* **2013**, *42*, 2861−2879.

(613) Froelich, P. N.; Hambrick, G. A.; Andreae, M. O.; Mortlock, R. A.; Edmond, J. M. The Geochemistry of Inorganic Germanium in Natural Waters. *J. Geophys. Res.* **1985**, *90*, 1133−1133.

(614) Simpson, T. L.; Gil, M.; Connes, R.; Diaz, J.; Paris, J. Effects of Germanium (Ge) on the Silica Spicules of the Marine Sponge *Suberites domuncula*: Transformation of Spicule Type. *J. Morphol.* **1985**, *183*, 117−128.

(615) Azam, F.; Hemmingsen, B. B.; Volcani, B. E. Germanium Incorporation into the Silica of Diatom Cell Walls. *Arch. Microbiol.* **1973**, *92*, 11−20.

(616) Micoulaut, M.; Cormier, L.; Henderson, G. S. The Structure of Amorphous, Crystalline and Liquid GeO₂. *J. Phys.: Condens. Matter* **2006**, *18*, 753−784.

(617) Laubengayer, A. W.; Morton, D. S. Germanium. XXXIX. The Polymorphism of Germanium Dioxide. *J. Am. Chem. Soc.* **1932**, *54*, 2303−2320.

(618) Murthy, M. K.; Hill, H. Studies in Germanium Oxide Systems: III, Solubility of Germania in Water. *J. Am. Ceram. Soc.* **1965**, *48*, 109−110.

(619) Deringer, V. L.; Dronskowski, R. Pauling's Third Rule Beyond the Bulk: Chemical Bonding at Quartz-Type GeO₂ Surfaces. *Chem. Sci.* **2014**, *5*, 894−894.

(620) Jing, C.; Hou, J.; Zhang, Y. Morphology Controls of GeO₂ Particles Precipitated by a Facile Acid-Induced Decomposition of Germanate Ions in Aqueous Medium. *J. Cryst. Growth* **2008**, *310*, 391−396.

(621) Boix, E.; Puddu, V.; Perry, C. C. Preparation of Hexagonal GeO₂ Particles With Particle Size and Crystallinity Controlled by Peptides, Silk and Silk-Peptide Chimeras. *Dalton Trans* **2014**, *43*, 16902−16910.

(622) Winn, D.; Doherty, M. F. Modeling Crystal Shapes of Organic Materials Grown From Solution. *AIChE J.* **2000**, *46*, 1348−1367.

(623) Wu, H. P.; Liu, J. F.; Ge, M. Y.; Niu, L.; Zeng, Y. W.; Wang, Y. W.; Lv, G. L.; Wang, L. N.; Zhang, G. Q.; Jiang, J. Z. Preparation of Monodisperse GeO₂ Nanocubes in a Reverse Micelle System. *Chem. Mater.* **2006**, *18*, 1817−1820.

(624) Kim, I.; Li, H.; Shin, N. H.; Ha, C.; Suh, H.; Batt, C. A. Diacetylene Phospholipid-Mediated Synthesis of Germania Nano-tubules and Nanoparticles. *Chem. Mater.* **2009**, *21*, 3782−3787.

(625) Stanic, V.; Pierre, A. C.; Etsell, T. H.; Mikula, R. J. Chemical Kinetics Study of the Sol-Gel Processing of GeS₂. *J. Phys. Chem. A* **2001**, *105*, 6136−6143.

(626) Cai, Q.; Xu, B.; Ye, L.; Tang, T.; Huang, S.; Du, X.; Bian, X.; Zhang, J.; Di, Z.; Jin, Q.; et al. Stable Functionalization of Germanium Surface and its Application in Biomolecules Immobilization. *Appl. Surf. Sci.* **2014**, *316*, 46−53.

(627) Zhong, N.; Zhu, X.; Liao, Q.; Wang, Y.; Chen, R. GeO₂-SiO₂-Chitosan-Medium-Coated Hollow Optical Fiber for Cell Immobiliza-tion. *Opt. Lett.* **2013**, *38*, 3115−8.

(628) Adachi, T.; Sakka, S. The Role of N,N-dimethylformamide, a DCCA, in the Formation of Silica Gel Monoliths by Sol-Gel Method. *J. Non-Cryst. Solids* **1988**, *99*, 118−128.

(629) Chauhan, N. P. S.; Gholipourmalekabadi, M.; Mozafari, M. Fabrication of Newly Developed Pectin − GeO₂ Nanocomposite Using Extreme Biomimetics Route and its Antibacterial Activities. *J. Macromol. Sci., Part A: Pure Appl.Chem.* **2017**, *54*, 655−661.

(630) Liao, Q.; Zhong, N.; Zhu, X.; Chen, R. High-Performance Biofilm Photobioreactor Based on a GeO₂−SiO₂−Chitosan-Medium-Coated Hollow Optical Fiber. *Int. J. Hydrogen Energy* **2014**, *39*, 10016−10027.

(631) Yi, W.; Xiong, D.; Zhang, W.; Su, H.; Liu, Q.; Gu, J.; Zhu, S.; Zhang, D. Bio-Templated Germanium Photonic Crystals by a Facile Liquid Phase Deposition Process. *RSC Adv.* **2016**, *6*, 73156−73159.

(632) Brahmi, Y.; Katir, N.; Castel, A.; El Kadib, A. Transformable Mesoporous Organo-Germano-Silicas. *Microporous Mesoporous Mater.* **2013**, *177*, 75−81.

(633) Sah, V. R.; Baier, R. E. Bacteria Inside Semiconductors as Potential Sensor Elements: Biochip Progress. *Sensors* **2014**, *14*, 11225−44.

(634) Dickerson, M. B.; Naik, R. R.; Stone, M. O.; Cai, Y.; Sandhage, K. H. Identification of Peptides That Promote the Rapid Precipitation of Germania Nanoparticle Networks *via* Use of a Peptide Display Library. *Chem. Commun.* **2004**, *0*, 1776.

(635) Banerjee, I. A.; Regan, M. R. Preparation of Gold Nanoparticle Templated Germania Nanoshells. *Mater. Lett.* **2006**, *60*, 915−918.

(636) Regan, M. R.; Banerjee, I. A. In Situ Growth of CoPt Nanoparticles in Porous Germania Nanospheres. *Mater. Lett.* **2007**, *61*, 71−75.

(637) Regan, M. R.; Banerjee, I. A. Immobilization of Invertase in Germania Matrix and a Study of its Enzymatic Activity. *J. Sol-Gel Sci. Technol.* **2007**, *43*, 27−33.

(638) Carter, C. J.; Ackerson, C. J.; Feldheim, D. L. Unusual Reactivity of a Silver Mineralizing Peptide. *ACS Nano* **2010**, *4*, 3883−8.

(639) Wang, H.; Tao, Y.; Zhang, G. Q.; Xia, Y. P.; Gong, F. H.; Wu, H. P.; Tao, G. L. Germanium Dioxide Nanocubes with Different Size Distributions and Its Gibbs Free Energy Theory. *Mater. Sci. Forum* **2011**, *688*, 135−140.

(640) Bujnowski, A. M.; Pitt, W. G. Water Structure Around Enkephalin Near a GeO₂ Surface: A Molecular Dynamics Study. *J. Biomater. Sci., Polym. Ed.* **2002**, *13*, 885−906.

(641) Chiu, S.; Lee, M.; Chen, H.; Chou, W.; Lin, L. Germanium Oxide Inhibits the Transition From G2 to M Phase of CHO Cells. *Chem.-Biol. Interact.* **2002**, *141*, 211−228.

(642) Horinek, D.; Serr, A.; Geisler, M.; Pirzer, T.; Slotta, U.; Lud, S. Q.; Garrido, J. A.; Scheibel, T.; Hugel, T.; Netz, R. R. Peptide Adsorption on a Hydrophobic Surface Results From an Interplay of Solvation, Surface, and Intrapeptide forces. *Proc. Natl. Acad. Sci. U. S. A.* **2008**, *105*, 2842−2847.

(643) Cole, M. A.; Voelcker, N. H.; Thissen, H.; Griesser, H. J. Stimuli-Responsive Interfaces and Systems for the Control of Protein-Surface and Cell-Surface Interactions. *Biomaterials* **2009**, *30*, 1827−1850.

(644) Köppen, S.; Langel, W. Simulation of Adhesion Forces and Energies of Peptides on Titanium Dioxide Surfaces. *Langmuir* **2010**, *26*, 15248−15256.

(645) Hildebrand, N.; Köppen, S.; Derr, L.; Li, K.; Koleini, M.; Rezwan, K.; Colombi Ciacchi, L. Adsorption Orientation and Binding Motifs of Lysozyme and Chymotrypsin on Amorphous Silica. *J. Phys. Chem. C* **2015**, *119*, 7295−7307.

(646) Kitadai, N.; Yokoyama, T.; Nakashima, S. ATR-IR Spectroscopic Study of L-lysine Adsorption on Amorphous Silica. *J. Colloid Interface Sci.* **2009**, *329*, 31−37.

(647) Maste, M. C.; Norde, W.; Visser, A. J. Adsorption-Induced Conformational Changes in the Serine Proteinase Savinase: a Tryptophan Fluorescence and Circular Dichroism Study. *J. Colloid Interface Sci.* **1997**, *196*, 224−230.

(648) Sekar, R.; Periasamy, A. Fluorescence Resonance Energy Transfer (FRET) Microscopy Imaging of Live Cell Protein Local-izations. *J. Cell Biol.* **2003**, *160*, 629−633.

(649) Durupthy, O.; Jeurgens, L. P. H.; Bill, J. Biomimetic Formation of Titania Thin Films: Effect of Amino Acids on the Deposition Process. *ACS Appl. Mater. Interfaces* **2011**, *3*, 1624−1632.

(650) Zhu, G.; Zhu, X.; Fan, Q.; Wan, X. Raman Spectra of Amino Acids and Their Aqueous Solutions. *Spectrochim. Acta, Part A* **2011**, *78*, 1187−1195.

(651) Yagola, A. G.; Kochikov, I. V.; Kuramshina, G. M. *Inverse Problems of Vibrational Spectroscopy*; VSP BV: Zeist, The Neverlands, 1999.

(652) Vankeirsbilck, T.; Vercauteren, A.; Baeyens, W.; Van der Weken, G.; Verpoort, F.; Vergote, G.; Remon, J. P. Applications of Raman Spectroscopy in Pharmaceutical Analysis. *TrAC, Trends Anal. Chem.* **2002**, *21*, 869−877.

(653) Bumbrah, G. S.; Sharma, R. M. Raman spectroscopy − Basic Principle, Instrumentation and Selected Applications for the Characterization of Drugs of Abuse. *Egyptian Journal of Forensic Sciences* **2016**, *6*, 209−215.

(654) Sela, M. N.; Badihi, L.; Rosen, G.; Steinberg, D.; Kohavi, D. Adsorption of Human Plasma Proteins to Modified Titanium Surfaces. *Clin. Oral Implants Res.* **2007**, *18*, 630−638.

(655) Martin, J.; Schwartz, Z.; Hummert, T.; Schraub, D.; Simpson, J.; Lankford, J.; Dean, D.; Cochran, D.; Boyan, B. Effect of Titanium Surface-Roughness on Proliferation, Differentiation, and Protein-

Synthesis of Human Osteoblast-Like Cells (Mg63). *J. Biomed. Mater. Res.* **1995**, *29*, 389−401.

(656) Kopac, T.; Bozgeyik, K. Effect of Surface Area Enhancement on the Adsorption of Bovine Serum Albumin onto Titanium Dioxide. *Colloids Surf., B* **2010**, *76*, 265−271.

(657) Maste, M. C. L.; Pap, E. H. W.; van Hoek, A.; Norde, W.; Visser, A. J. W. G. Spectroscopic Investigation of the Structure of a Protein Adsorbed on a Hydrophobic Latex. *J. Colloid Interface Sci.* **1996**, *180*, 632−633.

(658) Zhu, R.; Wang, W.; Sun, X.; Liu, H.; Wang, S. Enzyme Activity Inhibition and Secondary Structure Disruption of Nano-TiO$_2$ on Pepsin. *Toxicol. In Vitro* **2010**, *24*, 1639−1647.

(659) Xu, Z.; Liu, X.; Ma, Y.; Gao, H. Interaction of Nano-TiO2 With Lysozyme: Insights Into the Enzyme Toxicity of Nanosized Particles. *Environ. Sci. Pollut. Res.* **2010**, *17*, 798−806.

(660) Zhao, A. S.; Zhou, S.; Wang, Y.; Chen, J.; Ye, C. R.; Huang, N. Molecular Interaction of Fibrinogen With Thermally Modified Titanium Dioxide Nanoparticles. *RSC Adv.* **2014**, *4*, 40428−40434.

(661) Dolatshahi-Pirouz, A.; Rechendorff, K.; Hovgaard, M. B.; Foss, M.; Chevallier, J.; Besenbacher, F. Bovine Serum Albumin Adsorption on Nano-Rough Platinum Surfaces Studied by QCM-D. *Colloids Surf., B* **2008**, *66*, 53−59.

(662) Rodahl, M.; Höök, F.; Fredriksson, C.; Keller, C. A.; Krozer, A.; Brzezinski, P.; Voinova, M.; Kasemo, B. Simultaneous Frequency and Dissipation Factor QCM Measurements of Biomolecular Adsorption and Cell Adhesion. *Faraday Discuss.* **1997**, *107*, 229−46.

(663) Wei, Y.; Thyparambil, A. A.; Latour, R. A. Peptide−Surface Adsorption Free Energy Comparing Solution Conditions Ranging from Low to Medium Salt Concentrations. *ChemPhysChem* **2012**, *13*, 3782−3785.

(664) Allen, S.; Davies, M. C.; Roberts, C. J.; Tendler, S. J. B.; Williams, P. M. Atomic Force Microscopy in Analytical Biotechnology. *Trends Biotechnol.* **1997**, *15*, 101−105.

(665) Li, Q.; Zhang, T.; Pan, Y.; Ciacchi, L. C.; Xu, B.; Wei, G. AFM-Based Force Spectroscopy For Bioimaging and Biosensing. *RSC Adv.* **2016**, *6*, 12893−12912.

(666) Müller, D. J.; Dufrene, Y. F. Atomic Force Microscopy as a Multifunctional Molecular Toolbox in Nanobiotechnology. *Nat. Nanotechnol.* **2008**, *3*, 261−269.

(667) Allen, S.; Davies, J.; Davies, M. C.; Dawkes, A. C.; Roberts, C. J.; Tendler, S. J. B.; Williams, P. M. The Influence of Epitope Availability on Atomic-Force Microscope Studies of Antigen−Antibody Interactions. *Biochem. J.* **1999**, *341*, 173.

(668) Alsteens, D.; Pfreundschuh, M.; Zhang, C.; Spoerri, P. M.; Coughlin, S. R.; Kobilka, B. K.; Mueller, D. J. Imaging G Protein-Coupled Receptors While Quantifying Their Ligand-Binding Free-Energy Landscape. *Nat. Methods* **2015**, *12*, 845.

(669) Noy, A.; Friddle, R. W. Practical Single Molecule Force Spectroscopy: How To Determine Fundamental Thermodynamic Parameters of Intermolecular Bonds with an Atomic Force Microscope. *Methods* **2013**, *60*, 142−150.

(670) Friddle, R. W.; Noy, A.; De Yoreo, J. J. Interpreting the Widespread Nonlinear Force Spectra of Intermolecular Bonds. *Proc. Natl. Acad. Sci. U. S. A.* **2012**, *109*, 13573−13578.

(671) Meissner, R. H.; Wei, G.; Ciacchi, L. C. Estimation of the Free Energy of Adsorption of a Polypeptide on Amorphous SiO$_2$ From Molecular Dynamics Simulations and Force Spectroscopy Experiments. *Soft Matter* **2015**, *11*, 6254−6265.

(672) Razvag, Y.; Gutkin, V.; Reches, M. Probing the Interaction of Individual Amino Acids with Inorganic Surfaces Using Atomic Force Spectroscopy. *Langmuir* **2013**, *29*, 10102−10109.

(673) Li, Q.; Michaelis, M.; Wei, G.; Colombi Ciacchi, L. A Novel Aptasensor Based on Single-Molecule Force Spectroscopy For Highly Sensitive Detection of Mercury Ions. *Analyst* **2015**, *140*, 5243−5250.

(674) Cedervall, T.; Lynch, I.; Lindman, S.; Berggård, T.; Thulin, E.; Nilsson, H.; Dawson, K. A.; Linse, S. Understanding the Nanoparticle−Protein Corona Using Methods To Quantify Exchange Rates and Affinities of Proteins for Nanoparticles. *Proc. Natl. Acad. Sci. U. S. A.* **2007**, *104*, 2050−2055.

(675) Lindman, S.; Lynch, I.; Thulin, E.; Nilsson, H.; Dawson, K. A.; Linse, S. Systematic Investigation of the Thermodynamics of HSA Adsorption to N-Iso-Propylacrylamide/N-Tert-Butylacrylamide Copolymer Nanoparticles. Effects of Particle Size and Hydrophobicity. *Nano Lett.* **2007**, *7*, 914−920.

(676) Lynch, I.; Dawson, K. A. Protein-Nanoparticle Interactions. *Nano Today* **2008**, *3*, 40−47.

(677) Kettiger, H.; Québatte, G.; Perrone, B.; Huwyler, J. Interactions Between Silica Nanoparticles and Phospholipid Membranes. *Biochim. Biophys. Acta, Biomembr.* **2016**, *1858*, 2163−2170.

(678) Ababou, A.; Ladbury, J. E. Survey of the Year 2004: Literature on Applications of Isothermal Titration Calorimetry. *J. Mol. Recognit.* **2006**, *19*, 79−89.

(679) Chiad, K.; Stelzig, S. H.; Gropeanu, R.; Weil, T.; Klapper, M.; Mullen, K. Isothermal Titration Calorimetry: A Powerful Technique To Quantify Interactions in Polymer Hybrid Systems. *Macromolecules* **2009**, *42*, 7545−7552.

(680) Cliff, M. J.; Gutierrez, A.; Ladbury, J. E. A Survey of the Year 2003 Literature on Applications of Isothermal Titration Calorimetry. *J. Mol. Recognit.* **2004**, *17*, 513−523.

(681) Goobes, R.; Goobes, G.; Campbell, C. T.; Stayton, P. S. Thermodynamics of Statherin Adsorption onto Hydroxyapatite. *Biochemistry* **2006**, *45*, 5576−5586.

(682) Goobes, G.; Goobes, G.; Shaw, W. J.; Gibson, J. M.; Long, J. R.; Raghunathan, V.; Schueler-Furman, O.; Popham, J. M.; Baker, D.; Campbell, C. T.; et al. The structure, Dynamics, and Energetics of Protein Adsorption—Lessons Learned From Adsorption of Statherin to Hydroxyapatite. *Magn. Reson. Chem.* **2007**, *45*, S32−S47.

(683) Sprenger, K. G.; Pfaendtner, J. Strong Electrostatic Interactions Lead to Entropically Favorable Binding of Peptides to Charged Surfaces. *Langmuir* **2016**, *32*, 5690−5701.

(684) Gong, V.; França, R. Nanoscale Chemical Surface Characterization of Four Different Types of Dental Pulp-Capping Materials. *J. Dent.* **2017**, *58*, 11−18.

(685) Chittur, K. K. FTIR/ATR for Protein Adsorption to Biomaterial Surfaces. *Biomaterials* **1998**, *19*, 357−369.

(686) Grotzinger, J. P. Analysis of Surface Materials by the Curiosity Mars Rover. *Science* **2013**, *341*, 1475.

(687) Bruckman, V. J.; Wriessnig, K. Improved Soil Carbonate Determination by FT-IR and X-ray Analysis. *Environ. Chem. Lett.* **2013**, *11*, 65−70.

(688) Smith, B. C. *Fundamentals of Fourier Transform Infrared Spectroscopy*; CRC Press: New York, 1996.

(689) Whyburn, G. P.; Li, Y. J.; Huang, Y. Protein and Protein Assembly Based Material Structures. *J. Mater. Chem.* **2008**, *18*, 3755−3762.

(690) Naik, R. R.; Jones, S. E.; Murray, C. J.; McAuliffe, J. C.; Vaia, R. A.; Stone, M. O. Peptide Templates for Nanoparticle Synthesis Derived from Polymerase Chain Reaction-Driven Phage Display. *Adv. Funct. Mater.* **2004**, *14*, 25−30.

(691) Vodnik, M.; Zager, U.; Strukelj, B.; Lunder, M. Phage Display: Selecting Straws Instead of a Needle From a Haystack. *Molecules* **2011**, *16*, 790−817.

(692) Oren, E. E.; Tamerler, C.; Sarikaya, M. Metal Recognition of Septapeptides via Polypod Molecular Architecture. *Nano Lett.* **2005**, *5*, 415−419.

(693) Bedford, N. M.; Ramezani-Dakhel, H.; Slocik, J. M.; Briggs, B. D.; Ren, Y.; Frenkel, A. I.; Petkov, V.; Heinz, H.; Naik, R. R.; Knecht, M. R. Elucidation of Peptide-Directed Palladium Surface Structure for Biologically Tunable Nanocatalysts. *ACS Nano* **2015**, *9*, 5082−5092.

(694) Preedia Babu, E.; Subastri, A.; Suyavaran, A.; Lokeshwara Rao, P.; Suresh Kumar, M.; Jeevaratnam, K.; Thirunavukkarasu, C. Extracellularly Synthesized ZnO Nanoparticles Interact With DNA and Augment Gamma Radiation Induced DNA Damage Through Reactive Oxygen Species. *RSC Adv.* **2015**, *5*, 62067−62077.

(695) Wahab, R.; Kim, Y.; Hwang, I. H.; Shin, H. A Non-Aqueous Synthesis, Characterization of Zinc Oxide Nanoparticles and Their Interaction With DNA. *Synth. Met.* **2009**, *159*, 2443−2452.

(696) Litrán, R.; Blanco, E.; Ramírez-del-Solar, M. Aggregation Effects in Non-Linear Absorption of CuPc-SiO2 Sono-Xerogels. *J. Non-Cryst. Solids* **2004**, *333*, 327−332.

(697) Cheng, K.; Hong, Y.; Yu, M.; Lin, J.; Weng, W.; Wang, H. Modulation of Protein Behavior Through Light Responses of TiO2 Nanodots Films. *Sci. Rep.* **2015**, *5*, 13354.

(698) Oh, S.; Moon, K. S.; Lee, S. H. Effect of RGD Peptide-Coated TiO2 Nanotubes on the Attachment, Proliferation, and Functionality of Bone-Related Cells. *J. Nanomater.* **2013**, *2013*, 965864.

(699) Di Foggia, M.; Taddei, P.; Torreggiani, A.; Dettin, M.; Tinti, A. Interactions Between Oligopeptides and Oxidised Titanium Surfaces Detected by Vibrational Spectroscopy. *J. Raman Spectrosc.* **2011**, *42*, 276−285.

(700) Ahmed, M. H.; Byrne, J. A.; Keyes, T. E. Investigation of the Inhibitory Effects of TiO2 on the β-Amyloid Peptide Aggregation. *Mater. Sci. Eng., C* **2014**, *39*, 227−234.

(701) Marucco, A.; Fenoglio, I.; Turci, F.; Fubini, B. Interaction of Fibrinogen and Albumin With Titanium Dioxide Nanoparticles of Different Crystalline Phases. *J. Phys.: Conf. Ser.* **2013**, *429*, 012014.

(702) Dalai, S.; Pakrashi, S.; Chakravarty, S.; Hussain, S.; Chandrasekaran, N.; Mukherjee, A. Studies on Interfacial Interactions of TiO2 Nanoparticles With Bacterial Cells Under Light and Dark Conditions. *Bull. Mater. Sci.* **2014**, *37*, 371−381.

(703) York, R. L.; Mermut, O.; Phillips, D. C.; McCrea, K. R.; Ward, R. S.; Somorjai, G. A. Influence of Ionic Strength on the Adsorption of a Model Peptide on Hydrophilic Silica and Hydrophobic Polystyrene Surfaces: Insight From SFG Vibrational Spectroscopy. *J. Phys. Chem. C* **2007**, *111*, 8866−8871.

(704) Vertegel, A. A.; Siegel, R. W.; Dordick, J. S. Silica Nanoparticle Size Influences the Structure and Enzymatic Activity of Adsorbed Lysozyme. *Langmuir* **2004**, *20*, 6800−6807.

(705) Lundqvist, M.; Sethson, I.; Jonsson, B. Protein Adsorption Onto Silica Nanoparticles: Conformational Changes Depend on the Particles' Curvature and the Protein Stability. *Langmuir* **2004**, *20*, 10639−10647.

(706) Raghava, S.; Singh, P. K.; Ranga Rao, A.; Dutta, V.; Gupta, M. N. Nanoparticles of Unmodified Titanium Dioxide Facilitate Protein Refolding. *J. Mater. Chem.* **2009**, *19*, 2830−2834.

(707) Momeni, L.; Shareghi, B.; Saboury, A. A.; Evini, M. Interaction of TiO2 Nanoparticle With Trypsin Analyzed by Kinetic and Spectroscopic Methods. *Monatsh. Chem.* **2017**, *148*, 199−207.

(708) Eren, N. M.; Narsimhan, G.; Campanella, O. H. Protein Adsorption Induced Bridging Flocculation: The Dominant Entropic Pathway For Nano-Bio Complexation. *Nanoscale* **2016**, *8*, 3326−3336.

(709) Belay, A.; Kim, H. K.; Hwang, Y. Probing the Interaction of Caffeic Acid With ZnO Nanoparticles. *Luminescence* **2016**, *31*, 654−659.

(710) Allouni, Z. E.; Cimpan, M. R.; Høl, P. J.; Skodvin, T.; Gjerdet, N. R. Agglomeration and Sedimentation of TiO2 Nanoparticles in Cell Culture Medium. *Colloids Surf., B* **2009**, *68*, 83−87.

(711) Matsuyama, K.; Ihsan, N.; Irie, K.; Mishima, K.; Okuyama, T.; Muto, H. Bioimaging Application of Highly Luminescent Silica-Coated ZnO-Nanoparticle Quantum Dots with Biotin. *J. Colloid Interface Sci.* **2013**, *399*, 19−25.

(712) Estupiñán, D.; Bannwarth, M. B.; Mylon, S. E.; Landfester, K.; Muñoz-Espí, R.; Crespy, D. Multifunctional Clickable and Protein-Repellent Magnetic Silica Nanoparticles. *Nanoscale* **2016**, *8*, 3019−3030.

(713) Vergaro, V.; Carlucci, C.; Cascione, M.; Lorusso, C.; Conciauro, F.; Scremin, B. F.; Congedo, P. M.; Cannazza, G.; Citti, C.; Ciccarella, G. Interaction Between Human Serum Albumin and Different Anatase TiO2 Nanoparticles: A Nano-Bio Interface Study. *Nanomater. Nanotechnol.* **2015**, *5*, 30.

(714) Joshi, S.; Ghosh, I.; Pokhrel, S.; Maedler, L.; Nau, W. M. Interactions of Amino Acids and Polypeptides with Metal Oxide Nanoparticles Probed by Fluorescent Indicator Adsorption and Displacement. *ACS Nano* **2012**, *6*, 5668−5679.

(715) Arakha, M.; Saleem, M.; Mallick, B. C.; Jha, S. The Effects of Interfacial Potential on Antimicrobial Propensity of ZnO Nanoparticle. *Sci. Rep.* **2015**, *5*, 9578.

(716) Shahabi, S.; Döscher, S.; Bollhorst, T.; Treccani, L.; Maas, M.; Dringen, R.; Rezwan, K. Enhancing Cellular Uptake and Doxorubicin Delivery of Mesoporous Silica Nanoparticles Via Surface Functionalization: Effects of Serum. *ACS Appl. Mater. Interfaces* **2015**, *7*, 26880−26891.

(717) Lesniak, A.; Fenaroli, F.; Monopoli, M. P.; Åberg, C.; Dawson, K. A.; Salvati, A. Effects of the Presence or Absence of a Protein Corona on Silica Nanoparticle Uptake and Impact on Cells. *ACS Nano* **2012**, *6*, 5845−5857.

(718) Zhao, Y.; Sun, X.; Zhang, G.; Trewyn, B. G.; Slowing, I. I.; Lin, V. S. Interaction of Mesoporous Silica Nanoparticles With Human Red Blood Cell Membranes: Size and Surface Effects. *ACS Nano* **2011**, *5*, 1366−1375.

(719) Chen, C.; Liu, Y.; Wu, C.; Yeh, C.; Su, M.; Wu, Y. Preparation of Fluorescent Silica Nanotubes and their Application in Gene Delivery. *Adv. Mater.* **2005**, *17*, 404−407.

(720) Haran, G. Single-Molecule Fluorescence Spectroscopy of Biomolecular Folding. *J. Phys.: Condens. Matter* **2003**, *15*, R1291.

(721) Karlsson, M.; Carlsson, U. Protein Adsorption Orientation in the Light of Fluorescent Probes: Mapping of the Interaction Between Site-Directly Labeled Human Carbonic Anhydrase II and Silica Nanoparticles. *Biophys. J.* **2005**, *88*, 3536−3544.

(722) Eriksson, A. I. K.; Edwards, K.; Agmo Hernández, V. Cooperative Adsorption Behavior of Phosphopeptides on TiO2 Leads to Biased Enrichment, Detection and Quantification. *Analyst* **2015**, *140*, 303−312.

(723) Killian, M. S.; Krebs, H. M.; Schmuki, P. Protein Denaturation Detected by Time-of-Flight Secondary Ion Mass Spectrometry. *Langmuir* **2011**, *27*, 7510−7515.

(724) Deng, Z. J.; Mortimer, G.; Schiller, T.; Musumeci, A.; Martin, D.; Minchin, R. F. Differential Plasma Protein Binding to Metal Oxide Nanoparticles. *Nanotechnology* **2009**, *20*, 455101.

(725) Ruh, H.; Kuehl, B.; Brenner-Weiss, G.; Hopf, C.; Diabate, S.; Weiss, C. Identification of Serum Proteins Bound to Industrial Nanomaterials. *Toxicol. Lett.* **2012**, *208*, 41−50.

(726) Kim, Y.; Shon, H. K.; Shin, S. K.; Lee, T. G. Probing Nanoparticles and Nanoparticle-Conjugated Biomolecules using Time-Of-Flight Secondary Ion Mass Spectrometry. *Mass Spectrom. Rev.* **2015**, *34*, 237−247.

(727) Guo, C.; Holland, G. P. Investigating Lysine Adsorption on Fumed Silica Nanoparticles. *J. Phys. Chem. C* **2014**, *118*, 25792−25801.

(728) Nosaka, Y.; Nishikawa, M.; Nosaka, A. Y. Spectroscopic Investigation of the Mechanism of Photocatalysis. *Molecules* **2014**, *19*, 18248−18267.

(729) Payet, V.; Dini, T.; Brunner, S.; Galtayries, A.; Frateur, I.; Marcus, P. Pre-Treatment of Titanium Surfaces by Fibronectin: In Situ Adsorption and Effect of Concentration. *Surf. Interface Anal.* **2010**, *42*, 457−461.

(730) Pegueroles, M.; Tonda-Turo, C.; Planell, J. A.; Gil, F.; Aparicio, C. Adsorption of Fibronectin, Fibrinogen, and Albumin on TiO2: Time-Resolved Kinetics, Structural Changes, and Competition Study. *Biointerphases* **2012**, *7*, 48.

(731) Chang, C.; Chiu, N.; Lin, D. S.; Chu-Su, Y.; Liang, Y.; Lin, C. High-Sensitivity Detection of Carbohydrate Antigen 15−3 Using a Gold/Zinc Oxide Thin Film Surface Plasmon Resonance-Based Biosensor. *Anal. Chem.* **2010**, *82*, 1207−1212.

(732) Micksch, T.; Liebelt, N.; Scharnweber, D.; Schwenzer, B. Investigation of the Peptide Adsorption on ZrO2, TiZr, and TiO2 Surfaces as a Method for Surface Modification. *ACS Appl. Mater. Interfaces* **2014**, *6*, 7408−7416.

(733) Micksch, T.; Herrmann, E.; Scharnweber, D.; Schwenzer, B. A Modular Peptide-Based Immobilization System for ZrO2, TiZr and TiO2 Surfaces. *Acta Biomater.* **2015**, *12*, 290−297.

(734) Nishida, H.; Kajisa, T.; Miyazawa, Y.; Tabuse, Y.; Yoda, T.; Takeyama, H.; Kambara, H.; Sakata, T. Self-Oriented Immobilization

of DNA Polymerase Tagged by Titanium-Binding Peptide Motif. *Langmuir* **2015**, *31*, 732−740.

(735) Byun, K. M.; Kim, N.; Ko, Y. H.; Yu, J. S. Enhanced Surface Plasmon Resonance Detection of DNA Hybridization Based on ZnO Nanorod Arrays. *Sens. Actuators, B* **2011**, *155*, 375−379.

(736) Wang, L.; Sun, Y.; Wang, J.; Wang, J.; Yu, A.; Zhang, H.; Song, D. Water-Soluble ZnO-Au Nanocomposite-Based Probe For Enhanced Protein Detection in a SPR Biosensor System. *J. Colloid Interface Sci.* **2010**, *351*, 392−397.

(737) Brott, L. L.; Naik, R. R.; Pikas, D. J.; Kirkpatrick, S. M.; Tomlin, D. W.; Whitlock, P. W.; Clarson, S. J.; Stone, M. O. Ultrafast Holographic Nanopatterning of Biocatalytically Formed Silica. *Nature* **2001**, *413*, 291−293.

(738) Han, S.; Xu, W.; Meiwen, C.; Jiqian, W.; Xia, D.; Xu, H.; Zhao, X.; Lu, J. R. Interfacial Adsorption of Cationic Peptide Amphiphiles: A Combined Study of *In Situ* Spectroscopic Ellipsometry and Liquid AFM. *Soft Matter* **2012**, *8*, 645−652.

(739) Xu, H.; Wang, Y.; Ge, X.; Han, S.; Wang, S.; Zhou, P.; Shan, H.; Zhao, X.; Lu, J. R. Twisted Nanotubes Formed From Ultrashort Amphiphilic Peptide I$_3$K and Their Templating for the Fabrication of Silica Nanotubes. *Chem. Mater.* **2010**, *22*, 5165−5173.

(740) Guo, L. Q.; Hu, Y. W.; Yu, B.; Davis, E.; Irvin, R.; Yan, X. G.; Li, D. Y. Incorporating TiO$_2$ Nanotubes With a Peptide of D-Amino K122−4 (D) For Enhanced Mechanical and Photocatalytic Properties. *Sci. Rep.* **2016**, *6*, 22247.

(741) Santos, O.; Kosoric, J.; Hector, M. P.; Anderson, P.; Lindh, L. Adsorption Behavior of Statherin and a Statherin Peptide Onto Hydroxyapatite and Silica Surfaces by *In Situ* Ellipsometry. *J. Colloid Interface Sci.* **2008**, *318*, 175−182.

(742) Goyal, D. K.; Pribil, G. K.; Woollam, J. A.; Subramanian, A. Detection of Iltrathin Biological Films Using Vacuum Ultraviolet Spectroscopic Ellipsometry. *Mater. Sci. Eng., B* **2008**, *149*, 26−33.

(743) Höök, F.; Kasemo, B.; Nylander, T.; Fant, C.; Sott, K.; Elwing, H. Variations in Coupled Water, Viscoelastic Properties, and Film Thickness of a Mefp-1 Protein Film during Adsorption and Cross-Linking: A Quartz Crystal Microbalance with Dissipation Monitoring, Ellipsometry, and Surface Plasmon Resonance Study. *Anal. Chem.* **2001**, *73*, 5796−5804.

(744) Jedlicka, S. S.; Rickus, J. L.; Zemlyanov, D. Y. Surface Analysis by X-ray Photoelectron Spectroscopy of Sol−Gel Silica Modified with Covalently Bound Peptides. *J. Phys. Chem. B* **2007**, *111*, 11850−11857.

(745) Weidner, T.; Apte, J. S.; Gamble, L. J.; Castner, D. G. Probing the Orientation and Conformation of α-Helix and β-Strand Model Peptides on Self-Assembled Monolayers Using Sum Frequency Generation and NEXAFS Spectroscopy. *Langmuir* **2010**, *26*, 3433−3440.

(746) Iucci, G.; Battocchio, C.; Dettin, M.; Gambaretto, R.; Di Bello, C.; Borgatti, F.; Carravetta, V.; Monti, S.; Polzonetti, G. Peptides Adsorption on TiO$_2$ and Au: Molecular Organization Investigated by NEXAFS, XPS and IR. *Surf. Sci.* **2007**, *601*, 3843−3849.

(747) Hövel, S.; Kolczewski, C.; Wühn, M.; Albers, J.; Weiss, K.; Staemmler, V.; Wöll, C. Pyridine Adsorption on the Polar ZnO(0001) Surface: Zn Termination Versus O Termination. *J. Chem. Phys.* **2000**, *112*, 3909−3916.

(748) Kaznacheyev, K.; Osanna, A.; Jacobsen, C.; Plashkevych, O.; Vahtras, O.; Agren, H.; Carravetta, V.; Hitchcock, A. Innershell Absorption Spectroscopy of Amino Acids. *J. Phys. Chem. A* **2002**, *106*, 3153−3168.

(749) Larsericsdotter, H.; Oscarsson, S.; Buijs, J. Structure, Stability, and Orientation of BSA Adsorbed to Silica. *J. Colloid Interface Sci.* **2005**, *289*, 26−35.

(750) Larsericsdotter, H.; Oscarsson, S.; Buijs, J. Thermodynamic Analysis of Lysozyme Adsorbed to Silica. *J. Colloid Interface Sci.* **2004**, *276*, 261−268.

(751) Takahashi, H.; Li, B.; Sasaki, T.; Miyazaki, C.; Kajino, T.; Inagaki, S. Catalytic Activity in Organic Solvents and Stability of Immobilized Enzymes Depend on the Pore Size and Surface

Characteristics of Mesoporous Silica. *Chem. Mater.* **2000**, *12*, 3301−3305.

(752) Wang, Y.; Caruso, F. Mesoporous Silica Spheres as Supports For Enzyme Immobilization and Encapsulation. *Chem. Mater.* **2005**, *17*, 953−961.

(753) Berman, B. 3-D Printing: The New Industrial Revolution. *Bus. Horiz.* **2012**, *55*, 155−162.

(754) Ivanova, O.; Williams, C.; Campbell, T. Additive Manufacturing (AM) and Nanotechnology: Promises and Challenges. *Rapid Prototyping Journal* **2013**, *19*, 353−364.

(755) Horn, T. J.; Harrysson, O. L. Overview of Current Additive Manufacturing Technologies and Selected Applications. *Sci. Prog.* **2012**, *95*, 255−282.

(756) Wong, K. V.; Hernandez, A. A Review of Additive Manufacturing. *ISRN Mech. Eng.* **2012**, *2012*, 208760.

(757) Huang, S. H.; Liu, P.; Mokasdar, A.; Hou, L. Additive Manufacturing and Its Societal Impact: A Literature Review. *Int. J. Adv. Des. Manuf. Technol.* **2013**, *67*, 1191−1203.

(758) Murphy, S. V.; Atala, A. 3D Bioprinting of Tissues and Organs. *Nat. Biotechnol.* **2014**, *32*, 773−785.

(759) Feng, C.; Zhang, W.; Deng, C.; Li, G.; Chang, J.; Zhang, Z.; Jiang, X.; Wu, C. 3D Printing of Lotus Root-Like Biomimetic Materials for Cell Delivery and Tissue Regeneration. *J. Adv. Sci.* **2017**, *4*, 1700401.

(760) Huang, T. Q.; Qu, X.; Liu, J.; Chen, S. 3D Printing of Biomimetic Microstructures For Cancer Cell Migration. *Biomed. Microdevices* **2014**, *16*, 127−132.

(761) Porter, M. M.; Ravikumar, N. 3D-Printing a 'Family' of Biomimetic Models to Explain Armored Grasping in Syngnathid Fishes. *Bioinspiration Biomimetics* **2017**, *12*, 066007.

(762) Szojka, A.; Lalh, K.; Andrews, S. H. J.; Jomha, N. M.; Osswald, M.; Adesida, A. B. Biomimetic 3D Printed Scaffolds For Meniscus Tissue Engineering. *Bioprinting* **2017**, *8*, 1−7.

(763) Park, J. Y.; Gao, G.; Jang, J.; Cho, D. 3D Printed Structures For Delivery of Biomolecules and Cells: Tissue Repair and Regeneration. *J. Mater. Chem. B* **2016**, *4*, 7521−7539.

(764) Carrow, J. K.; Kerativitayanan, P.; Jaiswal, M. K.; Lokhande, G.; Gaharwar, A. K. Polymers for Bioprinting. In *Essentials of 3D Biofabrication and Translation*; Atala, A., Yoo, J. J., Eds.; Academic Press: Boston, 2015; pp 229−248.

(765) Fafenrot, S.; Grimmelsmann, N.; Wortmann, M.; Ehrmann, A. Three-Dimensional (3D) Printing of Polymer-Metal Hybrid Materials by Fused Deposition Modeling. *Materials* **2017**, *10*, 1199.

(766) Martin, J. H.; Yahata, B. D.; Hundley, J. M.; Mayer, J. A.; Schaedler, T. A.; Pollock, T. M. 3D Printing of High-Strength Aluminium Alloys. *Nature* **2017**, *549*, 365.

(767) Horst, D. J.; Tebcherani, S. M.; Kubaski, E. T.; de Almeida Vieira, R. Bioactive Potential of 3D-Printed Oleo-Gum-Resin Disks: *B. papyrifera*, *C. myrrha*, and *S. benzoin* Loading Nanooxides—TiO$_2$, P25, Cu$_2$O, and MoO$_3$. *Bioinorg. Chem. Appl.* **2017**, *2017*, 6398167.

(768) Salea, A.; Prathumwan, R.; Junpha, J.; Subannajui, K. Metal Oxide Semiconductor 3D Printing: Preparation of Copper(II) Oxide by Fused Deposition Modelling For Multi-Functional Semiconducting Applications. *J. Mater. Chem. C* **2017**, *5*, 4614−4620.

(769) Fielding, G. A.; Bandyopadhyay, A.; Bose, S. Effects of Silica and Zinc Oxide Doping on Mechanical and Biological Properties of 3D Printed Tricalcium Phosphate Tissue Engineering Scaffolds. *Dent. Mater.* **2012**, *28*, 113−122.

(770) Zhu, W.; Ma, X.; Gou, M.; Mei, D.; Zhang, K.; Chen, S. 3D Printing of Functional Biomaterials For Tissue Engineering. *Curr. Opin. Biotechnol.* **2016**, *40*, 103−112.

(771) Mandrycky, C.; Wang, Z.; Kim, K.; Kim, D. 3D Bioprinting For Engineering Complex Tissues. *Biotechnol. Adv.* **2016**, *34*, 422−434.

(772) Gimeno-Fabra, M.; Peroglio, M.; Eglin, D.; Alini, M.; Perry, C. C. Combined Release of Platelet-Rich Plasma and 3D-Mesenchymal Stem Cell Encapsulation in Alginate Hydrogels Modified by the Presence of Silica. *J. Mater. Chem.* **2011**, *21*, 4086−4089.

(773) Tarafder, S.; Koch, A.; Jun, Y.; Chou, C.; Awadallah, M. R.; Lee, C. H. Micro-Precise Spatiotemporal Delivery System Embedded in 3D Printing For Complex Tissue Regeneration. *Biofabrication* **2016**, *8*, 025003.

(774) Andrianantoandro, E.; Basu, S.; Karig, D. K.; Weiss, R. Synthetic Biology: New Engineering Rules for an Emerging Discipline. *Mol. Syst. Biol.* **2006**, *2*, 2006.

(775) Khalil, A. S.; Collins, J. J. Synthetic Biology: Applications Come of Age. *Nat. Rev. Genet.* **2010**, *11*, 367−379.

(776) McAdams, H.; Arkin, A. Gene Regulation: Towards a Circuit Engineering Discipline. *Curr. Biol.* **2000**, *10*, R318−R320.

(777) Gardner, T.; Cantor, C.; Collins, J. Construction of a Genetic Toggle Switch in *Escherichia coli*. *Nature* **2000**, *403*, 339−342.

(778) Elowitz, M.; Leibler, S. A Synthetic Oscillatory Network of Transcriptional Regulators. *Nature* **2000**, *403*, 335−338.

(779) Bashor, C. J.; Collins, J. J. Understanding Biological Regulation Through Synthetic Biology. *Annu. Rev. Biophys.* **2018**, *47*, 399.

(780) Breitling, R. What is Systems biology? *Front. Physiol.* **2010**, *1*, 9.

(781) Kitano, H. Systems Biology: A Brief Overview. *Science* **2002**, *295*, 1662−1664.

(782) Bruggeman, F. J.; Westerhoff, H. V. The Nature of Systems Biology. *Trends Microbiol.* **2007**, *15*, 45−50.

(783) Morra, M. *Water in Biomaterials Surface Science*; Wiley-VCH: Weinheim, 2001.

(784) Volkov, V. V.; Chelli, R.; Muniz-Miranda, F.; Righini, R. Structural Properties of a Membrane Associated Anchor Dipeptide. *J. Phys. Chem. B* **2011**, *115*, 5294−5303.

(785) Kataoka, S.; Gurau, M.; Albertorio, F.; Holden, M.; Lim, S.; Yang, R.; Cremer, P. Investigation of Water Structure at the TiO_2/Aqueous Interface. *Langmuir* **2004**, *20*, 1662−1666.

(786) Volkov, V. Sum-Frequency Generation Echo and Grating From Interface. *J. Chem. Phys.* **2014**, *141*, 144103.

(787) Ozboyaci, M.; Kokh, D. B.; Corni, S.; Wade, R. C. Modeling and Simulation of Protein-Surface Interactions: Achievements and Challenges. *Q. Rev. Biophys.* **2016**, *49*, 1−45.

(788) Robustelli, P.; Piana, S.; Shaw, D. E. Developing a Molecular Dynamics Force Field for Both Folded and Disordered Protein States. *Proc. Natl. Acad. Sci. U. S. A.* **2018**, *115*, E4758.

(789) Huang, J.; MacKerell, A. D. Force Field Development and Simulations of Intrinsically Disordered Proteins. *Curr. Opin. Struct. Biol.* **2018**, *48*, 40−48.

(790) Piana, S.; Donchev, A. G.; Robustelli, P.; Shaw, D. E. Water Dispersion Interactions Strongly Influence Simulated Structural Properties of Disordered Protein States. *J. Phys. Chem. B* **2015**, *119*, 5113−5123.

(791) Song, D.; Luo, R.; Chen, H. The IDP-Specific Force Field ff14IDPSFF Improves the Conformer Sampling of Intrinsically Disordered Proteins. *J. Chem. Inf. Model.* **2017**, *57*, 1166−1178.

(792) Heinz, H.; Lin, T.; Kishore Mishra, R.; Emami, F. S. Thermodynamically Consistent Force Fields for the Assembly of Inorganic, Organic, and Biological Nanostructures: The INTERFACE Force Field. *Langmuir* **2013**, *29*, 1754−1765.

(793) Zhang, H.; Liu, C.; Gazibegovic, S.; Xu, D.; Logan, J. A.; Wang, G.; van Loo, N.; Bommer, J. D. S.; de Moor, M. W. A.; Car, D.; et al. Quantized Majorana conductance. *Nature* **2018**, *556*, 74−79.

(794) Warshel, A.; Levitt, M. Theoretical Studies of Enzymic Reactions - Dielectric, Electrostatic and Steric Stabilization of Carbonium-Ion in Reaction of Lysozyme. *J. Mol. Biol.* **1976**, *103*, 227−249.

(795) Kohn, W.; Sham, L. J. Self-Consistent Equations Including Exchange and Correlation Effects. *Phys. Rev.* **1965**, *140*, A1133.

(796) Car, R.; Parrinello, M. Unified Approach for Molecular-Dynamics and Density-Functional Theory. *Phys. Rev. Lett.* **1985**, *55*, 2471−2474.

(797) Burke, K.; Werschnik, J.; Gross, E. Time-Dependent Density Functional Theory: Past, Present, and Future. *J. Chem. Phys.* **2005**, *123*, 062206.

(798) Volkov, V.; Belton, D.; Perry, C. C. Do Material Discontinuities in Silica Affect Vibration Modes? *J. Phys. Chem. A* **2018**, *122*, 4997−5003.

(799) Mozhdehi, D.; Luginbuhl, K. M.; Simon, J. R.; Dzuricky, M.; Berger, R.; Samet Varol, H.; Huang, F. C.; Buehne, K. L.; Mayne, N. R.; Weitzhandler, I.; et al. Genetically Encoded Lipid−Polypeptide Hybrid Biomaterials That Exhibit Temperature-Triggered Hierarchical Self-Assembly. *Nat. Chem.* **2018**, *10*, 496−505.